

The role of Cep78 and NPHP5 in centrosome homeostasis

Mohammad Delowar Hossain
Division of Experimental Medicine
McGill University
Montreal, Quebec, Canada
January 2019

A thesis submitted to McGill University in partial fulfillment of the
requirements for the degree of Doctor of Philosophy

Table of contents

List of figures	V
Abstract	VIII
Résumé	X
Acknowledgements	XII
Preface	XIII
Frequently used abbreviations	XVI
Introduction (rationale and objectives of the thesis)	1
Chapter 1. Literature reviews	2
1.1. The centrosome	2
1.1.1. Structure of the centrosome	2
1.1.2. Centrosome cycle	3
1.1.3. Functions of the centrosome	5
1.1.4. Centrosome in human diseases	6
1.2. The cilia	7
1.2.1. Structure and types of cilia	7
1.2.2. Assembly and disassembly of cilia	9
1.2.3. Functions of cilia	11
1.2.4. Ciliopathies	13
1.3. Centrosomal proteins and their functions	15
1.3.1. Centrin	15
1.3.2. POC5	15
1.3.3. CP110	16
1.3.4. Cep97	16
1.3.5. Cep76	16
1.3.6. γ -tubulin	17
1.3.7. DA proteins	17
1.3.8. SDA proteins	17
1.3.9. C-Nap1	18
1.3.10. Cep78	18
1.3.11. NPHP5	19

1.4. Vpr	21
1.5. Ubiquitylation as a mode of protein regulation in centrosome and cilia formation	23
1.6. Figures.....	25
Chapter 2. Cep78 controls centrosome homeostasis by inhibiting EDD-DYRK2-DDB1 ^{VprBP}	33
2.1. Preface.....	34
2.2. Abstract	35
2.3. Introduction.....	36
2.4. Results.....	38
2.4.1. Cep78 localizes to parental centrioles and is periodically expressed in the cell cycle.....	38
2.4.2. Cep78 specifically interacts with the EDD-DYRK2-DDB1 ^{VprBP} E3 ligase at the centrosome	39
2.4.3. Mapping domains critical for the function of Cep78 and its interaction with EDD-DYRK2-DDB1 ^{VprBP} ..	40
2.4.4. Cep78 is not a substrate of EDD-DYRK2-DDB1 ^{VprBP}	41
2.4.5. Cep78 prevents EDD-DYRK2-DDB1 ^{VprBP} from ubiquitinating substrates..	41
2.4.6. A Cep78-interacting protein CP110 is a novel EDD-DYRK2-DDB1 ^{VprBP} substrate	42
2.4.7. Mechanism of EDD-DYRK2-DDB1 ^{VprBP} inhibition by Cep78..	44
2.5. Discussion.....	45
2.6. Materials and methods.....	47
2.7. Acknowledgement.....	51
2.8. Author contributions.....	52
2.9. Conflict of interest.....	53
2.10. References.....	54
2.11. Figures.....	59
Chapter 3. HIV-1 Vpr hijacks EDD-DYRK2-DDB1 ^{DCAF1} to disrupt centrosome homeostasis... ..	85
3.1. Preface.....	86
3.2. Abstract	87
3.3. Introduction.....	88
3.4. Results.....	90

3.4.1. Vpr binds to Cep78 and EDD-DYRK2-DDB1 ^{DCAF1} and localizes to the centrosome.....	90
3.4.2. Vpr hijacks EDD-DYRK2-DDB1 ^{DCAF1} to enhance ubiquitination and degradation of CP110	90
3.4.3. Vpr induces centriole elongation through CP110 degradation.....	91
3.4.4. Vpr-induced CP110 degradation and centriole elongation are independent of G2/M arrest.....	91
3.4.5. Vpr induces CP110 degradation and centriole elongation in infected T cells.....	92
3.4.6. Elongated centrioles enhance microtubule nucleation.....	92
3.5. Discussion.....	94
3.6. Materials and methods.....	96
3.7. Acknowledgement.....	100
3.8. Author contributions.....	101
3.9. Conflict of interest.....	102
3.10. References.....	103
3.11. Figures.....	110
Chapter 4. Requirement of NPHP5 in the hierarchical assembly of basal feet	122
4.1. Preface.....	123
4.2. Abstract	124
4.3. Introduction.....	125
4.4. Results.....	128
4.4.1. SDA and BF are distinguishable.....	128
4.4.2. NPHP5 is a novel SDA and BF component.....	128
4.4.3. NPHP5 is required for BF assembly.....	129
4.4.4. Cells able to form basal bodies require NPHP5 for BF assembly.....	131
4.4.5. The BF and SDA assembly pathways are similar but not identical.....	132
4.4.6. BF assembly correlates with ciliogenesis.....	134
4.5. Discussion.....	135
4.6. Materials and methods.....	137
4.7. Acknowledgement.....	141
4.8. Author contributions.....	142

4.9. Conflict of interest..	143
4.10. References.....	144
4.11. Figures.....	148
Chapter 5. Conclusion and summary	163
References	171

List of figures

Figure 1.6.1. Centrosome structure	25
Figure 1.6.2. Centrosome cycle	26
Figure 1.6.3. Structure of a cilium	27
Figure 1.6.4. Types of cilia	28
Figure 1.6.5. Cilia and cell cycle progression.....	29
Figure 1.6.6. Cilia assembly and disassembly	30
Figure 1.6.7. Structural components of the centrosome	31
Figure 1.6.8. The ubiquitination system	32
Figure 2.11.1. Cep78 interacts with Cep76 and CP110, localizes to the distal region of centrioles and is cell cycle regulated	59
Figure 2.11.2. EDD-DYRK2-DDB1 ^{VprBP} -mediated ubiquitination and degradation of CP110 are regulated by Cep78	61
Figure 2.11.3. Characterization of Cep78	63
Figure 2.11.4. Cep78 interacts with EDD-DYRK2-DDB1 ^{VprBP} through VprBP	64
Figure 2.11.5. Cep78 binds to EDD-DYRK2-DDB1 ^{VprBP} through VprBP	65
Figure 2.11.6. EDD-DYRK2-DDB1 ^{VprBP} is present at the centrosome and mapping functional domains of Cep78 and VprBP	66
Figure 2.11.7. Mapping of the centrosomal localization and VprBP-binding domains of Cep78	68
Figure 2.11.8. Mapping of interaction domains of Cep78 and EDD-DYRK2-DDB1 ^{VprBP}	69
Figure 2.11.9. Cep78 and VprBP are independently recruited to the centrosome and Cep78 is not an EDD-DYRK2-DDB1 ^{VprBP} substrate	70
Figure 2.11.10. Cep78 is a negative regulator but not a substrate of EDD-DYRK2-DDB1 ^{VprBP} ..	72
Figure 2.11.11. Depletion or expression Cep78 had no effect on VprBP protein levels and Cep78 inhibits EDD-DYRK2-DDB1 ^{VprBP}	74
Figure 2.11.12. Cep78 modulates ubiquitination of two EDD-DYRK2-DDB1 ^{VprBP} substrates katanin p60 and TERT but not a CRL4 ^{VprBP} substrate MCM10	75
Figure 2.11.13. CP110 interacts with VprBP and its protein levels are dependent on EDD-DYRK2-DDB1 ^{VprBP} and Cep78.....	77
Figure 2.11.14. Cep76 protein levels are not affected by EDD-DYRK2-DDB1 ^{VprBP} or Cep78 ...	78

Figure 2.11.15. Cep78 regulates CP110 ubiquitination and protein levels through EDD-DYRK2-DDB1 ^{VprBP}	79
Figure 2.11.16. Cep78 and EDD-DYRK2-DDB1 ^{VprBP} control CP110-dependent centriole elongation in non-ciliated cells and cilia assembly in ciliated cells	80
Figure 2.11.17. Cep78 controls CP110-dependent centriole elongation in non-ciliated cells	82
Figure 2.11.18. Mechanism underlying EDD-DYRK2-DDB1 ^{VprBP} inhibition by Cep78	83
Figure 3.11.1 Vpr interacts with Cep78 and EDD-DYRK2-DDB1 ^{DCAF1} through DCAF1	110
Figure 3.11.2. Vpr but not Vpr(Q65R) localizes to the centrosome.....	111
Figure 3.11.3. Vpr enhances ubiquitination and degradation of CP110 but not Cep78	112
Figure 3.11.4. Vpr induces CP110 loss, centriole elongation, and centrosome amplification	114
Figure 3.11.5. Vpr-induced proteasomal degradation of CP110 occurs in a DCAF1-dependent manner.....	115
Figure 3.11.6. Vpr centrosomal localization and Vpr-induced ubiquitination and degradation of CP110 are independent of G2/M arrest	116
Figure 3.11.7. Vpr-induced centrosome amplification, but not CP110 loss or centriole elongation, is dependent of G2/M arrest.....	118
Figure 3.11.8. Degradation of CP110 induced by Vpr or Vpr(R80A) can be overcome by Cep78 expression	119
Figure 3.11.9. HIV-1 Vpr induces CP110 loss, centriole elongation, and centrosome amplification in infected T cells.....	120
Figure 3.11.10. Depletion of CP110 or expression of Vpr enhances microtubules nucleation ...	121
Figure 4.11.1. Cell lines vary in their ability to enter quiescence, form basal bodies, and ciliate	148
Figure 4.11.2. NPHP5 is a novel component of SDAs and BF, two distinguishable structures	149
Figure 4.11.3. Ablation of BF components inhibits ciliogenesis without affecting entry into quiescence and basal body formation	150
Figure 4.11.4. Ablation of BF components inhibits ciliogenesis without affecting recruitment of IFT88.....	151
Figure 4.11.5. Knockdown efficiency of NPHP5 in cycling versus quiescent RPE-1 cells	152
Figure 4.11.6. NPHP5 recruits Kif3a, ninein, and Cep170 to BF while preventing the recruitment of TCHP in quiescent RPE-1 cells	153

Figure 4.11.7. NPHP5 destabilizes TCHP, interacts with Kif3a and ninein at the centrosome, and is required for microtubule nucleation and anchoring in quiescent RPE-1 cells	154
Figure 4.11.8. NPHP5 does not affect SDA assembly in cycling RPE-1 cells.....	156
Figure 4.11.9. Cep290 specifically recruits ninein to BF but not SDAs.....	157
Figure 4.11.10. NPHP5-mediated BF assembly is cell type specific	158
Figure 4.11.11. Ablation of NPHP5 does not affect entry into quiescence or basal body formation in quiescent RPE-1, ARPE-19, HK-2, and HeLa cells.....	159
Figure 4.11.12. Hierarchical assembly of BF	160
Figure 4.11.13. BF loss due to ablation of NPHP5, Kif3a or ODF2 can be rescued.....	161
Figure 4.11.14. Cilia loss due to ablation of NPHP5, Kif3a or ODF2 can be rescued	162

Abstract

The centrosome is a microtubule based structure consisting of two centrioles surrounded by electron dense proteinaceous material called the pericentriolar matrix. The two centrioles in each centrosome are identified as mother and daughter centrioles and can be distinguished by the presence of distal and subdistal appendages at the mother centriole. Distal appendages are involved in the docking of the basal body to the cell membrane prior to ciliogenesis. Subdistal appendages are important for the anchoring and nucleation of microtubules, and have recently been found to play an important role in ciliogenesis. The role of centrosome in cells is to organize microtubules, thereby regulating cell shape, motility, polarity and cell migration, as well as act as a template to form the cilia. Cilia are hair-like protrusions found on the surface of the cell membrane that can help with fluid flow, cell locomotion or participate in cell signalling mechanisms based on the type and nature of the cilia. It is known that several diseases such as cancer, microcephaly and ciliopathies are caused by centrosome and cilia abnormalities. A better understanding of the assembly and function of centrosomes and cilia could shed light on many human diseases caused by mutations in the proteins associated with these organelles. Although more than one thousand centrosomal proteins have been identified, the precise role of most of them has not been fully characterized.

Here, I have characterized the functions of two centrosomal proteins: Cep78 and NPHP5. Cep78 was previously identified as a novel centrosomal component with no assigned function. I have shown that Cep78 is localized at the distal end of the centriole, suggesting that it carries an important biological function in this region of the centrosome. In addition, Cep78 interacts with VprBP/DCAF1, which is the substrate recognition subunit of both the RING-type CRL4^{VprBP} ubiquitin E3 ligase and the HECT-type EDD-DYRK2-DDB1^{VprBP} ubiquitin E3 ligase. Furthermore, Cep78 specifically binds with EDD-DYRK2-DDB1^{VprBP}, where EDD-DYRK2-DDB1^{VprBP} ubiquitinates and degrades the newly identified substrate CP110. CP110 is known to cap the distal end of the centriole and to suppress centriole elongation. Cep78 preferentially inhibits the ubiquitination activity of EDD-DYRK2-DDB1^{VprBP}, thereby leading to decreased CP110 ubiquitination. Moreover, expression of EDD-DYRK2-DDB1^{VprBP} or depletion of Cep78 promotes centriole elongation, a phenotype reminiscent of CP110 loss. Thus, we found that Cep78 has a role in centrosome homeostasis by regulating the ubiquitination of an EDD-DYRK2-DDB1^{VprBP} substrate.

Previously, it has been shown that HIV-1 accessory protein viral protein R (Vpr) interacts with VprBP. As VprBP acts as a substrate recognition subunit of abovementioned two types of ubiquitin E3 ligases, I would like to know if Vpr specifically interacts with EDD-DYRK2-DDB1^{VprBP} in the centrosome. Following up on this work, I found that Vpr interacts with Cep78 in the centrosome through the EDD-DYRK2-DDB1^{VprBP} ubiquitin E3 ligase. Furthermore, I have demonstrated that Vpr and its partner VprBP enhances the ubiquitination and degradation of previously characterized native substrate CP110 without affecting the non-substrate Cep78. Moreover, Vpr mediated loss of CP110 can be overcome by the expression of Cep78. Infection of T-cells with wild type HIV-1 leads to the degradation of CP110, thereby promoting centriole elongation. In addition, the elongated centriole, due to the loss of CP110, increases the microtubule nucleation activity at the centrosome. It is known that the microtubule facilitates HIV-1 trafficking inside the cell. Therefore, our research suggests that Cep78 might counteract the effects of HIV-1 and could play a role in modulating viral pathogenesis.

Finally, I focused on a nother poorly described centriolar distal region protein, NPHP5. Previously it has been shown that NPHP5 is involved in the regulation of the early steps of ciliogenesis. During early ciliogenesis, the mother centriole differentiates into a specialized structure called the basal body, while distal appendages and subdistal appendages are respectively converted into transition fibres and basal feet. To determine if NPHP5 might be involved in the abovementioned conversion process, I have investigated the proper localization of NPHP5 in detail using super-resolution microscopy images and found that NPHP5 localizes in both subdistal appendages and basal feet. In the absence of NPHP5, basal feet are not assembled properly, whereas the assembly of subdistal appendages was unaffected. I also confirmed a close association between NPHP5 and basal feet proteins by proximity ligation assay. Finally, I observed a positive correlation between basal feet assembly and ciliogenesis, suggesting that these two events are coupled to each other.

Résumé

Le centrosome est une organelle microtubulaire composée de deux centrioles entourés d'un électron dense en matière protéinique appelé matrice pericentriolaire. Les deux centrioles de chaque centrosome, identifiés mère et fille, se distinguent par la présence d'appendices distaux et subdistaux chez le centriole mère. Les appendices distaux sont impliqués dans l'arrimage du corps basal à la membrane cellulaire précédant la ciliogénèse. Les appendices subdistaux sont importants pour l'arrimage et la nucléation des microtubules et, on sait depuis peu, qu'ils sont aussi impliqués dans la ciliogénèse. Le rôle du centrosome est d'organiser les microtubules dans la cellule, régulant ainsi la forme, la motilité, la polarité et la migration cellulaire, tout en agissant comme modèle pour la formation des cils. Les cils sont des protusions filiformes situées à la surface de la membrane cellulaire qui facilitent la fluidité et la mobilité cellulaire ou qui participent aux mécanismes de signalisation cellulaire selon le type et la nature des cils. On sait que plusieurs maladies comme le cancer, la microcéphalie et les ciliopathies sont causées par des anomalies des centrosomes ou de s cils. Une meilleure connaissance de l'assemblage et du fonctionnement des centrosomes et des cils pourraient nous aider à mieux comprendre les maladies causées par les mutations des protéines de ces organelles. Bien que plus d'un millier de protéines centrosomales aient été identifiées, leur rôle précis n'a pas encore été complètement caractérisé.

Ici, j'ai caractérisé les fonctions de deux protéines centrosomales : Cep78 et NPHP5. Cep78 avait préalablement été identifiée comme une nouvelle composante centrosomale sans fonction précise. J'ai démontré que Cep78 se situe à l'extrémité distale du centriole, ce qui permet de croire qu'elle occupe une fonction biologique importante dans cette région du centrosome. De plus, Cep78 interagit avec VprBP/DCAF1, qui est la sous-unité de reconnaissance de substrat de l'ubiquitine E3 ligase CRL4^{VprBP} de type RING, et de l'ubiquitine E3 ligase EDD-DYRK2-DDB1^{VprBP} de type HECT. De plus, Cep78 se fixe spécifiquement à EDD-DYRK2-DDB1^{VprBP}, où EDD-DYRK2-DDB1^{VprBP} ubiquitine et dégrade le substrat CP110 nouvellement identifié. On sait que CP110 couvre l'extrémité distale du centriole et réprime l'allongement du centriole. Cep78 inhibe de préférence l'activité d'ubiquitination de EDD-DYRK2-DDB1^{VprBP}, ce qui entraîne la diminution d'ubiquitination de CP110. De plus, l'expression de EDD-DYRK2-DDB1^{VprBP} ou la déplétion de Cep78 favorise l'allongement du centriole, un phénotype similaire

à la perte de CP110. Par conséquent, nous avons trouvé que Cep78 joue un rôle dans l'homéostasie centrosomale en régulant l'ubiquitination du substrat EDD-DYRK2-DDB1^{VprBP}.

Au préalable, il a été démontré que la protéine accessoire du HIV-1 protéine virale R (Vpr) interagit avec VprBP. Puisque VprBP agit comme sous-unité de reconnaissance du substrat des deux types d'ubiquitine ligases E3 indiquées ci-dessus, j'ai tenté de savoir si Vpr interagissait spécifiquement avec EDD-DYRK2-DDB1^{VprBP} dans le centrosome. À la suite de ces travaux, j'ai constaté que Vpr interagit avec Cep78 dans le centrosome par le biais d'EDD-DYRK2-DDB1^{VprBP} ubiquitine ligase E3. De plus, j'ai démontré que Vpr et son partenaire VprBP augmentent l'ubiquitination et la dégradation du substrat endogène CP110 préalablement caractérisé sans affecter le non-substrat de CEP78. Aussi, la perte de CP110 provoquée par Vpr peut être compensée par l'expression de Cep78. L'infection des cellules-T par le HIV-1 de type naturel entraîne la dégradation de CP110, ce qui favorise l'allongement des centrioles. De plus, l'allongement du centriole causé par la perte de CP110 augmente la nucléation du microtubule dans le centrosome. On sait que le microtubule favorise la mobilité du HIV-1 à l'intérieur de la cellule. Par conséquent, nos recherches suggèrent que Cep78 pourrait neutraliser les effets du HIV-1 et serait impliquée dans la modulation de la pathogénèse virale.

Enfin, j'ai me suis concentré sur NPHP5, une protéine distale du centriole, encore peu connue. Auparavant, il a été démontré que NPHP5 est impliquée dans la régulation des premières phases de la ciliogénèse. Durant la phase initiale de la ciliogénèse, le centriole mère se différencie en une sustructure spécialisée appelée corps basal, alors que les appendices distaux et appendices subdistaux sont respectivement transformés en fibres de transition et pieds basaux. Pour déterminer si NPHP5 est impliquée dans le processus de conversion sus-mentionné, j'ai tenté de définir la position exacte de NPHP5 par microscopie à super-résolution, et j'ai découvert que NPHP5 se trouve à la fois dans les appendices subdistaux et les pieds basaux. En l'absence de NPHP5, les pieds basaux ne sont pas assemblés correctement, alors que l'assemblage des appendices subdistaux n'est pas affecté. J'ai aussi confirmé le lien étroit entre NPHP5 et les protéines des pieds basaux par test de ligature de proximité. Enfin, j'ai observé une corrélation positive entre l'assemblage des pieds basaux et la ciliogénèse, ce qui suggère que ces deux événements sont liés.

Acknowledgements

I would like to thank to my supervisor Dr. William Tsang for his mentorship, scientific guidance and valuable advice throughout my PhD studies in his lab. Dr. Tsang is an inspiring mentor from whom I have learned many lessons. I always remember the great experience he gave me while in his lab.

I also would like to thank to my committee members, Dr. David R. Hipfner, Dr. Javier Marcelo Di Noia and Dr. Khanh Huy Bui for their important advice, support and the time they spent attending meetings and reading the progress reports over the course of my studies. I am lucky to be a part of a group of talented scientists.

I have also had the opportunity to collaborate with famous virologist Dr. Éric A. Cohen throughout my PhD. Many thanks to Dr. Cohen for your valuable advice and the opportunity to work with some of your lab members. I am also grateful for the contributions of Dr. Robert Lodge and Jeremy Ferreira-Barbosa towards the publication of my second paper.

The company and help from the past and present members of Dr. Tsang's lab have been appreciated during my PhD studies and they have made the lab a great work place. Thank you to all of them. I would like to give special thanks to Nicole Rousseau for her assistance to edit my thesis and translate the abstract into French. I also want to thank to Dominic Filon and Dr. Erika Wee for their assistance to analyze the microscopy image.

Finally a special thanks to my partner Rumana Sultana for the support and encouraging me in the long journey. Most importantly thank you to my parents who actually inspire me to be a part of the scientific family.

Preface

Contributions to original knowledge

This thesis was written in accordance to the McGill University thesis guideline and has been chosen to manuscript based thesis preparation. The thesis was supported by McGill university graduate entrance fellowship and graduate excellence award.

Manuscripts are included in this thesis:

1. **Hossain D**, Javadi Esfehiani Y, Das A, Tsang WY (2017). Cep78 controls centrosome homeostasis by inhibiting EDD-DYRK2-DDB1^{VprBP}. *EMBO Rep.* 18 (4): 632-644.
2. **Hossain D**, Ferreira Barbosa JA, Cohen ÉA, Tsang WY (2018). HIV-1 Vpr hijacks EDD-DYRK2-DDB1^{DCAF1} to disrupt centrosome homeostasis. *J. Biol. Chem.* 293 (24): 9448-9460.
3. **Hossain D**, Barbelanne M, Tsang WY (2018). Requirement of NPHP5 in the hierarchical assembly of basal feet. Manuscript is under revision.

The centrosome is the major microtubule organizing center of animal cells that maintains cell shape, motility, polarity and cell signalling. It comprises of a pair of centrioles (called mother and daughter) surrounded by a proteinaceous material called the pericentriolar matrix. The distinguishable feature of mother centriole is the presence of distal and subdistal appendages which is absent in the daughter centriole. Centrosome also acts as a template to form the cilia. Cilia are hair-like protrusions found on many eukaryotic cells and function as fluid flow, locomotion as well as cell signalling. During ciliogenesis, mother centriole undergoes extensive modifications and converted to the basal bodies. Distal and sub-distal appendages of mother centriole are remodelled to transition fibres and basal feet respectively. Therefore, basal body serves as the nucleation site for the growth of the ciliary axoneme. Although centrosome plays an important role in cell biology, the function of many centrosomal proteins is still unknown.

In my first manuscript, I characterize a novel centrosomal protein Cep78, whose function is incompletely understood. I found that Cep78 is a key component in the distal region of the centriole suggesting that this protein plays a significant role in this region of the centriole. In this study, I report that Cep78 interacts with the VprBP which is the substrate recognition subunit of both the RING-type CRL4^{VprBP} ubiquitin E3 ligase and the HECT-type EDD-DYRK2-DDB1^{VprBP} ubiquitin E3 ligase. Moreover, Cep78 specifically inhibits the ubiquitination activity of EDD-DYRK2-DDB1^{VprBP} thereby leading to decrease ubiquitination of newly identified

substrate CP110. It is known that CP110 caps the distal end of the centriole and regulates the length of the centriole. Furthermore, depletion of Cep78 leads to the elongated centriole, a phenotype reminiscent of CP110 loss. Thus, Cep78 mediated regulation of EDD-DYRK2-DDB1^{VprBP} substrate highlighting the importance of Cep78 in centrosome homeostasis.

It is known that VprBP interacts with the HIV-1 accessory protein viral protein R (Vpr) and VprBP acts as a substrate recognition subunit of both the RING-type CRL4^{VprBP} ubiquitin E3 ligase and the HECT-type EDD-DYRK2-DDB1^{VprBP} ubiquitin E3 ligase. In my second manuscript, I want to know whether Vpr specifically interacts with EDD-DYRK2-DDB1^{VprBP} ubiquitin E3 ligase at the centrosome. I found that Vpr interacts with Cep78 through VprBP and increases the ubiquitination activity of EDD-DYRK2-DDB1^{VprBP} at the centrosome thereby degrades the newly identified substrate CP110. Moreover, the loss of CP110 by Vpr can be overcome by the expression of Cep78. I also demonstrated that Vpr mediated down regulation of CP110 promotes centriole elongation. In addition, the loss of CP110 by Vpr also increases the microtubule nucleation activity at the centrosome. As microtubules are needed for HIV-1 trafficking, it could presumably enhance the viral pathogenesis. Thus, our results suggest that Vpr mediated deregulation of centrosomal homeostasis could contribute to HIV-1 pathogenesis.

In my third manuscript, I characterize another centriolar distal region protein NPHP5, whose function is poorly understood. In this study, I found that NPHP5 is localized in subdistal appendages and basal feet, but specifically required for the basal feet assembly. Furthermore, ciliogenesis is affected in absence of NPHP5 or basal feet protein. Therefore, NPHP5 mediated hierarchical assembly of basal feet correlates with cilia assembly, indicating that these two events are linked to each other.

Contribution of the authors

1. **Hossain D**, Javadi Esfehiani Y, Das A, Tsang WY (2017). Cep78 controls centrosome homeostasis by inhibiting EDD-DYRK2-DDB1^{VprBP}. *EMBO Rep.* 18 (4): 632-644.

Contribution of Hossain D: All the experiments, figures, tables and statistical analysis except: Figure 2.11.1 (F-Tsang WY), Figure 2.11.2 (B-Tsang WY), Figure 2.11.2 (C-Tsang WY), Figure 2.11.2 (E-right portion-Tsang WY), Figure 2.11.2 (F-Tsang WY), Figure 2.11.4 (B-left portion-Tsang WY), Figure 2.11.7 (H-with the input of Tsang WY), Figure 2.11.9 (C-Tsang WY), Figure 2.11.9 (A-B-Tsang WY), Figure 2.11.12 (B-Tsang WY) and Figure 2.11.13 (A-Tsang WY).

2. **Hossain D**, Ferreira Barbosa JA, Cohen ÉA, Tsang WY (2018). HIV-1 Vpr hijacks EDD-DYRK2-DDB1^{DCAF1} to disrupt centrosome homeostasis. *J. Biol. Chem.* 293 (24): 9448-9460.

Contribution of Hossain D: All the experiments, figures, tables and statistical analysis except: Figure 3.11.6 (A-Ferreira Barbosa JA) and Figure 3.11.9 (A-Ferreira Barbosa JA infected the MT4 cells, Hossain D stained, analysed and prepared the figure).

3. **Hossain D**, Barbelanne M, Tsang WY (2018). Requirement of NPHP5 in the hierarchical assembly of basal feet. Manuscript is under revision.

Contribution of Hossain D: All the experiments, figures, tables and statistical analysis except: Figure 4.11.1 (A-graphics-Tsang WY), Figure 4.11.1 (E-graphics-Tsang WY), Figure 4.11.1 (F-Barbelanne M) and Figure 4.11.6 (A and C-Tsang WY).

Frequently used abbreviations

γ -TuRC	γ -tubulin ring complex
3D-SIM	Structured illumination microscopy
BBS	Bardet-Biedl syndrome
BF	Basal feet
CC	Coiled-coil domain
Cep	Centrosomal protein
CP110	Centriolar coiled coil protein 110
CRC	Colorectal cancer
DAs	Distal appendages
DT	Anti-detyrosinated tubulin
EM	Electron microscopy
GPCRs	G-protein-coupled receptors
GT335	Anti-glutamylated tubulin
HECT	<i>H</i> omologous to <i>E</i> 6-AP carboxy <i>T</i> erminus
HRP	Horseradish peroxidase
IFT	Intraflagellar transport
LRR	Leucine rich repeat
MCPH	Autosomal recessive primary microcephaly
MTOC	Microtubule organizing center
NPCs	Neural progenitor cells
NPHP	Nephronophthisis
NS	Non-specific
PCM	Pericentriolar matrix
PLA	Proximity ligation assay
PLK1	Polo like kinase-1
PLK4	Polo like kinase-4
Ptc1	Patched1
RBR	RING-between-RING
RING	<i>R</i> eally <i>I</i> nteresting <i>N</i> ew <i>G</i> ene type
ROI	Region of interest

RPE-1	Retinal pigmented epithelial cells
SDAs	Subdistal appendages
Shh	Sonic hedgehog
siRNA	Small interfering RNA
Smo	Smoothened
TCHP	Trichoplein
TERT	Telomerase reverse transcriptase
TFs	Transition fibres
Ub	Ubiquitin
Vpr	Viral protein R
VprBP	Viral protein R-binding protein
WT	Wild type

Introduction (rationale and objectives of the thesis)

The centrosome is considered as the major microtubule organizing center (MTOC) in the cell. It plays a significant role in the cell shape, motility, polarity and cilia formation. It is known that abnormalities of centrosome and cilia structures and functions are linked to diseases such as cancer. Despite the significance of this organelle to cell biology, the function of many centrosomal proteins is still unknown. In this thesis, I characterized two novel centrosomal proteins, Cep78 and NPHP5 whose functions are poorly understood. This is the objectives of this thesis.

The present study aims to answer the intriguing question of how Cep78 participates in centrosome biology which was the first goal of my research. In addition, the following questions need to be answered regarding the exact location of Cep78 at the centrosome: whether and how it is involved in centrosome assembly and function, and what are the major interacting partners involved in this process are. Furthermore, it is important to investigate whether deregulation of Cep78 is associated with disease. These important questions formed the rationale for the second and third chapters of this thesis.

I have further expanded my knowledge to another novel centrosomal protein, NPHP5. In our lab, we showed that NPHP5 is localized at the distal region of centriole and is involved in ciliogenesis. But the mechanism of ciliogenesis by NPHP5 is poorly understood. To gain further insight into the biological functions corresponding to NPHP5, it is important to investigate the precise localization of NPHP5 with high resolution microscopy, as well as its association with other proteins in that particular region. This is the rationale for the fourth chapter of my thesis.

Chapter 1

Literature reviews

1.1. The centrosome

The centrosome is a small organelle located at the center of the cell, usually close to the nucleus, and is composed of two centrioles called mother and daughter. Nearly all the animal cells have this organelle that plays an important role in organizing most of the microtubules in cells. The term centrosome was introduced by Theodor Boveri in 1887 (1). To understand the importance of studying the centrosome, I will briefly discuss the structure and functions of the centrosomes in cells.

1.1.1. Structure of the centrosome

The centrosome is composed of a pair of orthogonally arranged centrioles (called mother and daughter centrioles) surrounded by pericentriolar matrix (PCM). The centrioles in each centrosome are characterized by a precise nine fold bundle of three microtubules (A, B and C) (2, 3) (Figure 1.6.1). The length and diameter of this cylindrical structure is about 500 nm and 200 nm respectively. Each A microtubule (innermost) consists of 13 complete α - and β -tubulin containing protofilaments. B (middle) and C (outermost) microtubules are composed of 10 incomplete α - and β -tubulin containing protofilaments. A and B microtubules span the entire length of the centriole, whereas C microtubule does not extend all the way to the distal end of the centriole (3, 4) (Figure 1.6.1). α - and β -tubulin dimers at the centrosome undergo extensive posttranslational modifications such as glutamylation, acetylation and detyrosination. The microtubule modification of the centriole is important to stabilize the centrosome and provides its integrity. The cylinder pattern of the centriole exhibits proximal-distal orientation in which the distal end corresponds to the plus end of the centriolar microtubules. The appearance of distal appendages (DAs) and subdistal appendages (SDAs) are the distinguishing characteristics of the mother centriole (often called the mature centriole), as these appendages are absent in the daughter centriole (2-8) (Figure 1.6.1).

1.1.2. Centrosome cycle

The centrosome cycle is a series of events where a single centrosome duplicates to generate two centrosomes in a cell cycle dependent manner (Figure 1.6.2). The centrosome duplication is properly controlled so that only one newly synthesized centriole (also called procentriole) per existing one is gathered. There are four major events in the centrosome cycle: disengagement, duplication, maturation and separation. In brief, the loosening of the orthogonal arrangement between the mother and daughter centrioles in late mitosis or early G1 phase allows the synthesis of the procentriole in S phase and its elongation during the G2 phase. When the proliferating cell exits mitosis, the two centrosomes separate with a pair of centrioles (2, 9).

Centriole disengagement

In late mitosis or early G1 phase, the two centrioles in a centrosome are disengaged (loosening the orthogonal arrangement between the two centrioles) and get licensed to allow the synthesis of the procentriole. Centriole disengagement is restricted to once per cell cycle and is important for duplication. Despite the loosening of the orthogonal arrangement, the two centrioles are still attached to each other through a flexible linker between their proximal ends (2, and 9-11).

Centrosome duplication

Centriole duplication starts during the S phase where a procentriole forms adjacent to each existing centriole. When the procentriole is initiated, it looks like a cartwheel like structure at the proximal end of the existing centriole resulting in the stabilization of the microtubules 9-fold symmetry. Once formed, the procentrioles start to elongate until they reach the same size as the existing centrioles (12-16).

Centrosome maturation

Following elongation, procentrioles mature into daughter centrioles whereas the existing daughter centriole becomes mother centriole by acquiring its own DAs and SDAs. It takes one and a half cell cycle to reach to this stage from the procentriole formation. The important event at this step is the enlargement of the PCM at the onset of mitosis (17).

Centrosome separation

Progression through the centrosome cycle involves the formation and dissolution of linkers, which are important for proper segregation at the end of the centrosome cycle. During S and G2 transition, the existing centrioles are attached by a flexible linker which is formed preceding the

G1 phase. The dissolution of the flexible linker is the critical step for the separation of the two centrosomes. At the onset of mitosis, the existing centrioles are separated into two centrosomes in a process called centrosome separation (18-20). Once separated, the two centrosomes move to the opposite poles. After mitosis, the cell can enter the G1 phase and progress through another round of cell division or can exit the cell cycle where cilia formation is favoured (Figure 1.6.2).

1.1.3. Functions of the centrosome

The centrosome is a tubulin-based structure with a pair of centrioles (called mother and daughter centrioles) surrounded by PCM. DAs of the mother centriole are involved in the docking of the basal body (modified form of the mother centriole, will be discussed in the cilia section) to the cell membrane during ciliogenesis whereas SDAs are important for microtubule anchoring and ciliogenesis. PCM is responsible for microtubule nucleation in cells, leading to the term MTOC (8, and 21-23). The centrosome plays a significant role in cell polarity, shape, motility and intracellular signalling (23). For example, proper positioning of the golgi apparatus around the centrosome is important for cell polarization. This happens by maintaining the microtubule network intact (24).

The centrosome is also necessary for the cell cycle progression (25). If the centrosome is not working properly (due to the loss of centrosome, core centrosomal proteins or centrosome implication), it will lead to the activation of centrosome dependent checkpoints which causes cell cycle arrest in normal cells in p53 dependent manner (25). Moreover, in mitosis the centrosome establishes the bipolar spindle poles where spindle microtubules are anchored to segregate the DNA. It has been shown that mitosis can be delayed due to the loss of centrosome or centrosome amplification (26, 27). Overall, centrosomes are required to ensure a timely cell division and for proper cell maintenance (28-30). Besides these functions, the centrosome is also involved in forming the cilia which will be discussed later in this chapter.

1.1.4. Centrosome in human diseases

The function of the centrosome is known to significantly contribute to cell behaviour. It has been shown that several diseases are caused by centrosome deregulations. For example, multiple centrioles cause cell division errors which lead to genetic instability and aneuploidy (31-33). It is known that extra centrosomes, genetic instability and aneuploidy are hallmarks of cancer. During mitosis, the extra centrosomes are prone to multipolar spindle formation which might lead to cell death (34, 35). To avoid cell death, cancer cells form the normal bipolar spindle poles with an extra number of centrosomes in a process called centrosome clustering. In this case, centrosomes are pulled together in order to form bipolar spindles with increased frequency of lagging chromosomes at anaphase (36).

Aside from cancer, several developmental diseases like microcephaly and dwarfism have been linked to mutations in centrosomal proteins. Autosomal recessive primary microcephaly (MCPH) is a rare human disease where the brain does not develop properly leaving it smaller in size than normal. There are 18 genes that have been linked to MCPH, and some of these genes are related to centrosome duplication and maturation (37). It is known that the brain develops from the neural progenitor cells (NPCs). The number of NPCs increases through symmetrical division (generating two identical NPCs). Thereafter, NPCs begin asymmetrical division to generate one NPC to maintain the pool, and a precursor that migrates and differentiates into a neuron. It is important to maintain the proper balance between symmetrical and asymmetrical division to determine the final number of neurons in the brain. It is suggested that improper balance between symmetric vs. asymmetric divisions perturb the number of NPCs and neurons, thereby reducing the size of the brain. In addition, cell death or growth arrest due to delayed mitosis might also impair brain development (37-39).

1.2. The cilia

Cilia are membrane bound hair-like protrusions found on the surface of most eukaryotic cells. The structure of the cilia was first discovered by Leewenhoek (40). To form the cilia, the mother centriole is converted to a specialized structure called the basal body. Therefore, the basal body serves as a template to nucleate the growth of cilia. Although cilia formation is favoured in G0 phase, they are also present in the interphase. In mitosis, cilia need to be disassembled where the basal body switches back to mother centriole. Thereafter, the centrosome assists to establish the bipolar spindle poles. The length of cilia can vary from 1 μm to more than 2 mm depending on their nature or cell types, and their width is 0.25 μm (41). In this section, I will briefly discuss the structure and functions of cilia.

1.2.1. Structure and types of cilia

Cilia are microtubule-based projections that grow as a ninefold symmetry starting from the basal body. The axoneme, ciliary membrane and the transition zone are the basic structure of the cilia (42) (Figure 1.6.3). The basal body is located at the base of the cilia. It is a modified form of the mother centriole where DAs and SDAs are remodelled to the transition fibres (TFs) and basal feet (BF) respectively. Once formed, the basal body serves as the nucleation site for the growth of the axoneme. The axoneme is the inner core of the cilia. Cilia are broadly classified into two types, motile and non-motile or primary cilia (8, 43). Motile cilia have a 9+2 configuration in which nine microtubules doublets surrounds a central pair. In the case of the primary cilia, it appears as a 9+0 configuration in which the central pair is absent (Figure 1.6.4). Some studies have shown that there are exceptions with the 9+2 or 9+0 microtubule organization in motile, versus primary cilia respectively. For example, 9+0 motile cilia are present in the mouse embryonic node, and 9+2 primary cilia in kinocilia of fish (44-47). Both types of ciliary axonemes are surrounded by the ciliary membrane. The ciliary membrane differs from the plasma membrane in terms of their protein and lipid composition. As the subset of transmembrane proteins is concentrated into the ciliary membrane, it plays a significant role in signalling. For example, sonic hedgehog (Shh) signalling involves the reciprocal movement of two transmembrane proteins called smoothened (Smo) and patched 1 (Ptc1) into the cilia. It is known that the receptor Ptc1 is localized into the ciliary membrane and prevents the accumulation of Smo in the absence of ligand Shh. When Shh binds with Ptc1, Ptc1 is lost from the cilia which allows the enrichment of the Smo and activates the signal transduction. In this

way they help to communicate with the rest of the cell. It is known that cilia lack the protein synthesizing machinery. Thus, proteins need to traffic from elsewhere in order for cilia assembly to occur (48, 49). There is a postulated barrier called the ciliary gate that controls the entry of proteins in and out of the cilia. The features associated with the ciliary gate include TFs, transition zone and ciliary necklace. The ciliary transition zone appears as Y-shaped fibres, located at the base of the cilia that controls the entry of soluble proteins (50-52), whereas the ciliary necklace consists of several strands of intramembrane particles that are associated with the outer part of the Y-shaped fibres. It controls the entry of transmembrane proteins into the cilia that require a special sequence motif. For example, C-terminal VxPx is required for rhodopsin to get in to the cilia.

Motile cilia have their own motor protein dynein (the outer and inner motor dynein arms), thus facilitating motion (44-48) (Figure 1.6.4). The dynein arms produce asynchronous forces that generate the doublet microtubules sliding motion in respect to one another. The progression of the sliding activity around the axoneme causes the cilia to beat (49). They are present on a restricted number of cell types, but appear in large numbers.

In contrast, primary cilia lack the motor protein dynein responsible for ciliary movement and are usually referred to as non-motile (50) (Figure 1.6.4). Primary cilia are present in many different types of cells which appear once per cell. Primary cilia are the basis for different specialized sensory architectures such as mechanosensor, chemosensor and photosensor.

1.2.2. Assembly and disassembly of cilia

Cilia assembly begins as the cell cycle exits the mitotic phase. Although the process of ciliogenesis is mostly seen in quiescence, the cilia can also be found in interphase (53) (Figure 1.6.5). The cilia assembly process in motile vs. primary cilia are not the same (Figure 1.6.6). There are several events in primary cilia assembly: basal body formation, recruitment of the vesicle, transition zone formation, growth of the cilia and length control (42, and 53-55). The early event is the modification of the mother centriole into a specialized structure called the basal body. Once the basal body forms, it recruits the vesicles which eventually dock and fuse with the plasma membrane. Whether the basal body-vesicle moves to the cell surface is not clearly understood (42). In addition, another event called invagination of the vesicles to create the ciliary membrane is also associated in primary cilia assembly. Therefore, the transition zone formation is favoured, which controls the entry and exit of proteins to control the ciliary trafficking. In the case of the motile cilia, after the basal body formation, it migrates to the cell surface and starts to form the transition zone. As this organelle lacks the protein synthesizing machinery, the proteins required to build the cilia need to traffic from other places inside the cell. This process is dependent on intraflagellar transport (IFT). IFT is a bidirectional transport system that moves along with the motor proteins onto the axonemal microtubules. The IFT complex can be divided into 2 sub-complexes, IFTA and IFTB. IFTA is composed of 6 subunits (IFT144, IFT140, IFT139, IFT122, IFT121 and IFT43), whereas IFTB is a combination of several proteins (IFT172, IFT88, IFT81, IFT80, IFT74, IFT70, IFT57, IFT56, IFT54, IFT52, IFT46, IFT38, IFT27, IFT25, IFT22 and IFT20) (55-57). Cargos are used to build the axoneme and are delivered to the ciliary tip by anterograde transport. Unwanted cargos are returned to the basal body via retrograde transport. Although IFTA and IFTB respectively move the cargo in retrograde and anterograde directions, IFTA also regulates to direct anterograde transport (8). Finally the cilia start to elongate depending on the types of cells and cilia. For example it has been shown that the length and number of cilia are increased in serum starved conditions rather than interphase (58-60). On the other hand, it has been shown that brain ependymal cilia are much longer than cilia in lung (61). Cilia disassembly is the reverse process of cilia assembly where the basal body is converted back to the mother centriole. The mechanism underlying the cilia disassembly is favoured by growth stimulation that activates the deacetylase, histone deacetylase 6 to deacetylate the tubulin. As a result, tubulin becomes destabilized, leading to

ciliary disassembly (53, and 62-64) (Figure 1.6.6). In addition, G-protein coupled receptors (GPCRs) signalling pathway is also involved in cilia disassembly. Upon ligand binding to the GPCR, it increases the concentration of cyclic AMP which leads to the activation of a kinase called protein kinase A. Therefore, protein kinase A phosphorylates another kinase NEK10 (member of the NEK family, essential for cilia assembly). Subsequent degradation of NEK10 with the E3 ligase (CHIP) triggers the disassembly of the cilia (53, 58, 62).

1.2.3. Functions of cilia

Motile cilia are found in a small number of cells in organs such as the middle ear, respiratory tract, the fallopian tubes and the ventricles of the central nervous system. Motile cilia have a rhythmic motion or beating wave by relying on microtubule motor protein. This back and forth coordinated movement helps fluid flow or cell propulsion. Hence, they actually keep the airways clear of mucus at all times, thereby allowing breathing without irritation. Motile cilia in the fallopian tubes help the ovum to move to the site of fertilization. In addition, motile cilia are also associated with sperm motility (61, and 65-67).

Primary cilia have been detected in various types of cells. They are recognized as a major player in a number of organs acting as a sensory antenna of the cell to transmit or receive signals from extracellular environment. Many signalling pathways have been linked to the primary cilia including sonic hedgehog (Shh), wingless/integrated (Wnt), platelet-derived growth factor receptor alpha (PDGFR α), hippo pathway, G-protein coupled receptors (GPCRs) and transforming growth factor beta (TGF- β) (68, 69). For example, it is believed that the primary cilia bend in response to fluid flow which triggers to enhance the intracellular calcium ions. It is known that the members of the polycystin family called PC1 and PC2 are localized at the primary cilia. PC2 is a calcium channel. The bending of the primary cilia results in the opening of PC2 (PC2 is bound to the tail of PC1) channel to increase the calcium ions. Increased concentrations of calcium ions act as a second messenger for several signalling pathways inside the cell. One of the studies found that calcium influx were not observed in primary cilia dependent mechanosensors (70). This group measured the calcium response to fluid flow in the primary cilia in several cell lines including kidney thick ascending tubules and kidney epithelial cells. And they concluded that primary cilia mediated mechanosensation is not via calcium signalling. Moreover, photoreceptor sensory cilia which are equivalent of primary cilia localize to the light sensitive cells (photoreceptor) in the retina. There are two types of photoreceptors called rod and cone and each photoreceptor consists of the outer segment, the inner segment, the nucleus and the short axon. The axoneme of the photoreceptor sensory cilia extends to the outer segment. It is believed that the outer segment provides the structural backbone of the receptor protein rhodopsin (GPCR) required for phototransduction in rod. In response to light, GPCR pathway is activated, which hydrolyzes the second messenger cyclic GMP into 5'-GMP. It

reduces the concentration of cycling GMP in the cell. This phototransduction cascade generates an electrical impulse to mediate the first step in vision (71-73).

1.2.4. Ciliopathies

Ciliopathies are referred to as a group of disorders related to genetic mutations resulting from abnormalities in cilia structure, formation or function. As cilia are found in almost all cells, defects in ciliogenesis lead to a complex set of problems including renal failure, kidney disease, retinal degeneration and cerebral anomalies (74, 75). So far, 187 ciliopathy-associated genes in 35 ciliopathies have been reported. Here are brief descriptions of some of the ciliopathies. Bardet-Biedl syndrome (BBS), where one or more of the subunits in this complex, called the BBSome, are genetically mutated. BBSome is composed of eight subunits including BBS1, BBS2, BBS4, BBS5, BBS7, BBS8, BBS9 and BBIP10. The primary clinical manifestations in BBS are diabetes, polydactyly, renal abnormalities, rod-cone dystrophy and hypogonadism (76, 77). The Joubert syndrome is a rare ciliopathy characterized by ataxia, hypotonia, oculomotor apraxia and irregular beating patterns. As the ciliopathies from different genetic mutations overlap with regards to clinical symptoms, the phenotype of Meckel-Gruber syndrome partially overlaps with the Joubert syndrome. Clinical manifestations of Meckel-Gruber syndrome include cystic dysplastic kidneys, polydactyly, occipital encephalocele and hepatic bile duct proliferation (74). Nephronophthisis (NPHP) is an autosomal recessive ciliopathy causing cystic kidney disease and retinal dystrophy (78). Although the size of the kidney appears normal in nephronophthisis, there is an increased interstitial fibrosis and corticomedullary cyst caused by the disappearance of nephron (79-81). Most of the NPHP genes that produce proteins are localized at the primary cilia, basal body or centrosome. A large number of genes have been implicated in NPHP including mutations in nephrocystin-1, nephrocystin-2 (inversin), nephrocystin-3, nephrocystin-4, nephrocystin-5 (IQCB1), nephrocystin-6 (Cep290), nephrocystin-7 (GLIS2), nephrocystin-8 (RPGRIP1L), nephrocystin-9 (NEK8), nephrocystin-10 (SDCCAG8), nephrocystin-11 (TMEM67/MKS3), nephrocystin-12 (IFT139), nephrocystin-13 (IFT144), nephrocystin-14 (ZNF423), nephrocystin-15 (Cep164), nephrocystin-16 (ANKS6), nephrocystin-17 (IFT172), nephrocystin-18 (Cep83), nephrocystin-1L (XPNPEP3), and nephrocystin-2L (SLC41A1) (79). Based on the abovementioned ciliopathies, it is obvious that the phenotypes of one ciliopathy overlap with one another, and that mutation in the same gene give different clinical symptoms. This might be due to the expression of genes in different tissues, genetic modifiers and types of mutations (81).

As the primary cilia provides a platform for several diverse arrays of signalling pathways, changes in cilia formation, structure and function also lead to many types of cancer. For example, loss of cilia has been associated in breast cancer, glioblastoma, pancreatic cancer and renal cell carcinoma. Moreover, medulloblastoma (brain tumor in children) is favoured in both the absence or presence of the primary cilia depending on the oncogenic initiating events (81-83). In brief, at the first step of Shh signalling, it binds with receptor Ptc1. Therefore, Shh transmits a signal through Smo to regulate the activity of the transcription factor, Gli. There are three types of Gli: Gli1, Gli2 and Gli3. Gli1 acts as a transcriptional activator whereas Gli2 and Gli3 have both activator and repressor functions. Thus, in the presence of Shh, it blocks the Gli3 repressor form to stabilize the Gli2 (activator form) that allows for properly coordinated signalling events. Previously it has been shown that hyperactivation of Shh signalling by constitutively expression of Smo to the primary cilia induce medulloblastoma. They have also shown that medulloblastoma can be induced in the absence of primary cilia in the case of Gli2 activation. The plausible explanation for medulloblastoma formation is the elimination of the Gli3 repressor when primary cilia are removed (83).

1.3. Centrosomal proteins and their functions

The centrosome is considered as the primary microtubule organizing center of the cell and acts as a template to form a cilium. It also plays a crucial role in cell division by forming bipolar mitotic spindle poles, therefore equally segregating the chromosome between the dividing cells. Although this organelle plays an important role in cell biology, many aspects related to its structure, function and assembly are still poorly understood. Previously, several proteomic analyses were performed on isolated human centrosomes and they discovered a group of novel proteins, as well as known centrosomal proteins important for the structure, duplication and assembly of the centrosome (84-86). However, it is difficult to determine the exact number of centrosomal proteins, as mass spectrometry based studies have limited sensitivity to detect transiently associated proteins. In addition, contaminants are also present during isolation of the centrosomes. This is why the Anderson group used protein correlation profiling assay to identify true centrosomal proteins from a vast array of initial proteomic analysis. They further validated their findings based on centrosomal localization by immunofluorescence microscopy. In addition, MiCroKit database provides detailed information for the localization and distribution of centrosomal proteins from seven different model organisms. In this study, they present 1489 MiCroKit proteins, including 677 and 132 entries in human and mouse respectively based on their localization at the centrosome, midbody and kinetochore (87). In this section I will discuss some of the centrosomal proteins that I have studied along with Cep78 and NPHP5 in my thesis (Figure 1.6.7).

1.3.1. Centrin

Several proteins at the distal end of the centriole including the appendages have been identified and characterized. Centrin, also known as caltractin, has been localized to the lumen of the distal end. Centrin was found in both centrioles and procentrioles. Depletion of centrin inhibits centriole duplication and leads to distorted spindle pole formation, suggesting that it plays a central role in centrosome regulation (88-90). Recently it has been reported that a subset of centrin also exists in the cytoplasm and is associated with nuclear pore. Its role is to facilitate the nuclear export of proteins and mRNAs (91).

1.3.2. POC5

POC5 is another centriolar protein that is localized at the distal region of the centriole. It is known that POC5 interacts with centrin. POC5 is absent in the S phase where the new centriole

starts to synthesize (procentriole), but is present from G2 until full maturation. Studies have shown that POC5 has no role in centriole duplication, but it promotes centriolar assembly to form the mature centriole (92, 93).

1.3.3. CP110

Centriolar coiled-coil protein 110 (CP110 or Ccp110) is a cap binding protein that caps the distal end of the centriole. CP110 protein is expressed in high quantities during the G1 to S transition, and starts to reduce at G2/M where the newly formed centriole elongates until it reaches the same size as the existing centriole (8, and 94-96). Depletion of CP110 in the non-ciliated cells increases the length of the centriole suggesting that it regulates the length of the centriole (96-99). It was also reported that CP110 regulates the centrosome duplication and separation in a cyclin-dependent kinase manner (99-101). In ciliated cells, CP110 has unique functions, acting as a negative regulator of ciliogenesis. Loss of CP110 from the mother centriole is crucial for the basal body formation. Once formed, the basal body serves as the template to nucleate the ciliary axoneme (101-104).

1.3.4. Cep97

Cep97, another centriolar distal end protein, was first identified in a proteomic screening for CP110-interacting proteins (102). Cep97 is localized in distal ends in all stages (except in G0, where mother centriole specific Cep97 needs to be removed during cilia formation) of the cell cycle much like centrin. Although CP110 interacts with centrin, Cep97 fails to interact with centrin indicating that CP110 binds with Cep97 in a specific region. Depletion of Cep97 leads to the disappearance and reduction in amount of CP110 in the centrosome. The role of Cep97 is to stabilize the CP110 at the centrosome. Loss of Cep97 also gives the same phenotype much like the depletion of CP110 (8, 102, and 104).

1.3.5. Cep76

Cep76 is another distal end centriolar protein that interacts with CP110. Based on current knowledge, the expression of Cep76 is low in G1, starts to increase from the S to the G2 phase and appears to diminish during mitosis indicating its role in duplication. Depletion of Cep76 increases the number of dots relevant to centriolar proteins including CP110 and centrin, but not PCM proteins (for example γ -tubulin) suggesting the accumulation of centriolar intermediates. In conclusion, the role of Cep76 in the centrosome is to control the copy number of centrioles in cells (105, 106).

1.3.6. γ -tubulin

γ -tubulin localizes at the PCM and is a component of the γ -tubulin ring complex (γ -TuRC). In most cases, PCM is organized around the centrioles during entry into mitosis in a process called centrosome maturation. PCM plays a critical role in nucleating the microtubules through localization and regulation of γ -TuRC. Although the majority of PCM assembles during mitosis, a small amount of PCM is also recruited during interphase. Thus, it is plausible that centrosome maturation leads to the organization of a lot of microtubules during mitosis, hence properly enhancing the spindle function (22, and 107-109).

1.3.7. DA proteins

DAs are thought to be nine sets pinwheel-like structures protruding from the distal periphery of the mother centriole. DAs are composed of five core components and they are Cep164, Cep89 (ccdc123), Cep83 (ccdc41), SCLT1 and FBF1. Depletion of Cep83 disrupts the localization of the rest of DA components. It suggests that the hierarchy of DA assembly is regulated by Cep83, which is further divided into two branches through Cep89 and SCLT1. Further downstream, FBF1 and Cep164 branch out from SCLT1. Previous studies revealed that DA plays a role in docking the basal body to the cell membrane and thereby in ciliogenesis (110). TFs are the propeller like structures and are thought to originate from DAs. TF protein Cep164 recruits a kinase TTBK2 which in turn removes the centriolar cap binding protein CP110. It is a prerequisite to initiate the ciliary events (111-114). Both structures share some proteins such as Cep164 is localized in both DAs and TFs, whereas TTBK2 resides only in TFs.

1.3.8. SDA proteins

Another important feature of the mother centriole is the presence of SDAs which are located at the distal region (114). It has been shown that DAs are important for ciliogenesis, while SDAs are for microtubule anchoring and ciliogenesis. Several candidates that form the key structure of SDAs have been identified, but the exact mechanism of their assembly is poorly understood.

Previously described kinesin-2 motor protein (Kif3a) interacts and recruits the SDA component p150^{Glued} which in turn recruits ninein. As cilia lack the protein synthesizing machinery, proteins need to be transported from elsewhere in the cell. Kif3a is involved in the transport of the IFT complex to build the ciliary axoneme (115, 116). p150^{Glued} is considered as the largest component of dynactin protein complex. It also localizes at the SDAs of the mother centriole. p150^{Glued} is required for microtubule anchoring (117, 118), whereas, ninein localizes at

the proximal end of the centrioles, as well as at the SDAs of the mother centriole. It is known to act as a microtubule anchoring protein (119). Likewise, the staining associated with well characterized SDA protein ninein diminishes during kif3a depletion. Another SDA component, ODF2 is also required to recruit ninein. Further studies showed that ODF2 and ninein staining were much reduced in the absence of another established SDA protein, Cc2d2a (120). Recently, two new SDA components were identified, CCDC120 and CCDC68 at the centrosome. Both of these proteins are reported to interact with ODF2. CCDC68 is not recruited to the SDAs directly by ODF2, but it interacts and competes with CCDC120 to recruit Cep170 (known SDAs) at the centrosome (121). Trichoplein (TCHP) is a protein that is also considered as SDA protein and is a negative regulator of ciliogenesis. It is present in both mother and daughter centrioles and the mother centriole specific TCHP must be removed to form cilia (122). Based on literature reviews, it is obvious that there are several hierarchies of SDAs assembly processes. Altogether, how they contribute to the maintenance of functional SDAs is poorly understood. Surprisingly, the loss of SDA proteins has failed to anchor microtubules and ciliogenesis in some cases. BF is the equivalent structure of SDAs and it has been reported that there are always 9 SDAs. Whereas, the number of BF is not the same, and is larger in size depending on the nature and types of cilia. For example, one basal foot is formed in the motile cilia and BF can vary from 2 to 5 in primary cilia (114, and 123-126). Both structures share some proteins such as kif3a and ODF2 are localized in both SDAs and BF, whereas TCHP resides only in SDAs.

1.3.9. C-Nap1

C-Nap1 localizes at the proximal region of the centriole and participates in linking the mother and daughter centrioles in a cell cycle dependent manner (2, 19). This linker must be dissolved to form the two distinct centrosomes which are regulated by a kinase NeK2. In brief, NeK2 phosphorylates C-Nap1 leading to their removal from the centrosome. The untethered centrosomes are separated into two individual ones by a kinesin related motor protein called, Eg5 (10, 19 and 20).

1.3.10. Cep78

Before I started working on the Cep78 project there were no comprehensive studies on this particular centrosomal protein. Cep78 was first identified by proteomic screening of the isolated centrosome (84). While its structure is known to consist of 6 leucine rich repeats (LRR) and one coiled-coil (CC) domain, the role of Cep78 is not understood. It is 722 amino acids long, has a

molecular weight of 78 kDa, and is located on c chromosome 9q2r. Previous studies have suggested that Cep78 interacts with other centrosomal proteins involved in centrosome duplication and ciliogenesis (127, 128), such as Cep78 interacts with the polo like kinase-4 (PLK4) through its N-terminal region and is also colocalized with PLK4 at the centrosome. From the literature review, we know that PLK4 is involved in centrosome duplication and the interaction between Cep78 and PLK4 is necessary to regulate the duplication process (15, 129). Other studies have screened a group of patients who have been suffering from cone-rod degeneration (CRD), a rare ciliopathy. They found that *Cep78* gene was mutated and the disease was characterized by deafness and blindness. They studied two families who had been suffering from symptoms including retinal degeneration causing severe central vision loss. After sequencing, they found that the *Cep78* gene is mutated in both of these families. According to their studies, Cep78 was located on the inner segment of the retinal photoreceptor, cone and at the base of primary cilia in fibroblasts. In addition, Cep78 interacts with another ciliary protein, called FAM161A, whose loss is also associated with retinal degeneration (130, 131). Cep78 also plays a role in the progression of colorectal cancer (CRC). CRC is the most prevalent cancer worldwide and is a combination of activation and inactivation of oncogene and tumor suppressor gene respectively. The authors showed in different patient samples that the mRNA level of Cep78 was decreased. On the other hand, the overexpression of Cep78 inhibits the growth and proliferation of CRC, making it a potential marker to diagnose CRC in the future (132). Cep78 protein is also known to play a role in prostate cancers associated with autoantigen reactivity (133). Prostate cancer patients treated with radiotherapy or neoadjuvant hormone therapy induce expression of tumor specific immune responses. Therefore, immunoscreening of cDNA provides evidence of several antigens recognize by treatment related autoantibodies and Cep78 is one of them.

1.3.11. NPHP5

NPHP5 was identified as a causative gene of ciliopathies (78). NPHP5 is 598 amino acids long and is localized at the centrosomal distal region of the centriole (134). It was shown that NPHP5 interacts with another ciliopathy protein Cep290. The interaction between Cep290 and NPHP5 is required for ciliogenesis as depletion of NPHP5 gives the same phenotypes as found in Cep290 depletion. NPHP5 also has a role in controlling the integrity of a multisubunit complex called the BBSome (134, 135). As mentioned earlier, BBSome is composed of eight

subunits (BBS1, BBS2, BBS4, BBS5, BBS7, BBS8, BBS9 and BBIP10) organized in a hierarchical manner. The role of BBSome in cilia is trafficking the subsets of membrane proteins. IFT is responsible for transporting BBSome at the ciliary tip in an anterograde direction and back to the basal body in retrograde (75-77). Depletion of NPHP5 affects the localization of BBS2 and BBS5 in the cilia whereas other BBSome subunits remain unaffected. This suggests that the integrity of BBSome is regulated by NPHP5 during ciliogenesis (135). Experimental evidence indicates that NPHP5 is regulated by the ubiquitin E3 ligase BBS11 and deubiquitinase USP9x in a cell cycle dependent manner. In G0, G1, S and G2, NPHP5 recruits a pool of cytoplasmic USP9x into the centrosome and USP9x protects NPHP5 from ubiquitination. In mitosis, USP9x is mislocalized from the centrosome which allows BBS11 to ubiquitinate NPHP5 (136). Due to the ubiquitination of NPHP5 by BBS11, the centrosomal localization of NPHP5 is affected. As NPHP5 is required for the early events of ciliogenesis, the delocalization of NPHP5 might lead to the removal of downstream events in cilia assembly.

1.4. Vpr

HIV-1 is one of the most dangerous pathogenic viruses which preferentially infect T cells (expressing high levels of CD4 and CCR5, especially in memory T cells). In brief, to infect the T lymphocytes, HIV-1 must first come into contact with co-receptors, either CCR5 or CXCR4, and then with CD4 receptor which causes the HIV-1 envelope to fuse with the cell membrane and gain entry into the cell. Once inside the cell, it releases the viral RNA, which is reverse transcribed into double stranded DNA. HIV-1 enzyme integrase promotes integration of the viral double stranded DNA into the host genome. Therefore, the host machinery creates the long chain of HIV-1 proteins, which is the building block of more mature HIV-1. Then, they assemble and exit the cell, upon which they are processed by viral protease to become mature HIV-1. This makes the mature HIV-1 ready for another round of infection (137-139). There are at least nine proteins in the HIV-1 genome that can be divided into three subgroups: 1) structural proteins such as Gag, Pol and Env, 2) regulatory proteins such as Tat and Rev and 3), as well as accessory proteins Vpr, Vpu, Vif and Nef (140, 141).

Here, I will discuss one of the HIV-1 accessory proteins: viral protein R (Vpr). Vpr is a multifunctional accessory protein which is critical for the development of efficient viral infections. Vpr is 96 amino acids long, and a 14KDa protein (141, 142). Vpr mediates several functions including: facilitating the transport of the viral genome with the preintegration complex (PIC) to the nucleus, induction of G2/M arrest, modulation and coactivation of apoptosis in both host and viral genes, regulation the nuclear factor kappa B, as well as activation of HIV-1 long terminal repeats (142-144). Vpr also interacts with the ubiquitin E3 ligase to ubiquitinate the substrate and alter substrate activity or stabilization. For example, Vpr binds with HECT E3 ligase to load more substrate, TERT (catalytic subunit of telomerase) onto the complex. In the presence of Vpr, ubiquitination of TERT is increased and is degraded, suggesting that Vpr negatively regulates the telomerase activity. The TERC-RNA template and TERT-reverse transcriptase are the components of telomerase. Loss of telomerase gradually leads to growth arrest and cell death (145, 146).

It is thought that centrosome polarization controls the positioning and movement of various molecules between immune cells to generate a better immune response. The human immune system is composed of different cell types to protect against infection and disease. For example, CD4 T cells release cytokine during an immune response (147, 148). On the other

hand, cytotoxic T- lymphocytes (CTL) release lytic proteins to kill infected cells. These immune cells typically interact with other cells called antigen-presenting cells (APCs) to function properly. Most of the interaction is based on receptor-mediated recognition (for example, by T cell receptors (TCRs) in T cells) followed by changes in protein organization and cell morphology. The membrane proteins between cell-to-cell contact sites are supposed to remodelled into a distinct arrangement typically referred as an immunological synapse (147, 148). Given that cell polarization and migration are significant during the immune response, and centrosome-mediated microtubules organization plays an important role in these processes. Centrosome positioning in the migratory T cells differs from other migratory cells, which are at the back and are called uropod. Thus, T cells always move with the nucleus at the front. During antigen recognition, cells are supposed to halt their movement and form a stable contact (cell-to-cell) with their target. At this point, positioning of the centrosome within the migratory T cell changes and move back at the front to reorganize the formation of cell-to-cell contact with the target, production of cytokine and their release of cytotoxic components (147, 149). The centrosome also docks at the plasma membrane during ciliogenesis where the mother centriole is converted into a basal body from where the ciliary axoneme extends. Although centrosome docking at the T cell seems like the docking of the basal bodies to the cell cortex during ciliogenesis, it is reported that cilia do not form in T cells. Another group also showed that cilia are formed in T cells, but they are fewer in number (147, 150).

1.5. Ubiquitylation as a mode of protein regulation in centrosome and cilia formation

The centrosome duplicates in a coordinated manner with the cell cycle. The number of centrioles is tightly controlled so that the centrosome duplicates only once per cell cycle with two centrioles per centrosome. Defects in centrosome regulation can lead to issues such as inappropriate chromosome segregation which plays a role in human diseases. It is important to focus on the mechanisms regulating centrosome structure, function and cycle in order to understand the findings in centrosome biology. Complex sets of protein networks are involved in maintaining the number and structure of the centrosome in each cell. The necessary modifications of proteins in these networks are controlled by posttranslational modifications such as ubiquitination, acetylation, phosphorylation, deubiquitination and sumoylation (146, 151).

As my thesis project is based on ubiquitination, I will briefly discuss protein ubiquitination. Ubiquitination is an intracellular protein modification system that gives a versatile molecular signal to their substrate leading to their final outcome. Ubiquitin is a 76 amino acids long protein that is brought to the substrate through an enzymatic cascade including (1) activating enzyme E1, (2) conjugating enzyme E2, and (3) ubiquitin ligase E3. There is a small number of E1 (about ten), over a hundred of E2, and more than a thousand of E3 in the human body. Initially, ubiquitin molecules are attached to activating enzyme E1 in an ATP dependent manner by forming a thiol-ester bond with the c- terminal end of glycine residue of ubiquitin. The activated ubiquitin is then transferred to the catalytic cystic residue of the conjugating enzyme E2. In the last step of the cascade, ubiquitin linked E2 associates with ubiquitin E3 ligase. Thereafter, ubiquitin is covalently attached to the lysine residue of the substrate depending on the type of ubiquitin E3 ligase (152) (Figure 1.6.8).

There are three major classes of ubiquitin ligases, also called E3 ligases, which have been described. They differ in how ubiquitin molecules are transferred to the substrate. The first one is called RING type (*R* really *I* nteresting *N* ew *G* ene) E3 ligase. The RING E3 ligase has a coordinated organization in which members of the cullin group of scaffold proteins bind with the RING containing catalytic subunit Rbx1 or Rbx2 (also called Roc1 or Roc2), and with the adaptor protein. For example, DDB1 is the adaptor protein for Cullin4 E3 ligase that directly binds with the substrate recognition subunit viral protein R-binding protein (VprBP) in this case. In RING type E3 ligase, the ubiquitin linked E2 associates with the E3 ligase and then directly

transfers to the substrate. Whereas in HECT (*homologous to E6-AP carboxy terminus*), the second type of E3 ligase, ubiquitin linked E2 associates with E3 ligase as usual, and undergoes a trans-thioesterification at an active cysteine residue in the HECT E3 ligase before being transferred to the substrate. For instance, the HECT family contains: EDD, kinase DYRK2, adaptor protein DDB1, and substrate recognition subunit VprBP. In brief, the substrate is recognized by VprBP and phosphorylated by DYRK2. The Ubiquitin molecule is then transferred by EDD to the substrate (153). The third type of E3 ligase is RBR (RING-in-Between-RING) E3 ligase. It is a kind of middle E3 ligase that shares common features with RING and HECT types of E3 ligases. RBR is characterized by a RING1 domain used for E2 binding, and a second domain called RING2 that contains active cysteine residue to form a covalent intermediate before being transferred to the substrate (154) (Figure 1.6.8).

Ubiquitination can be mono, di, tri or polyubiquitination, depending on the addition of ubiquitin molecules onto the specific lysine residues (K6, K11, K27, K33, K48, and K63). The final fate of the substrate depends on the type of chain that is formed. It has shown that to target proteosomal degradation, 4 ubiquitin molecules are required. For example, ubiquitin chains are formed through K48, trigger proteosomal degradation. Although a single ubiquitin molecule is attached to the substrate in monoubiquitination, there is evidence that monoubiquitination also undergoes protein degradation (155-160).

1.6. Figures

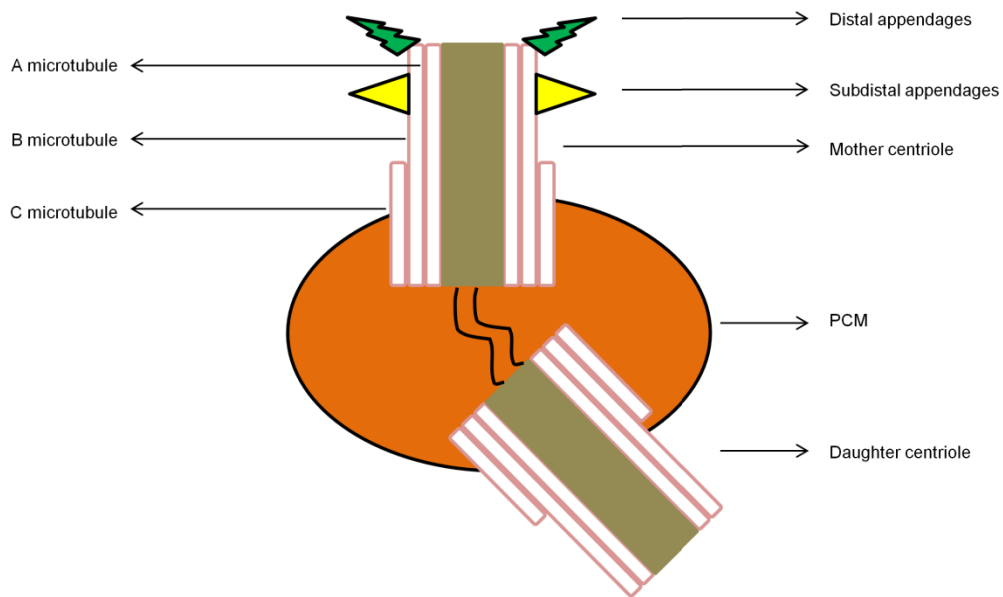


Figure 1.6.1. Centrosome structure

Schematic representation of a centrosome. It consists of two centrioles called mother (three parallel open lines with two protrusions at the top) and daughter (three parallel open lines) surrounded by a PCM (orange oval shape). The mother centriole has DA (black blade like protrusion filled with green color) and SDA (black triangular protrusion filled with yellow color) which is absent in the daughter centriole. Each centriole is characterized by precise nine triplet microtubules (marked by A, B and C).

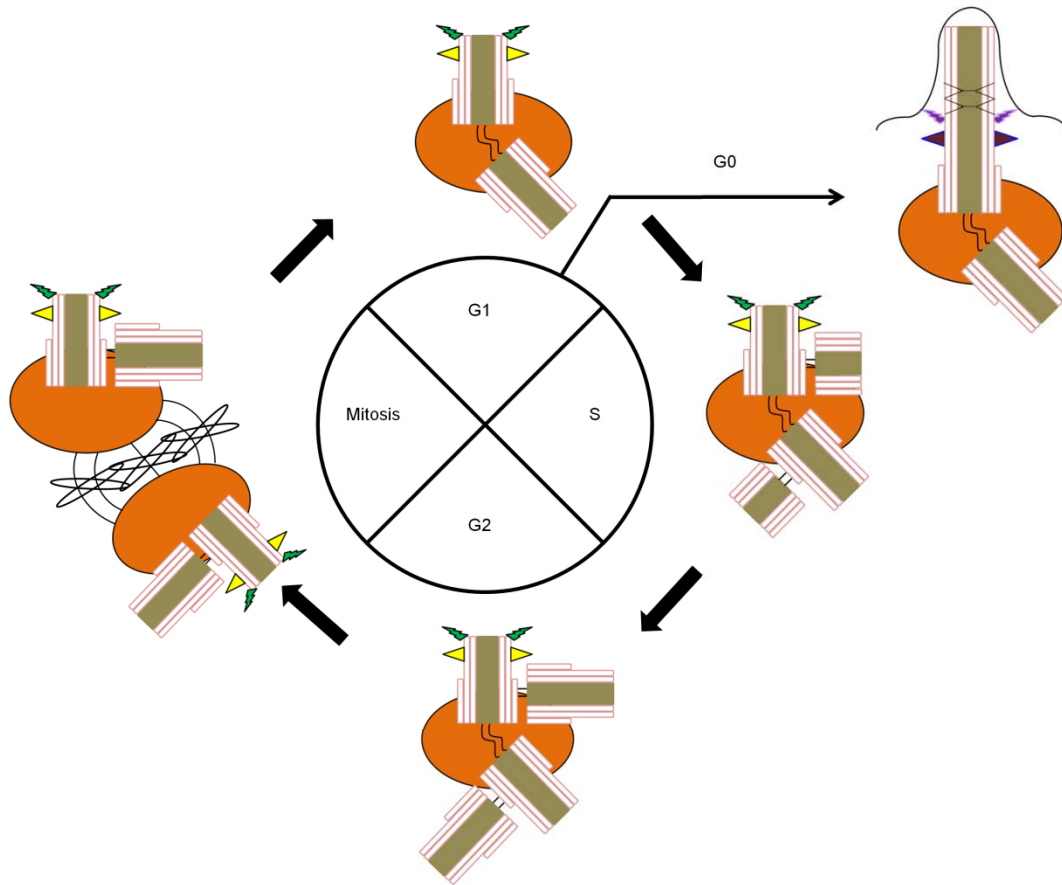


Figure 1.6.2. Centrosome cycle

In G1 phase, centrosome possesses mother (three parallel open lines with two protrusions at the top) and daughter centrioles (three parallel open lines) embedded by a PCM (orange oval shape). Upon disengagement of mother and daughter centrioles at the end of mitosis allow them to duplicate. Procentrioles (small perpendicular to the existing one) are formed in S phase which is tightly attached with the existing one. Subsequently the procentrioles elongate and mature into daughter centrioles whereas the daughter centriole in G1 phase matures into a mother centriole by acquiring DAs and SDAs in S and G2 transition. At the onset of mitosis, the centriole accumulates more PCM, centrosomes segregate and move to the opposite poles. Each cell can then enter into the G1 phase at the end of mitosis or exit to the cell cycle where cilia are formed.

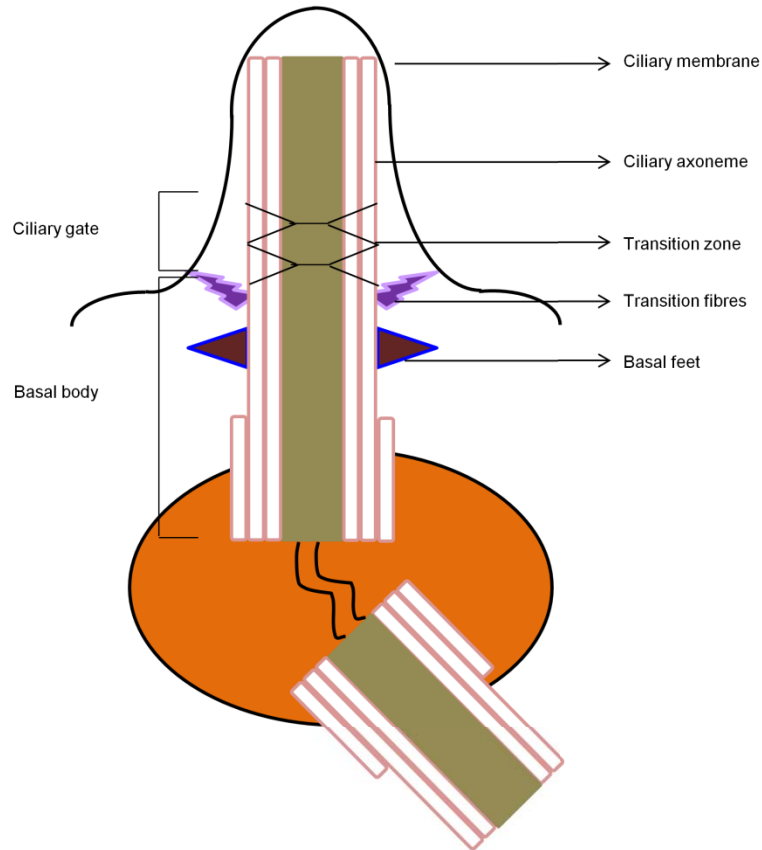


Figure 1.6.3. Structure of a cilium

The basal body (three parallel open lines with pink blade like protrusion filled with purple color and blue triangular protrusion filled with dark brown color at the middle typified by TF and BF respectively) is located at the base of a cilium. The axoneme (two parallel open lines starting from the TF), the ciliary membrane (black surface covering the axoneme) and the transition zone (black Y shape) are the basic structure of a cilium.

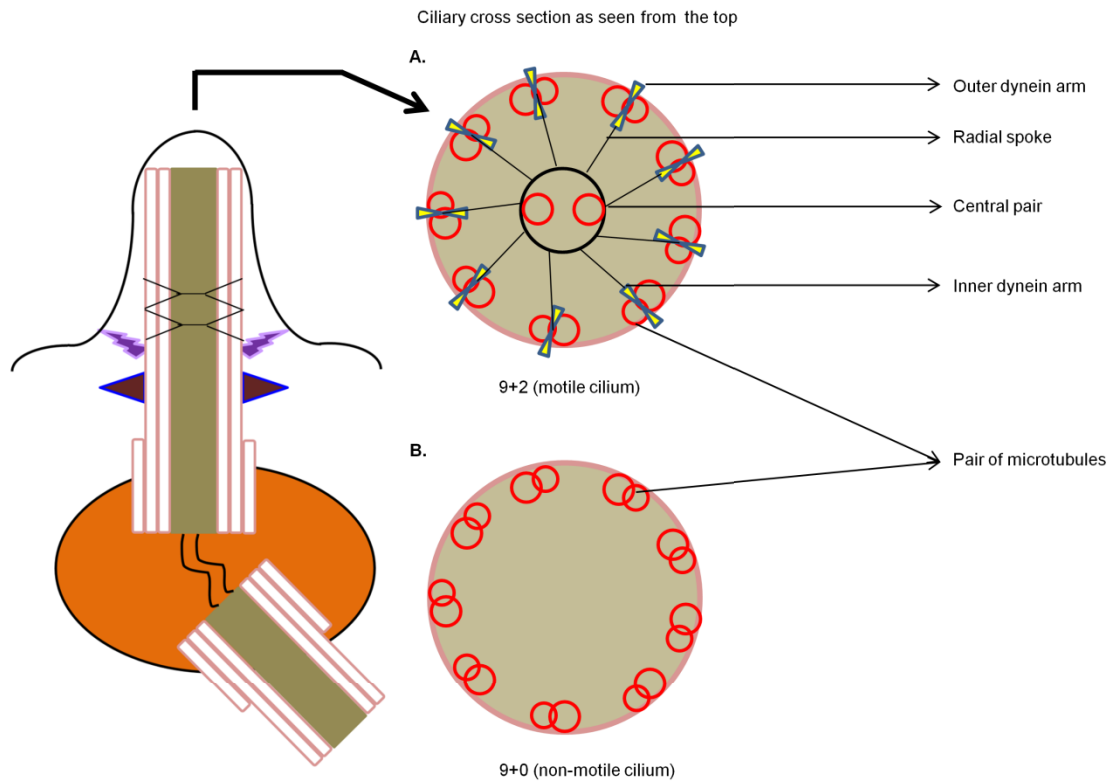


Figure 1.6.4. Types of cilia

Schematic representation of crosssection of motile and non-motile ciliary axoneme. Motile cilia (A) consist of nine outer pair of microtubules (two red circles) along a central pair of microtubules (two red circles inside the black circle at the center). Motile cilia also have inner and outer motor proteins dynein (blue triangular filled with yellow color) and radial spokes (black line connecting the outer microtubules to the central pair). Whereas non-motile cilia (B) consist of nine outer pair of microtubules (two red circles).

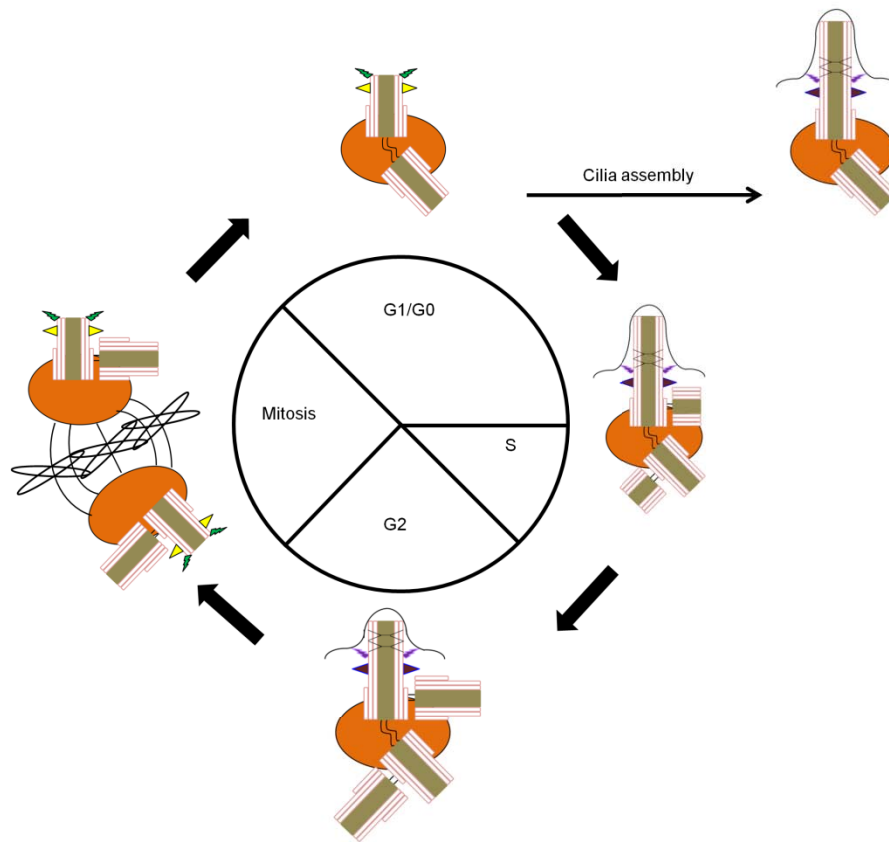


Figure 1.6.5. Cilia and cell cycle progression

To form a cilium, mother centriole needs to be converted to a specialized structure called the basal body. Thereafter, the basal body serves to nucleate the ciliary axoneme. Although cilia formation is typically favoured in G0, it also assembles in G1, S and G2. But in mitosis, cilia are completely disassembled.

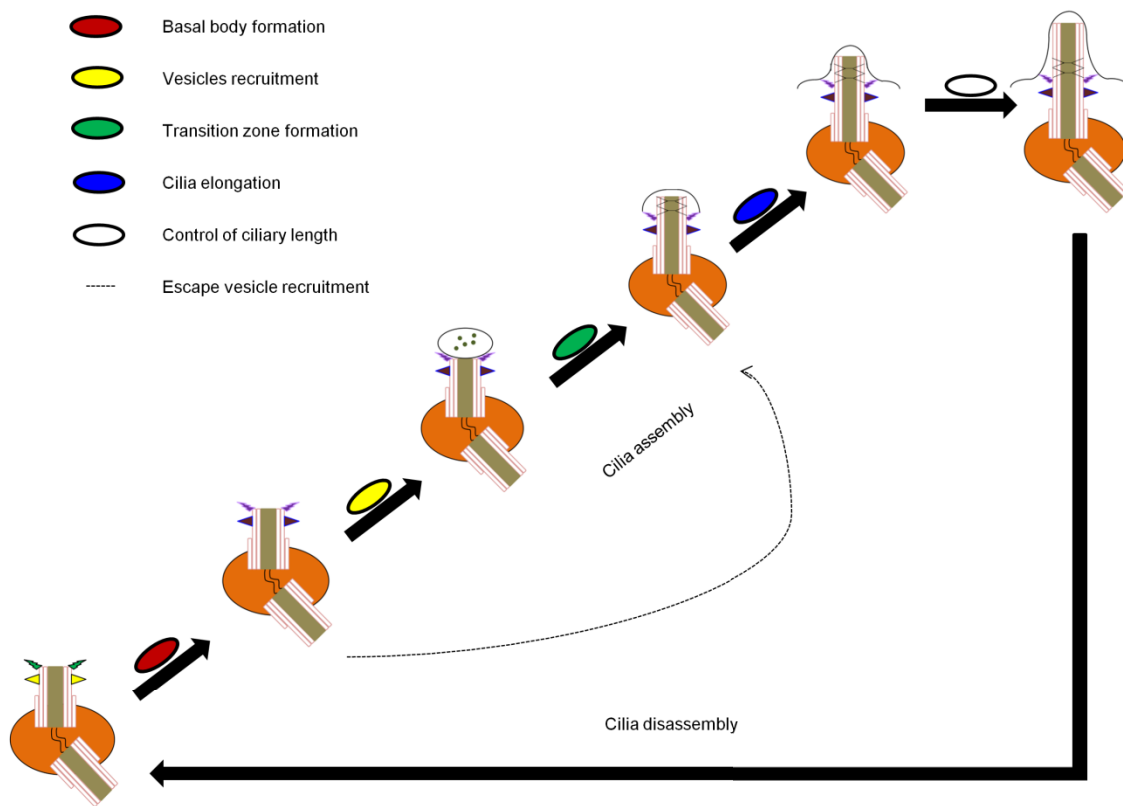


Figure 1.6.6. Cilia assembly and disassembly

There are several steps to assemble the cilia including the basal body formation (black oval shape filled with red color), vesicles recruitment (black oval shape filled with yellow color), transition zone formation (black oval shape filled with green color), elongation of ciliary axoneme (black oval shape filled with blue color) and control of the ciliary length (black oval shape filled with white color). Although primary cilia follow the abovementioned events, motile cilia escape the vesicles recruitment. Thereafter they follow the rest of the steps (indicated by dash arrow). Disassembly of the cilia involves the reverse process.

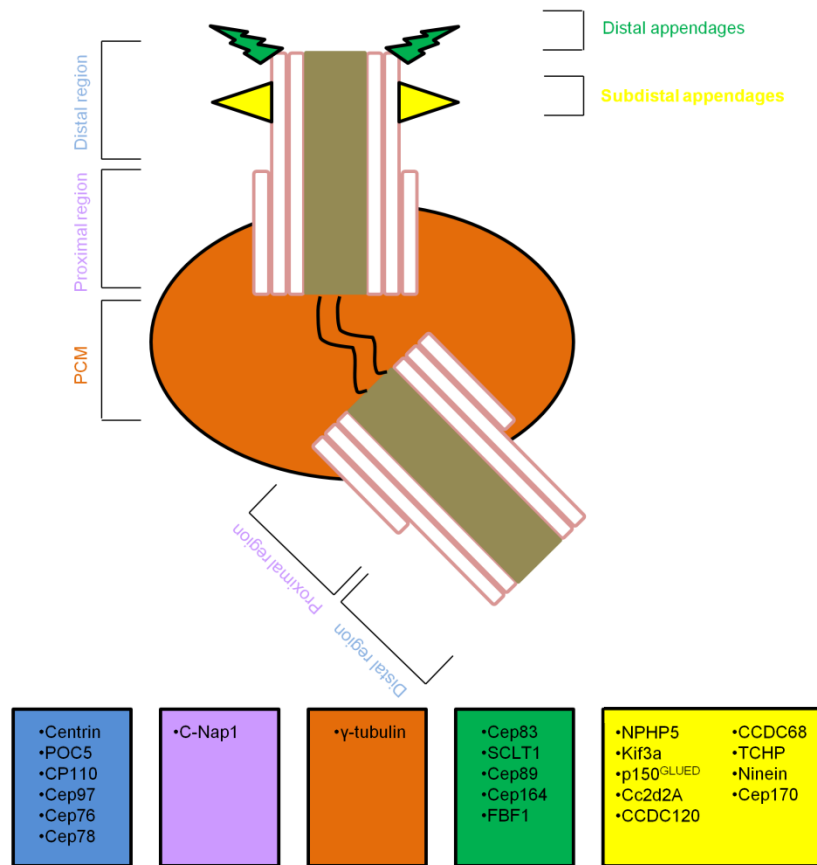


Figure 1.6.7. Structural components of the centrosome

Schematic representation of different sub-structures of the centrosome and their core components. They are distal region (black rectangular shape filled with blue color), proximal region (black rectangular shape filled with pink color), PCM (black rectangular shape filled with orange color), DAs (black rectangular shape filled with green color), and SDAs (black rectangular shape filled with yellow color).

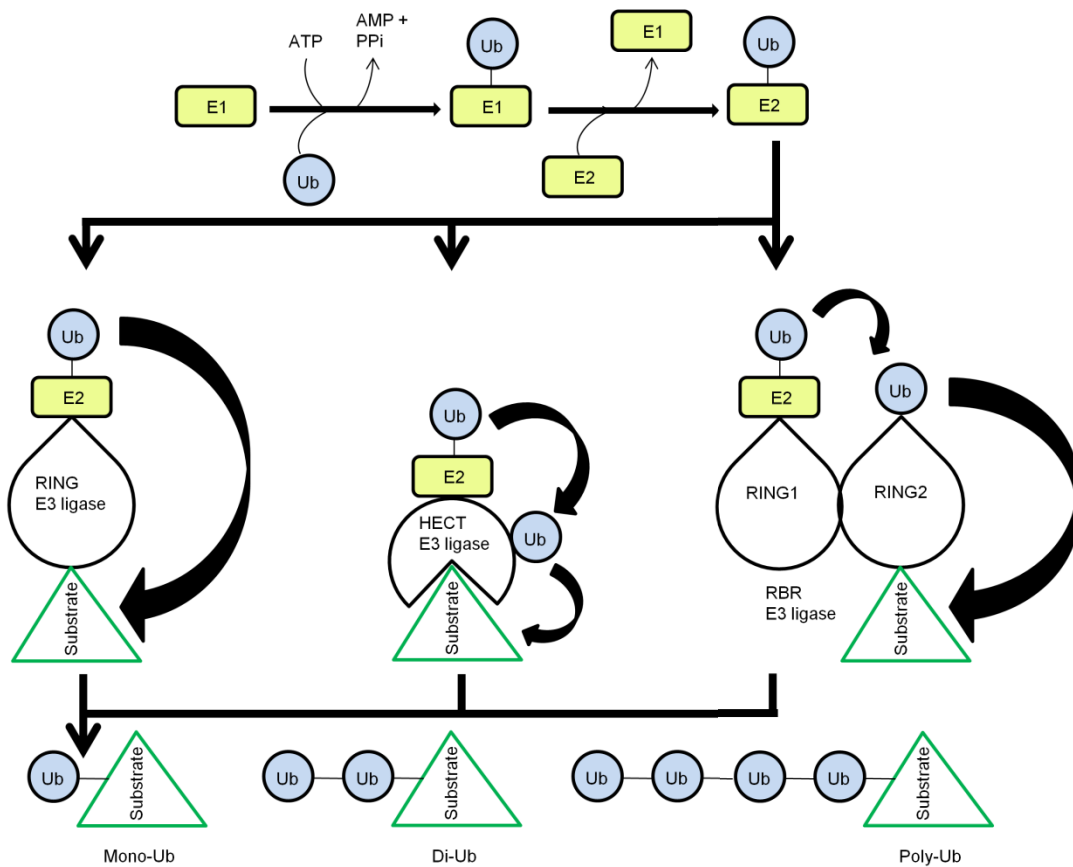


Figure 1.6.8. The ubiquitination system

Ubiquitin (Ub) is activated by an ubiquitin activating enzyme E1 in an ATP dependent manner which is then transfer to the ubiquitin conjugating enzyme E2. The ubiquitin conjugated E2 is then joins to the ubiquitin ligase E3. There are three types of E3 ligases which allow the adding of the ubiquitin molecule into the substrate. In RING E3 ligase, E2-Ub associates with the ligase and then ubiquitin is directly transferred to the substrate. Whereas E2-Ub first joins with the HECT E3 ligase and form a covalent intermediate before being transfer to the substrate. In case of RBR E3 ligase, ubiquitin conjugated E2 joins to the RING1 domain and then form a covalent intermediate with RING2 domain. This allows the transfer of ubiquitin molecule to the substrate. Monoubiquitination is the addition of a single ubiquitin molecule to the substarte. Subsequent addition of ubiquitin molecules to the substarte might be di-ubiquitination, tri-ubiquitination (not shown) or polyubiquitination.

Chapter 2

Cep78 controls centrosome homeostasis by inhibiting EDD-DYRK2- DDB1^{VprBP}

Delowar Hossain^{1,2}, Yalda Javadi Esfehiani^{1,3}, Arindam Das^{1,3} and William Y. Tsang^{1,2,3,*}

¹ Institut de recherches cliniques de Montréal, 110 avenue des Pins Ouest, Montréal, Québec H2W 1R7, Canada

² Division of Experimental Medicine, McGill University, Montréal, Québec H3A 1A3, Canada

³ Faculté de Médecine, Université de Montréal, Montréal, Québec H3C 3J7, Canada

* To whom correspondence should be addressed: william.tsang@ircm.qc.ca

Phone: 1 (514) 987-5719

Fax: 1 (514) 987-5685

Keywords: centrosome/Cep78/E3 ligase/inhibitor/ubiquitin

Running title: Cep78 regulates centrosome homeostasis

2.1. Preface

In chapter 2, I characterized a novel centrosomal protein Cep78 whose function was poorly understood. Here, I confirmed the localization of Cep78 at the centrosome and did a proteomic screen for Cep78 interacting proteins. Furthermore, the interaction between Cep78 and the candidates from the proteomic screen were confirmed by immunoprecipitation/western blot and their role in centrosome homeostasis were elucidated.

2.2. Abstract

The centrosome plays a critical role in various cellular processes including cell division and cilia formation, and deregulation of centrosome homeostasis is a hallmark feature of many human diseases. Here, we found that centrosomal protein of 78kDa (Cep78) localizes to mature centrioles and directly interacts with viral protein R binding protein (VprBP). Although VprBP is a component of two distinct E3 ubiquitin ligases, EDD-DYRK2-DDB1^{VprBP} and CRL4^{VprBP}, Cep78 binds to EDD-DYRK2-DDB1^{VprBP} only. Cep78 is an inhibitor but not a substrate of EDD-DYRK2-DDB1^{VprBP}. A pool of EDD-DYRK2-DDB1^{VprBP} is active at the centrosome and mediates ubiquitination of a novel centrosomal substrate CP110. De-regulation of Cep78 or EDD-DYRK2-DDB1^{VprBP} perturbs CP110 ubiquitination and protein stability, thereby affecting centriole length and cilia assembly. Mechanistically, ubiquitination of CP110 entails its phosphorylation by DYRK2 and binding to VprBP. Cep78 specifically impedes the transfer of ubiquitin from EDD to CP110 without affecting CP110 phosphorylation and binding to VprBP. Thus, we have identified Cep78 as a new player that regulates centrosome homeostasis by inhibiting the last step of an enzymatic reaction catalyzed by EDD-DYRK2-DDB1^{VprBP}.

2.3. Introduction

The centrosome is the major microtubule-organizing center in most eukaryotic cells and controls a number of cellular processes including cell division, cell shape, motility and polarity, and cilia formation (1). Beginning in G1 phase, a cell possesses one centrosome comprising two centrioles, the mother and daughter centrioles, embedded in the pericentriolar material (PCM) (2). Centrosome duplication commences in S phase, wherein a new centriole or procentriole grows perpendicularly at the proximal end of each existing centriole. Procentrioles elongate in S and G2 phases, while the daughter centriole matures into a mother centriole. At the same time, parental centrioles recruit and accumulate increasing amounts of PCM. Two functional centrosomes, fully capable of nucleating and organizing microtubules, are formed at the G2/M phase. At the onset of mitosis, the two centrosomes separate, migrating to the opposite end of a cell and establishing the mitotic spindle. These events ensure accurate chromosome segregation and allow each of the two incipient daughter cells to receive a diploid set of DNA along with a single centrosome. When a cell exits the cell cycle and enters the G0 phase, the centrosome migrates to the cell cortex where the mother centriole templates the assembly of a cilium, a cellular antenna critical for locomotion and sensation (3). Because centrosome duplication occurs once per cell cycle, the number of centrosomes in a cell is under strict control. Defects in centrosome duplication or function can give rise to human disorders such as cancer, ciliopathies and microcephaly (4-7).

The molecular makeup of the centrosome is complex, consisting of hundreds of proteins as revealed by recent bioinformatic, genomic, transcriptomic and proteomic studies (8-10). Centrosomal protein of 78 kDa (Cep78) was first discovered as a novel component through proteomic analysis of isolated centrosomes (9). Human full-length Cep78 is composed of 722 amino acids and possesses a putative coiled-coil (CC) domain and a leucine-rich repeat (LRR) domain with 6 consecutive LRR repeats. De-regulation of *Cep78* causes retinal degeneration and hearing loss (11-13), and is associated with prostate and colorectal cancer (14,15). The *Cep78* gene is found in ciliated organisms but absent from non-ciliated organisms, suggesting that the encoded product could be involved in cilia biogenesis and/or function (16). Another recent study shows that Cep78 is involved in regulating centrosome duplication (17). Despite these observations, the biological function of Cep78 remains poorly characterized.

Ubiquitination is common mechanism for regulating protein stability and function (18). The process of ubiquitination is controlled by three main classes of enzymes wherein ubiquitin (Ub) is transferred from an activating enzyme E1 to a conjugating enzyme E2 and finally to lysine residue(s) of the target substrate via a ligating enzyme E3. E3 ligases are responsible for substrate recognition and can be categorized into three types, really interesting new gene (RING), homologous to the E6AP carboxyl terminus (HECT) and RING-between-RING (RBR), depending on the presence of functional domains and the mechanism of Ub transfer to the substrate (19). Given that deregulation of some E3 ligases is associated with cancer, it is therefore critical to understand how their activities are controlled at the molecular level. The connection between Cep78 and protein ubiquitination is unknown.

In this study, we identified Cep78 as playing a role in controlling protein ubiquitination at the centrosome. We found that (1) Cep78 mostly associates with parental centrioles; (2) Cep78 directly interacts with viral protein R binding protein/DDB1 and Cullin4-associated factor 1 (VprBP/DCAF1), a subunit of two distinct E3 ligases: the HECT-type EDD-DYRK2-DDB1^{VprBP} consisting of EDD, DYRK2, DDB1 and VprBP, and the RING-type CRL4^{VprBP} consisting of Roc1, Cullin4A, DDB1 and VprBP (20); (3) Cep78 specifically interacts with EDD-DYRK2-DDB1^{VprBP}; (4) Cep78 is not a substrate of EDD-DYRK2-DDB1^{VprBP}; (5) Cep78 inhibits EDD-DYRK2-DDB1^{VprBP}; (6) a fraction of EDD-DYRK2-DDB1^{VprBP} is present at the centrosome and mediates ubiquitination of a novel substrate CP110; (7) de-regulation of Cep78 or EDD-DYRK2-DDB1^{VprBP} alters CP110 ubiquitination, thereby disrupting protein stability and cellular processes that are dependent on CP110. Finally, we dissected the molecular mechanism by which Cep78 inhibits ubiquitination of CP110.

2.4. Results

2.4.1. Cep78 localizes to parental centrioles and is periodically expressed in the cell cycle

We previously used a combination of biochemistry, cell biology and proteomics to characterize Cep76, a protein that suppresses centriole amplification (21,22). During the course of these studies, we identified Cep78 from a proteomic screen for Cep76-interacting partners. The interaction between Cep78 and Cep76 was subsequently confirmed by immunoprecipitation (IP)/Western blot (WB) (Figure 2.11.1A). Furthermore, both recombinant and endogenous Cep78 associated with a known Cep76-interacting protein CP110 (22) (Figures 2.11.1A and 2.11.2A). By transfecting a plasmid expressing Flag-tagged Cep78 into normal diploid RPE-1 cells and performing immunofluorescence (IF) experiments, we found that the staining of recombinant Cep78 overlaps with a distal centriolar marker CP110 but not with a proximal centriolar marker C-Nap1 (Figure 2.11.1B). Likewise, IF experiments performed with an anti-Cep78 antibody revealed that endogenous Cep78 co-localizes with a distal centriolar marker centrin but not with C-Nap1 or another proximal marker glutamylated tubulin (GT335) (Figure 2.11.1C). A second anti-Cep78 antibody also exhibited staining that overlapped with centrin (Figure 2.11.3A). Cep78 is an intrinsic component of centrosomes since its localization was not affected by treatment with nocodazole, a microtubule-depolymerizing drug (Figure 2.11.3B). Examination of endogenous Cep78 staining pattern at different stages of the cell cycle revealed one bright dot or two dots, one bright and one weak, in G0 cells (Figure 2.11.1D). The bright dot is always associated with the mother centriole able to template a cilium (Figure 2.11.1C). This staining pattern of Cep78 remains unchanged in G0, G1 and S phases (Figure 2.11.1D). In late G2 and M phases, two additional weak dots, presumably associated with maturing procentrioles, could be detected occasionally (Figure 2.11.1D). By quantifying the intensity of Cep78 IF in the vicinity of centrosomes, we showed that the Cep78 signal is low in G0 and G1, increases in S and G2, and diminishes in M phase (Figure 2.11.1E). Similarly, Cep78 protein levels were low in G0 and G1, increased in G1/S, peaked in S and G2, and decreased in M and the next G1 phase (Figure 2.11.1F). Cep78 IF and WB signals were greatly diminished in Cep78-depleted cells (Figures 2.11.3C-D), indicating that our antibody specifically recognizes endogenous Cep78. Taken together, our data suggest that Cep78 is a distal centriolar protein primarily associated with parental centrioles and that it may function in late G1, S and G2 phases.

2.4.2. Cep78 specifically interacts with the EDD-DYRK2-DDB1^{VprBP} E3 ligase at the centrosome

To obtain insights into the biological relevance of Cep78, we performed a proteomic screen for Cep78-interacting partners. We identified three putative partners--EDD, DDB1 and VprBP (Figure 2.11.4A)--components of EDD-DYRK2-DDB1^{VprBP} (23). Because the highest number of peptides recovered in our mass spectrometric analysis besides Cep78 corresponded to VprBP, we first tested and confirmed the interaction between endogenous Cep78 and VprBP in multiple cell lines, including HEK293, HeLa and RPE-1 (Figure 2.11.5A). To further explore whether Cep78 binds to EDD-DYRK2-DDB1^{VprBP}, we transfected a plasmid expressing Flag-Cep78 into cells, performed anti-Flag IPs, and showed that Flag-Cep78 co-immunoprecipitates with endogenous DYRK2, EDD, DDB1 and VprBP (Figure 2.11.4B). In striking contrast, Flag-Cep78 did not co-immunoprecipitate with Cullin4A, a component of CRL4^{VprBP} (Figure 2.11.4B). Similarly, endogenous Cep78, VprBP, DDB1 and EDD were detected in Flag-DYRK2 immunoprecipitates (Figure 2.11.5B). The interaction between Cep78 and EDD-DYRK2-DDB1^{VprBP} is physiologically relevant since endogenous Cep78 specifically co-immunoprecipitated with endogenous DYRK2, EDD, DDB1 and VprBP (Figure 2.11.4C) and these proteins co-fractionated in a discrete protein complex at ~670 kDa (Figure 2.11.4D). Of note, the interaction between Cep78 and VprBP appeared to be very robust (Figures 2.11.4B-C), suggesting that these two proteins may directly interact. Indeed, *in vitro* binding experiments using purified Cep78 and individual EDD-DYRK2-DDB1^{VprBP} subunits revealed that Cep78 directly binds to VprBP only (Figure 2.11.4E). Furthermore, since VprBP is thought to directly interact with DDB1, which in turn binds to DYRK2/EDD (23), we determined whether Cep78 interacts with DDB1 through VprBP. The Cep78-VprBP interaction remained intact upon DDB1 depletion (Figure 2.11.5C), whereas the interaction between Cep78 and DDB1, DYRK2 or EDD was substantially reduced in VprBP-depleted cells (Figure 2.11.5D). Thus, our results suggest that Cep78 specifically binds to EDD-DYRK2-DDB1^{VprBP} and that VprBP likely forms a scaffold linking Cep78 to DDB1/DYRK2/EDD (Figure 2.11.4F).

Although EDD-DYRK2-DDB1^{VprBP} subunits are present in the nucleus and cytoplasm (24-27), their localization to the centrosome has not been documented. Since EDD-DYRK2-DDB1^{VprBP} binds to Cep78, we speculate that a pool of this E3 ligase is targeted to the centrosome. To biochemically demonstrate the localization of EDD-DYRK2-DDB1^{VprBP}, we

purified centrosomes through sucrose gradient centrifugation and found that endogenous Cep78, EDD, DYRK2, DDB1 and VprBP co-sedimented with γ -tubulin and centrin on a sucrose gradient (Figure 2.11.6A). As a negative control, these gradient fractions were devoid of a non-centrosomal marker giantin (Figure 2.11.6A). Furthermore, IF experiments revealed that in addition to their nuclear localization, endogenous DYRK2, EDD and VprBP co-localize with centrin in about 5-65% of cells depending on the phase of the cell cycle (Figures 2.11.6B-C). Together, these data suggest that Cep78 likely interacts with EDD-DYRK2-DDB1^{VprBP} at the centrosome.

2.4.3. Mapping domains critical for the function of Cep78 and its interaction with EDD-DYRK2-DDB1^{VprBP}

To delineate the functional domain(s) of Cep78 that enable its localization to the centrosome and association with VprBP, a series of Flag-tagged truncated, deletion and point mutants of Cep78 were expressed in cells. After IPs with anti-Flag antibodies, we found that only a fragment (1-520) containing the entire LRR domain can interact with endogenous VprBP (Figures 2.11.6D and 2.11.7A), and that deletion of any one repeat within the domain is sufficient to abolish VprBP binding (Figures 2.11.6D and 2.11.7B). Deletion of the CC domain, in contrast, did not affect binding to VprBP (Figures 2.11.6D and 2.11.7B). Furthermore, disruption of the LRR domain but not the CC domain compromised centrosomal localization (Figures 2.11.6D and 2.11.7C), suggesting that the LRR domain or the horseshoe conformation it adopts is critical for centrosomal targeting and VprBP binding. To further dissect the centrosomal localization and VprBP-binding domains, we mutated single amino acids within the LRR domain that lie on the concave or convex surface of the horseshoe (28) and thus are predicted to induce minimal structural perturbations. We found that a point mutation in the fifth (D262A) or sixth (D290A) LRR repeat is sufficient to abrogate VprBP binding without affecting centrosomal localization (Figures 2.11.6E and 2.11.8A-B). Likewise, depletion of VprBP did not impinge on Cep78 localization (Figure 2.11.9A), suggesting that centrosomal targeting of Cep78 and its association with VprBP are separate events.

VprBP possesses an armadillo-like and a cr omo-like domain in the N-terminal region, a LisH domain in the middle region, and a WD40 and an acidic domain in the C-terminal region (20). When VprBP fragments of various sizes were expressed, we observed that the C-terminal end (1377-1507) encompassing the acidic domain is responsible for Cep78 binding (Figures

2.11.6F and 2.11.8C-D). The Cep78-binding domain of VprBP is therefore distinct from the WD40 domain required for DDB1 binding (29,30).

2.4.4. Cep78 is not a substrate of EDD-DYRK2-DDB1^{VprBP}

To explore the functional relationship between Cep78 and EDD-DYRK2-DDB1^{VprBP}, we first asked if Cep78 is a substrate of EDD-DYRK2-DDB1^{VprBP} by setting up *in vivo* ubiquitination assays. Flag-Cep78, HA-Ub and Myc-VprBP expressed in cells were left untreated or treated with MG132 to stabilize ubiquitinated products. Lysates were immunoprecipitated with anti-Flag in the presence of 1% SDS to prevent interacting proteins such as VprBP from co-immunoprecipitating with Flag-Cep78 (Figure 2.11.9B). Under this assay condition, any observable ubiquitinated products with an apparent molecular weight above 78 kDa were likely attributed to Flag-Cep78 ubiquitination. Although ubiquitination of Flag-Cep78 could be detected, the levels of ubiquitination did not change upon VprBP expression irrespective of MG132 (Figure 2.11.10A). Likewise, expression of VprBP did not significantly increase the levels of Cep78 ubiquitination in mitosis (Figure 2.11.9C) during which Cep78 was down-regulated (Figures 2.11.1E-F). In contrast, two previously known EDD-DYRK2-DDB1^{VprBP} substrates, katanin p60 and TERT (23,31), became highly ubiquitinated in the presence of VprBP (Figures 2.11.9D-E). Consistent with the notion that VprBP does not impinge on Cep78 ubiquitination, depletion or expression of VprBP did not alter the protein levels or centrosomal localization of Cep78 (Figures 2.11.10B and 2.11.9A). Depletion of VprBP also did not affect Cep78 protein levels in mitosis (Figure 2.11.9F), and both wild type Cep78 and VprBP-binding mutant of Cep78 (D290A) exhibited similar levels of ubiquitination in mitosis (Figure 2.11.9G). Moreover, depletion or expression of Cep78 had no effect on VprBP protein levels or centrosomal localization (Figure 2.11.9A and 2.11.11A-B). From these results, we conclude that Cep78 is not a substrate of EDD-DYRK2-DDB1^{VprBP} and that neither protein affects the localization or stability of the other.

2.4.5. Cep78 prevents EDD-DYRK2-DDB1^{VprBP} from ubiquitinating substrates

Next, we investigated whether Cep78 can modulate the activity of EDD-DYRK2-DDB1^{VprBP}. For this purpose, we performed *in vivo* ubiquitination assays without SDS to immunoprecipitate recombinant VprBP and associated proteins from cells expressing recombinant VprBP and Ub. VprBP co-immunoprecipitated with ubiquitinated products having apparent molecular weights from 50kDa to 250 kDa (Figure 2.11.10C). These products were

present in greater abundance in MG132-treated cells as opposed to untreated cells (Figure 2.11.10C) and likely represent substrates that get ubiquitinated by, and remain bounded to, VprBP throughout IP. Remarkably, co-expression of Cep78 dramatically reduced the levels of ubiquitinated products in a dose-dependent manner (Figure 2.11.10C). In contrast, the D290A mutant was less efficient in preventing the appearance of ubiquitinated products compared to wild type Cep78 (Figure 2.11.11C). Likewise, depletion of Cep78 under the same assay condition led to enhanced accumulation of ubiquitinated products (Figure 2.11.10D and 2.11.11D), and these results together suggest that Cep78 suppresses EDD-DYRK2-DDB1^{VprBP}. To further confirm a role of Cep78 in suppressing EDD-DYRK2-DDB1^{VprBP}, we examined the effects of expressing a VprBP mutant refractory to Cep78 binding (1-1377) on the levels of ubiquitinated products. Importantly, while the levels of ubiquitinated products associated with wild type VprBP were drastically reduced in the presence of Cep78, those associated with 1-1377 exhibited no reduction (Figure 2.11.10E). Collectively, our data support the notion that Cep78 inhibits the ubiquitination activity of EDD-DYRK2-DDB1^{VprBP} by directly binding to VprBP.

To unambiguously and biochemically prove that Cep78 regulates EDD-DYRK2-DDB1^{VprBP} but not CRL4^{VprBP}, we found that depletion of Cep78 leads to enhanced ubiquitination of katanin p60 and TERT, whereas its overexpression diminishes ubiquitination (Figures 2.11.12A-D). On the other hand, the ubiquitination levels of a CRL4^{VprBP} substrate MCM10 (32) remained unaffected by Cep78 (Figures 2.11.12E-F). In light of these results, we suggest that Cep78 specifically regulates ubiquitination of EDD-DYRK2-DDB1^{VprBP} substrates in a negative manner.

2.4.6. A Cep78-interacting protein CP110 is a novel EDD-DYRK2-DDB1^{VprBP} substrate

Next, we sought to determine whether EDD-DYRK2-DDB1^{VprBP} could target certain substrates for ubiquitination at the centrosome and whether this event is regulated by Cep78. To this end, we demonstrated that recombinant or endogenous VprBP interacts with a Cep78-interacting protein CP110 (Figure 2.11.2A and 2.11.13A), and conversely, recombinant or endogenous CP110 associates with VprBP (Figures 2.11.2A-B). Furthermore, CP110 co-immunoprecipitated with VprBP, DDB1, DYRK2 and EDD but not with Cullin4A (Figure 2.11.2B), consistent with the idea that it specifically binds to EDD-DYRK2-DDB1^{VprBP}. Ectopic expression of VprBP or depletion of Cep78 enhanced CP110 ubiquitination (Figures 2.11.2C-D),

whereas expression of wild type but not mutant (D290A) Cep78 reduced ubiquitination (Figure 2.11.2E), suggesting that CP110 is an EDD-DYRK2-DDB1^{VprBP} substrate. Indeed, CP110 ubiquitination could be induced by EDD-DYRK2-DDB1^{VprBP} and suppressed by Cep78 *in vitro* using purified proteins (Figure 2.11.2F). Ubiquitination of CP110 likely signals the protein for proteasomal degradation since ectopic expression of EDD, DDB1 or VprBP, or depletion of Cep78, decreased the steady-state levels of CP110 in HEK293, RPE-1 and HeLa cells (Figure 2.11.2G and 2.11.13A-D). The decrease in CP110 levels caused by Cep78 depletion could be rescued by expression of exogenous Cep78 (Figure 2.11.13D). In sharp contrast, expression of Cep78 or depletion of VprBP increased CP110 levels in these cell lines (Figures 2.11.1A, 2.11.2H-I). As a control, we found that the levels of another Cep78-interacting protein Cep76 are not affected by Cep78 or VprBP (Figures 2.11.14A-B). Taken together, our results indicate that EDD-DYRK2-DDB1^{VprBP} specifically ubiquitinates CP110, leading to its degradation, and these effects can be counteracted by Cep78.

To validate these results, we were able to distinguish the activity of EDD-DYRK2-DDB1^{VprBP} from Cyclin F and Neuralized homologue 4 (Neurl4), two E3 ligases previously known to modulate CP110 ubiquitination and stability (33,34). Cyclin F ubiquitinates CP110 in G2 phase, whereas Neurl4 may ubiquitinate CP110 throughout the cell cycle. We showed that Cep78 specifically suppresses ubiquitination of CP110 induced by EDD-DYRK2-DDB1^{VprBP}, but not by Cyclin F or Neurl4 (Figure 2.11.15A). Furthermore, although CP110 protein levels decreased in the presence of VprBP, they could be further reduced by co-expression with Cyclin F or Neurl4 (Figure 2.11.15B). Thus, the mechanism by which EDD-DYRK2-DDB1^{VprBP} ubiquitinates CP110 appears to be unique since only this enzyme is subjected to regulation by Cep78.

To further interrogate the relationship between Cep78, EDD-DYRK2-DDB1^{VprBP} and CP110, we investigated the functional consequences of CP110 degradation *in vivo*. We employed two sensitive assays to monitor the loss of CP110. First, it has been shown that ablation of CP110 or a CP110 chaperone Cep97 leads to excessive growth or elongation of centrioles in non-ciliated HeLa cells (35-38). We thus examined the effects of manipulating the protein levels of Cep78 or EDD-DYRK2-DDB1^{VprBP} on the formation of elongated centrioles in this cell line. Remarkably, depletion of Cep78 promoted centriole elongation (Figures 2.11.16A-B and 2.11.17A-D) which could be rescued by expression of exogenous Cep78 (Figures

2.11.17C-D), whereas ectopic expression of wild type Cep78 but not the D290A mutant suppressed the elongation phenotype induced by Cep97 loss (Figures 2.11.16C-D). Similarly, expression of EDD, DDB1 or VprBP provoked elongation of centrioles (Figures 2.11.16E-F). Second, it is known that CP110 can suppress cilia assembly in RPE-1 cells able to form cilia (35,39). A loss of CP110 therefore results in ectopic formation of cilia in proliferating cells, while its expression inhibits cilia assembly in quiescent cells. We demonstrated that expression of wild type Cep78, in contrast to the D290A mutant, efficiently inhibits cilia formation in quiescent RPE-1 cells (Figures 2.11.16G-H). Conversely, expression of EDD, DDB1 and VprBP promoted cilia formation in proliferating cells (Figures 2.11.16I-J). Taken together, these data suggest that Cep78 maintains centrosome homeostasis by counteracting EDD-DYRK2-DDB1^{VprBP}-mediated ubiquitination and degradation of CP110.

2.4.7. Mechanism of EDD-DYRK2-DDB1^{VprBP} inhibition by Cep78

To obtain mechanistic details into how Cep78 precludes CP110 ubiquitination, we revisited our current knowledge of substrate ubiquitination carried out by EDD-DYRK2-DDB1^{VprBP} (23,31). First, it is believed that the substrate must be phosphorylated by DYRK2 prior to ubiquitination. Substrate recognition by VprBP is also important since VprBP helps bring the substrate into close proximity with EDD. Once the substrate is physically close to EDD, Ub is transferred from EDD to the substrate. CP110 contains five putative DYRK2 phosphorylation sites (Figure 2.11.18A) and was readily phosphorylated by DYRK2 alone or EDD-DYRK2-DDB1^{VprBP} *in vitro* (Figure 2.11.18B), suggesting that it is a DYRK2 substrate. When four of these sites were mutated to alanine (S287AS366AS551AS906A), phosphorylation of the mutant protein was significantly diminished (Figure 2.11.18C). The mutant protein exhibited impaired binding to VprBP (Figure 2.11.18D) and became less susceptible to ubiquitination (Figure 2.11.18E), suggesting that CP110 phosphorylation is a prerequisite for VprBP binding and subsequent ubiquitination. Importantly, Cep78 suppressed ubiquitination of CP110 (Figure 2.11.2E) without compromising its ability to undergo phosphorylation (Figure 2.11.18F) and associate with VprBP (Figure 2.11.18G). These results imply that Cep78 specifically prevents the transfer of Ub to CP110.

2.5. Discussion

The centrosome is a dynamic organelle which undergoes numerical and structural changes during the cell cycle. To achieve dynamicity, the stability and function of proteins involved in different aspects of centrosome biology must be kept in check at all times. Failure to achieve or maintain centrosome homeostasis can have deleterious consequences and can give rise to human diseases such as cancer and ciliopathies. E3 ligases play an important role in modulating protein stability and function (19), and in this study, we demonstrated that a pool of the E3 ligase EDD-DYRK2-DDB1^{VprBP} operates at the centrosome and that a poorly studied protein Cep78 is dedicated to controlling its activity. To our knowledge, Cep78 is the first centrosomal protein shown to possess inhibitory activity against an E3 ligase through direct binding.

Although the precise manner in which EDD-DYRK2-DDB1^{VprBP} ubiquitinates its substrates is not fully clear, distinct components of this E3 ligase are thought to participate in substrate phosphorylation, binding to VprBP and ubiquitination (23,31). Our data show that although Cep78 inhibits CP110 ubiquitination, it does not prevent CP110 from undergoing phosphorylation or from interacting with VprBP. Therefore, it appears that Cep78 explicitly hinders the addition of Ub to CP110, the last step of the enzymatic reaction catalyzed by EDD-DYRK2-DDB1^{VprBP}. We postulate that Cep78 binding to VprBP triggers a conformational change in VprBP, thereby precluding CP110 from staying close to EDD (Figure 2.11.18H). As a result, the transfer of Ub from EDD to CP110 is hampered.

One interesting finding from our work is that the C-terminal acidic domain of VprBP binds to Cep78 and plays a crucial role in controlling the ubiquitination activity of EDD-DYRK2-DDB1^{VprBP}. In this regard, it is intriguing that Merlin, a protein that inhibits CRL4^{VprBP}, binds to the same domain on VprBP (40). It has been proposed that Merlin acts as a competitive inhibitor to prevent substrates from binding to VprBP (40). This mode of inhibition is undoubtedly different from that of Cep78 which appears to be non-competitive. Since deregulation of some E3 ligases has been linked to cancer and very few inhibitors of the HECT-type E3 ligases are currently available (41,42), our results on Cep78 may provide new insights into targeting this particular type of E3 ligases for therapeutic intervention.

Although we do not yet know how many centrosomal substrates EDD-DYRK2-DDB1^{VprBP} can target, this E3 ligase seems to be highly selective since it specifically ubiquitinates and influences the steady-state levels of two centrosomal proteins, CP110 (this work) and katanin

p60 (23), but not the other (Cep76; this work). EDD-DYRK2-DDB1^{VprBP} is believed to function during mitosis (23,31). We postulate that EDD-DYRK2-DDB1^{VprBP} is responsible for directing ubiquitination of a subset of substrates in mitosis when Cep78 levels are low, and that regulation of this E3 ligase by Cep78 in other phases of the cell cycle is critical to maintain centrosome homeostasis. In support of this idea, the protein levels of Cep78 correlate with those of CP110 (43) and the two cellular processes associated with CP110 function, centriole length and cilia assembly, go awry when there is insufficient or excessive amount of Cep78 or EDD-DYRK2-DDB1^{VprBP}. Future proteomic studies will identify additional EDD-DYRK2-DDB1^{VprBP} substrates at the centrosome.

2.6. Materials and methods

Cell culture and plasmids

Human U2OS, hTERT RPE-1, HeLa, Jurkat and HEK293 cells were grown in DMEM supplemented with 5% FBS at 37°C in a humidified 5% CO₂ atmosphere. To generate Flag-tagged Cep78 fusion proteins, human Cep78 cDNA fragments encoding residues 1-722 (full-length), 1-520, 221-445, 446-722 and 221-722 were amplified by PCR using Phusion High-Fidelity DNA polymerase (New England Biolabs) and cloned into mammalian expression vector pCBF-Flag. Full-length cDNA was also sub-cloned into pEGFP-C1 vector to generate GFP-Cep78. The following Cep78 deletions/point mutations (Δ 122-146, Δ 147-174, Δ 175-225, Δ 226-254, Δ 255-282, Δ 283-308, Δ 450-497, E126A, S154A, N182A, T233A, D262A and D290A) and CP110 mutation (S287AS366AS551AS906A) were introduced into full-length cDNA by employing a two-step PCR mutagenesis strategy and sub-cloned into pCBF-Flag or pEGFP-C1. To generate Flag-VprBP fusion proteins, human VprBP cDNA fragments encoding residues 1-1507 (full-length), 1-796, 797-1040 and 1041-1507 were cloned into pCBF-Flag. All constructs were verified by DNA sequencing. The following proteins were also expressed from plasmids in mammalian cells: HA-Ub (J. Archambault), Flag-TERT (C. Autexier), GFP-DDB1, Myc-VprBP (1-1507), Myc-VprBP (1-1377), Myc-VprBP (981-1377), Myc-VprBP (1040-1377) (E. Cohen), HA-CP110, Flag-CP110, Flag-SCAPER, Flag-Cyclin F and Flag-Neurl4 (B. Dynlacht), Myc-MCM10 (S. Saxena), Flag-katanin p60 (J. Singer), Flag-EDD (D. Saunders and C. Watts, Addgene plasmid #37188) and Flag-DYRK2 (A. Rao, Addgene plasmid #20005).

Antibodies

Antibodies used in this study included anti-CP110, anti-Cep78, anti-VprBP, anti-EDD, anti-DDB1, anti-Cullin4A (Bethyl Laboratories), anti-centrin (Millipore), anti-GFP (Roche), anti-C-Nap1, anti-HA, anti-myc, anti-phosphoserine (Santa Cruz), anti- α -tubulin, anti-Flag, anti- γ -tubulin, anti- β -actin (Sigma-Aldrich), anti-glutamylated tubulin GT335 (Cedarlane), anti-DYRK2 (Abcam) and anti-Ub (Dako). To generate rabbit anti-Cep78 antibodies, a glutathione-S-transferase (GST) fusion protein containing residues 590-722 (IRCM6) of Cep78 was expressed in *E. coli* and purified to homogeneity. Antibodies against Cep78 were purified by affinity chromatography.

Mass spectrometric identification of Cep78 interacting proteins

To identify interacting proteins, Flag-Cep78 was expressed in HEK293 and immunoprecipitated with anti-Flag agarose beads (Sigma-Aldrich) for 2 hours at 4°C. Bounded proteins were eluted with Flag peptide for 30 minutes, and the resultant eluates were precipitated with trichloroacetic acid and fractionated by SDS-PAGE. Six gel slices containing polypeptides were excised after Coomassie staining and subjected to proteolytic digestion mass spectrometric analysis. Analyses were performed at the mass spectrometry core facility from IRCM by micro-capillary LC/MS/MS.

Immunoprecipitation, immunoblotting, and immunofluorescence microscopy

Immunoprecipitation, immunoblotting and immunofluorescence were performed as described (44,45). Briefly, cells were lysed with lysis buffer (50 mM HEPES/pH 7.4, 250 mM NaCl, 5 mM EDTA/pH 8, 0.1% NP-40, 1 mM DTT, 0.2 mM AEBSF, 2 µg/ml leupeptin, 2 µg aprotinin, 10 mM NaF, 50 mM β-glycerophosphate and 10% glycerol) at 4°C for 30 minutes and extracted proteins were recovered in the supernatant after centrifugation at 16,000g. For immunoprecipitation, 2 mg of the resulting supernatant was incubated with an appropriate antibody at 4°C for 1 hour and collected using protein A- or G-Sepharose beads. The beads were washed with lysis buffer, and bound proteins were analyzed by SDS-PAGE and immunoblotting with primary antibodies and horseradish peroxidase-conjugated secondary antibodies (VWR). 100 µg of lysate was typically loaded into the input (IN) lane. For indirect immunofluorescence, cells were grown on glass coverslips, fixed with cold methanol and permeabilized with 1% Triton X-100/PBS. Slides were blocked with 3% BSA in 0.1% Triton X-100/PBS prior to incubation with primary antibodies. Secondary antibodies used were Cy3-, Cy5- or Alexa488-conjugated donkey anti-mouse, anti-rat or anti-rabbit IgG (Jackson Immunolabs and Molecular Probes). Cells were then stained with DAPI (Sigma), and slides were mounted, observed, and photographed using a Leitz DMRB (Leica) microscope (100×, NA 1.3) equipped with a Retiga EXi cooled camera. To quantify Cep78 signal at the centrosome, the background fluorescence between slides was normalized and the function measurement by region of interest (ROI) from the software Volocity was used.

Cell cycle synchronization and FACS analysis

To obtain U2OS cells synchronized in the G1, G1/S, S, G2, M, M/G1 and next G1 phases, cells were treated with 0.4 mM mimosine for 24 hours, 2 mM HU for 24 hours, 2 mM HU for 24 hours and release for 5 hours, 2 mM HU for 24 hours and release for 9 hours, 40ng/ml

nocodazole for 24 hours, 40ng/ml nocodazole for 24 hours and release for 4 hours, and 40ng/ml nocodazole for 24 hours and release for 9 hours, respectively. To obtain RPE-1 cells synchronized in the G₀, G₁, G₁/S, S/G₂ and M phases, cells were brought to quiescence by serum starvation for 48 hours and re-stimulated for 0, 12, 24, 28 and 34 hours. HEK293 cells were synchronized in mitosis with 40ng/ml nocodazole for 24 hours. Cell cycle distribution was confirmed by FACS as described previously (46).

RNA interference

Synthetic siRNA oligonucleotides were purchased from GE Dharmacon. The 21-nucleotide siRNA sequence for the non-specific (NS) control was 5'-AATTCTCCGAACGTGTCACGT-3'. The 21-nucleotide siRNA sequences for Cep78 were 5'-GAGGAGTTGTCCAGAAATA-3' (oligo 1), 5'-GCGATAAGATACAAAGATG-3' (oligo 2), 5'-GGTCGTTCTGGATATAAGA-3' (oligo 6) and 5'-CAAAGAACTAGGGAACTAG-3' (oligo 7). Oligo 1 was used unless stated otherwise. Oligo 7 targets the 3'UTR of Cep78 mRNA and was used in rescue experiments. The siRNAs for VprBP, DDB1 and Cep97 were described previously (23,35).

Production of recombinant proteins

Purified DDB1 and DYRK2 were obtained from Cedarlane. Flag-Cep78, Flag-EDD or Flag-VprBP expressed in HEK293 cells was immunoprecipitated with anti-Flag beads for 2 hours. Beads were washed twice with lysis buffer containing 500 mM NaCl. Proteins were eluted with Flag peptide for 30 minutes and collected through poly-prep chromatography columns (BioRad). A small sample was run on a gel and Coomassie stained to ensure protein purity.

***In vitro* binding assay**

1 µg of purified Cep78 protein was mixed with 1 µg of purified EDD, DYRK2, DDB1 or VprBP at 4°C for 1 hour, followed by incubation with an anti-Cep78 antibody for 1 hour and Protein A beads for 2 hours. After extensive washing with lysis buffer, bound proteins were analyzed by SDS-PAGE and immunoblotting.

Size exclusion chromatography

2 mg of cell extract was chromatographed (ÄKTA FPLC; GE Healthcare) over a Superose-6 10/300 GL column (GE Healthcare). 1 ml fractions were collected, and proteins were precipitated with trichloroacetic acid and analyzed by SDS-PAGE. The column was calibrated with Gel Filtration Standard (Bio-Rad) containing a mixture of molecular weight markers from 17 to 670 kDa.

Centrosome purification

Centrosomes were isolated as described (47). Briefly, Approximately 1×10^9 Jurkat cells treated with $0.2 \mu\text{M}$ nocodazole and $1 \mu\text{g/ml}$ cytochalasin D at 37°C for 1 hour were collected and lysed. The lysate was treated with 1 mg/ml DNase I before placing onto a 60% sucrose cushion. After centrifugation, the bottom $\frac{1}{4}$ of the suspension was added to a discontinuous sucrose gradient consisting of 5 ml of 70% sucrose solution at the bottom, 3 ml of 50% sucrose solution in the middle and 3 ml of 40% sucrose solution at the top. 1 ml fractions were collected after another round of centrifugation.

***In vivo* ubiquitination assay**

HEK293 cells were typically transfected with various combinations of plasmids including HA-Ub. 48 hours after transfection, cells were left untreated or treated with $10 \mu\text{M}$ MG132 for 6 hours and lysed with lysis buffer. The desired protein was immunoprecipitated without SDS or with 1% SDS to prevent interacting partners from co-immunoprecipitating with the desired protein. After extensive washing, bound proteins were analyzed by SDS-PAGE and immunoblotting with an anti-HA antibody.

***In vitro* ubiquitination assay**

HA-CP110 bound to beads was used as substrate for the assay. Briefly, HA-CP110 expressed in HEK293 cells was immunoprecipitated with anti-HA beads, and beads were washed twice with lysis buffer containing 500 mM NaCl. Reactions were performed at 30°C for 1 hour in 30ul of ubiquitination buffer (40 mM Tris-HCl/pH 7.6, 2 mM DTT, 5 mM MgCl_2 , 0.1 M NaCl, 2 mM ATP) containing various combinations of the following components: $100 \mu\text{M}$ Ub (Boston Biochem), 20 nM E1/UBE1 (Boston Biochem), 100 nM UbcH5b (Boston Biochem), 50 ng EDD, 50 ng DYRK2 (Abcam), 50 ng DDB1 (Abnova), 50 ng VprBP and 50 ng Cep78. After the reaction, beads were washed with lysis buffer and bound proteins were analyzed by SDS-PAGE and immunoblotting.

***In vitro* kinase assay**

HA-CP110 bound to beads was used as substrate for the assay. Reactions were performed at 30°C for 1 hour in 30ul of kinase buffer (25 mM Tris-HCl/pH 7.5, 2 mM DTT, 10 mM MgCl_2 , 5 mM β -glycerophosphate, 0.1 mM Na_3VO_4) containing 50 ng DYRK2 or 50 ng each of EDD, DYRK2, DDB1 and VprBP. After the reaction, beads were washed with lysis buffer and bound proteins were analyzed by SDS-PAGE and immunoblotting.

2.7. Acknowledgements

We thank all members of the Tsang laboratory for constructive advice; N. Al-Bader, M. Hudson, H. Ling, R. Rouget, J. Song and X. Deng for initial efforts on this project; J. Archambault, C. Autexier, E. Cohen, B. Dynlacht, A. Rao, D. Saunders, S. Saxena, J. Singer and C. Watts for providing plasmids; E. Cohen for critical reading of the manuscript; and Denis Faubert for assistance with mass spectrometric identification of Cep78-interacting proteins. W.Y.T. was a Canadian Institutes of Health Research New Investigator and a Fonds de recherche Santé Junior 1 Research Scholar. This work was supported by the Canadian Institutes of Health Research (MOP-115033 to WYT) and the Natural Sciences and Engineering Research Council of Canada.

2.8. Author Contributions

W.Y.T. designed the experiments. D.H., Y.J.E., A.D. and W.Y.T. conducted the experiments. D.H. and W.Y.T. wrote the paper.

2.9. Conflict of Interest

The authors declare no conflict of interest.

2.10. References

1. Bornens M (2012) The centrosome in cells and organisms. *Science* **335**, 422-426.
2. Fu J, Hagan IM and Glover DM (2015) The centrosome and its duplication cycle. *Cold Spring Harb Perspect Biol* **7**, a015800.
3. Goetz SC and Anderson KV (2010) The primary cilium: a signalling centre during vertebrate development. *Nat Rev Genet* **11**, 331-344.
4. Barbelanne M and Tsang WY (2014) Molecular and cellular basis of autosomal recessive primary microcephaly. *Biomed Res Int* **2014**, 547986.
5. Nigg EA and Raff JW (2009) Centrioles, centrosomes, and cilia in health and disease. *Cell* **139**, 663-678.
6. Gonczy P (2015) Centrosomes and cancer: revisiting a long-standing relationship. *Nat Rev Cancer* **15**, 639-652.
7. Hildebrandt F, Benzing T and Katsanis N (2011) Ciliopathies. *N Engl J Med* **364**, 1533-1543.
8. Nogales-Cadenas R, Abascal F, Diez-Perez J, Carazo JM and Pascual-Montano A (2009) CentrosomeDB: a human centrosomal proteins database. *Nucleic Acids Res* **37**, D175-180.
9. Andersen JS, Wilkinson CJ, Mayor T, Mortensen P, Nigg EA and Mann M (2003) Proteomic characterization of the human centrosome by protein correlation profiling. *Nature* **426**, 570-574.
10. Firat-Karalar E, N Sante J, Elliott S and Stearns T (2014) Proteomic analysis of mammalian sperm cells identifies new components of the centrosome. *J Cell Sci* **127**, 4128-4133.
11. Fu Q, Xu M, Chen X, Sheng X, Yuan Z, Liu Y, Li H, Sun Z, Yang L, Wang K, Zhang F, Li, Y, Zhao C, Sui R and Chen R (2016) CEP78 is mutated in a distinct type of Usher syndrome. *J Med Genet* **54**, 190-195.
12. Namburi P, Ratnapriya R, Khateb S, Lazar CH, Kinarty Y, Obolensky A, Erdinest I, Marks-Ohana, D, Pras E, Ben-Yosef T, Newman H, Gross M, Swaroop A, Banin E and Sharon D (2016) Bi-allelic Truncating Mutations in CEP78, Encoding Centrosomal Protein 78, Cause Cone-Rod Degeneration with Sensorineural Hearing Loss. *Am J Hum Genet* **99**, 777-784.

13. Nikopoulos K, Farinelli P, Giangreco B, Tsika C, Royer-Bertrand B, Mbefo MK, Bedoni N, Kjellstrom U, El Zaoui I, Di Gioia SA, Balzano S, Cisarova K, Messina A, Decembrini S, Plainis S, Blazaki SV, Khan MI, Micheal S, Boldt K, Ueffing M, Moulin AP, Cremers FP, Roepman R, Arsenijevic Y, Tsilimbaris MK, Andreasson S and Rivolta, C (2016) Mutations in CEP78 cause cone-rod dystrophy and hearing loss associated with Primary-Cilia Defects. *Am J Hum Genet* **99**, 770-776.
14. Zhang M, Duan T, Wang L, Tang J, Luo R, Zhang R and Kang T (2016) Low expression of centrosomal protein 78 (CEP78) is associated with poor prognosis of colorectal cancer patients. *Chin J Cancer* **35**, 62.
15. Nesslinger NJ, Sahota R A, Stone B, Johnson K, Chima N, King C, Rasmussen D, Bishop D, Rennie PS, Gleave M, Blood P, Pai H, Ludgate C and Nelson BH (2007) Standard treatments induce antigen-specific immune responses in prostate cancer. *Clin Cancer Res* **13**, 1493-1502.
16. Azimzadeh J, Wong ML, Downhour DM, Sanchez Alvarado A and Marshall WF (2012) Centrosome loss in the evolution of planarians. *Science* **335**, 461-463.
17. Brunk K, Zhu M, Barenz F, Kratz AS, Haselmann-Weiss U, Antony C and Hoffmann I (2016) Cep78 is a new centriolar protein involved in Plk4-induced centriole overduplication. *J Cell Sci* **129**, 2713-2718.
18. Komander D and Rape M (2012) The ubiquitin code. *Annu Rev Biochem* **81**, 203-229.
19. Berndsen CE and Wolberger C (2014) New insights into ubiquitin E3 ligase mechanism. *Nat Struct Mol Biol* **21**, 301-307.
20. Nakagawa T, Mondal K and Swanson PC (2013) VprBP (DCAF1): a promiscuous substrate recognition subunit that incorporates into both RING-family CRL4 and HECT-family EDD/UBR5 E3 ubiquitin ligases. *BMC Mol Biol* **14**, 22.
21. Barbelanne M, Chiu A, Qian J and Tsang WY (2016) Opposing post-translational modifications regulate Cep76 function to suppress centriole amplification. *Oncogene* **35**, 5377-5387.
22. Tsang WY, Spektor A, Vijayakumar S, Bista BR, Li J, Sanchez I, Duensing S and Dynlacht BD (2009) Cep76, a centrosomal protein that specifically restrains centriole reduplication. *Dev Cell* **16**, 649-660.

23. Maddika S and Chen J (2009) Protein kinase DYRK2 is a scaffold that facilitates assembly of an E3 ligase. *Nat Cell Biol* **11**, 409-419.
24. Becker W, Weber Y, Wetzel K, Eirmbter K, Tejedor FJ and Joost HG (1998) Sequence characteristics, subcellular localization, and substrate specificity of DYRK-related kinases, a novel family of dual specificity protein kinases. *J Biol Chem* **273**, 25893-25902.
25. Belzile JP, Abrahamyan LG, Gerard FC, Rougeau N and Cohen EA (2010) Formation of mobile chromatin-associated nuclear foci containing HIV-1 Vpr and VPRBP is critical for the induction of G2 cell cycle arrest. *PLoS Pathog* **6**, e1001080.
26. Chu G and Chang E (1988) Xeroderma pigmentosum group E cells lack a nuclear factor that binds to damaged DNA. *Science* **242**, 564-567.
27. Henderson MJ, Russell AJ, Hird S, Munoz M, Clancy JL, Lehrbach GM, Calanni ST, Jans DA, Sutherland RL and Watts CK (2002) EDD, the human hyperplastic discs protein, has a role in progesterone receptor coactivation and potential involvement in DNA damage response. *J Biol Chem* **277**, 26468-26478.
28. Matsushima N, Tachi N, Kuroki Y, Enkhbayar P, Osaki M, Kamiya M and Kretsinger RH (2005) Structural analysis of leucine-rich-repeat variants in proteins associated with human diseases. *Cell Mol Life Sci* **62**, 2771-2791.
29. Le Rouzic E, Belaïdouni N, Estrabaud E, Morel M, Rain JC, Transy C and Margottin-Goguet F (2007) HIV1 Vpr arrests the cell cycle by recruiting DCAF1/VprBP, a receptor of the Cul4-DDB1 ubiquitin ligase. *Cell Cycle* **6**, 182-188.
30. Gérard FC, Yang R, Romani B, Poisson A, Belzile JP, Rougeau N and Cohen EA (2014) Defining the interactions and role of DCAF1/VPRBP in the DDB1-cullin4A E3 ubiquitin ligase complex engaged by HIV-1 Vpr to induce a G2 cell cycle arrest. *PLoS One* **9**, e89195.
31. Jung HY, Wang X, Jun S and Park JI (2013) Dyrk2-associated EDD-DDB1-VprBP E3 ligase inhibits telomerase by TERT degradation. *J Biol Chem* **288**, 7252-7262.
32. Kaur M, Khan MM, Kar A, Sharma A and Saxena S (2012) CRL4-DDB1-VPRBP ubiquitin ligase mediates the stress triggered proteolysis of Mcm10. *Nucleic Acids Res* **40**, 7332-7346.

33. D'Angiolella V, Donato V, Vijayakumar S, Saraf A, Florens L, Washburn MP, Dynlacht B and Pagano M (2010) SCF(Cyclin F) controls centrosome homeostasis and mitotic fidelity through CP110 degradation. *Nature* **466**, 138-142.
34. Li J, Kim S, Kobayashi T, Liang FX, Korzeniewski N, Duensing S and Dynlacht BD (2012) Neurl4, a novel daughter centriole protein, prevents formation of ectopic microtubule organizing centres. *EMBO Rep* **13**, 547-553.
35. Spektor A, Tsang WY, Khoo D and Dynlacht BD (2007) Cep97 and CP110 suppress a cilia assembly program. *Cell* **130**, 678-690.
36. Schmidt TI, Kleylein-Sohn J, Westendorf J, Le Clech M, Lavoie SB, Stierhof YD and Nigg EA (2009) Control of centriole length by CPAP and CP110. *Curr Biol* **19**, 1005-1011.
37. Kohlmaier G, Loncarek J, Meng X, McEwen BF, Mogensen MM, Spektor A, Dynlacht BD, Khodjakov A and Gönczy P. (2009) Overly long centrioles and defective cell division upon excess of the SAS-4-related protein CPAP. *Curr Biol* **19**, 1012-1018.
38. Tang CJ, Fu RH, Wu KS, Hsu WB and Tang TK (2009) CPAP is a cell-cycle regulated protein that controls centriole length. *Nat Cell Biol* **11**, 825-831.
39. Tsang WY, Bossard C, Khanna H, Peränen J, Swaroop A, Malhotra V and Dynlacht BD (2008) CP110 suppresses primary cilia formation through its interaction with CEP290, a protein deficient in human ciliary disease. *Dev Cell* **15**, 187-197.
40. Li W, You L, Cooper J, Schiavon G, Pepe-Caprio A, Zhou L, Ishii R, Giovannini M, Hanemann CO, Long SB, Erdjument-Bromage H, Zhou P, Tempst P and Giancotti FG (2010) Merlin/NF2 suppresses tumorigenesis by inhibiting the E3 ubiquitin ligase CRL4(DCAF1) in the nucleus. *Cell* **140**, 477-490.
41. Mund T, Lewis MJ, Maslen S and Pelham HR (2014) Peptide and small molecule inhibitors of HECT-type ubiquitin ligases. *Proc Natl Acad Sci U S A* **111**, 16736-16741.
42. Rossi M, Rotblat B, Ansell K, Amelio I, Caraglia M, Misso G, Bernassola F, Cavasotto CN, Knight RA, Ciechanover A and Melino G (2014) High throughput screening for inhibitors of the HECT ubiquitin E3 ligase ITCH identifies antidepressant drugs as regulators of autophagy. *Cell Death Dis* **5**, e1203.

43. Chen Z, Indjeian VB, McManus M, Wang L and Dynlacht BD (2002) CP110, a cell cycle-dependent CDK substrate, regulates centrosome duplication in human cells. *Dev Cell* **3**, 339-350.
44. Barbelanne M, Song J, Ahmadzai M and Tsang WY (2013) Pathogenic NPHP5 mutations impair protein interaction with Cep290, a prerequisite for ciliogenesis. *Hum Mol Genet* **22**, 2482-2494.
45. Barbelanne M, Hossain D, Chan DP, Peränen J and Tsang WY (2015) Nephrocystin proteins NPHP5 and Cep290 regulate BBSome integrity, ciliary trafficking and cargo delivery. *Hum Mol Genet* **24**, 2185-2200.
46. Tsang WY, Wang L, Chen Z, Sánchez I and Dynlacht BD (2007) SCAPER, a novel cyclin A-interacting protein that regulates cell cycle progression. *J Cell Biol* **178**, 621-633.
47. Moudjou M, Bordes N, Paintrand M and Bornens M (1996) gamma-Tubulin in mammalian cells: the centrosomal and the cytosolic forms. *J Cell Sci* **109**, 875-887.

2.11. Figures

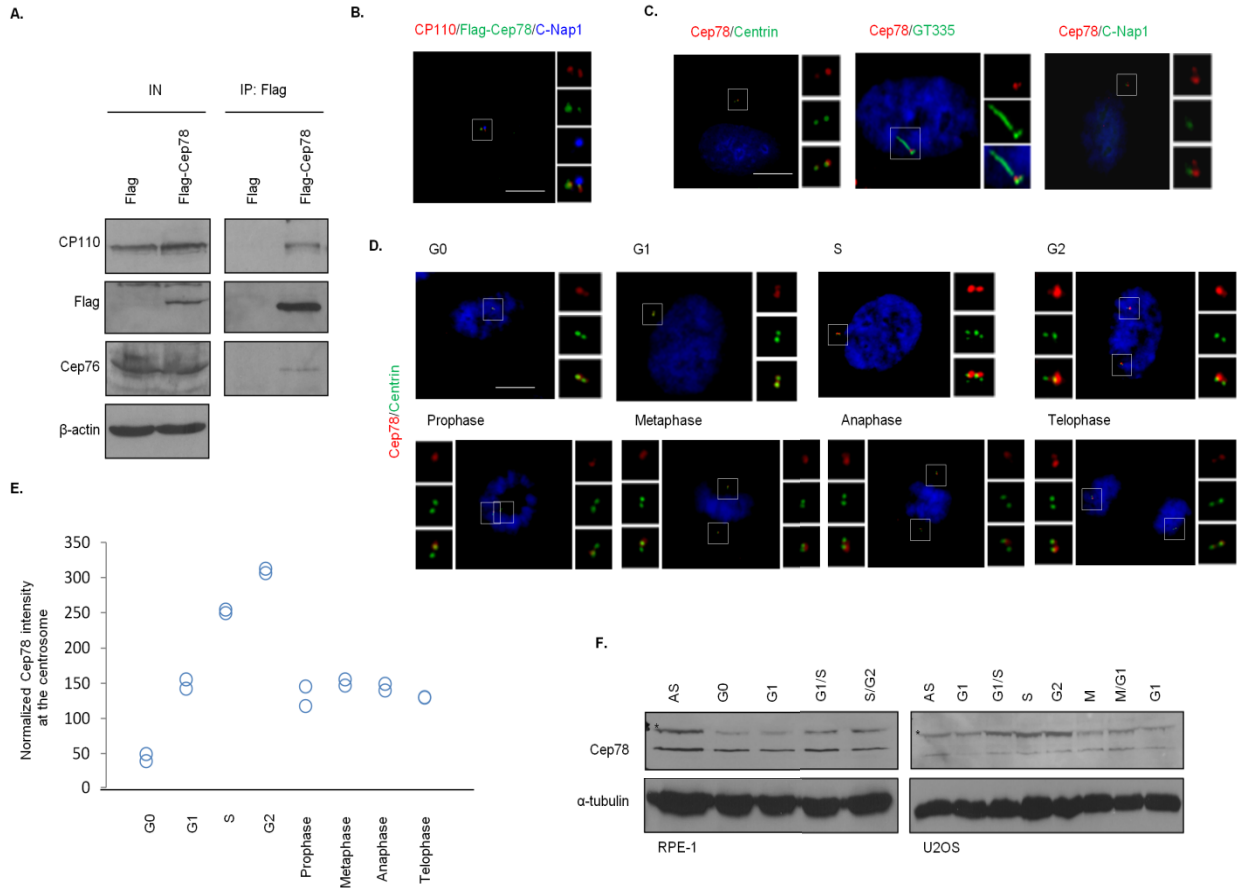


Figure 2.11.1. Cep78 interacts with Cep76 and CP110, localizes to the distal region of centrosomes and is cell cycle regulated.

(A) Flag or Flag-Cep78 was expressed in HEK293 cells. Lysates were immunoprecipitated with an anti-Flag antibody and Western blotted with the indicated antibodies. IN, input. β-actin was used as loading control. (B) RPE-1 cells expressing Flag-Cep78 were stained with antibodies against CP110 (red), Flag (green) and C-Nap1 (blue). Scale bar, 1 μm. (C) RPE-1 cells were stained with DAPI (blue) and antibodies against Cep78 (red) and centrin, glutamylated tubulin (GT335) or C-Nap1 (green). Scale bar, 1 μm. (D) RPE-1 cells in different phases of the cell cycle were stained with DAPI (blue) and antibodies against Cep78 (red) and centrin (green). Scale bar, 1 μm. (E) Cep78 fluorescence intensity at centrosomes was measured and quantitated.

At least 75 cells were quantitated in each cell cycle phase and two independent experiments were performed. (F) RPE-1 (left) and U2OS (right) lysates from different cell cycle phases were Western blotted with antibodies against Cep78. α -tubulin was used as loading control. AS, asynchronous. * denotes full-length Cep78.

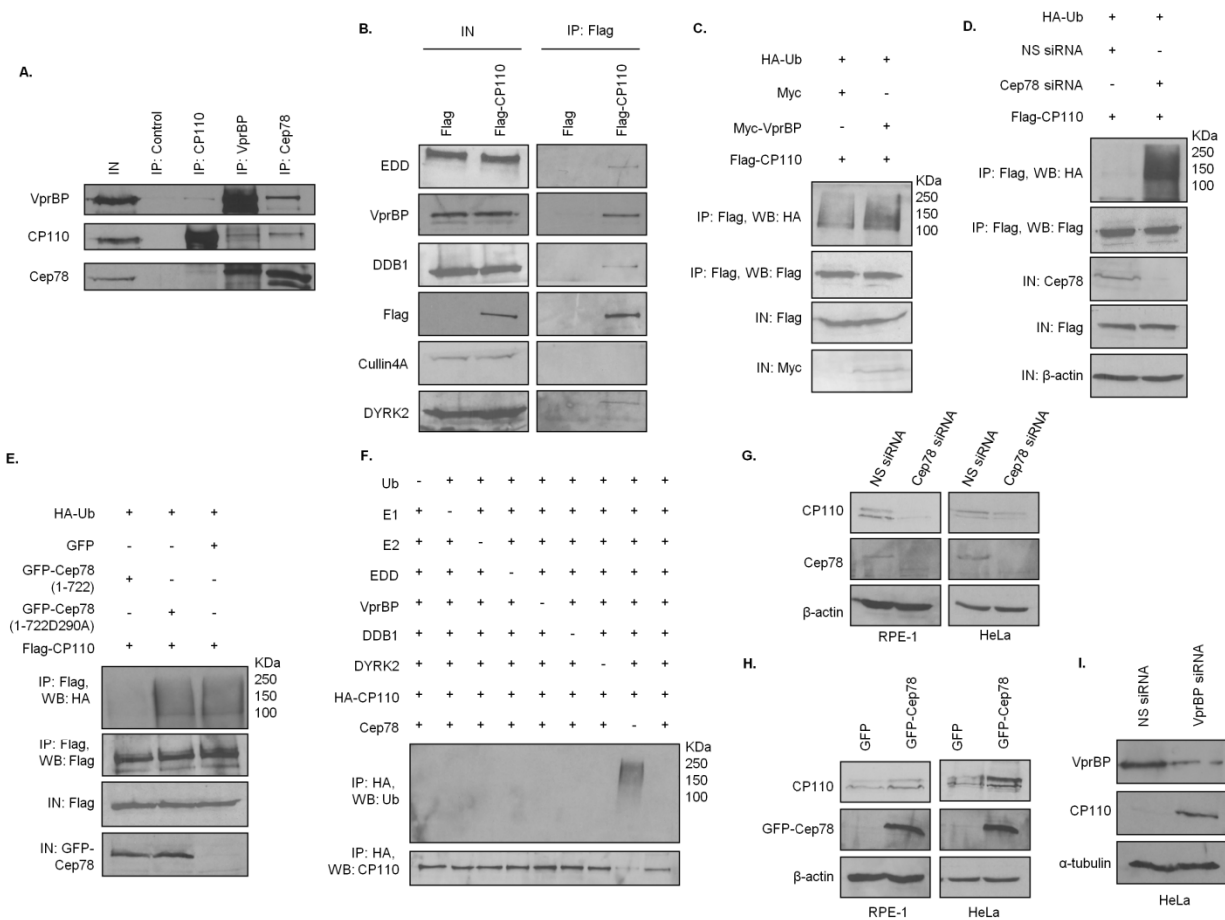


Figure 2.11.2. EDD-DYRK2-DDB1^{VprBP}-mediated ubiquitination and degradation of CP110 are regulated by Cep78

(A) HEK293 lysates were immunoprecipitated with an irrelevant (control), anti-CP110, anti-VprBP or anti-Cep78 antibody and Western blotted with the indicated antibodies. IN, input. (B) Flag or Flag-CP110 was expressed in HEK293 cells. Lysates were immunoprecipitated with an anti-Flag antibody and Western blotted with the indicated antibodies. IN, input. (C) Flag-CP110 was co-expressed with HA-Ub and Myc or Myc-VprBP in HEK293 cells. Lysates were immunoprecipitated with an anti-Flag antibody in 1% SDS and Western blotted with the indicated antibodies. IN, input. (D) HEK293 cells were transfected with NS siRNA or Cep78 siRNA and constructs expressing Flag-CP110 and HA-Ub. Lysates were immunoprecipitated with an anti-Flag antibody in 1% SDS and Western blotted with the indicated antibodies. IN, input. β -actin was used as loading control. (E) Flag-CP110 was co-expressed with HA-Ub and GFP, GFP-tagged Cep78 wild type (1-722) or mutant refractory to VprBP binding (1-722D290A) in HEK293 cells. Lysates were immunoprecipitated with an anti-Flag antibody in

1% SDS and Western blotted with the indicated antibodies. IN, input. (F) *In vitro* ubiquitination assays were performed with HA-CP110 as a substrate in the presence of purified Ub, E1, E2, EDD1, DYRK2, DDB1, VrpBP and Cep78 in various combinations. Ubiquitinated and non-ubiquitinated CP110 were detected by immunoblotting with anti-Ub and anti-CP110 antibodies, respectively. (G) RPE-1 or HeLa cells were transfected with NS siRNA or Cep78 siRNA. Lysates were Western blotted with the indicated antibodies. β -actin was used as loading control. (H) RPE-1 or HeLa cells were transfected with construct expressing GFP or GFP-Cep78. Lysates were Western blotted with the indicated antibodies. β -actin was used as loading control. (I) HeLa cells were transfected with NS siRNA or VrpBP siRNA. Lysates were Western blotted with the indicated antibodies. α -tubulin was used as loading control.

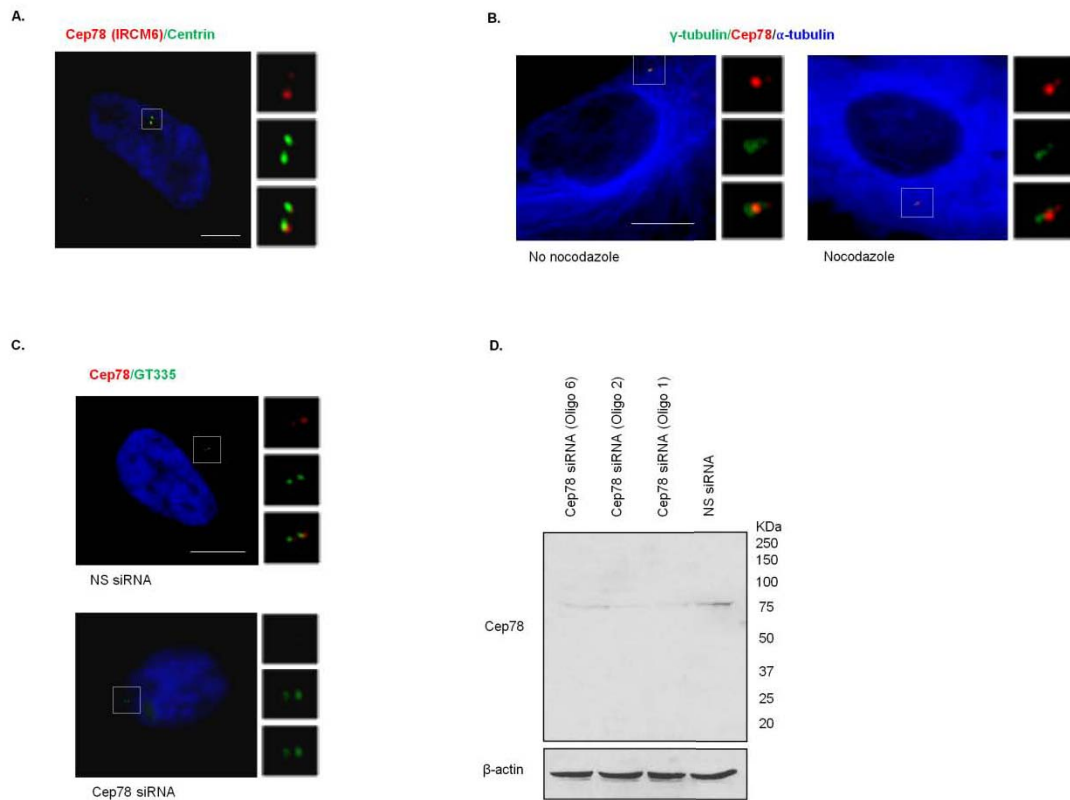


Figure 2.11.3. Characterization of Cep78

(A) RPE-1 cells were stained with DAPI (blue) and antibodies against centrin (green) and Cep78 raised against the C-terminal region of the protein (IRCM6, red). Scale bar, 1 μ m. (B) RPE-1 cells untreated or treated with 10 μ M nocodazole for 1 hour to induce microtubule depolymerization were stained with antibodies against γ -tubulin (green), α -tubulin (blue) and Cep78 (red). Scale bar, 1 μ m. (C) RPE-1 cells transfected with NS siRNA or Cep78 siRNA were stained with DAPI (blue) and antibodies against Cep78 (red) and polyglutamylated tubulin (GT335, green). Scale bar, 1 μ m. (D) RPE-1 cells were transfected with NS siRNA or Cep78 siRNA (oligo 1, 2 or 6). Lysates were Western blotted with antibody against Cep78. β -actin was used as loading control.

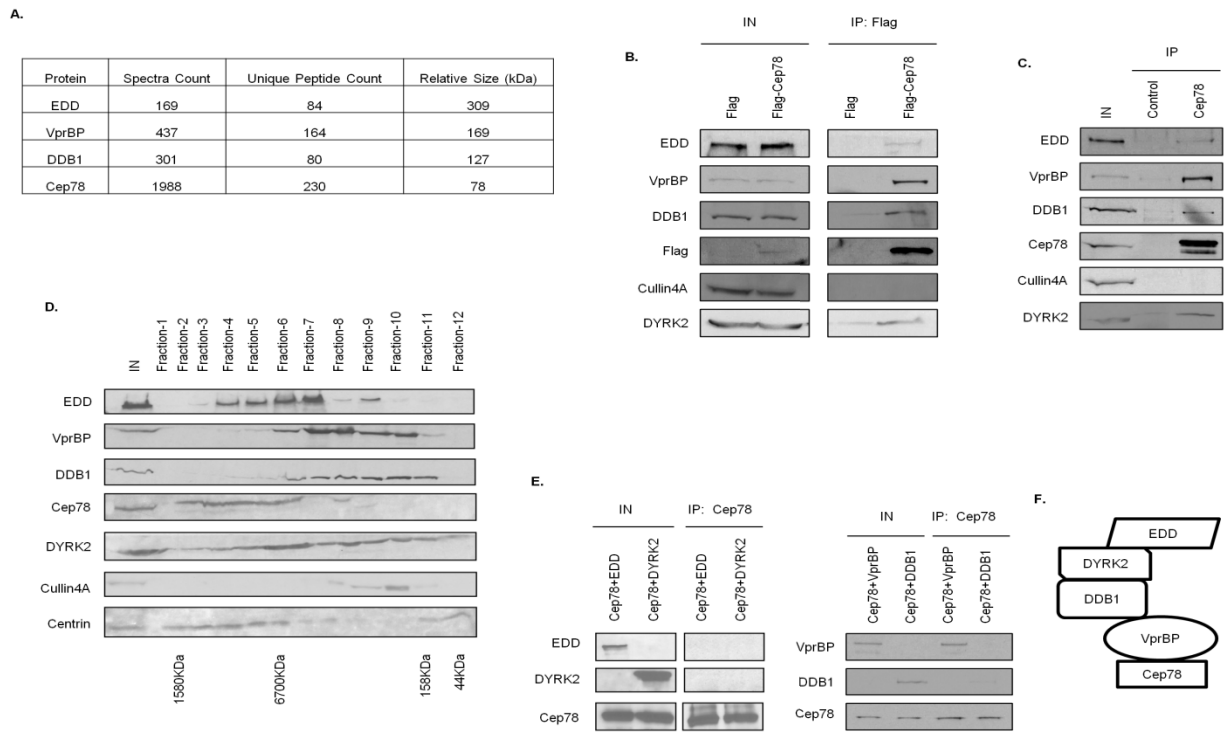


Figure 2.11.4. Cep78 interacts with EDD-DYRK2-DDB1^{VprBP} through VprBP

(A) Flag-Cep78 protein complexes from HEK293 cells were immuno-purified and subjected to mass spectrometric analysis. (B) Flag or Flag-Cep78 was expressed in HEK293 cells. Lysates were immunoprecipitated with an anti-Flag antibody and Western blotted with the indicated antibodies. IN, input. (C) HEK293 lysates were immunoprecipitated with an irrelevant (control) or anti-Cep78 antibody and Western blotted with the indicated antibodies. IN, input. (D) HEK293 cell extracts were chromatographed on a Superpose-6 column and the resulting fractions (Fraction-1 to -12) were Western blotted with the indicated antibodies. IN, input. (E) Purified Cep78 was mixed with purified EDD, DYRK2, DDB1 or VprBP. Proteins were immunoprecipitated with an anti-Cep78 antibody and Western blotted with the indicated antibodies. IN, input. (F) Proposed architecture of the Cep78-bounded EDD-DYRK2-DDB1^{VprBP} complex.

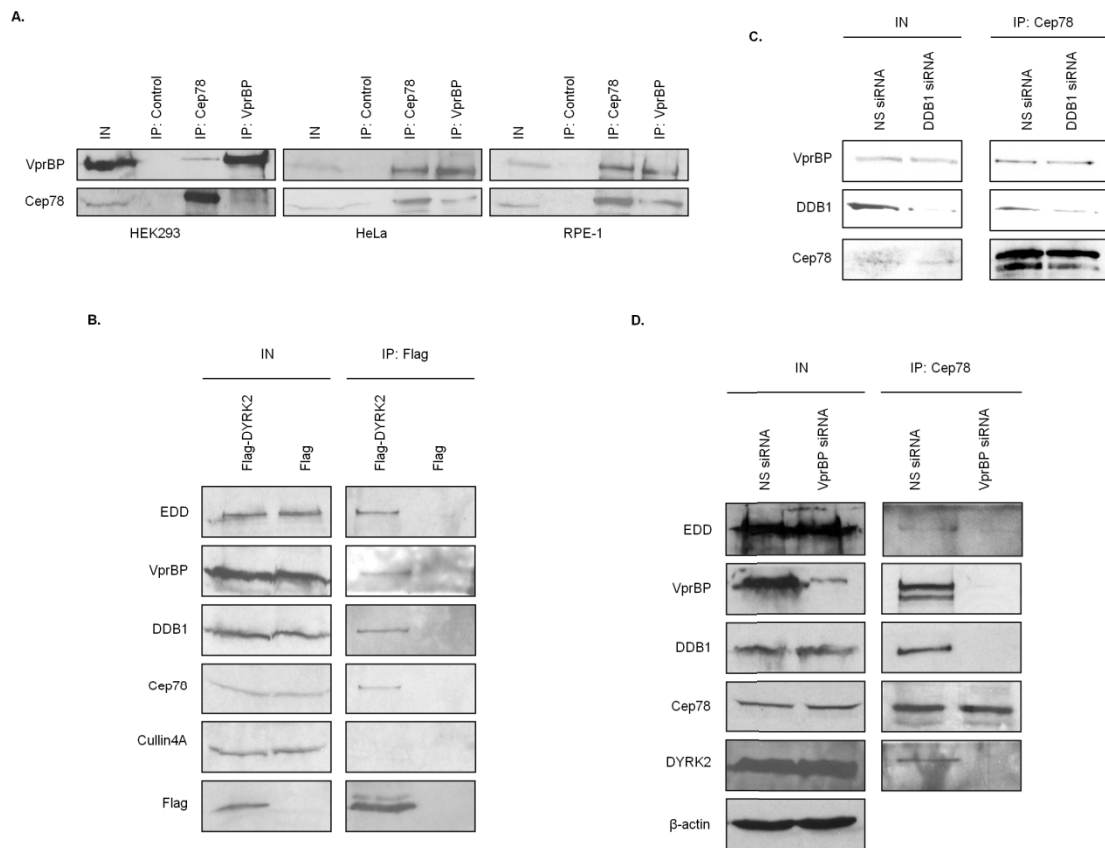


Figure 2.11.5. Cep78 binds to EDD-DYRK2-DDB1^{VprBP} through VprBP

(A) HEK293, HeLa or RPE-1 lysates were immunoprecipitated with an anti-Flag (control), anti-Cep78 or anti-VprBP antibody and Western blotted with the indicated antibodies. IN, input. (B) Flag or Flag-DYRK2 was expressed in HEK293 cells. Lysates were immunoprecipitated with an anti-Flag antibody and Western blotted with the indicated antibodies. IN, input. (C, D) HEK293 cells were transfected with NS, DDB1 or VprBP siRNA. Lysates were immunoprecipitated with an anti-Cep78 antibody and Western blotted with the indicated antibodies. IN, input. β -actin was used as loading control.

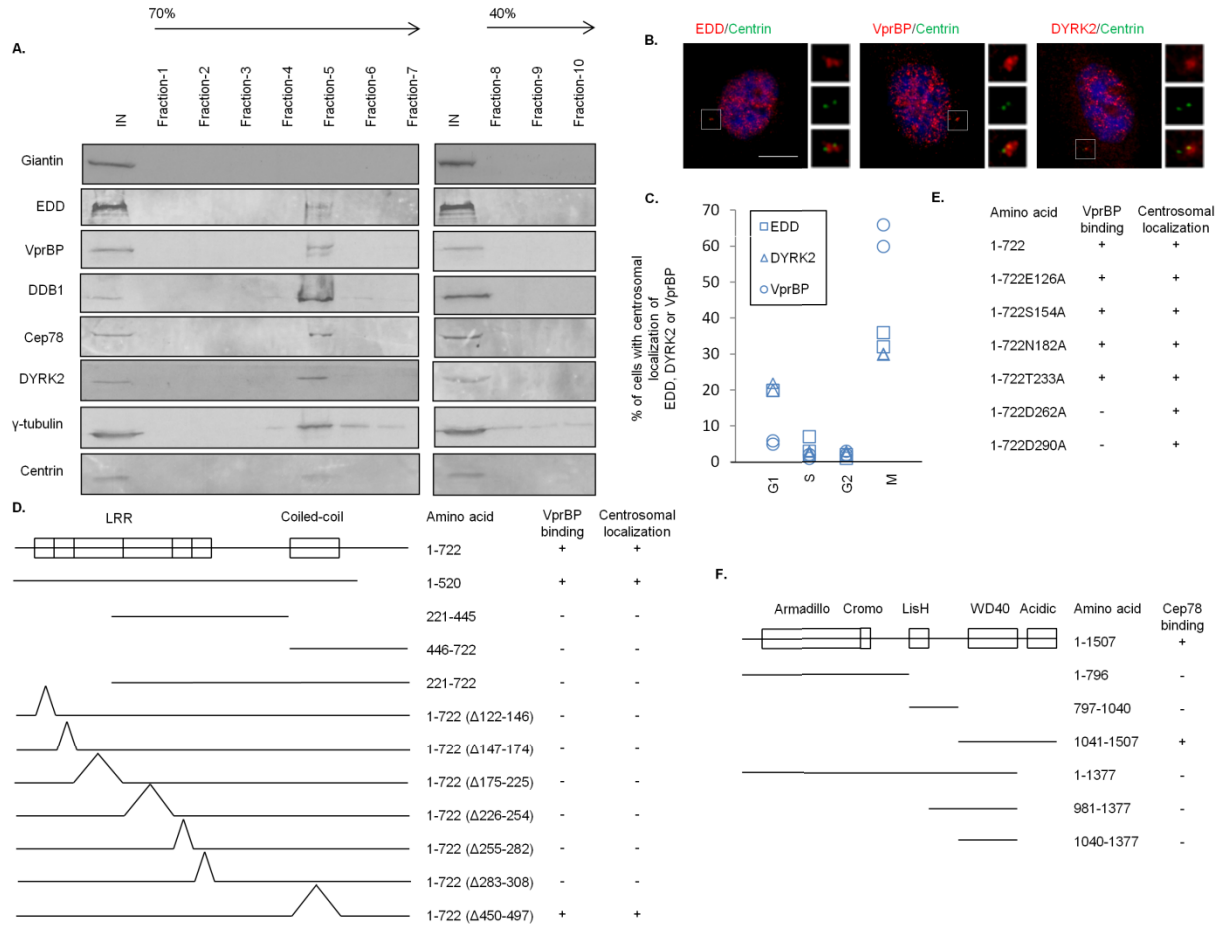


Figure 2.11.6. EDD-DYRK2-DDB1^{VprBP} is present at the centrosome and mapping functional domains of Cep78 and VprBP

(A) Centrosomes from Jurkat cells were purified through a 40%-70% sucrose gradient, and the resulting fractions were Western blotted with the indicated antibodies. IN, input. γ -tubulin and centrin, positive control; giantin, negative control. (B) RPE-1 cells were stained with DAPI (blue) and antibodies against centrin (green) and EDD, DYRK2 and VprBP (red). Scale bar, 1 μ m. (C) The percentage of cells with centrosomal EDD, DYRK2 or VprBP staining across the cell cycle. At least 100 cells were scored in each cell cycle phase and two independent experiments were performed. (D, E) The ability of various Cep78 truncated, deletion and point mutants to interact with VprBP and localize to centrosomes. 1-722, full-length; Δ 122-146, deletion of the first LRR repeat; Δ 147-174, deletion of the second LRR repeat; Δ 175-225, deletion of the third LRR repeat; Δ 226-254, deletion of the fourth LRR repeat; Δ 255-282, deletion of the fifth LRR repeat; Δ 283-308, deletion of the sixth LRR repeat; Δ 450-497, deletion

of the coiled-coil domain. E126A, S154A, N182A, T233A, D262A and D290A, point mutations of the first, second, third, fourth, fifth and sixth LRR repeats, respectively. (F) The ability of various VprBP truncates to interact with Cep78. 1-1507, full-length.

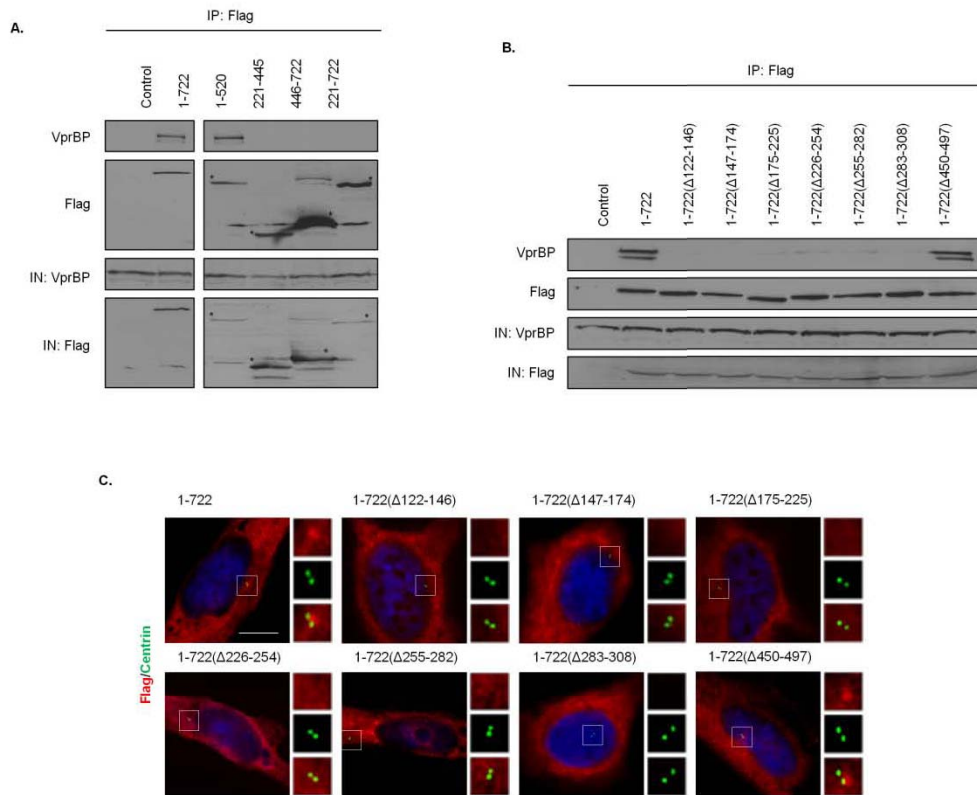


Figure 2.11.7. Mapping of the centrosomal localization and VprBP-binding domains of Cep78

(A, B) Flag (control), Flag-Cep78 full-length (1-722) or Flag-Cep78 truncated/deletion mutant was expressed in HEK293 cells. Lysates were immunoprecipitated with an anti-Flag antibody and Western blotted with the indicated antibodies. IN, input. * denotes bands corresponding to the expected proteins. (C) RPE-1 cells expressing Flag-Cep78 full-length or truncated/deletion mutant were stained with DAPI (blue) and antibodies against Flag (red) and centrin (green). Scale bar, 1 μ m.

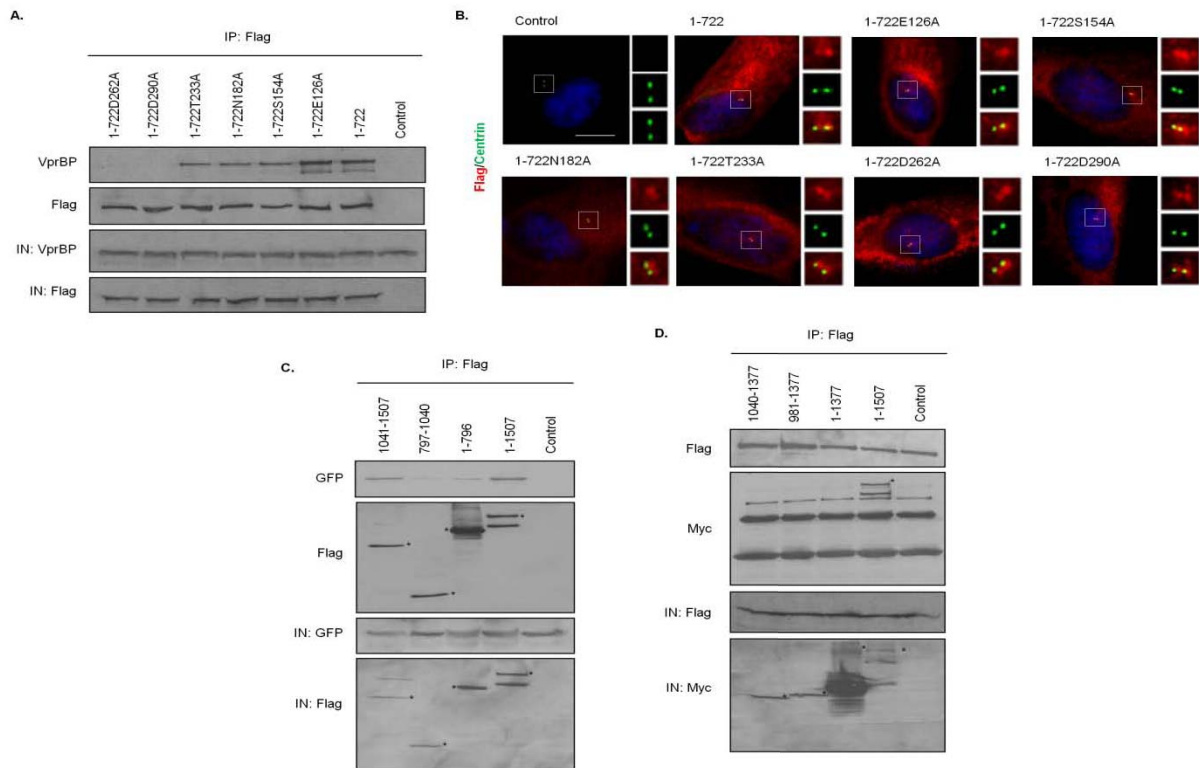


Figure 2.11.8. Mapping of interaction domains of Cep78 and EDD-DYRK2-DDB1^{VprBP}

(A) Flag (control), Flag-Cep78 full-length (1-722) or Flag-Cep78 point mutant was expressed in HEK293 cells. Lysates were immunoprecipitated with an anti-Flag antibody and Western blotted with the indicated antibodies. IN, input. (B) RPE-1 cells expressing Flag (control), Flag-Cep78 full-length or point mutant were stained with DAPI (blue) and antibodies against Flag (red) and centrin (green). Scale bar, 1 μ m. (C) Flag (control), Flag-VprBP full-length (1-1507) or Flag-VprBP truncated mutant was co-expressed with GFP-Cep78 in HEK293 cells. Lysates were immunoprecipitated with an anti-Flag antibody and Western blotted with the indicated antibodies. IN, input. (D) Myc, Myc-VprBP full-length or Myc-VprBP truncated mutant was co-expressed with Flag-Cep78 in HEK293 cells. Lysates were immunoprecipitated with an anti-Flag antibody and Western blotted with the indicated antibodies. IN, input; * de notes bands corresponding to the expected proteins.

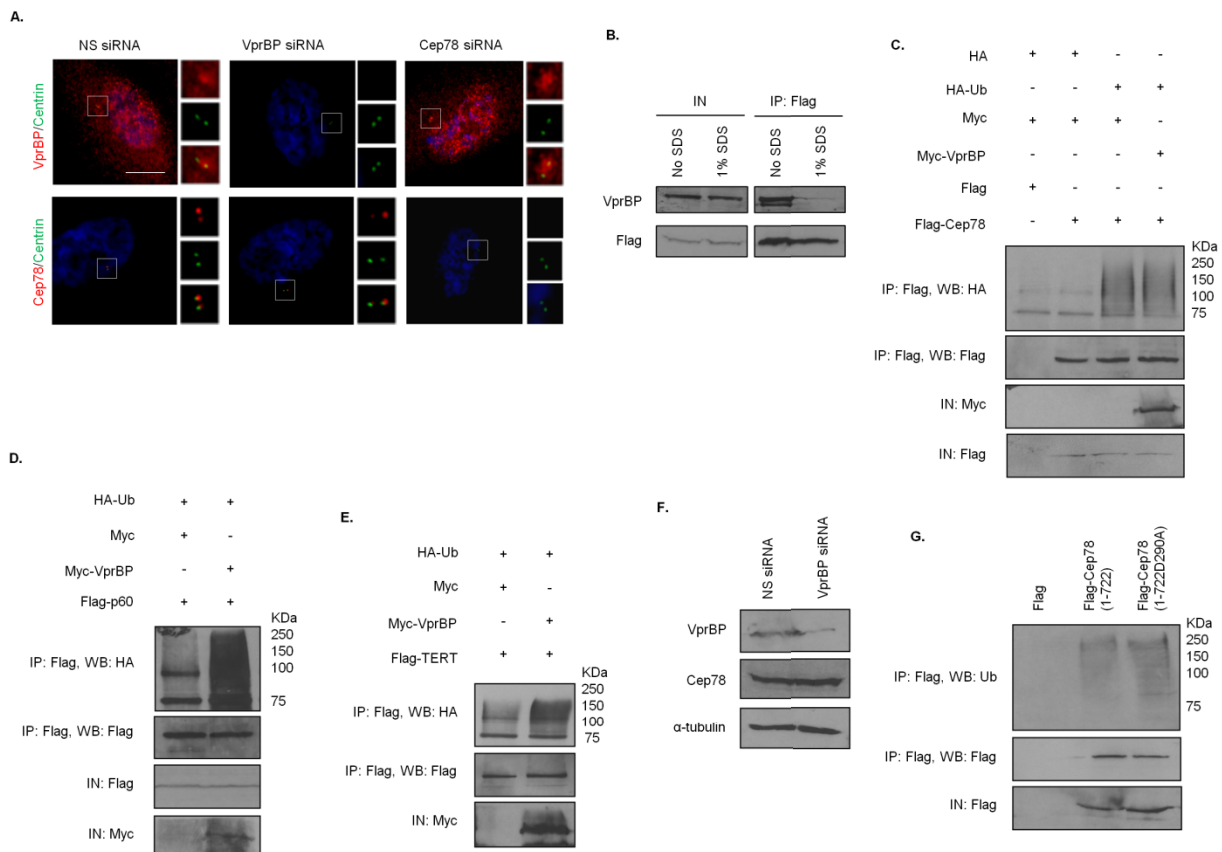


Figure 2.11.9. Cep78 and VprBP are independently recruited to the centrosome and Cep78 is not an EDD-DYRK2-DDB1^{VprBP} substrate

(A) RPE-1 cells transfected with NS siRNA, Cep78 siRNA or VprBP siRNA were stained with DAPI (blue) and antibodies against centrin (green) and Cep78 or VprBP (red). Scale bar, 1 μ m. (B) Flag-Cep78 was expressed in HEK293 cells. Lysates were immunoprecipitated with an anti-Flag antibody in the presence or absence of 1% SDS and Western blotted with the indicated antibodies. IN, input. (C) HEK293 cells expressing Flag or Flag-Cep78, HA or HA-Ub and Myc or Myc-VprBP, were synchronized in mitosis with nocodazole. Lysates were immunoprecipitated with an anti-Flag antibody in 1% SDS and Western blotted with the indicated antibodies. IN, input. (D, E) HA-Ub, Flag-katanin p60 or Flag-TERT, and Myc or Myc-VprBP, were co-expressed in HEK293 cells. Lysates were immunoprecipitated with an anti-Flag antibody in 1% SDS and Western blotted with the indicated antibodies. IN, input. (F) HEK293 cells transfected with NS siRNA or VprBP siRNA were synchronized in mitosis. Lysates were Western blotted with the indicated antibodies. α -tubulin was used as loading

control. (G) HEK293 cells expressing Flag, Flag-Cep78 wild type (1-722) or mutant (1-722D290A) were synchronized in mitosis. Lysates were immunoprecipitated with an anti-Flag antibody in 1% SDS and Western blotted with the indicated antibodies. IN, input.

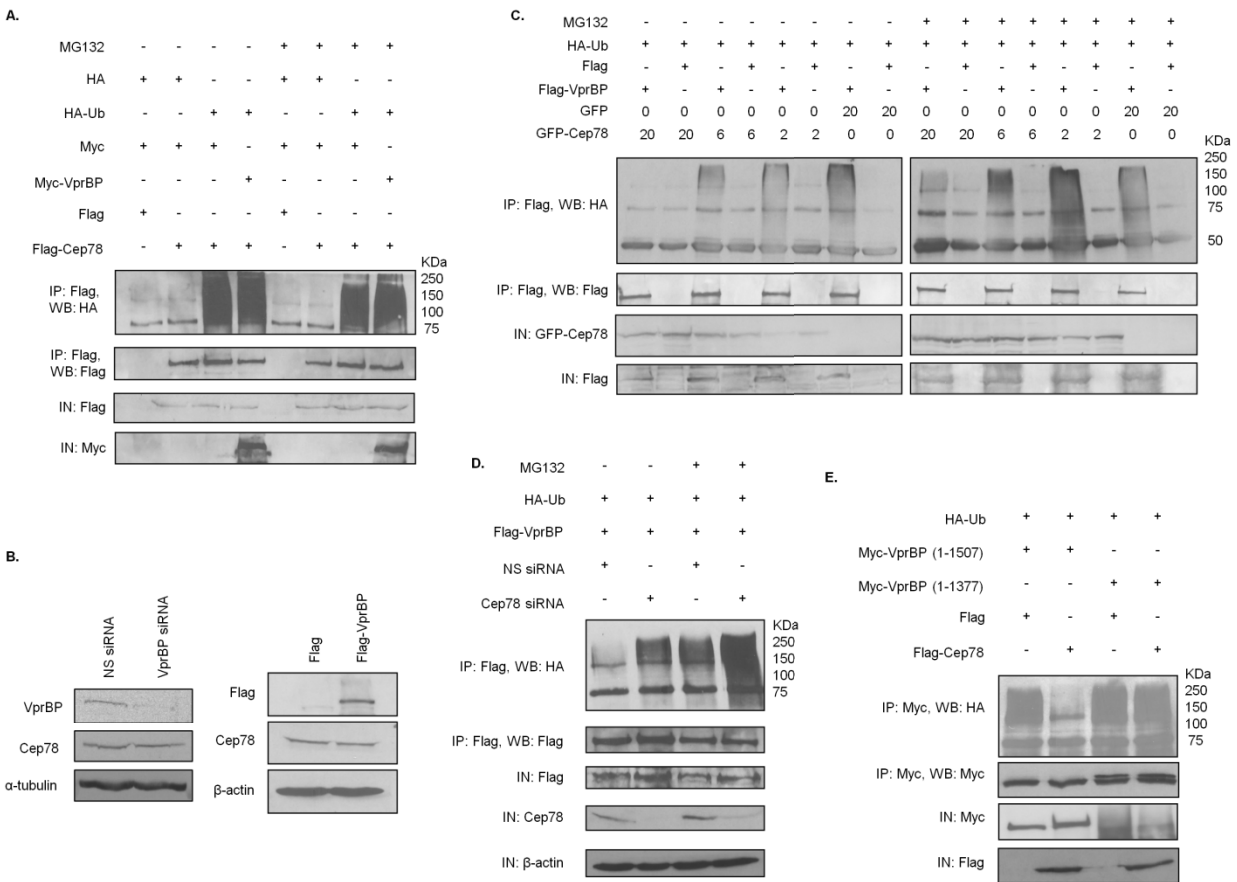


Figure 2.11.10. Cep78 is a negative regulator but not a substrate of EDD-DYRK2-DDB1^{VprBP}

(A) Flag or Flag-Cep78 was co-expressed with HA or HA-Ub and Myc or Myc-VprBP in HEK293 cells untreated or treated with MG132. Lysates were immunoprecipitated with an anti-Flag antibody in 1% SDS and Western blotted with the indicated antibodies. IN, input. (B) HEK293 cells were transfected with NS siRNA or VprBP siRNA (left) or construct expressing Flag or Flag-VprBP (right). Lysates were Western blotted with the indicated antibodies. α -tubulin (left) or β -actin (right) was used as loading control. (C) HEK293 cells transfected with HA-Ub, Flag or Flag-VprBP, and the indicated amount of GFP or GFP-Cep78 constructs in μ g were left untreated or treated with MG132. Lysates were immunoprecipitated with an anti-Flag antibody without SDS and Western blotted with the indicated antibodies. IN, input. (D) HEK293 cells transfected with NS siRNA or Cep78 siRNA and constructs expressing Flag-VprBP and HA-Ub were left untreated or treated with MG132. Lysates were immunoprecipitated with anti-Flag antibody without SDS and Western blotted with the indicated antibodies. IN, input. β -actin

was used as loading control. (E) Flag or Flag-Cep78 was co-expressed with HA-Ub and Myc-tagged VprBP full-length (1-1507) or VprBP refractory to Cep78 binding (1-1377) in HEK293 cells. Lysates were immunoprecipitated with anti-Myc antibody without SDS and Western blotted with the indicated antibodies. IN, input.

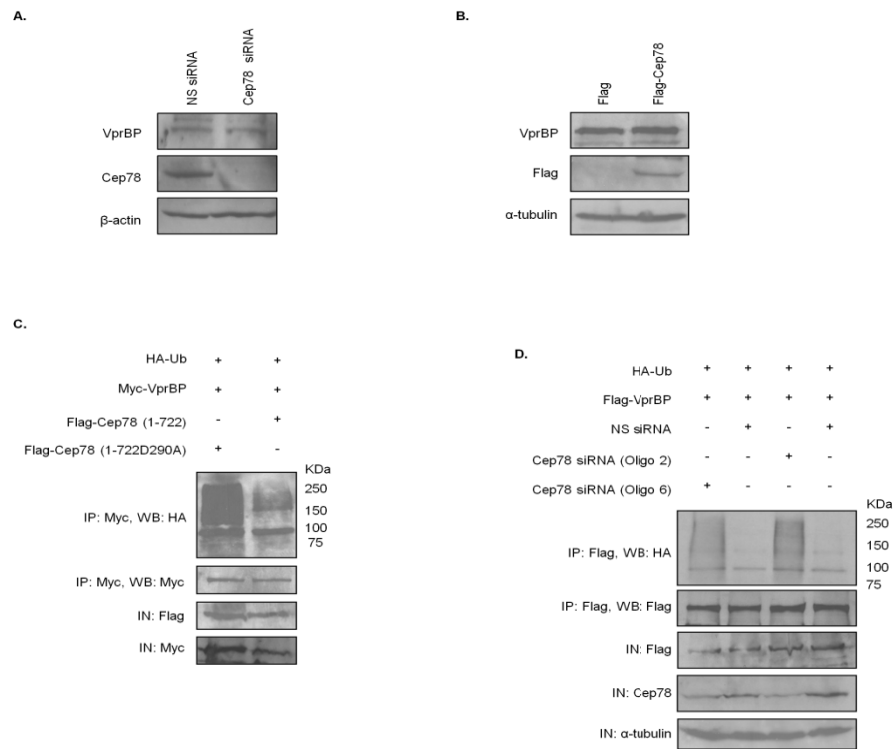


Figure 2.11.11. Depletion or expression Cep78 had no effect on VprBP protein levels and Cep78 inhibits EDD-DYRK2-DDB1^{VprBP}

(A) HEK293 cells were transfected with NS siRNA or Cep78 siRNA. Lysates were Western blotted with the indicated antibodies. β -actin was used as a loading control. (B) Flag or Flag-Cep78 was expressed in HEK293 cells. Lysates were Western blotted with the indicated antibodies. α -tubulin was used as a loading control. (C) Flag-Cep78 wild type (1-722) or mutant (1-722D290A) was co-expressed with HA-Ub and Myc-VprBP in HEK293 cells. Lysates were immunoprecipitated with an anti-Myc antibody without SDS and Western blotted with the indicated antibodies. IN, input. (D) HEK293 cells were transfected with NS siRNA or Cep78 siRNA (oligo 2 or oligo 6) and constructs expressing Flag-VprBP and HA-Ub. Lysates were immunoprecipitated with an anti-Flag antibody without SDS and Western blotted with the indicated antibodies. IN, input. α -tubulin was used as a loading control.

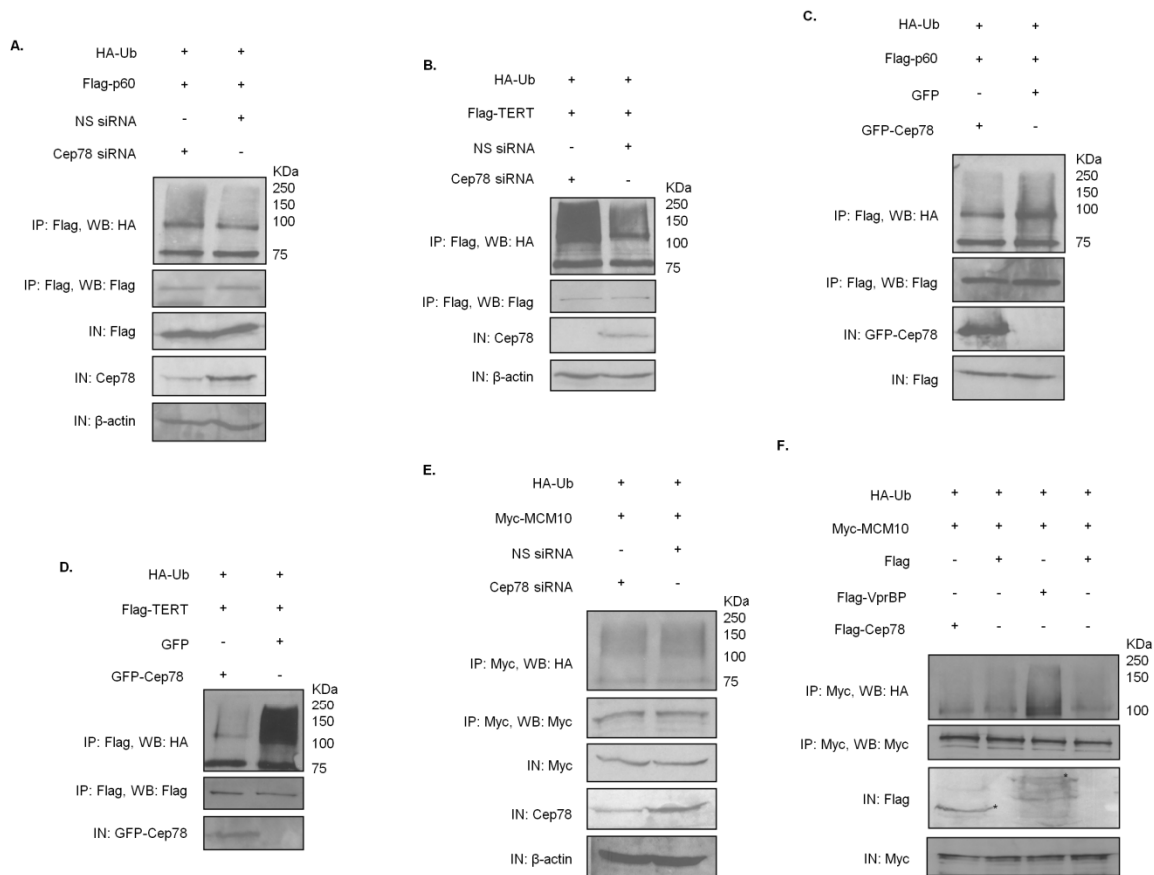


Figure 2.11.12. Cep78 modulates ubiquitination of two EDD-DYRK2-DBB1^{VprBP} substrates katanin p60 and TERT but not a CRL4^{VprBP} substrate MCM10

(A, B) HEK293 cells were transfected with NS siRNA or Cep78 siRNA and constructs expressing HA-Ub and Flag-katanin p60 or Flag-TERT. Lysates were immunoprecipitated with an anti-Flag antibody in 1% SDS and Western blotted with the indicated antibodies. IN, input. β -actin was used as a loading control. (C, D) HEK293 cells were transfected with constructs expressing HA-Ub, Flag-katanin p60 or Flag-TERT, and GFP or GFP-Cep78. Lysates were immunoprecipitated with an anti-Flag antibody in 1% SDS and Western blotted with the indicated antibodies. IN, input. (E) HEK293 cells were transfected with NS siRNA or Cep78 siRNA and constructs expressing HA-Ub and Myc-MCM10. Lysates were immunoprecipitated with an anti-Myc antibody in 1% SDS and Western blotted with the indicated antibodies. IN, input. β -actin was used as a loading control. (F) HEK293 cells were transfected with constructs expressing HA-Ub, Myc-MCM10, and Flag, Flag-Cep78 or Flag-VprBP. Lysates were

immunoprecipitated with an anti-Myc antibody in 1% SDS and Western blotted with the indicated antibodies. IN, input. * denotes bands corresponding to the expected proteins.

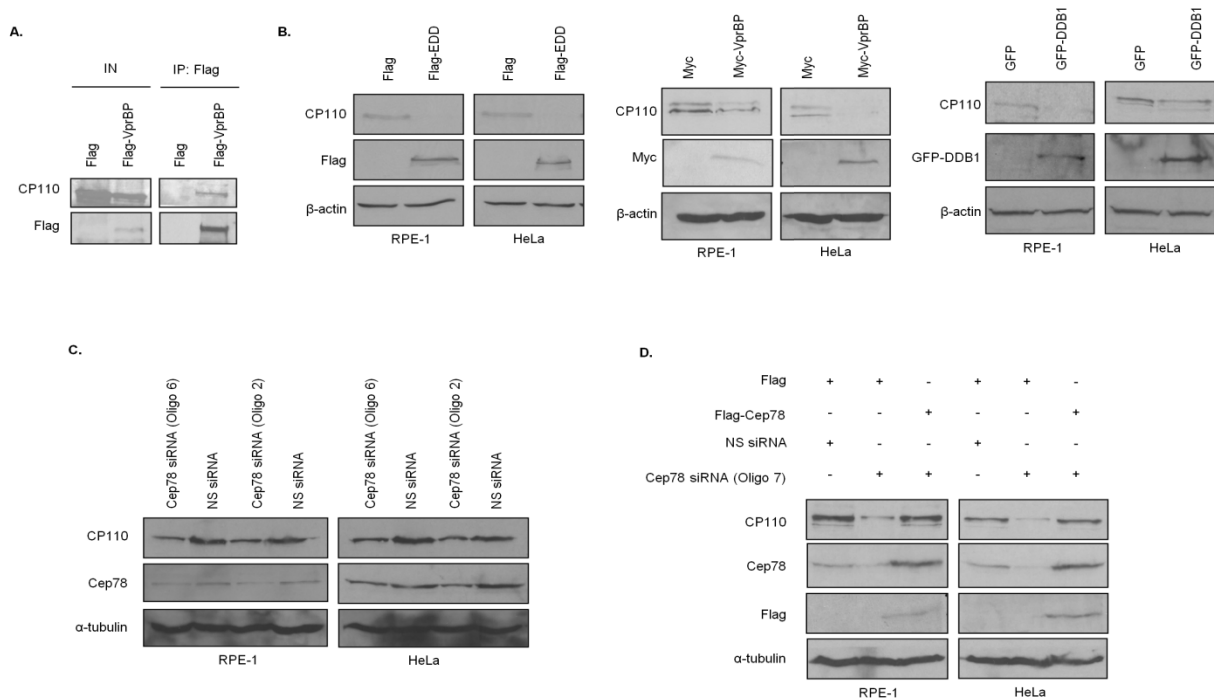


Figure 2.11.13. CP110 interacts with VprBP and its protein levels are dependent on EDD-DYRK2-DDB1^{VprBP} and Cep78

(A) Flag or Flag-VprBP was expressed in HEK293 cells. Lysates were immunoprecipitated with an anti-Flag antibody and Western blotted with the indicated antibodies. IN, input. (B) RPE-1 or HeLa cells were transfected with construct expressing Myc, Myc-VprBP, Flag, Flag-EDD, GFP or GFP-DDB1. Lysates were Western blotted with the indicated antibodies. β -actin was used as a loading control. (C) RPE-1 or HeLa cells were transfected with NS siRNA or Cep78 siRNA (oligo 2 or 6). α -tubulin was used as a loading control. (D) RPE-1 or HeLa cells were transfected with NS siRNA or Cep78 siRNA that targets the 3'UTR of Cep78 mRNA (oligo 7) and construct expressing Flag or Flag-Cep78. Lysates were Western blotted with the indicated antibodies. α -tubulin was used as a loading control.

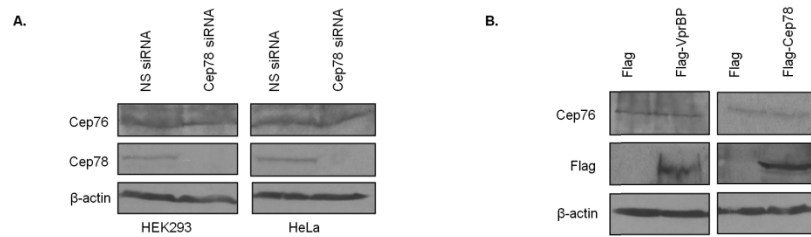


Figure 2.11.14. Cep76 protein levels are not affected by EDD-DYRK2-DDB1^{VprBP} or Cep78
 (A) HEK293 and HeLa cells were transfected with NS siRNA or Cep78 siRNA. Lysates were Western blotted with the indicated antibodies. β -actin was used as a loading control. (B) Flag, Flag-Cep78 or Flag-VprBP was expressed in HEK293 cells. Lysates were Western blotted with the indicated antibodies. β -actin was used as a loading control.

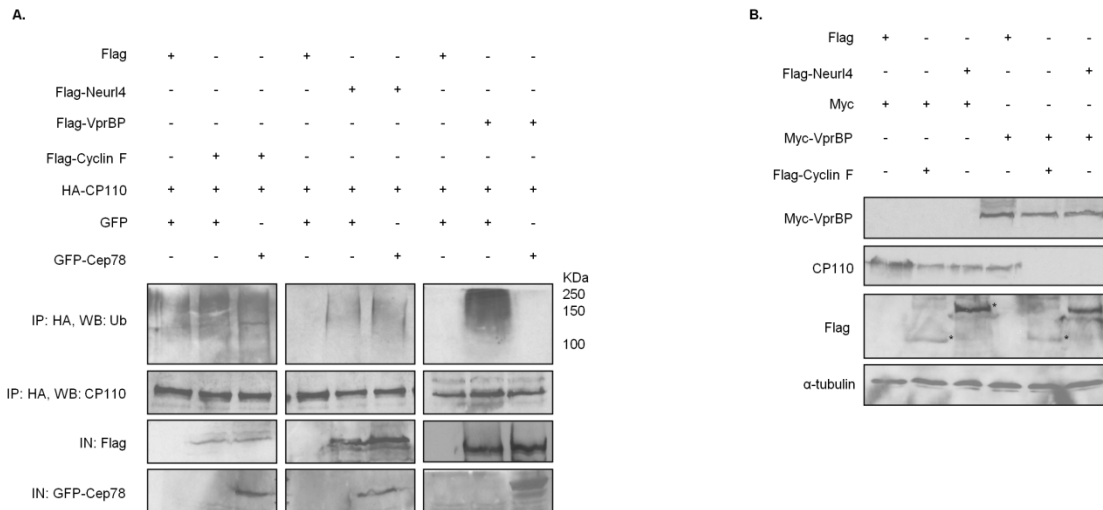


Figure 2.11.15. Cep78 regulates CP110 ubiquitination and protein levels through EDD-DYRK2-DDB1^{VprBP}

(A) HEK293 cells were transfected with constructs expressing Flag-Cyclin F, Flag-Neur14 or Flag-VprBP, GFP or GFP-Cep78, and HA-CP110. Lysates were immunoprecipitated with an anti-HA antibody in 1% SDS and Western blotted with the indicated antibodies. IN, input. (B) Flag-Cyclin F, Flag-Neur14 and Myc-VprBP were expressed singly or in combination in HeLa cells. Lysates were Western blotted with the indicated antibodies. α -tubulin was used as a loading control.* denotes bands corresponding to the expected proteins.

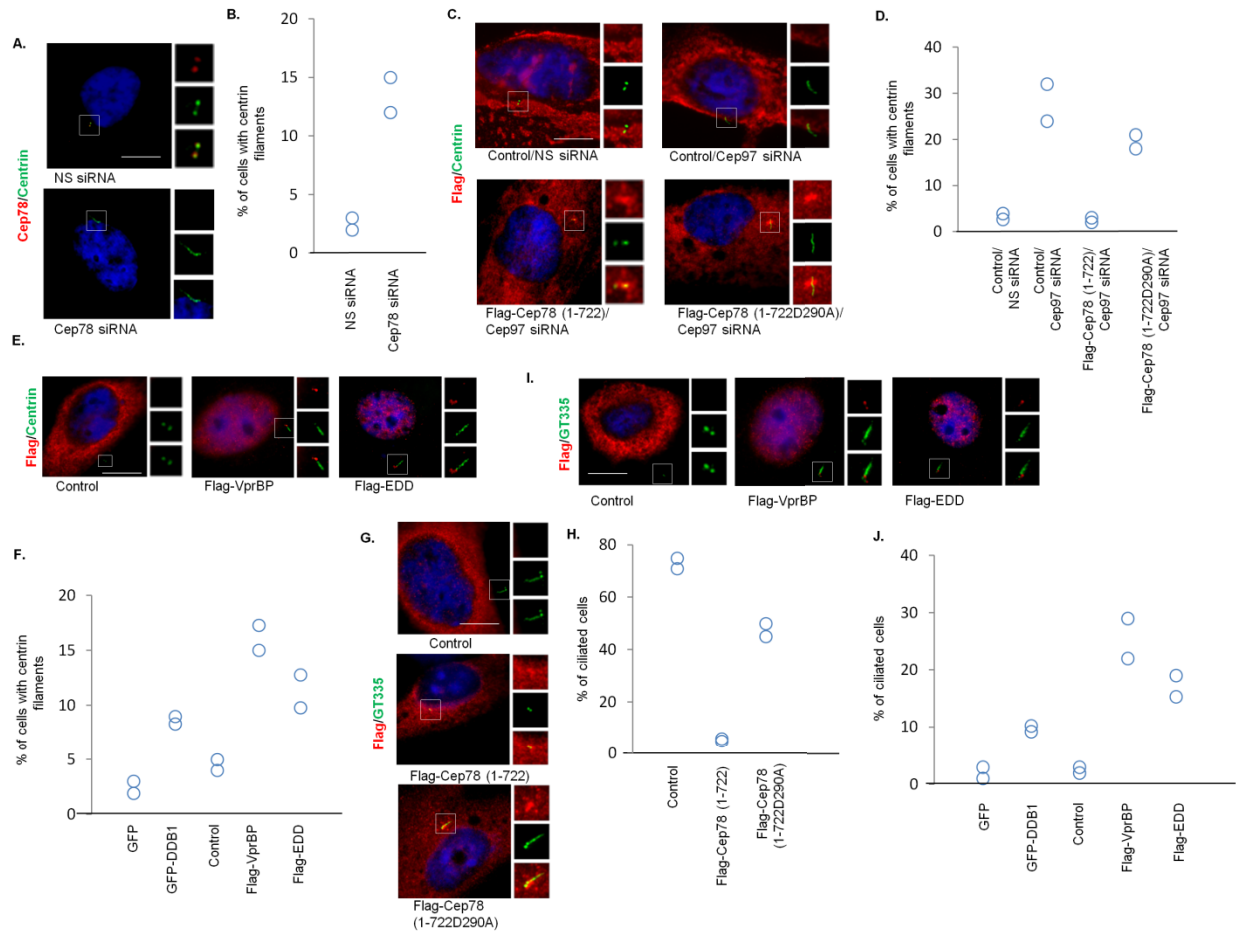


Figure 2.11.16. Cep78 and EDD-DYRK2-DDB1^{VprBP} control CP110-dependent centriole elongation in non-ciliated cells and cilia assembly in ciliated cells

(A) HeLa cells transfected with NS siRNA and Cep78 siRNA were stained with DAPI (blue) and antibodies against Cep78 (red) and centrin (green). Scale bar, 1 μ m. (C) HeLa cells transfected with NS siRNA or Cep97 siRNA and construct expressing an irrelevant Flag-tagged protein (control), Flag-Cep78 (1-722) or Flag-Cep78 (1-722D290A) were stained with DAPI (blue) and antibodies against Flag (red) and centrin (green). Scale bar, 1 μ m. (E) HeLa cells transfected with construct expressing an irrelevant Flag-tagged protein (control), Flag-EDD, Flag-VprBP were stained with DAPI (blue) and antibodies against Flag (red) and centrin (green). Scale bar, 1 μ m. (G) Quiescent RPE-1 cells expressing an irrelevant Flag-tagged protein (control), Flag-Cep78 (1-722) or Flag-Cep78 (1-722D290A) were stained with DAPI (blue) and antibodies against Flag (red) and glutamylated tubulin (GT335, green). Scale bar, 1 μ m. (I) Proliferating RPE-1 cells expressing an irrelevant Flag-tagged protein (control), Flag-EDD, Flag-VprBP were stained with DAPI (blue) and antibodies against Flag (red) and glutamylated tubulin (GT335,

green). Scale bar, 1 μm . (B, D, F) The percentage of cells with elongated centrioles (centrin filaments) was determined. (H, J) The percentage of ciliated cells was determined. In (B, D, F, H, J), at least 100 cells were scored in each condition and two independent experiments were performed.

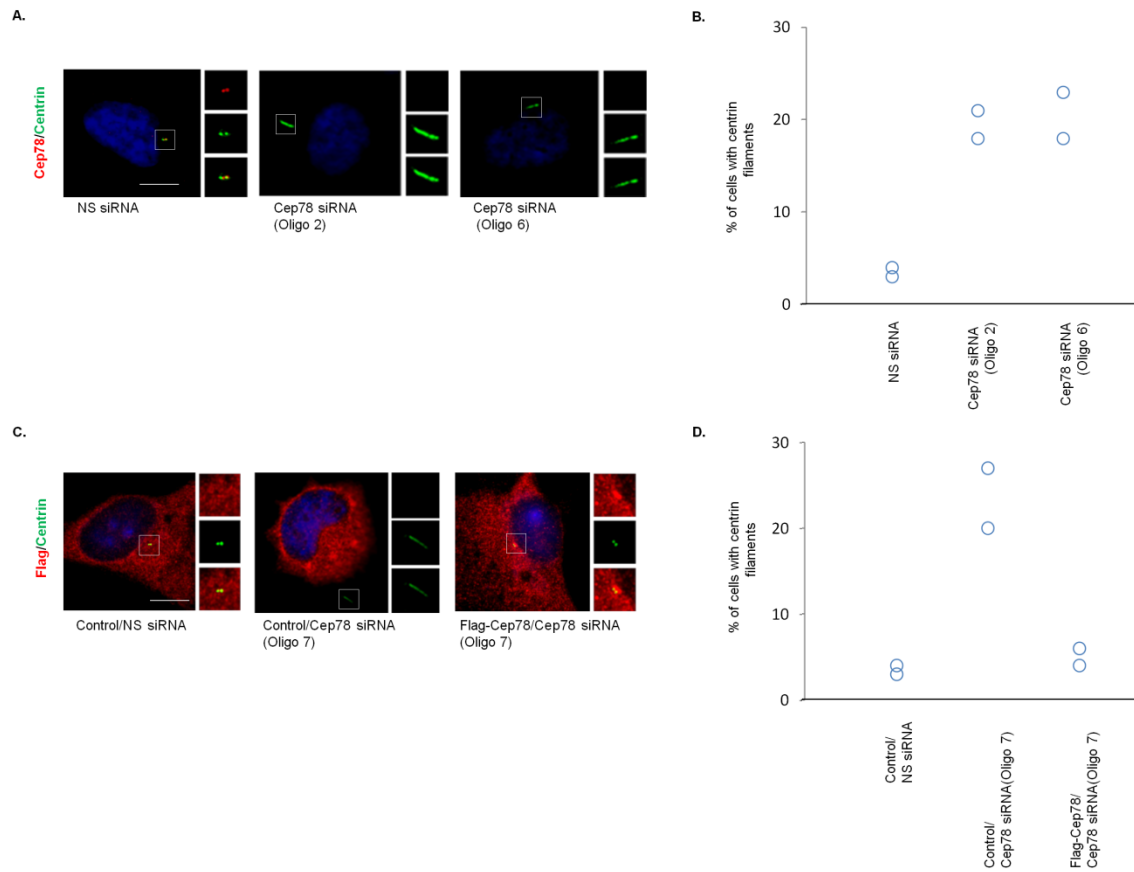


Figure 2.11.17. Cep78 controls CP110-dependent centriole elongation in non-ciliated cells

(A) HeLa cells transfected with NS siRNA and Cep78 siRNA (oligo 2 or oligo 6) were stained with DAPI (blue) and antibodies against Cep78 (red) and centrin (green). Scale bar, 1 μ m. (C) HeLa cells were transfected with NS siRNA or Cep78 siRNA that targets the 3'UTR of Cep78 mRNA (oligo 7) and construct expressing an irrelevant Flag-tagged protein (control) or Flag-Cep78. Cells were stained with DAPI (blue) and antibodies against Flag (red) and centrin (green). Scale bar, 1 μ m. (B and D) The percentage of cells with elongated centrioles (centrin filaments) was determined. At least 100 cells were scored in each condition and two independent experiments were performed.

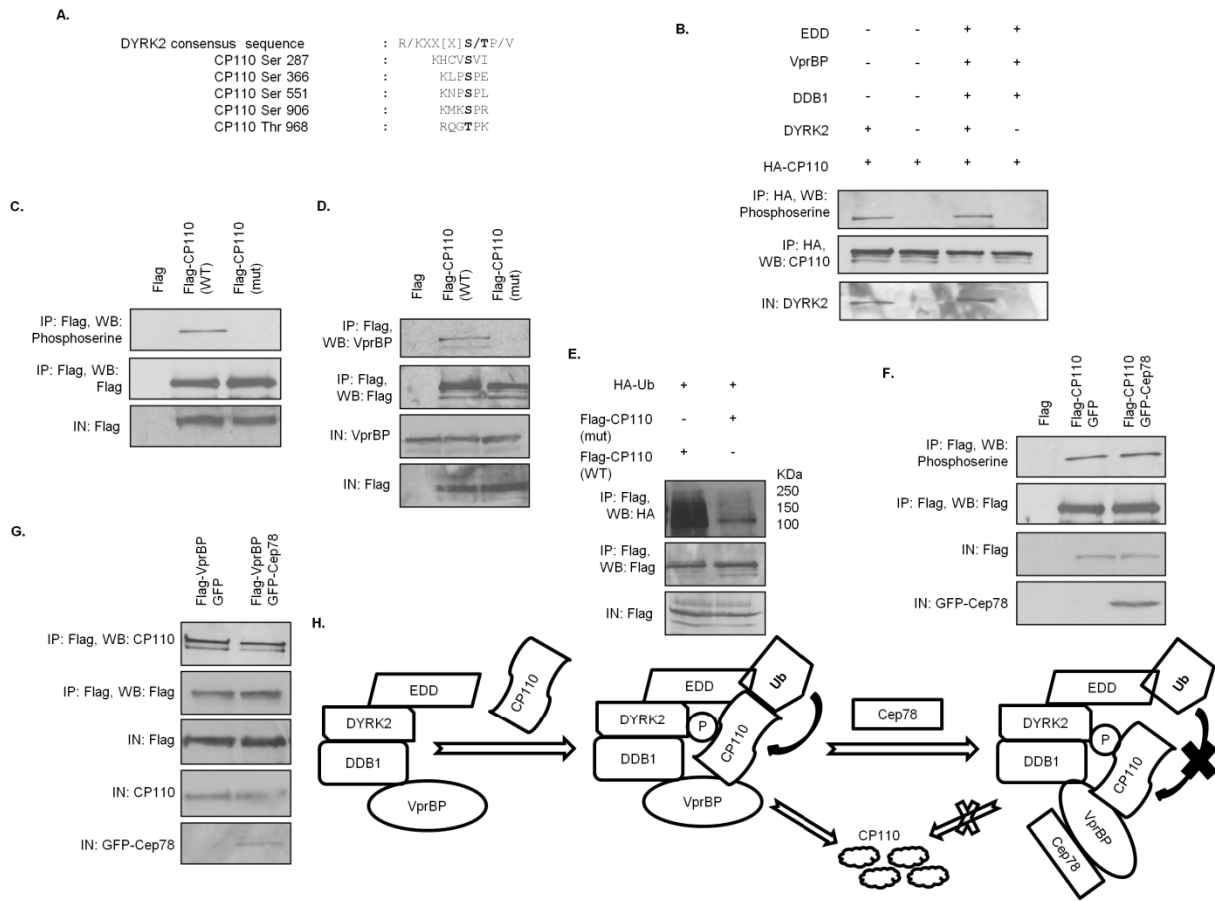


Figure 2.11.18. Mechanism underlying EDD-DYRK2-DDB1^{VprBP} inhibition by Cep78

(A) Putative DYRK2 phosphorylation sites of CP110. (B) *In vitro* kinase assays were performed using HA-CP110 as a substrate in the presence of DYRK2 or DYRK2, EDD, DDB1 and VprBP. Phosphorylation of CP110 was detected by immunoblotting with an anti-phosphoserine antibody. IN, input. (C-D) Flag, Flag-CP110 wild type (WT) or S287AS366AS551AS906A mutant (mut) was expressed in HEK293 cells. Lysates were immunoprecipitated with an anti-Flag antibody and Western blotted with the indicated antibodies. IN, input. (E) Flag-CP110 wild type (WT) or S287AS366AS551AS906A mutant (mut) was co-expressed with HA-Ub in HEK293 cells. Lysates were immunoprecipitated with an anti-Flag antibody in 1% SDS and Western blotted with the indicated antibodies. IN, input. (F) Flag-CP110 was co-expressed with GFP or GFP-Cep78 in HEK293 cells. Lysates were immunoprecipitated with an anti-Flag antibody and Western blotted with the indicated antibodies. IN, input. (G) Flag-VprBP was co-expressed with GFP or GFP-Cep78 in HEK293 cells. Lysates were immunoprecipitated with an anti-Flag antibody and Western blotted with the indicated antibodies. IN, input. (H) A model

illustrating the role of Cep78 in regulating the activity of EDD-DYRK2-DDB1^{VprBP}. Upon binding to VprBP, Cep78 induces a conformational change in VprBP. As a result, EDD is not longer in close proximity to CP110 and Ub cannot be transferred to CP110.

Chapter 3

HIV-1 Vpr hijacks EDD-DYRK2-DDB1^{DCAF1} to disrupt centrosome homeostasis

Delowar Hossain^{1,2}, Jérémy A. Ferreira Barbosa¹, Éric A. Cohen^{1,2,3}, and William Y. Tsang^{1,2,4,*}

¹ Institut de recherches cliniques de Montréal, Montreal, Quebec, Canada

² Division of Experimental Medicine, McGill University, Montreal, Quebec, Canada

³ Department of Microbiology, Infectiology and Immunology, Université de Montréal, Montreal, Quebec, Canada

⁴ Department of Pathology and Cell Biology, Université de Montréal, Montreal, Quebec, Canada

* To whom correspondence should be addressed: william.tsang@ircm.qc.ca

Phone: 1 (514) 987-5719

Fax: 1 (514) 987-5685

Keywords: centrosome/centriole/microtubule/HIV-1/Vpr/ubiquitin ligase/Cep78/CP110

Running title: Vpr usurps EDD-DYRK2-DDB1^{DCAF1} at the centrosome

3.1. Preface

As from the literature reviews, it is known that VprBP interacts with HIV-1 accessory protein Vpr, I would like to follow-up on my findings from chapter 2. In order to understand the role of Vpr in centrosome biology, I design the experiment whether Vpr specifically targets EDD-DYRK2-DDB1^{VprBP} (in chapter 2, I reported that this particular type of E3 ligase are localized at the centrosome) at the centrosome, and what are the consequences of being targeting the centrosomal substrate.

3.2. Abstract

Viruses exploit the host cell machinery for their own profit. To evade innate immune sensing and promote viral replication, the human immunodeficiency virus type 1 (HIV-1) subverts DNA repair regulatory proteins and induces G2/M arrest. The pre-integration complex of HIV-1 is known to traffic along microtubules and accumulate near the microtubule-organizing center. The centrosome is the major microtubule-organizing center in most eukaryotic cells, but precisely how HIV-1 impinges on centrosome biology remains poorly understood. We report that HIV-1 accessory protein viral protein R (Vpr) localizes to the centrosome through binding to DCAF1 and forms a complex with the ubiquitin ligase EDD-DYRK2-DDB1^{DCAF1} and Cep78, a resident centrosomal protein previously shown to inhibit EDD-DYRK2-DDB1^{DCAF1}. Vpr does not affect ubiquitination of Cep78. Rather, it enhances ubiquitination of an EDD-DYRK2-DDB1^{DCAF1} substrate CP110, leading to its degradation, and this effect can be overcome by Cep78 expression. Down-regulation of CP110 and elongation of centrioles provoked by Vpr are independent of G2/M arrest. Infection of T lymphocytes with HIV-1, but not with HIV-1 lacking Vpr, promotes CP110 degradation and centriole elongation. Elongated centrioles recruit more γ -tubulin to the centrosome and results in increased microtubule nucleation. Our results suggest that Vpr is targeted to the centrosome where it hijacks an ubiquitin ligase, disrupting organelle homeostasis which might contribute to HIV-1 pathogenesis.

3.3. Introduction

Viruses are pathogens that infect all life forms and reproduce inside living cells. To do so, they must be able to counteract and evade immune defences, and utilize cellular machinery from the host for their own replication. Human immunodeficiency virus type 1 (HIV-1) belongs to the lentivirus subgroup of retroviruses and is the casual agent of acquired immunodeficiency syndrome (1,2). The HIV-1 genome encodes five proteins essential for viral replication and four accessory proteins, namely, viral infectivity factor (Vif), viral protein U (Vpu), negative regulatory factor (Nef), and viral protein R (Vpr) (3,4). These accessory proteins are not absolutely essential for viral replication *in vitro*, but nevertheless play critical roles in viral infection, survival, and propagation *in vivo* (5-12). Vpr is among the least characterized in terms of function and mechanism of action. As a predominantly nuclear protein, Vpr is able to exert multiple effects on host cells by interacting with a cohort of cellular proteins (13-24). Among these, viral protein R binding protein (VprBP/DCAF1) is the first protein identified to bind Vpr (15,25). Current evidence suggests that DCAF1 can function as a protein kinase (26), a transcriptional repressor (27), and a substrate recognition subunit of two distinct multi-subunit ubiquitin ligases, EDD-DYRK2-DDB1^{DCAF1} and CRL4^{DCAF1} (28). EDD-DYRK2-DDB1^{DCAF1} is composed of DYRK2, EDD, DDB1, and DCAF1 subunits (29), whereas CRL4^{DCAF1} consists of Roc1, Cullin4, DDB1, and DCAF1 (30-32). Upon binding to an ubiquitin ligase, Vpr directs ubiquitination of novel substrates and accelerates ubiquitination of native substrates, leading to their premature degradation (16,18,20,33-35).

In contrast to CRL4^{DCAF1} which is present in the nucleus, EDD-DYRK2-DDB1^{DCAF1} exists in two distinct subcellular compartments, the nucleus and centrosome, which comprises a pair of centrioles surrounded by pericentriolar material from which microtubules emanate and elongate (36,37). In the nucleus, EDD-DYRK2-DDB1^{DCAF1} functions to suppress telomerase activity by targeting telomerase reverse transcriptase TERT for ubiquitination and degradation (36). The down-regulation of TERT is further enhanced by Vpr binding to EDD-DYRK2-DDB1^{DCAF1} (19). On the other hand, EDD-DYRK2-DDB1^{DCAF1} at the centrosome is known to ubiquitinate and induce the degradation of CP110, a protein which controls centriole length (37-41). The ability of EDD-DYRK2-DDB1^{DCAF1} to ubiquitinate CP110 is subjected to regulation by Cep78, a resident centrosomal protein which directly associates with, and inhibits, EDD-DYRK2-

DDB1^{DCAF1} in a cell cycle-dependent manner (37). It is currently unknown if Vpr has the capacity to hijack EDD-DYRK2-DDB1^{DCAF1} at the centrosome.

The centrosome is the major microtubule-organizing centers in most eukaryotic cells and acts as a central hub for coordinating a multitude of cellular events. Various molecules and cargos are known to transit through this organelle (42). The viral core of HIV-1 disassembles upon entry into the host cells and the resulting pre-integration complex traffics along microtubules and accumulates near the microtubule-organizing center (43-46). Another study reported that HIV-1 sub-viral particles accumulate at the centrosome under resting T cells through an unknown mechanism, and resumes infection upon stimulation (47). Interestingly, Vpr has been observed to disrupt certain protein interactions at the centrosome (48) and induce centrosome amplification and multipolar spindle formation (49,50), suggesting that this viral protein is capable of exerting an effect on the centrosome, either directly or indirectly. In spite of these observations, the extent to which Vpr modulates different aspects of centrosome biology and the underlying mechanisms have not been studied in detail.

3.4. Results

3.4.1. Vpr binds to Cep78 and EDD-DYRK2-DDB1^{DCAF1} and localizes to the centrosome

We have recently demonstrated that Cep78 forms a complex with EDD-DYRK2-DDB1^{DCAF1} through DCAF (37). Given that Vpr is known to associate with DCAF (15,25), we first asked if Vpr and Cep78 interact. Endogenous Cep78 and DCAF1 co-immunoprecipitated with HA-Vpr in HEK293 cells (Figure 3.11.1A-B). When DCAF1 was depleted with siRNA, very little Cep78 was detected in Vpr immunoprecipitates (Figure 3.11.1A). Moreover, endogenous DCAF1 and Cep78 bound to wild type Vpr, but neither protein interacted with a Vpr mutant refractory to DCAF1 binding (Vpr(Q65R)) (Figure 3.11.1B). Thus, Vpr is likely to associate with Cep78 through DCAF1, and these results are consistent with the findings that the Vpr- and Cep78-binding sites of DCAF1 are non-overlapping. Vpr binds to the WD40 domain of DCAF (15,51), whereas Cep78 binds to the acidic domain of DCAF1(37).

Next, we explored whether Vpr might specifically bind to the Cep78/EDD-DYRK2-DDB1^{DCAF1} complex, which normally forms at the centrosome. We expressed Flag-Cep78 and HA-Vpr in HEK293 cells, performed anti-Flag immunoprecipitations, and demonstrated that Cep78 binds to EDD-DYRK2-DDB1^{DCAF1} but not to CRL4^{DCAF1}, as expected (37), and Vpr (Figure 3.11.1C). Wild type Vpr co-localized with endogenous Cep78 in ~20-25% of transfected HeLa cells, indicating that this viral protein is targeted to the centrosome in some contexts (Figure 3.11.2A-B). In contrast, Vpr(Q65R) did not exhibit centrosomal localization (Figure 3.11.2A-B). Taken together, these data suggest that Vpr engages in a complex with EDD-DYRK2-DDB1^{DCAF1} and Cep78 at the centrosome through binding to DCAF1.

3.4.2. Vpr hijacks EDD-DYRK2-DDB1^{DCAF1} to enhance ubiquitination and degradation of CP110

To explore the relevance of Vpr-binding to EDD-DYRK2-DDB1^{DCAF1} and Cep78, we tested if Vpr might promote ubiquitination of proteins at the centrosome. The ubiquitination levels of Cep78, an inhibitor and non-substrate of EDD-DYRK2-DDB1^{DCAF1} (37), remained the same upon Vpr expression (Figure 3.11.3A). Likewise, centrosomal localization and steady-state levels of Cep78 were not altered by wild type Vpr or Vpr(Q65R) (Figures 3.11.2A, 3.11.2C, 3.11.3A-C). On the contrary, ubiquitination of CP110, a known centrosomal EDD-DYRK2-DDB1^{DCAF1} substrate (37), became greatly enhanced by Vpr (Figure 3.11.3D). This was accompanied by a decrease in CP110 protein levels (Figure 3.11.3D-H), and a loss of

centrosomal CP110 staining by immunofluorescence (Figure 3.11.4A-B). Notably, diminished levels of CP110 were specifically induced by wild type Vpr but not Vpr(Q65R) mutant (Figures 3.11.3G-H, 3.11.4A-B), and could be rescued by addition of a proteasome inhibitor MG132 (Figure 3.11.5A-B) or depletion of DCAF1 (Figure 3.11.5C-D). Furthermore, co-expression of Cep78 drastically reduced ubiquitination of CP110 (Figure 3.11.3D) and restored endogenous CP110 to wild type levels (Figures 3.11.3E-F and 3.11.8A-B). These data indicate that Vpr subverts centrosomal EDD-DYRK2-DDB1^{DCAF1} to accelerate ubiquitination and proteasomal degradation of a native substrate CP110, and these effects can be counteracted by over-expression of Cep78.

3.4.3. Vpr induces centriole elongation through CP110 degradation

Previously, it has been shown that depletion of CP110 induces the formation of overly long or elongated centrioles, represented by γ -tubulin filaments, in non-ciliated or poorly ciliated cells including HeLa (38-41). This phenotype can also be recapitulated by CP110 loss resulting from ablation of Cep78 or over-expression of EDD-DYRK2-DDB1^{DCAF1} (37). To further substantiate our observations that Vpr enhances degradation of CP110, we found that wild type Vpr provokes centriole elongation, whereas Vpr(Q65R) mutant could not (Figure 3.11.4A, C). Of note, wild type Vpr also induced centrosome amplification (>2 γ -tubulin foci; Figure 3.11.4A, D), consistent with a previous report (50), but this phenotype is unlikely to be a consequence of CP110 loss since excessive CP110, rather than loss of CP110, drives centrosome amplification (52).

3.4.4. Vpr-induced CP110 degradation and centriole elongation are independent of G2/M arrest

A recent study showed that Vpr associates with the SLX4 complex to induce chromosomal instability, triggering activation of DNA damage response (DDR) pathways and cell cycle arrest at the G2/M phase (20), although this is debated (53). Coincidentally, CP110 has been documented to undergo ubiquitination by SCF^{cyclinF} and EDD-DYRK2-DDB1^{DCAF1} (37,52), and subsequently proteasomal degradation, in G2/M. Thus, we sought to address whether, or not, down-regulation of CP110 induced by Vpr is due to prolonged G2/M arrest. For this purpose, we utilized a well-characterized Vpr mutant Vpr(R80A), which, in contrast to Vpr(Q65R), can bind to DCAF1 but is unable to provoke G2/M arrest ((54,55) and Figure 3.11.6A). Similar to wild type Vpr, Vpr(R80A) was detected at the centrosome in ~20-25% of transfected cells (Figure

3.11.6B-C). Next, we investigated the consequences of expressing Vpr(R80A) on CP110 and centriole length. Wild type Vpr and Vpr(R80A) were equally able to enhance CP110 ubiquitination (Figure 3.11.6D), causing a diminution of CP110 levels (Figure 3.11.6E-F) and immunostaining at the centrosome (Figure 3.11.7A-B). Furthermore, wild type Vpr and Vpr(R80A) induced γ -tubulin filament formation to similar extent (Figure 3.11.7A, C). Down-regulation of CP110 provoked by wild type Vpr or Vpr(R80A) could be rescued by ectopic expression of Cep78 (Figure 3.11.8A-D). Remarkably, unlike wild type Vpr, Vpr(R80A) did not induce centrosome amplification (Figure 3.11.7A, D). These data suggest that CP110 down-regulation and centriole elongation could be attributed to subversion of EDD-DYRK2-DDB1^{DCAF1} rather than G2/M arrest. On the contrary, the other phenotype caused by Vpr, namely centrosome amplification, is dependent on cell cycle arrest at the G2/M phase.

3.4.5. Vpr induces CP110 degradation and centriole elongation in infected T cells

We have thus far shown that Vpr induces the loss of CP110 in two model cell lines, HEK293 and HeLa. However, it remains unknown if this accessory protein could trigger the same response in CD4⁺ T lymphocytes that HIV-1 normally infects. To interrogate the relationship between Vpr and CP110 in a more physiologically relevant cell line, we infected CD4⁺ MT4 T cells, which are highly susceptible to, and permissive for, infection with HIV-1. We found that a significant percentage of cells infected with wild type HIV-1 (HIV-1 Vpr+) exhibit CP110 loss and centriole elongation (Figure 3.11.9A-C), in addition to centrosome amplification (Figure 3.11.9A, D). In contrast, very few mock infected cells or cells infected with HIV-1 lacking Vpr (HIV-1 Vpr-) possessed these phenotypes (Figure 3.11.9A-D). These results indicate that HIV-1 can also induce CP110 degradation and centriole elongation in T cells in a Vpr-dependent manner.

3.4.6. Elongated centrioles enhance microtubule nucleation

In order to shed light on the net effects of down-regulating CP110 for Vpr, we studied how elongated centrioles might influence centrosome function. When a centriole becomes abnormally long, the surrounding pericentriolar material becomes distorted into the shape of a filament (38-41). Given that γ -tubulin present in the pericentriolar material plays a crucial role in microtubule nucleation, we addressed whether, or not, elongated centrioles might alter nucleation. We quantified the staining area occupied by γ -tubulin and found that it is substantially bigger in CP110-depleted or Vpr-expressing cells than in control cells (Figure 3.11.10A-C). γ -tubulin

staining intensity was likewise higher upon depletion of CP110 or expression of Vpr (Figure 3.11.10A-B, D). Next, we performed microtubule re-growth assays following microtubule depolymerization with nocodazole. Shortly after removal of nocodazole, control cells nucleated an aster of microtubules emanating from the centrosome (1'; Figure 3.11.10A-B). With time, the aster enlarged, signifying an increase in the length and number of microtubules (5'; Figure 3.11.10A-B). Strikingly, cells depleted of CP110 or expressing Vpr formed a bigger aster and nucleated more microtubules at comparable time points (1', 5'; Figure 3.11.10A-B, E). In contrast, no gross microtubule anchoring defects were observed (45'; Figure 3.11.10A-B). Together, these data strongly suggest that elongated centrioles have the capacity to recruit more γ -tubulin, resulting in enhanced microtubule nucleation.

3.5. Discussion

In this work, we sought to obtain molecular insights into how HIV-1 Vpr exploits host machinery at the centrosome. While an intimate connection exists between HIV-1, Vpr, and centrosomes (42,47-50,56), the extent to which Vpr orchestrates its effects on this organelle remains poorly understood. Our data show that Vpr associates with a resident centrosomal protein Cep78 through DCAF1 and that it localizes to the centrosome by engaging in a complex with the ubiquitin ligase EDD-DYRK2-DDB1^{DCAF1} and Cep78. Because Vpr and Vpr(R80A) localize to the centrosome with similar efficiency and EDD-DYRK2-DDB1^{DCAF1} components are known to be present at this organelle throughout the cell cycle (37), it seems likely that centrosomal localization of Vpr is independent of G2/M arrest. Vpr is able to hijack EDD-DYRK2-DDB1^{DCAF1}, accelerating ubiquitination and degradation of a native centrosomal substrate CP110. Down-regulation of CP110 triggers the formation of abnormally long centrioles which recruit excess γ -tubulin, and as a consequence, nucleation of cytoplasmic microtubules becomes greatly enhanced. In addition, Vpr can provoke other centrosome anomalies such as amplification ((50) and this study), indicating that proteins involved in the regulation of organelle copy number might also be affected. It would therefore be interestingly to identify novel Vpr-interacting partners and/or EDD-DYRK2-DDB1^{DCAF1} substrates, and test if any of these might be responsible for the centrosome amplification phenotype.

Although Vpr triggers centriole elongation and centrosome amplification, it is clear that these phenotypes occur through two distinct mechanisms. We show that centriole elongation as a result of Vpr-mediated CP110 loss is independent of G2/M arrest, whereas centrosome amplification necessitates G2/M arrest. How then does Vpr-induced G2/M arrest result in centrosome amplification? It is reported that Vpr targets DNA repair factors such as HLF and UNG (33,35) for degradation and inappropriately activates the SLX4 complex in the nucleus(20), conditions that could contribute to replication stress and induction of DDR (57). The DDR protein Ataxia Telangiectasia-Mutated (ATM) and Rad3-related protein (ATR), once activated, initiates downstream signalling cascades that involve activation of Checkpoint Kinase 1 (CHK1) and inhibition of Cell Division Cycle 25C (CDC25C) and Cyclin B/Cyclin-Dependent Kinase 1 (CDK1), ultimately leading to G2/M arrest(58). Curiously, other studies have shown that DNA damage alone is sufficient to induce centrosome amplification (59), and several DDR proteins, such as ATM, ATR and CHK1, are found in the nucleus and at the centrosome (60).

While the precise functions of DDR proteins at the centrosome await future investigation, it is plausible that a DDR signal originating from the nucleus impinges on the centrosome through DDR proteins, causing amplification to occur.

What are the benefits HIV-1 might receive by hijacking EDD-DYRK2-DDB1^{DCAF1} at the centrosome? Regulation of microtubule dynamics and microtubule-associated proteins such as end-binding proteins and motor proteins is an important facet during the HIV-1 replication cycle. For example, HIV-1 promotes the formation of stable microtubules, an event crucial for early infection and translocation of the viral core in the cytoplasm *en route* to the nucleus (45). Intact microtubules are needed to facilitate HIV-1 uncoating, and disruption of microtubules by nocodazole impairs this process (46). In macrophages, HIV-1 Vpr perturbs the localization of End-Binding 1 to impair the maturation of phagosomes, leading to defects in innate immunity (61). Moreover, HIV-1 Tat can promote or hinder microtubule stability in a context-dependent fashion (62-64). Thus, it is clear that HIV-1 employs different strategies to remodel the host microtubule network during infection. Further studies will be needed to decipher how CP110 loss, elongated centrioles, and enhanced microtubule nucleation provoked by Vpr might affect various stages of HIV-1 infection.

One interesting finding from our studies is that Cep78 counteracts the effects of Vpr on CP110, raising the possibility that it might have anti-viral properties. It would therefore be interesting to test if this protein might safeguard the centrosome to inhibit viral infection.

3.6. Materials and methods

Cell culture and plasmids

HeLa, HEK293, and HEK293T cells were grown in DMEM (Wisent Inc, 319-005-CL) supplemented with 5% FBS (Wisent Inc, 080150) at 37°C in a humidified 5% CO₂ atmosphere. MT4 T cells were grown in RPMI1640 (Wisent Inc, 350-000-CL) supplemented with 10% FBS at 37°C in a humidified 5% CO₂ atmosphere. The following proteins were expressed from plasmids in mammalian cells: HA-Ub (65), pCBF-Flag-Cep78 (37), pEGFP-C1-Cep78(37), pCBF-Flag-CP110(66), pQBI25, SVCMV-HA-Vpr, SVCMV-HA-Vpr(Q65R), and SVCMV-HA-Vpr(R80A) (55).

Viral production and infection

Infectious GFP-marked HIV-1 NL4.3 or NL4.3ΔVpr viruses were generated by calcium phosphate transfection of HEK293T cells. Virus-containing supernatants were recovered 2 days post transfection, clarified, pelleted by ultracentrifugation, and titrated by analyzing the percentage of GFP positive MT4 T cells using flow cytometry. MT4 T cells were infected with the different GFP-expressing NL4.3 viruses at a multiplicity of infection of 0.75. Three days post infection, cells were plated on coated coverslips and processed for immunofluorescence.

Antibodies

Antibodies used in this study included anti-CP110 (Bethyl Laboratories, A301-344A), anti-Cep78 (Bethyl Laboratories, A301-799A and IRCM6(37)), anti-DCAF1 (Proteintech, 11612-1-AP), anti-EDD (Bethyl Laboratories, A300-573A), anti-DDB1 (Bethyl Laboratories, A300-462A), anti-Cullin4A (Bethyl Laboratories, A300-739A), anti-GFP (Roche, 11814460001), anti-HA (Santa Cruz, sc-7392 and Novus Biologicals, NB600-362), anti-Flag (Sigma-Aldrich, F7425 and F3165), anti- α -tubulin (Sigma-Aldrich, T5168), anti- γ -tubulin (Sigma-Aldrich, T3559 and T6557) and anti-DYRK2 (Abcam, ab37912). The anti-p24 monoclonal antibodies were produced from hybridomas 31-90-25 (HB9725) obtained from the American Type Culture Collection (ATCC).

RNA interference and transient expression of recombinant proteins

For RNA interference, synthetic siRNAs for non-specific (NS) control, DCAF1 and CP110 were described previously (29,67,68) and purchased from GE Dharmacon. Transfection of siRNA into HEK293 or HeLa cells was performed using siIMPORTER (Millipore, 64-101) per manufacturer's instructions, and cells were processed for immunoprecipitation, immunoblotting,

or immunofluorescence 72 hours post transfection. For expression of recombinant proteins, expression vector(s) was/were transfected into HEK293 cells using calcium phosphate or HeLa cells using polyethylenimine, and cells were processed 72 hours post transfection. For experiments involving both RNA interference and recombinant protein expression, HEK293 cells were transfected with siRNA, followed by transfection of expression vector 24 hours later. Cells were processed 72 hours after siRNA transfection. Optimal knockdown and recombinant protein expression were achieved 72 hours and 48-72 hours, respectively, post transfection.

Immunoprecipitation, immunoblotting, and immunofluorescence

Immunoprecipitation, immunoblotting and immunofluorescence were performed as described (67,68). Cells were lysed in a lysis buffer (50 mM HEPES/pH 7.4, 250 mM NaCl, 5 mM EDTA/pH 8, 0.1% NP-40, 1 mM DTT, 0.5 mM PMSF, 2 µg/ml leupeptin, 2 µg aprotinin, 10 mM NaF, 50 mM β-glycerophosphate and 10% glycerol) at 4°C for 30 minutes. Extracted proteins were recovered in the supernatant after centrifugation at 16,000g. For immunoblotting, 100µg of extract was used as input. For immunoprecipitation, 2 mg of extract was incubated with anti-Flag (Sigma-Aldrich, A2220) or anti-HA agarose (Sigma-Aldrich, A2095) beads at 4°C for 2 hours. The beads were washed three times with a lysis buffer, and bound proteins were analyzed by SDS-PAGE and immunoblotted with primary antibodies and horseradish peroxidase (HRP)-conjugated secondary antibodies (Rockland Inc, 610-703-002 and 611-7302). For indirect immunofluorescence, cells were fixed with cold methanol and permeabilized with 1% Triton X-100/PBS. Slides were blocked with 3% BSA in 0.1% Triton X-100/PBS prior to incubation with primary antibodies. Secondary antibodies used were Cy3- (Jackson Immunolabs, 711-165-151 and 715-165-152), Alexa647- (Jackson Immunolabs, 711-605-152), DyLight649- (Jackson Immunolabs, 715-495-151), or Alexa488- (Thermo Fisher Scientific, A11008, A11055, A11001) conjugated donkey anti-mouse, anti-goat or anti-rabbit IgG. Cells might also be stained with DAPI (Molecular Probes, D3571), and slides were mounted, observed, and photographed using a Leitz DMRB (Leica) microscope (100×, NA 1.3) equipped with a Retiga EXi cooled camera.

***In vivo* ubiquitination assay**

In vivo ubiquitination assays were performed as described (37,69). Briefly, HEK293 cells were transfected with various plasmids including HA-Ub. Cells were lysed 72 hours post transfection and the desired protein was immunoprecipitated with 1% SDS (Bio Basic Inc, SB0485) to prevent non-covalently linked binding partners from co-immunoprecipitating with

the desired protein. After extensive washing, bound proteins were analyzed by SDS-PAGE and immunoblotting with an anti-HA antibody.

Microtubule regrowth assay

Cells were treated with 10 μ M nocodazole (Sigma-Aldrich, M1404) for 1 hour at 4°C. After washing the cells several times with cold medium, they were placed in a pre-warmed medium at 37°C. Cells were fixed at various time points (0', 1', 5', 45') after 37°C and processed for immunofluorescence.

Cell cycle analysis

HEK293T cells were co-transfected plasmids expressing GFP (pQBI25) and wild type or mutant HA-Vpr. 48 hours post transfection, cells were fixed, permeabilized and stained with propidium iodide as described (55). Cell cycle analysis was performed on the GFP⁺ population by flow cytometry (BD FACSCalibur, Becton Dickinson). The ModFit mathematical model (ModFit LT v4.1.7, Verity Software House) was used to enumerate proportions of cells in G1 and G2/M phases.

Quantitation of γ -tubulin staining area and intensity

A region of interest (ROI) was drawn around γ -tubulin which marks the centrosome and the area of the ROI was calculated by using Volocity6 (PerkinElmer). The area of the ROI was used to measure the fluorescence intensity of γ -tubulin by using Volocity6. Image conditions were identical in all cases and none were saturated as confirmed by the pixel intensity range.

Quantitation of cytoplasmic microtubules

The number of microtubules emanated from the centrosome at 0' after microtubule regrowth was subtracted from that at 1' after regrowth, and presented as microtubules nucleated per minute.

Quantitation of Western blots

Protein bands from Western blot films were quantitated with ImageJ. Different film exposure lengths were used to prevent saturation. Quantitation was normalized with respect to the loading control.

Data and statistical analysis

Each experiment was conducted three times. The statistical significance of the difference between two means was calculated using a two-tailed Student's t-test. Differences were considered significant when $p < 0.01$.

3.7. Acknowledgements

We thank all members of the Tsang laboratory for constructive advice, M. Bego and R. Lodge for helpful discussions, and J. Archambault for providing plasmids. WYT was a Canadian Institutes of Health Research New Investigator and a Fonds de recherche Santé Junior 2 Research Scholar. This work was supported by grants from the Natural Sciences and Engineering Research Council of Canada to WYT and Canadian Institutes of Health Research (HOP143169) to EAC.

3.8. Author contributions

D. H. and J. A. F. B. data curation; D. H. software; D. H. and J. A. F. B. formal analysis; D. H., J. A. F. B., E. A. C., and W. Y. T. validation; D. H., E. A. C., and W. Y. T. investigation; D. H. visualization; D. H., J. A. F. B., E. A. C., and W. Y. T. methodology; D. H., J. A. F. B., E. A. C., and W. Y. T. writing-review and editing; E. A. C. and W. Y. T. conceptualization; E. A. C. And W. Y. T. supervision; E. A. C. and W. Y. T. funding acquisition; W. Y. T. resources; W. Y. T. writing-original draft; W. Y. T. Project administration.

3.9. Conflict of interest

The authors declare that they have no conflicts of interest with the contents of this article.

3.10. References

1. Barré-Sinoussi F, Chermann JC, Rey F, Nugeyre MT, Chamaret S, Gruest J, Dautquet C, Axler-Blin C, Vézinet-Brun F, Rouzioux C, Rozenbaum W and Montagnier L (1983) Isolation of a T-lymphotropic retrovirus from a patient at risk for acquired immune deficiency syndrome (AIDS). *Science* **220**, 868-871.
2. Gallo RC, Sarin PS, Gelmann EP, Robert-Guroff M, Richardson E, Kalyanaraman VS, Mann D, Sidhu GD, Stahl RE, Zolla-Pazner S, Leibowitch J and Popovic M (1983) Isolation of human T-cell leukemia virus in acquired immune deficiency syndrome (AIDS). *Science* **220**, 865-867.
3. Frankel AD and Young JA (1998) HIV-1: fifteen proteins and an RNA. *Annu Rev Biochem* **67**, 1-25.
4. Coffin JM, Hughes SH and Varmus HE (1997) The Interactions of Retroviruses and their Hosts. Cold Spring Harbor Laboratory Press, Cold Spring Harbor, NY.
5. Sato K, Misawa N, Iwami S, Satou Y, Matsuoka M, Ishizaka Y, Ito M, Aihara K, An DS and Koyanagi Y (2013) HIV-1 Vpr accelerates viral replication during acute infection by exploitation of proliferating CD4+ T cells in vivo. *PLoS Pathog* **9**, e1003812.
6. Krisko JF, Martinez-Torres F, Foster JL and Garcia JV (2013) HIV restriction by APOBEC3 in humanized mice. *PLoS Pathog* **9**, e1003242.
7. Sato K, Izumi T, Misawa N, Kobayashi T, Yamashita Y, Ohmichi M, Ito M, Takaori-Kondo A and Koyanagi Y (2010) Remarkable lethal G-to-A mutations in vif-proficient HIV-1 provirus by individual APOBEC3 proteins in humanized mice. *J Virol* **84**, 9546-9556.
8. Sato K, Takeuchi JS, Misawa N, Izumi T, Kobayashi T, Kimura Y, Iwami S, Takaori-Kondo A, Hu WS, Aihara K, Ito M, An DS, Pathak VK and Koyanagi Y (2014) APOBEC3D and APOBEC3F potentially promote HIV-1 diversification and evolution in humanized mouse model. *PLoS Pathog* **10**, e1004453.
9. Dave VP, Hajjar F, Dieng MM, Haddad É and Cohen ÉA (2013) Efficient BST2 antagonism by Vpu is critical for early HIV-1 dissemination in humanized mice. *Retrovirology* **10**, 128.

10. Sato K, Misawa N, Fukuhara M, Iwami S, An DS, Ito M and Koyanagi Y (2012) Vpu augments the initial burst phase of HIV-1 propagation and downregulates BST2 and CD4 in humanized mice. *J Virol* **86**, 5000-5013.
11. Watkins RL, Zou W, Denton PW, Krisko JF, Foster JL and Garcia JV (2013) In vivo analysis of highly conserved Nef activities in HIV-1 replication and pathogenesis. *Retrovirology* **10**, 125.
12. Zou W, Denton PW, Watkins RL, Krisko JF, Nochi T, Foster JL and Garcia JV (2012) Nef functions in BLT mice to enhance HIV-1 replication and deplete CD4⁺CD8⁺ thymocytes. *Retrovirology* **9**, 44.
13. Belzile JP, Abrahamyan LG, Gérard FC, Rougeau N and Cohen EA (2010) Formation of mobile chromatin-associated nuclear foci containing HIV-1 Vpr and VPRBP is critical for the induction of G2 cell cycle arrest. *PLoS Pathog* **6**, e1001080.
14. Gérard FC, Yang R, Romani B, Poisson A, Belzile JP, Rougeau N and Cohen EA (2014) Defining the interactions and role of DCAF1/VPRBP in the DDB1-cullin4A E3 ubiquitin ligase complex engaged by HIV-1 Vpr to induce a G2 cell cycle arrest. *PLoS One* **9**, e89195.
15. Zhang S, Feng Y, Narayan O and Zhao LJ (2001) Cytoplasmic retention of HIV-1 regulatory protein Vpr by protein-protein interaction with a novel human cytoplasmic protein VprBP. *Gene* **263**, 131-140.
16. Wen X, Casey Klockow L, Nekorchuk M, Sharifi HJ and de Noronha CM (2012) The HIV1 protein Vpr acts to enhance constitutive DCAF1-dependent UNG2 turnover. *PLoS One* **7**, e30939.
17. Ahn J, Vu T, Novince Z, Guerrero-Santoro J, Rapic-Otrin V and Gronenborn AM (2010) HIV-1 Vpr loads uracil DNA glycosylase-2 onto DCAF1, a substrate recognition subunit of a cullin 4A-ring E3 ubiquitin ligase for proteasome-dependent degradation. *J Biol Chem* **285**, 37333-37341.
18. Schröfelbauer B, Yu Q, Zeitlin SG and Landau NR (2005) Human immunodeficiency virus type 1 Vpr induces the degradation of the UNG and SMUG uracil-DNA glycosylases. *J Virol* **79**, 10978-10987.

19. Wang X, Singh S, Jung HY, Yang G, Jun S, Sastry KJ and Park JI (2013) HIV-1 Vpr protein inhibits telomerase activity via the EDD-DDB1-VPRBP E3 ligase complex. *J Biol Chem* **288**, 15474-15480.
20. Laguette N, Brégnard C, Hue P, Basbous J, Yatim A, Larroque M, Kirchhoff F, Constantinou A, Sobhian B and Benkirane M (2014) Premature activation of the SLX4 complex by Vpr promotes G2/M arrest and escape from innate immune sensing. *Cell* **156**, 134-145.
21. Sawaya BE, Khalili K, Mercer WE, Denisova L and Amini S (1998) Cooperative actions of HIV-1 Vpr and p53 modulate viral gene transcription. *J Biol Chem* **273**, 20052-20057.
22. Forget J, Yao XJ, Mercier J and Cohen EA (1998) Human immunodeficiency virus type 1 vpr protein transactivation function: mechanism and identification of domains involved. *J Mol Biol* **284**, 915-923.
23. Schröfelbauer B, Hakata Y and Landau NR (2007) HIV-1 Vpr function is mediated by interaction with the damage-specific DNA-binding protein DDB1. *Proc Natl Acad Sci U S A* **104**, 4130-4135.
24. Hrecka K, Gierszewska M, Srivastava S, Kozackiewicz L, Swanson SK, Florens L, Washburn MP and Skowronski J (2007) Lentiviral Vpr usurps Cul4-DDB1[VprBP] E3 ubiquitin ligase to modulate cell cycle. *Proc Natl Acad Sci U S A* **104**, 11778-11783.
25. Zhao LJ, Mukherjee S and Narayan O (1994) Biochemical mechanism of HIV-I Vpr function. Specific interaction with a cellular protein. *J Biol Chem* **269**, 15577-15582.
26. Kim K, Kim JM, Kim JS, Choi J, Lee YS, Neamati N, Song JS, Heo K and An W (2013) VprBP has intrinsic kinase activity targeting histone H2A and represses gene transcription. *Mol Cell* **52**, 459-467.
27. Kim K, Heo K, Choi J, Jackson S, Kim H, Xiong Y and An W (2012) Vpr-binding protein antagonizes p53-mediated transcription via direct interaction with H3 tail. *Mol Cell Biol* **32**, 783-796.
28. Nakagawa T, Mondal K and Swanson PC. (2013) VprBP (DCAF1): a promiscuous substrate recognition subunit that incorporates into both RING-family CRL4 and HECT-family EDD/UBR5 E3 ubiquitin ligases. *BMC Mol Biol* **14**, 22.
29. Maddika S and Chen J (2009) Protein kinase DYRK2 is a scaffold that facilitates assembly of an E3 ligase. *Nat Cell Biol* **11**, 409-419.

30. Angers S, Li T, Yi X, MacCoss MJ, Moon RT and Zheng N (2006) Molecular architecture and assembly of the DDB1-CUL4A ubiquitin ligase machinery. *Nature* **443**, 590-593.
31. He YJ, McCall CM, Hu J, Zeng Y and Xiong Y (2006) DDB1 functions as a linker to recruit receptor WD40 proteins to CUL4-ROC1 ubiquitin ligases. *Genes Dev* **20**, 2949-2954.
32. Higa LA, Wu M, Ye T, Kobayashi R, Sun H and Zhang H (2006) CUL4-DDB1 ubiquitin ligase interacts with multiple WD40-repeat proteins and regulates histone methylation. *Nat Cell Biol* **8**, 1277-1283.
33. Lahouassa H, Blondot ML, Chauveau L, Chougui G, Morel M¹, Leduc M, Guillonneau F, Ramirez BC, Schwartz O and Margottin-Goguet F (2016) HIV-1 Vpr degrades the HLTF DNA translocase in T cells and macrophages. *Proc Natl Acad Sci U S A* **113**, 5311-5316.
34. Zhou X, DeLucia M, Hao C, Hrecka K, Monnie C, Skowronski J and Ahn J (2017) HIV-1 Vpr protein directly loads helicase-like transcription factor (HLTF) onto the CUL4-DCAF1 E3 ubiquitin ligase. *J Biol Chem* **292**, 21117-21127.
35. Hrecka K, Hao C, Shun MC, Kaur S, Swanson SK, Florens L, Washburn MP and Skowronski J (2016) HIV-1 and HIV-2 exhibit divergent interactions with HLTF and UNG2 DNA repair proteins. *Proc Natl Acad Sci U S A* **113**, E3921-3930.
36. Jung HY, Wang X, Jun S and Park JI (2013) Dyrk2-associated EDD-DDB1-VprBP E3 ligase inhibits telomerase by TERT degradation. *J Biol Chem* **288**, 7252-7262.
37. Hossain D, Javadi Esfehiani Y, Das A and Tsang WY (2017) Cep78 controls centrosome homeostasis by inhibiting EDD-DYRK2-DDB1^{VprBP}. *EMBO Rep* **18**, 632-644.
38. Spektor A, Tsang WY, Khoo D and Dynlacht BD (2007) Cep97 and CP110 suppress a cilia assembly program. *Cell* **130**, 678-690.
39. Schmidt TI, Kleylein-Sohn J, Westendorf J, Le Clech M, Lavoie SB, Stierhof YD and Nigg EA (2009) Control of centriole length by CPAP and CP110. *Curr Biol* **19**, 1005-1011.
40. Kohlmaier G, Loncarek J, Meng X, McEwen BF, Mogensen MM, Spektor A, Dynlacht BD, Khodjakov A and Gönczy P (2009) Overly long centrioles and defective cell division upon excess of the SAS-4-related protein CPAP. *Curr Biol* **19**, 1012-1018.

41. Tang CJ, Fu RH, Wu KS, Hsu WB and Tang TK (2009) CPAP is a cell-cycle regulated protein that controls centriole length. *Nat Cell Biol* **11**, 825-831.
42. Afonso PV, Zamborlini A, Saïb A and Mahieux R (2007) Centrosome and retroviruses: the dangerous liaisons. *Retrovirology* **4**, 27
43. McDonald D, Vodicka MA, Lucero G, Svitkina TM, Borisy GG, Emerman M and Hope TJ (2002) Visualization of the intracellular behavior of HIV in living cells. *J Cell Biol* **159**, 441-452
44. Fackler, O. T., and Krausslich, H. G. (2006) Interactions of human retroviruses with the host cell cytoskeleton. *Curr Opin Microbiol* **9**, 409-415.
45. Sabo Y, Walsh D, Barry DS, Tinaztepe S, de Los Santos K, Goff SP, Gundersen GG and Naghavi MH (2013) HIV-1 induces the formation of stable microtubules to enhance early infection. *Cell Host Microbe* **14**, 535-546.
46. Lukic Z, Dharan A, Fricke T, Diaz-Griffero F and Campbell EM (2014) HIV-1 uncoating is facilitated by dynein and kinesin 1. *J Virol* **88**, 13613-13625.
47. Zamborlini A, Lehmann-Che J, Clave E, Giron ML, Tobaly-Tapiero J, Roingeard P, Emiliani S, Toubert A, de Thé H and Saïb A (2007) Centrosomal pre-integration latency of HIV-1 in quiescent cells. *Retrovirology* **4**, 63.
48. Bolton DL, Barnitz RA, Sakai K and Lenardo MJ (2008) 14-3-3 theta binding to cell cycle regulatory factors is enhanced by HIV-1 Vpr. *Biol Direct* **3**, 17.
49. Chang F, Re F, Sebastian S, Sazer S and Luban J (2004) HIV-1 Vpr induces defects in mitosis, cytokinesis, nuclear structure, and centrosomes. *Mol Biol Cell* **15**, 1793-1801.
50. Watanabe N, Yamaguchi T, Akimoto Y, Rattner JB, Hirano H and Nakauchi H (2000) Induction of M-phase arrest and apoptosis after HIV-1 Vpr expression through uncoupling of nuclear and centrosomal cycle in HeLa cells. *Exp Cell Res* **258**, 261-269.
51. Le Rouzic E, Belaïdouni N, Estrabaud E, Morel M, Rain JC, Transy C and Margottin-Goguet F (2007) HIV1 Vpr arrests the cell cycle by recruiting DCAF1/VprBP, a receptor of the Cul4-DDB1 ubiquitin ligase. *Cell Cycle* **6**, 182-188.
52. D'Angiolella V, Donato V, Vijayakumar S, Saraf A, Florens L, Washburn MP, Dynlacht B and Pagano M (2010) SCF(Cyclin F) controls centrosome homeostasis and mitotic fidelity through CP110 degradation. *Nature* **466**, 138-142.

53. Fregoso OI and Emerman M (2016) Activation of the DNA Damage Response Is a Conserved Function of HIV-1 and HIV-2 Vpr That Is Independent of SLX4 Recruitment. *MBio* **7**, pii: e01433-16.
54. Gaynor EM and Chen IS (2001) Analysis of apoptosis induced by HIV-1 Vpr and examination of the possible role of the hHR23A protein. *Exp Cell Res* **267**, 243-257.
55. Belzile JP, Duisit G, Rougeau N, Mercier J, Finzi A and Cohen EA (2007) HIV-1 Vpr-mediated G2 arrest involves the DDB1-CUL4AVPRBP E3 ubiquitin ligase. *PLoS Pathog* **3**, e85.
56. Minemoto Y, Shimura M, Ishizaka Y, Masamune Y and Yamashita K (1999) Multiple centrosome formation induced by the expression of Vpr gene of human immunodeficiency virus. *Biochem Biophys Res Commun* **258**, 379-384.
57. Romani B and Cohen EA (2012) Lentivirus Vpr and Vpx accessory proteins usurp the cullin4-DDB1 (DCAF1) E3 ubiquitin ligase. *Curr Opin Virol* **2**, 755-763.
58. Bregnard C, Benkirane M and Laguette N (2014) DNA damage repair machinery and HIV escape from innate immune sensing. *Front Microbiol* **5**, 176.
59. Bourke E, Dodson H, Merdes A, Cuffe L, Zachos G, Walker M, Gillespie D and Morrison CG (2007) DNA damage induces Chk1-dependent centrosome amplification. *EMBO Rep* **8**, 603-609.
60. Mullee LI and Morrison CG (2016) Centrosomes in the DNA damage response--the hub outside the centre. *Chromosome Res* **24**, 35-51.
61. Dumas A, Lê-Bury G, Marie-Anaïs F, Herit F, Mazzolini J, Guilbert T, Bourdoncle P, Russell DG, Benichou S, Zahraoui A and Niedergang F (2015) The HIV-1 protein Vpr impairs phagosome maturation by controlling microtubule-dependent trafficking. *J Cell Biol* **211**, 359-372.
62. Chen D, Wang M, Zhou S and Zhou Q (2002) HIV-1 Tat targets microtubules to induce apoptosis, a process promoted by the pro-apoptotic Bcl-2 relative Bim. *EMBO J* **21**, 6801-6810.
63. de Mareuil J, Carre M, Barbier P, Campbell GR, Lancelot S, Opi S, Esquieu D, Watkins JD, Prevot C, Braguer D, Peyrot V and Loret EP (2005) HIV-1 Tat protein enhances microtubule polymerization. *Retrovirology* **2**, 5.

64. Aprea S, Del Valle L, Mameli G, Sawaya BE, Khalili K and Peruzzi F (2006) Tubulin-mediated binding of human immunodeficiency virus-1 Tat to the cytoskeleton causes proteasomal-dependent degradation of microtubule-associated protein 2 and neuronal damage. *J Neurosci* **26**, 4054-4062.
65. Treier M, Staszewski LM and Bohmann D (1994) Ubiquitin-dependent c-Jun degradation in vivo is mediated by the delta domain. *Cell* **78**, 787-798.
66. Tsang WY, Bossard C, Khanna H, Peränen J, Swaroop A, Malhotra V and Dynlacht BD (2008) CP110 suppresses primary cilia formation through its interaction with CEP290, a protein deficient in human ciliary disease. *Dev Cell* **15**, 187-197.
67. Barbelanne M, Song J, Ahmadzai M and Tsang WY (2013) Pathogenic NPHP5 mutations impair protein interaction with Cep290, a prerequisite for ciliogenesis. *Hum Mol Genet* **22**, 2482-2494.
68. Barbelanne M, Hossain D, Chan DP, Peränen J and Tsang WY (2015) Nephrocystin proteins NPHP5 and Cep290 regulate BBSome integrity, ciliary trafficking and cargo delivery. *Hum Mol Genet* **24**, 2185-2200.
69. Das A, Qian J and Tsang WY (2017) USP9X counteracts differential ubiquitination of NPHP5 by MARCH7 and BBS11 to regulate ciliogenesis. *PLoS Genet* **13**, e1006791.

3.11. Figures

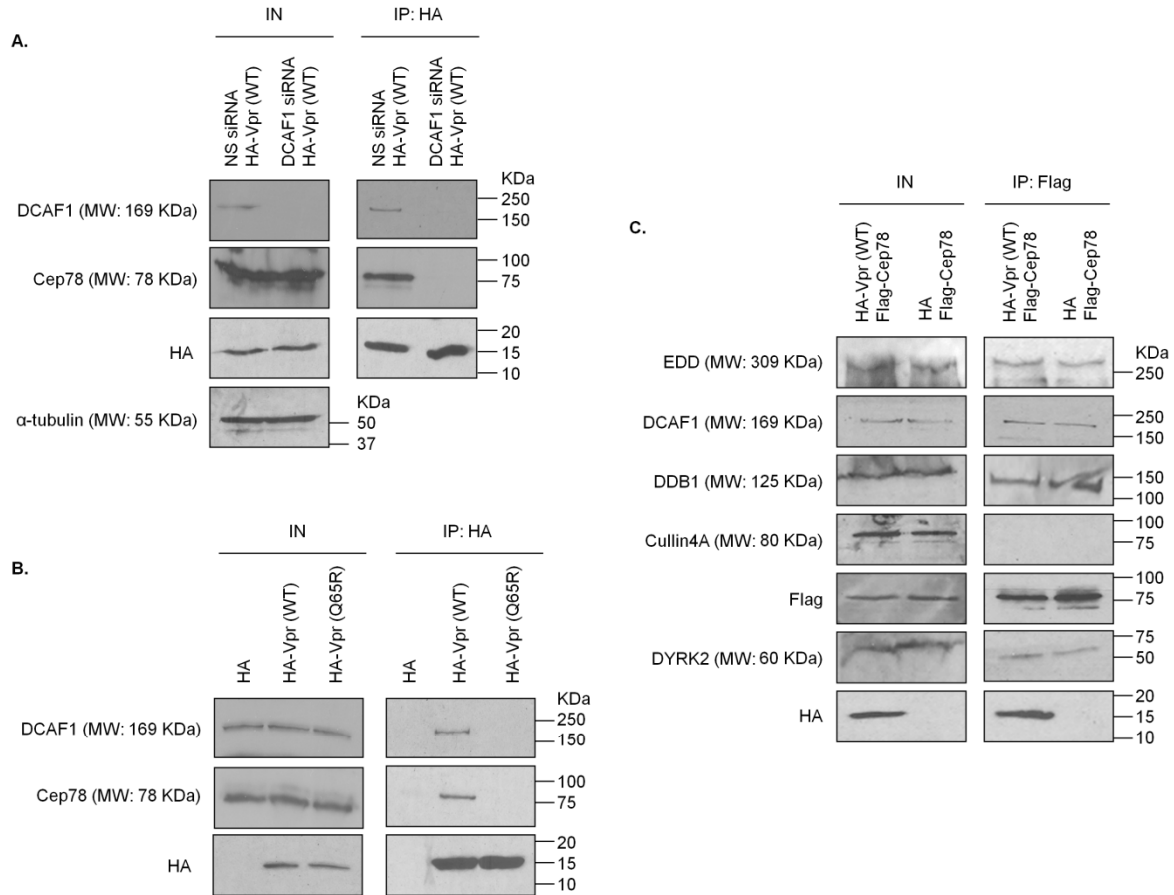


Figure 3.11.1. Vpr interacts with Cep78 and EDD-DYRK2-DDB1^{DCAF1} through DCAF1

A) HEK293 cells were transfected with NS (non-specific) or DCAF1 siRNA, followed by plasmid expressing HA-Vpr wild type (WT). Lysates were immunoprecipitated with an anti-HA antibody and Western blotted with the indicated antibodies. IN, input. α -tubulin was used as loading control. B) HEK293 cells were transfected with plasmid expressing HA, HA-Vpr(WT), or HA-Vpr mutant refractory to DCAF1 binding (Q65R). Lysates were immunoprecipitated with an anti-HA antibody and Western blotted with the indicated antibodies. IN, input. C) HEK293 cells were co-transfected with plasmids expressing Flag-Cep78 and HA or HA-Vpr(WT). Lysates were immunoprecipitated with an anti-Flag antibody and Western blotted with the indicated antibodies. IN, input.

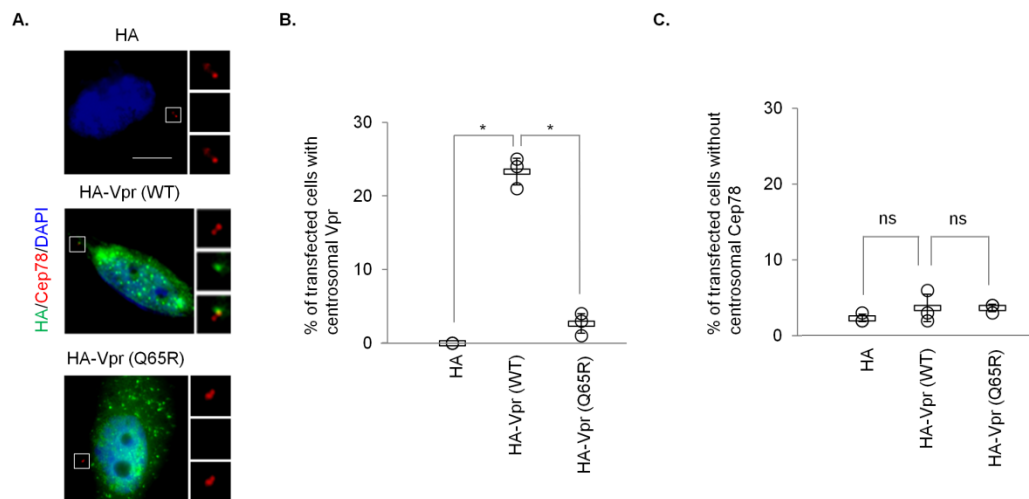


Figure 3.11.2. Vpr but not Vpr(Q65R) localizes to the centrosome

A) HeLa cells transfected with plasmid expressing HA, HA-Vpr(WT), or HA-Vpr(Q65R) were processed for immunofluorescence and stained with antibodies against HA (green) and Cep78 (red). DNA was stained with DAPI (blue). Scale bar, 2 μ m. B-C) The percentage of HA-expressing cells showing centrosomal localization of Vpr B) or no centrosomal Cep78 staining C) was determined. For B-C), at least 100 cells were scored for each condition in each experiment, and mean (thick open line) and standard error (bar) of three independent experiments (o) are shown in the graph. *, $p < 0.01$; ns, non-significant.

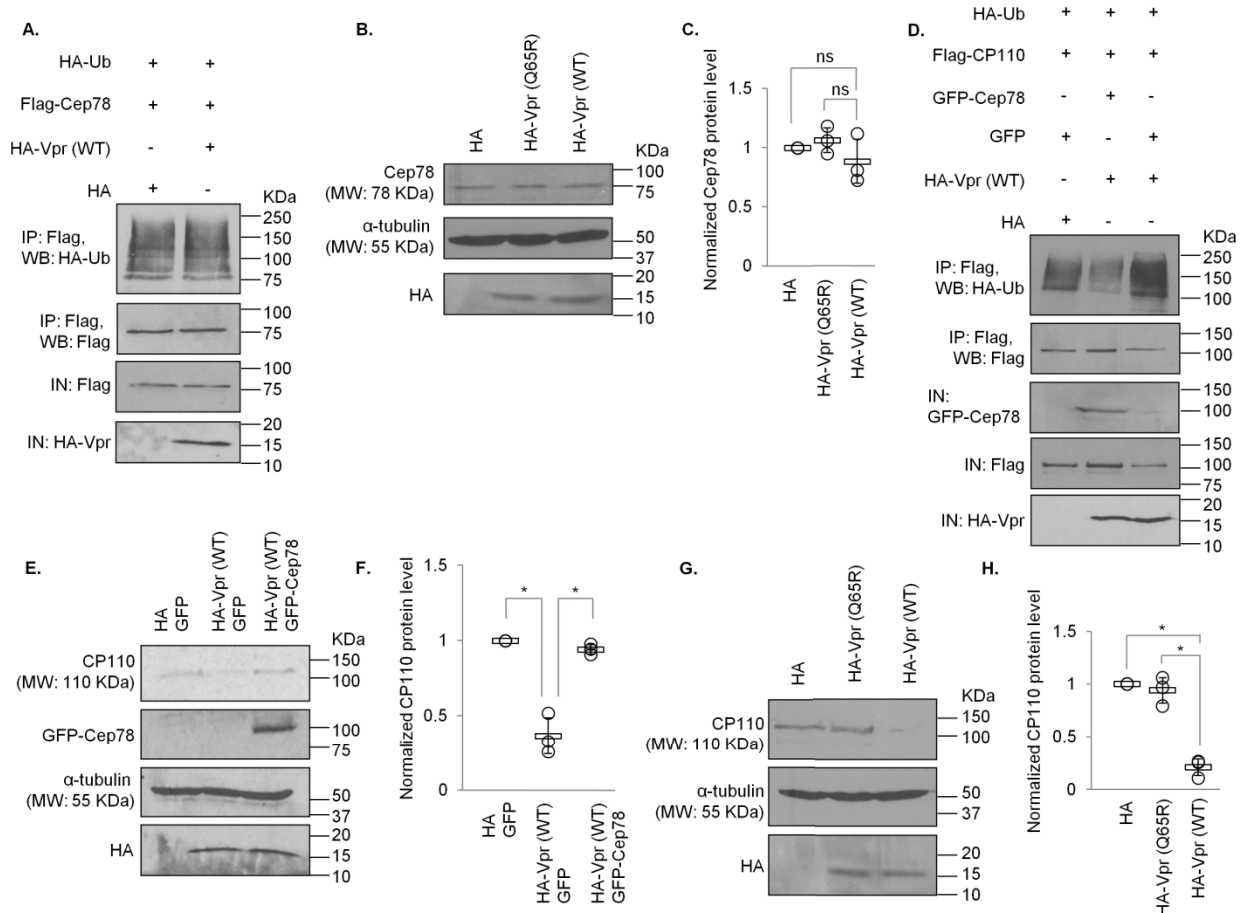


Figure 3.11.3. Vpr enhances ubiquitination and degradation of CP110 but not Cep78

A) HEK293 cells were co-transfected with plasmids expressing HA-Ub, Flag-Cep78, and HA or HA-Vpr(WT). Lysates were immunoprecipitated with an anti-Flag antibody in 1% SDS and Western blotted with the indicated antibodies. IN, input. B) HEK293 cells were transfected with plasmid expressing HA, HA-Vpr(WT), or HA-Vpr(Q65R). Lysates were Western blotted with the indicated antibodies. α -tubulin was used as loading control. C) Normalized Cep78 protein level. Mean (thick open line) and standard error (bar) of three independent experiments (o) are shown in the graph. ns, non-significant. D) HEK293 cells were co-transfected with plasmids expressing HA-Ub, Flag-CP110, GFP or GFP-Cep78, and HA or HA-Vpr(WT). Lysates were immunoprecipitated with an anti-Flag antibody in 1% SDS and Western blotted with the indicated antibodies. IN, input. E) HEK293 cells were co-transfected with plasmids expressing HA and GFP, HA-Vpr(WT) and GFP, or HA-Vpr(WT) and GFP-Cep78. Lysates were Western blotted with the indicated antibodies. α -tubulin was used as loading control. F) Normalized CP110 protein level. Mean (thick open line) and standard error (bar) of three independent

experiments (o) are shown in the graph. *, $p < 0.01$. G) HEK293 cells were transfected with plasmid expressing HA, HA-Vpr(WT), or HA-Vpr(Q65R). Lysates were Western blotted with the indicated antibodies. α -tubulin was used as loading control. H) Normalized CP110 protein level. Mean (thick open line) and standard error (bar) of three independent experiments (o) are shown in the graph. *, $p < 0.01$.

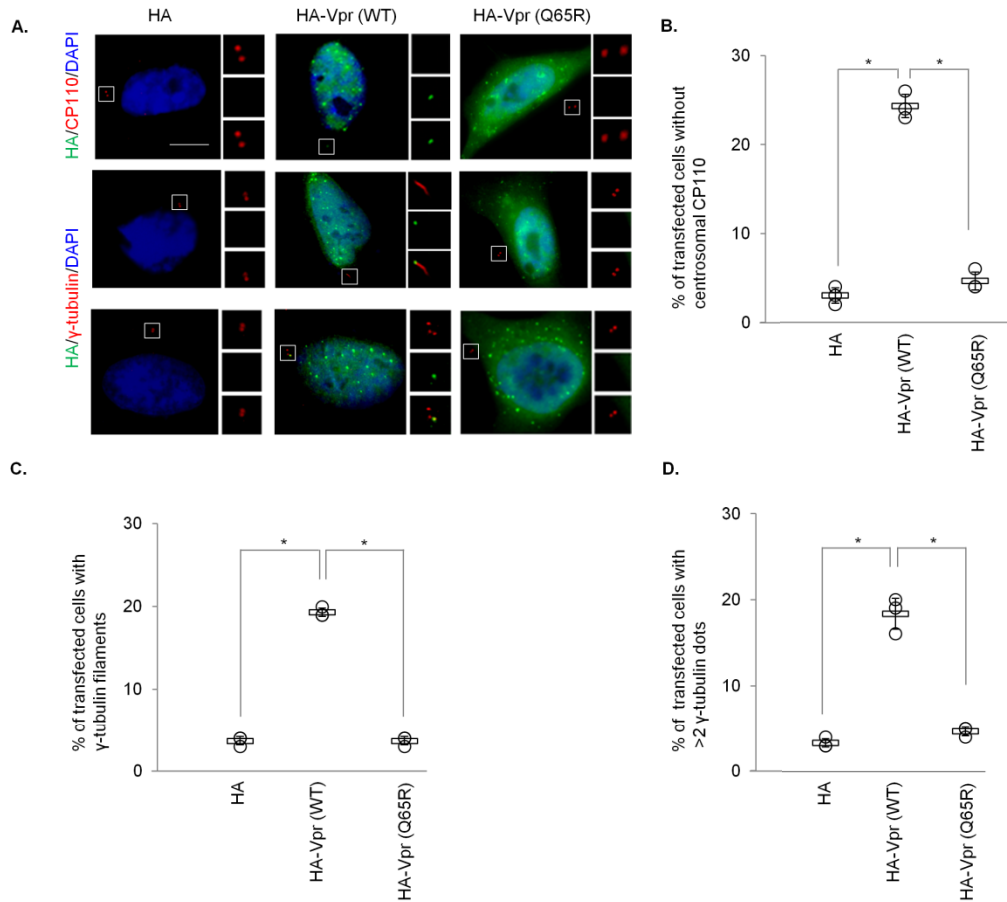


Figure 3.11.4. Vpr induces CP110 loss, centriole elongation, and centrosome amplification

A) HeLa cells transfected with plasmid expressing expressing HA, HA-Vpr(WT), or HA-Vpr(Q65R) were processed for immunofluorescence and stained with antibodies against HA (green) and CP110 or γ -tubulin (red). DNA was stained with DAPI (blue). Scale bar, 2 μ m. B) The percentage of HA-expressing cells with no centrosomal CP110 staining was determined. C- D) The percentage of HA-expressing cells with elongated centrioles (γ -tubulin filaments) C) or centrosome amplification (>2 γ -tubulin dots) D) was determined. For B-D), at least 100 cells were scored for each condition in each experiment, and mean (thick open line) and standard error (bar) of three independent experiments (o) are shown in the graph. *, $p < 0.01$.

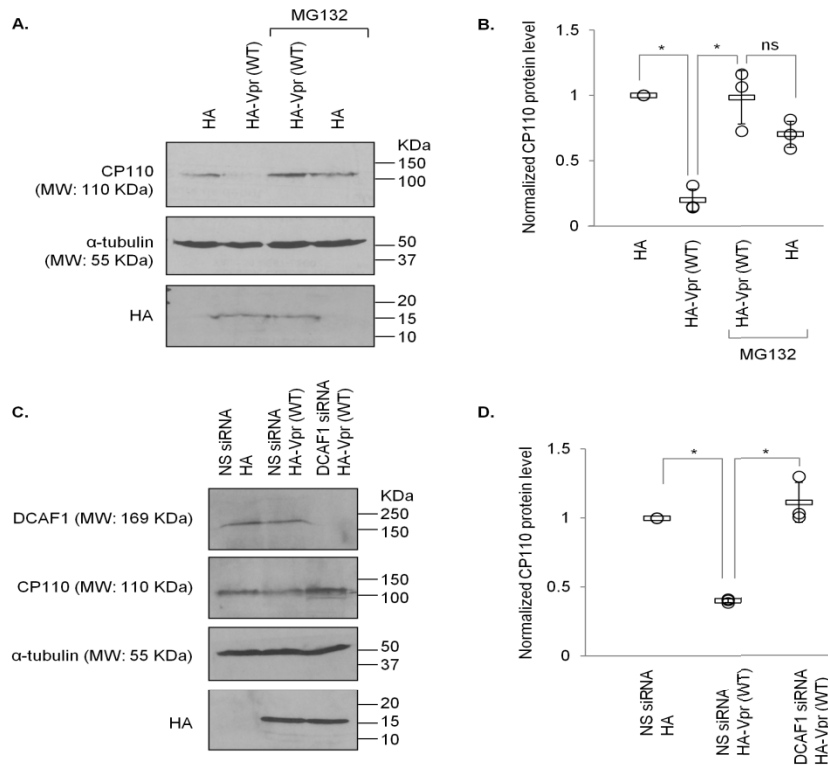


Figure 3.11.5. Vpr-induced proteasomal degradation of CP110 occurs in a DCAF1-dependent manner

A) HEK293 cells transfected with plasmid expressing HA or HA-Vpr(WT) were treated with or without 10 μ M MG132 for 6 hours. Lysates were Western blotted with the indicated antibodies. α -tubulin was used as loading control. B) Normalized CP110 protein level. Mean (thick open line) and standard error (bar) of three independent experiments (o) are shown in the graph. *, p < 0.01; ns, non-significant. C) HEK293 cells were transfected with NS (non-specific) or DCAF1 siRNA, followed by plasmid expressing HA or HA-Vpr(WT). Lysates were Western blotted with the indicated antibodies. α -tubulin was used as loading control. D) Normalized CP110 protein level. Mean (thick open line) and standard error (bar) of three independent experiments (o) are shown in the graph. *, p < 0.01.

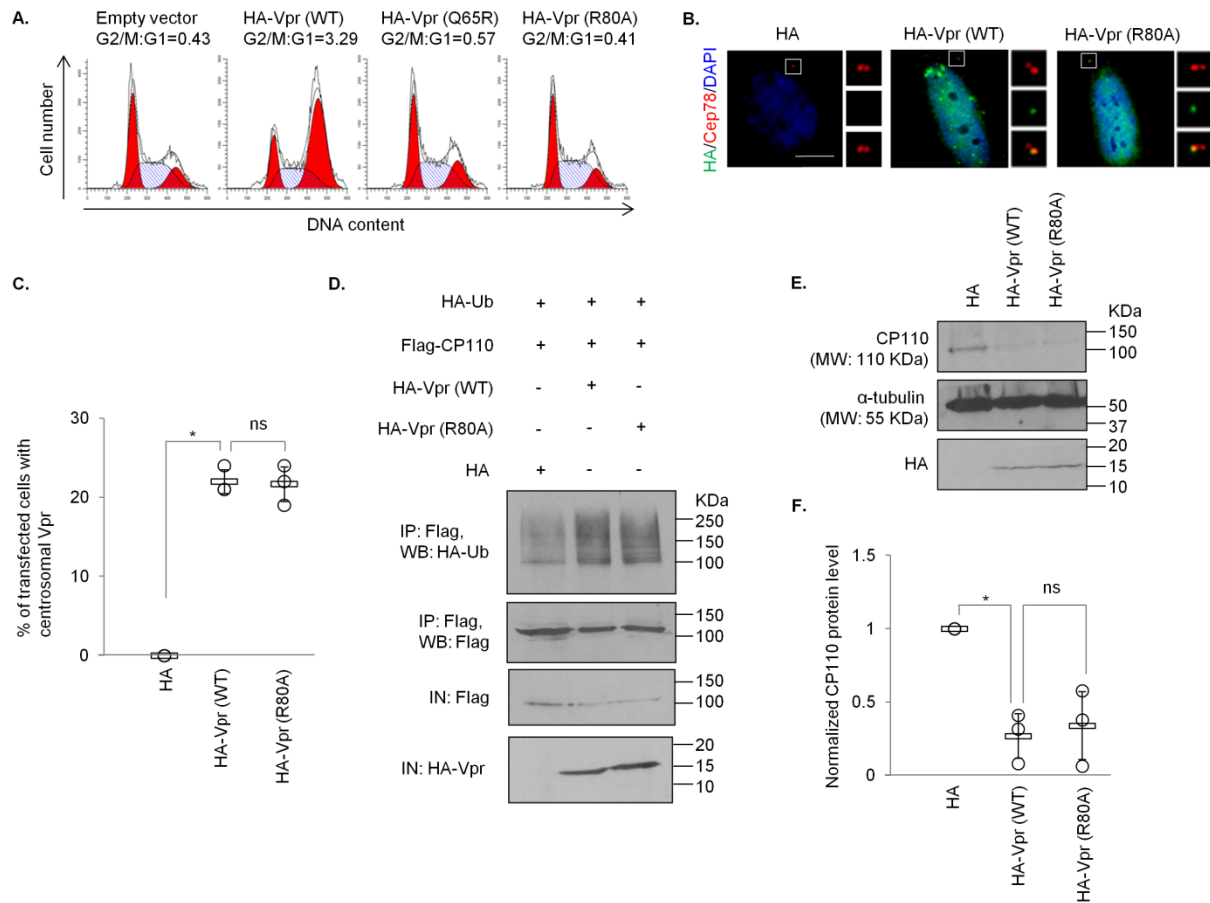


Figure 3.11.6. Vpr centrosomal localization and Vpr-induced ubiquitination and degradation of CP110 are independent of G2/M arrest

A) HEK293T cells co-transfected with plasmids expressing GFP and HA (empty vector), HA-Vpr(WT), HA-Vpr(Q65R), or HA-Vpr(R80A). Cell cycle profiles were determined by flow cytometry gating on the GFP⁺ population. G2/M:G1 ratio is presented for each condition. B) HeLa cells transfected with plasmid expressing HA, HA-Vpr(WT), or HA-Vpr(R80A) were processed for immunofluorescence and stained with antibodies against HA (green) and Cep78 (red). DNA was stained with DAPI (blue). Scale bar, 2 μ m. C) The percentage of HA-expressing cells showing centrosomal localization of Vpr was determined. At least 100 cells were scored for each condition in each experiment, and mean (thick open line) and standard error (bar) of three independent experiments (o) are shown in the graph. *, $p < 0.01$; ns, non-significant. D) HEK293 cells were co-transfected with plasmids expressing HA-Ub, Flag-CP110, and HA, HA-Vpr(WT), or HA-Vpr(R80A). Lysates were immunoprecipitated with an anti-Flag antibody in 1% SDS and Western blotted with the indicated antibodies. IN, input. E) HEK293 cells were transfected with

plasmid expressing HA, HA-Vpr(WT), or HA-Vpr(R80A). Lysates were Western blotted with the indicated antibodies. α -tubulin was used as loading control. F) Normalized CP110 protein level. Mean (thick open line) and standard error (bar) of three independent experiments (o) are shown in the graph. *, $p < 0.01$; ns, non-significant.

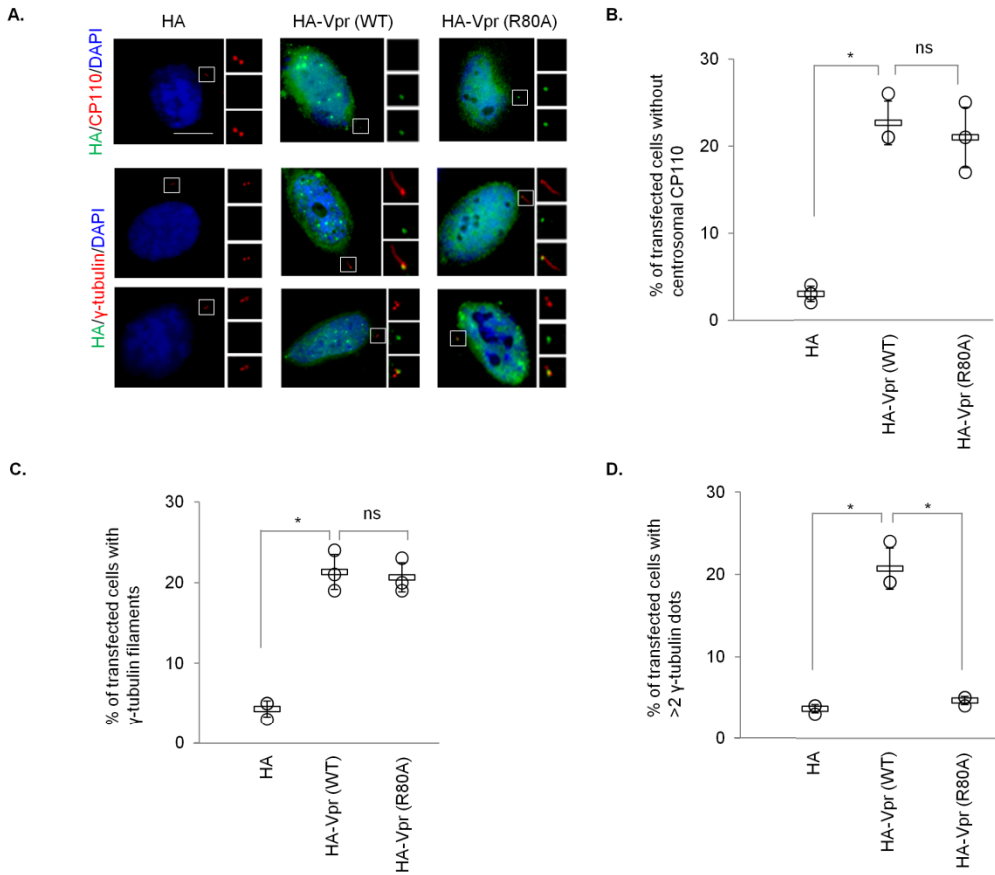


Figure 3.11.7. Vpr-induced centrosome amplification, but not CP110 loss or centriole elongation, is dependent of G2/M arrest

A) HeLa cells transfected with plasmid expressing HA, HA-Vpr(WT), or HA-Vpr(R80A) were processed for immunofluorescence and stained with antibodies against HA (green) and CP110 or γ -tubulin (red). DNA was stained with DAPI (blue). Scale bar, 2 μ m. B) The percentage of HA-expressing cells with no centrosomal CP110 staining was determined. C-D) The percentage of HA-expressing cells with elongated centrioles (γ -tubulin filaments) C) or centrosome amplification (>2 γ -tubulin dots) D) was determined. For B-D), at least 100 cells were scored for each condition in each experiment, and mean (thick open line) and standard error (bar) of three independent experiments (o) are shown in the graph. *, p<0.01; ns, non-significant.

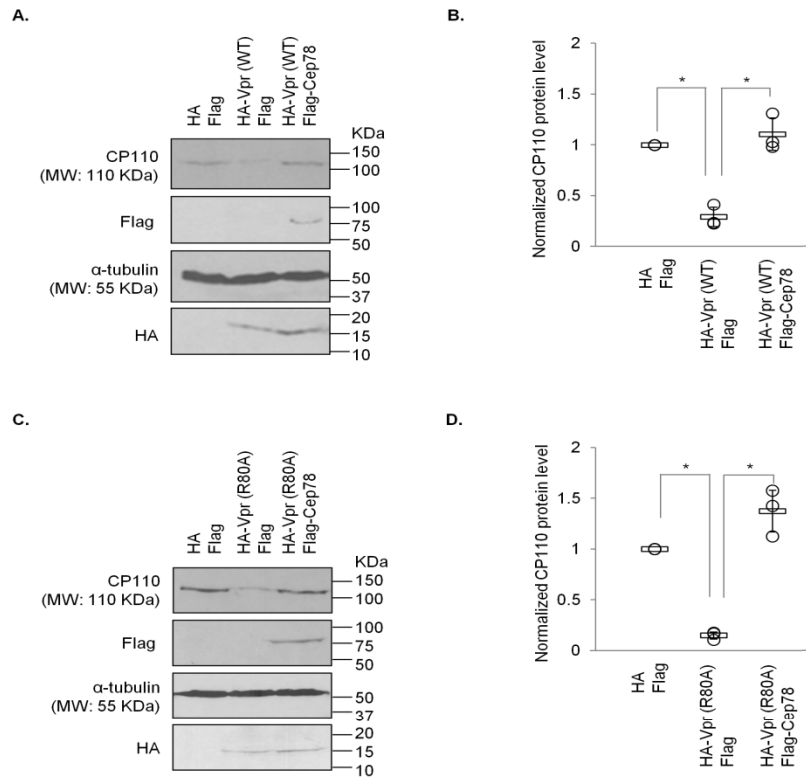


Figure 3.11.8. Degradation of CP110 induced by Vpr or Vpr(R80A) can be overcome by Cep78 expression

A) HEK293 cells were transfected with plasmids expressing HA and Flag, HA-Vpr(WT) and Flag, or HA-Vpr(WT) and Flag-Cep78. Lysates were Western blotted with the indicated antibodies. α -tubulin was used as loading control. B) Normalized CP110 protein level. Mean (thick open line) and standard error (bar) of three independent experiments (o) are shown in the graph. *, $p < 0.01$. C) HEK293 cells were transfected with plasmids expressing HA and Flag, HA-Vpr(R80A) and Flag, or HA-Vpr(R80A) and Flag-Cep78. Lysates were Western blotted with the indicated antibodies. α -tubulin was used as loading control. D) Normalized CP110 protein level. Mean (thick open line) and standard error (bar) of three independent experiments (o) are shown in the graph. *, $p < 0.01$.

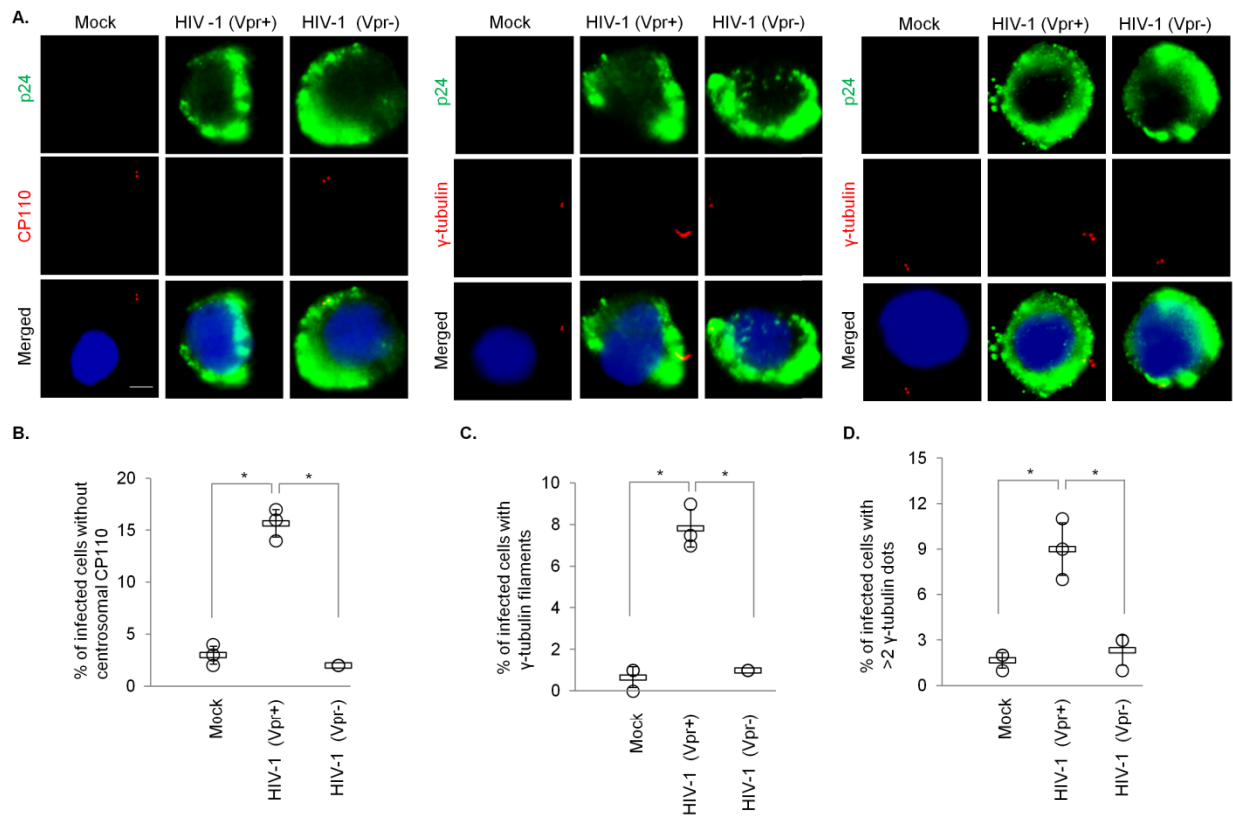


Figure 3.11.9. HIV-1 Vpr induces CP110 loss, centriole elongation, and centrosome amplification in infected T cells

A) MT4 cells mock infected or infected with either wild type HIV-1 (Vpr+) or HIV-1 missing Vpr (Vpr-) were processed for immunofluorescence and stained with antibodies against p24 (green) and CP110 or γ -tubulin (red). DNA was stained with DAPI (blue). Scale bar, 2 μ m. B) The percentage of p24-positive cells with no centrosomal CP110 staining was determined. C-D) The percentage of p24-positive cells with elongated centrioles (γ -tubulin filaments) C) or centrosome amplification (>2 γ -tubulin dots) D) was determined. For B-D), at least 100 cells were scored for each condition in each experiment, and mean (thick open line) and standard error (bar) of three independent experiments (o) are shown in the graph. *, $p < 0.01$.

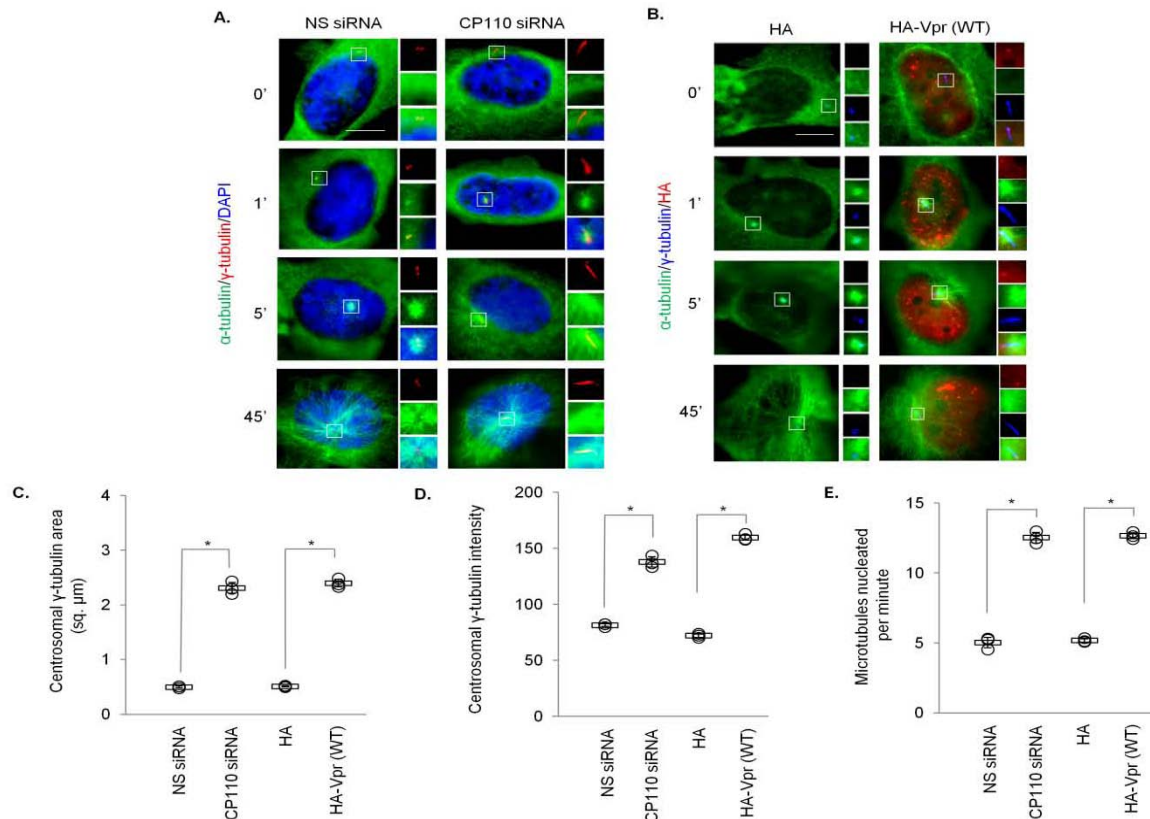


Figure 3.11.10. Depletion of CP110 or expression of Vpr enhances microtubule nucleation

A) HeLa cells transfected with NS (non-specific) or CP110 siRNA were subjected to a microtubule regrowth assay. Cells were processed for immunofluorescence at the indicated time points after release and stained with antibodies against α -tubulin (green) and γ -tubulin (red). DNA was stained with DAPI (blue). B) HeLa cells transfected with plasmid expressing HA or HA-Vpr(WT) were subjected to a microtubule regrowth assay. Cells were processed for immunofluorescence at the indicated time points after release and stained with antibodies against HA (red), α -tubulin (green) and γ -tubulin (blue). C) The staining area of γ -tubulin at the centrosome was quantitated. D) The staining intensity of γ -tubulin at the centrosome was quantitated. E) The number of cytoplasmic microtubules emanated from the centrosome was determined at the 1' time point. For C-E), at least 20 cells were scored for each condition in each experiment, and mean (thick open line) and standard error (bar) of three independent experiments (o) are shown in the graph. *, $p < 0.01$.

Chapter 4

Requirement of NPHP5 in the hierarchical assembly of basal feet

Delowar Hossain^{1,3}, Marine Barbelanne^{1,2} and William Y. Tsang^{1,2,3,*}

¹ Institut de recherches cliniques de Montréal, 110 avenue des Pins Ouest, Montréal, Québec H2W 1R7, Canada

² Faculté de Médecine, Département de pathologie et biologie cellulaire, Université de Montréal, Montréal, Québec H3C 3J7, Canada

³ Division of Experimental Medicine, McGill University, Montréal, Québec H3A 1A3, Canada

* To whom correspondence should be addressed: william.tsang@ircm.qc.ca

Phone: 1 (514) 987-5719

Fax: 1 (514) 987-5685

Keywords: centrosome/cilium/centriole/basal body/sub-distal appendage/basal foot/NPHP5

Running title: NPHP5 is required for basal feet formation

4.1. Preface

In chapter 4, I characterized another poorly described centrosomal protein NPHP5. Previously, it was shown that NPHP5 is localized at the distal region of the centriole and is required for ciliogenesis. As there are substructures associated with the distal region of the mother centriole (DAs and SDAs) and basal bodies (TFs and BF), it is necessary to know the precise localization of NPHP5 in order to understand the mechanism of ciliogenesis by NPHP5. In this study, I demonstrated the exact localization of NPHP5 using super resolution microscopy as well as the close association of NPHP5 with other proteins at this particular region, focusing on our understanding the structure and composition of this region, which is linked to ciliogenesis.

4.2. Abstract

During ciliogenesis, the mother centriole transforms into a basal body competent to nucleate a cilium. The mother centriole and basal body possess sub-distal appendages (SDAs) and basal feet (BF), respectively. SDAs and BF are thought to be equivalent structures. In contrast to SDA assembly, little is known about the players involved in BF assembly and its assembly order. Furthermore, the contribution of BF to ciliogenesis is not understood. Here, we found that SDAs are distinguishable from BF and that the protein NPHP5 is a novel SDA and BF component. Remarkably, NPHP5 is specifically required for BF assembly in cells able to form basal bodies, but is dispensable for SDA assembly. Determination of the hierarchical assembly reveals that NPHP5 cooperates with a subset of SDA/BF proteins to organize BF. The assembly pathway of BF is similar but not identical to that of SDA. Loss of NPHP5 or a BF protein simultaneously inhibits BF assembly and ciliogenesis, and these phenotypes could be rescued by manipulating the expression of certain components in the BF assembly pathway. These findings define a novel role for NPHP5 in specifically regulating BF assembly, a process which is tightly coupled to ciliogenesis.

4.3. Introduction

The centrosome participates in the organization of the microtubule network in most eukaryotic cells and coordinates a number of microtubule-related processes such as cell division, cell polarity, cell motility, and cell signalling (1). As a dynamic organelle, its structure and function are subjected to tight spatial and temporal regulation (2,3). A cell in the G1 phase contains a single centrosome comprised of two centrioles, the mother and daughter centrioles, which are surrounded by the pericentriolar material (PCM) from which microtubules emanate and elongate. The mother centriole is structurally distinct from the daughter centriole in that the former possesses sub-distal appendages (SDAs) and distal appendages (DAs) (2,4). After the centrosome duplicates in the S phase and the PCM enlarges and matures in the G2 phase, two fully functional centrosomes with increased capacity to nucleate microtubules are formed. At the onset of mitosis, the two centrosomes separate, migrating to opposite poles and establishing the mitotic spindle. When a cell exits the cell cycle, the mother centriole transforms into a basal body, a structure essential for the nucleation of a cilium (2,4). At the molecular level, the mother centriole-to-basal body transformation is thought to entail targeting of TTBK2 to, followed by loss of CP110 from and recruitment of intraflagellar transport (IFT) proteins to, the mother centriole (5).

The basal body is accompanied by basal feet (BF) and transition fibers (TFs) (2,4). TFs are analogous to DAs and the two structures exist in a mutually exclusive manner. Nine DAs are present at the distal end of the mother centriole (6,7), and the same number of TFs, which serve to dock vesicles/membranes during ciliogenesis, occupy a similar location at the basal body (8,9). Likewise, BF and SDAs are believed to be equivalent but mutually exclusive. While there are nine sub-distal appendages projecting laterally from the sides of the mother centriole close to the distal end (7), the number of basal feet associated with the basal body appears to vary depending on cilia type. Based on preliminary electron microscopy (EM) studies, basal bodies that template motile cilia reportedly possess one basal foot which is larger than an individual SDA (8,9), whereas those that template primary cilia are alleged to contain one to several BF(10-12). Thus, structural differences likely exist between BF and SDAs.

On the other hand, there seems to be a considerable overlap between BF and SDAs in terms of function and molecular composition. Both BF and SDAs are able to nucleate and anchor microtubules (8,13,14). The molecular composition of SDA is beginning to emerge and a

handful of SDA proteins have been identified. ODF2/Cenexin1, ninein, Cep170, centriolin, ϵ -tubulin, CCDC120, and CCDC68 are considered core SDA components based on immuno-EM and/or super-resolution microscopy studies (15-20), and a loss of any one of them compromises SDA assembly and/or function. Ablation of ODF2 also disrupts BF assembly (15), suggesting that this protein is shared among SDAs and BF. Other proteins such as Kif3a, p150^{Glued}, Sec15, CC2D2A, and Cep128 are found to be present at the sub-distal ends of the mother centriole and play a critical role in SDA assembly and/or function (10,21-23). Kif3a and CC2D2A, in particular, are also involved in BF assembly (10,21). Another protein TCHP is enriched at the sub-distal to medial region of centrioles, including the mother centriole, where it regulates SDA assembly in a positive manner (24). Paradoxically, TCHP disappears from the basal body of quiescent cells and might play an inhibitory role in BF formation (25). Identification of novel proteins that specifically localize to and/or participate in the assembly of SDAs or BF would greatly enhance our understanding of the similarities and differences between the two structures. In addition, while the assembly order of SDA components has been partially revealed (10,22,24), little is known about the players involved in BF assembly and their assembly hierarchy.

In contrast to TFs, the requirement of BF for ciliogenesis is controversial. The Tsukita group showed that basal bodies lacking BF can still template cilia, indicating that BF are not required for ciliogenesis (26). Likewise, by using CRISPR-mediated gene targeting to inactivate SDA/BF components, Mazo *et al.* found that SDAs/BF are not needed for cilia assembly (22). Moreover, depletion of CCDC120 has no impact on ciliogenesis (18). In contrast, several other studies showed that ablation of ODF2, ninein, Kif3a, or CC2D2A inhibits ciliogenesis (10,15,21,27-31), although it is not clear whether this is attributed to defects in cell cycle exit, mother centriole-to-basal body conversion, and/or BF formation. While the aforementioned proteins positively regulate ciliogenesis, TCHP is unique among SDA proteins in that it is a negative regulator of ciliogenesis, and a loss of this protein in cycling cells leads to aberrant formation of cilia (25).

Here, by using three-dimensional structured illumination microscopy (3D-SIM), we found that SDAs are distinguishable from BF in normal diploid retinal pigmented epithelial cells (RPE-1), a well-established model for primary cilia assembly. We then identified NPHP5 as a novel SDAs and BF component. NPHP5 specifically regulated BF assembly by coordinating with a subset of SDA/BF proteins in cell lines able to form basal bodies. In striking contrast, NPHP5 did not organize SDAs of mother centrioles. We determined the assembly pathway of BF and

found it to be similar but not identical to the SDA assembly pathway, consistent with the notion that BF and SDAs are distinct entities. Finally, we observed a positive correlation between BF assembly and ciliogenesis and demonstrated a tight coupling between these two processes.

4.4. Results

4.4.1. SDA and BF are distinguishable

To explore the notion that SDAs of mother centrioles and BF associated with basal bodies of primary cilia might not be identical at the structural level, we used 3D-SIM to examine the sub-cellular localization pattern of two SDA/BF proteins, ninein and Cep170, under cycling versus quiescent conditions. When grown in the presence of serum, the majority of RPE-1 cells were cycling (27% of cells were Ki67 negative), lacked a primary cilium (19% of cells had cilia), and possessed a mother centriole (78% of cells had two/four centriolar CP110 dots) (Figure 4.11.1). Antibodies against ninein, Cep170, or a DA/TF protein Cep164 stained a ring-like structure indicative of nine appendages when viewed from the top (Figure 4.11.2A, E). The ring diameter of Cep164 was substantially smaller than that of ninein or Cep170 (Figure 4.11.2A, E), in agreement with published data (32). In the side view, a single ninein or Cep170 focus corresponding to SDAs was located slightly proximal to Cep164 (Figure 4.11.2A). A ninein dot representing the proximal end of the mother centriole could also be seen (Figure 4.11.2A). In contrast, most RPE-1 cells grown in serum-free medium were quiescent (78% of cells were Ki67 negative) and possessed a basal body (77% of cells with one CP110 dot) and a cilium (73% of cell had cilia) (Figure 4.11.1). Under this condition, the ring-like structure of Cep164 remained (Figure 4.11.2B, E), which is consistent with a previous report (33). Remarkably, we observed ninein or Cep170 in four dots instead of a ring from the top (Figure 4.11.2B, E). Two of the four dots, which were very close to each other, and the remaining two dots appeared to form three equidistant points on a circle (Figure 4.11.2B, E). The side view picture showed only one ninein or Cep170 focus proximal to Cep164 (Figure 4.11.2B). Another ninein focus corresponding to the proximal end of the mother centriole was observed (Figure 4.11.2B). Together, these results indicate that mother centrioles possess nine DAs and nine SDAs, whereas basal bodies carry nine TFs and three to four BF.

4.4.2. NPHP5 is a novel SDA and BF component

We previously reported NPHP5 as a centrosomal protein which localizes to the distal region of centrioles (34,35). In particular, two NPHP5 dots could be seen in quiescent RPE-1 cells and cycling cells in the G1 phase (34,35). Upon closer examination, one dot appeared to be brighter than the other, and the dot associated with the cilium-nucleating basal body was always more intense than the dot associated with the daughter centriole (Figure 4.11.2C). Use of limiting

amounts of antibody resulted in the disappearance of the weaker dot (Figure 4.11.2C), suggesting that NPHP5 might be enriched at the mother centriole and basal body. We examined NPHP5 localization in greater detail by using 3D-SIM. When viewed from the top, NPHP5 exhibited a ring-like structure reminiscent of ninein and Cep170 under cycling conditions (Figure 4.11.2A, E). The NPHP5 ring had a smaller diameter than the ninein and Cep170 ring (Figure 4.11.2A, E), suggesting that this protein is located closer to the outer surface of the centriole barrel. In the side view, a single focus of NPHP5 was located slightly proximal to Cep164 (Figure 4.11.2A). Under quiescent conditions, the top view picture revealed that the NPHP5 ring has disappeared and is replaced by four dots (Figure 4.11.2B, E), while the side view pictures showed one NPHP5 focus in close proximity to Cep164 (Figure 4.11.2B). These patterns were similar to those of ninein and Cep170 but distinct from Cep164 (Figure 4.11.2B, E). Thus, our results argue that NPHP5 is preferentially enriched at SDAs of mother centrioles and BF of basal bodies.

4.4.3. NPHP5 is required for BF assembly

Next, we explored whether NPHP5 might contribute to the assembly of SDAs and BF. Although depletion of NPHP5 with siRNA did not affect the ninein ring in cycling RPE-1 cells as revealed by 3D-SIM (Figure 4.11.2D), it led to the disappearance of ninein staining in quiescent cells (Figure 4.11.2D), suggesting that BF formation might be compromised. To confirm this finding, we examined centrosomes in control and NPHP5-depleted quiescent cells by ultrathin section EM. Most control cells had primary cilia emanating from basal bodies with BF (Figure 4.11.2F). In contrast, very few cells depleted of NPHP5 possessed cilia, as expected (34), or BF (Figure 4.11.2F). When centrioles were scored at random, 50% were expected to be basal bodies and 50% were expected to be daughter centrioles. We found that 24 out of 51 (47%) control centrioles possessed basal feet, in comparison to 14 out of 56 (25%) centrioles from NPHP5-depleted cells. Importantly, unlike Cep164 depletion, depletion of NPHP5 in quiescent cells did not compromise basal body formation since CP110 disappeared from one of the two centrioles (Figure 4.11.3) and IFT88 was properly recruited to the centrosome (Figure 4.11.4). Considering that the knockdown efficiency of NPHP5 was actually better in cycling cells than quiescent cells (Figure 4.11.5), our data suggest that in addition to cilia formation, NPHP5 is specifically required for, and/or plays a prominent role in, BF assembly.

To confirm a critical role of NPHP5 in BF assembly, we studied the effects of depleting this protein on a panel of known SDA/BF markers in quiescent RPE-1 cells by using epi-

fluorescence microscopy. Due to the resolution limit of this microscope, ninein and Cep170 signals were observed as four dots, two corresponding to BF and the other two corresponding to proximal end of centrioles (Figure 4.11.6A). Upon NPHP5 depletion, ninein and Cep170 staining intensities were substantially reduced and two of the four dots were lost (Figure 4.11.6A-B). The two remaining ninein dots did not overlap with Sec15 (Figure 4.11.6A), a SDA/BF marker, suggesting that ninein stays at the proximal end of centrioles but is de-localized from BF. These results are consistent with our earlier 3D-SIM and EM studies (Figure 4.11.2D and 4.11.2F) that BF assembly is compromised in NPHP5-depleted quiescent cells. For Kif3a, one single dot on BF was observed in control cells, and this signal completely disappeared in NPHP5-depleted cells (Figure 4.11.6A-B). Of note, although ablation of NPHP5 affected the localization of ninein, Cep170, and Kif3a, it did not affect their protein levels (Figure 4.11.7A, quiescent). TCHP was present on the daughter centriole only in control cells (Figure 4.11.6A). In cells depleted of NPHP5, TCHP stayed on the daughter centriole and basal body (Figure 4.11.6A), and its centrosomal staining (Figure 4.11.6B) and protein level dramatically increased (Figure 4.11.7A, quiescent). We also found that depletion of NPHP5 in quiescent cells has no effect on the localization of three other SDA/BF proteins CC2D2A, ODF2, and Sec15 (Figure 4.11.6A-B). Moreover, NPHP5 loss did not affect the localization of proteins residing at the TFs (Cep164 and Cep83; Figure 4.11.6C-D) or within the distal lumen of centrioles (centrin and POC5; Figure 4.11.6E-F). Thus, NPHP5 organizes BF by modulating the abundance of TCHP and the localization of a subset of SDA/BF proteins including Kif3a, ninein, Cep170, and TCHP.

To validate the requirement of NPHP5 for BF as opposed to SDA assembly, four additional experiments were conducted. First, we confirmed that depletion of NPHP5 does not impinge on the localization of SDA proteins (Kif3a, ninein, Cep170, TCHP, CC2D2A, ODF2, and Sec15; Figure 4.11.8A-B), DA proteins (Cep164 and Cep83; Figure 4.11.8C-D), and distal centriolar lumen proteins (centrin and POC5; Figure 4.11.8E-F), or the protein level of selected SDA proteins (Kif3a, ninein, Cep170, TCHP; Figure 4.11.7A, cycling) in cycling RPE-1 cells. Second, as impaired SDA and BF assembly have functional consequences, we examined SDA and BF function in the absence of NPHP5 by conducting a microtubule re-growth assay. In control cycling and quiescent RPE-1 cells, an aster of microtubules radiating out from the centrosome, indicative of microtubule nucleation, was seen as early as 1' after removal of the microtubule-depolymerizing drug nocodazole (Figure 4.11.7B). 60' after nocodazole washout, a

large network of long microtubules centered at/near the centrosome, indicative of microtubule anchoring, was observed (Figure 4.11.7B). Upon ablation of NPHP5, we found that the aster size is substantially smaller at early time points and microtubules are less focused around the centrosome at the 60' time point in quiescent cells (Figure 4.11.7B), but not in cycling cells (Figure 4.11.7B). These results indicate that BF rather than SDA function is specifically impaired. Third, Cep290 is known to anchor NPHP5 to the centrosome (34,36), and we further showed here that a loss of the former disrupts the centrosomal localization of the latter in both cycling and quiescent RPE-1 cells (Figure 4.11.9). Ablation of Cep290 reduced the number of ninein dots from four to two (Figure 4.11.9A) and the staining intensity of ninein (Figure 4.11.9B), phenotypes reminiscent of NPHP5 loss, in quiescent cells only. Fourth, we reasoned that NPHP5 might cooperate and interact with other SDA/BF proteins to assemble BF. *In situ* proximity ligation assays (PLA) were performed to assess the interaction between NPHP5 and Kif3a or ninein in cycling versus quiescent RPE-1 cells. Robust NPHP5:Kif3a and NPHP5:ninein PLA signals were detected in quiescent cells, but not in cycling cells (Figure 4.11.7C), suggesting that NPHP5 binds and/or is close proximity to Kif3a and ninein only when BF are assembled. In contrast, a strong NPHP5:Cep290 PLA signal observed under both cycling and quiescent conditions (Figure 4.11.7C) was consistent with our previous results (37). Taken together, these data further strengthen the role of NPHP5 in BF assembly.

4.4.4. Cells able to form basal bodies require NPHP5 for BF assembly

To assess whether the requirement of NPHP5 for BF assembly might extend beyond RPE-1 cells, we studied the consequences of depleting this protein in a number of different cell lines that are either able or unable to quiescence, or form basal bodies. Similar to RPE-1, >70% of APRE-19 cells subjected to serum starvation were quiescent (Ki67 negative) and possessed a basal body (one CP110 dot) and a cilium (Figures 4.11.1, 4.11.10A and 4.11.11A). A significant percentage of serum-starved HK-2 (37-43%) or HeLa (31-36%) cells also exhibited the same properties (Figures 4.11.1, 4.11.10A and 4.11.11A). Ablation of NPHP5 in quiescent RPE-1, APRE-19, HK-2, and HeLa cells induced a decrease in ninein dots (Figure 4.11.10A) and staining intensity (Figure 4.11.10B), in addition to reduced ciliation (Figure 4.11.10A), without affecting basal body formation or cell cycle exit (Figure 4.11.11A). In contrast, the same ablation in these four cell lines did not affect the number of ninein dots (Figure 4.11.10C) and ninein intensity (Figure 4.11.10D) under cycling conditions where cells were Ki67 positive and

possessed a mother centriole (two CP110 dots) (Figures 4.11.11B). These results suggest that a loss of NPHP5 specifically disrupts ninein localization, and presumably BF assembly, in quiescent cells that possess basal bodies. A second set of cell lines examined (U2OS, PC-3, MCF-7) did not readily undergo quiescence upon serum withdrawal (0-7% of cells were Ki67 negative) and did not form a cilium (0-5% of cells had cilia) or basal body (90-96% of cells with two/four CP110 dots) (Figures 4.11.1, 4.11.10A and 4.11.11A). In other words, these cells possessed mostly a mother centriole regardless of the presence or absence of serum (Figure 4.11.11). Interestingly, the staining pattern and intensity of ninein in these cells remained unchanged upon NPHP5 depletion in serum or serum-free conditions (Figures 4.11.10 and 4.11.11), reinforcing the idea that NPHP5 is not needed for the assembly of mother centriole-specific SDAs. Moreover, we studied two other cell lines (DU-5 and SAOS-2) that possessed unique properties: upon serum starvation, a significant percentage of cells (18-20%) entered quiescence, yet their mother centrioles could not be converted to basal bodies (4% of cells had one CP110 dot) and therefore lacked cilia (Figures 4.11.1, 4.11.10A and 4.11.11A). When focused on this particular quiescent cell population, we found that the number of ninein dots and ninein staining intensity are also unaffected by NPHP5 loss (Figures 4.11.10A-B and 4.11.11A), indicating that this protein is dispensable in cells that lack basal bodies. Altogether, our data suggest that the ninein phenotype provoked by NPHP5 depletion can be attributed to a loss of BF in cell lines that are able to form basal bodies.

4.4.5. The BF and SDA assembly pathways are similar but not identical

Having established a role of NPHP5 in BF assembly, we next investigated the hierarchical assembly of BF. Because of the similar protein makeup between BF and SDAs, we surmised that the assembly pathway of BF might resemble that of SDA. For SDA assembly, it is known that 1) Kif3a recruits and lies upstream of ninein to organize SDAs (10); 2) ninein recruits Cep170 (27); 3) ODF2 lies upstream of TCHP which in turn is upstream of ninein(24); and 4) ODF2 is upstream of Sec15 (23) (Figure 4.11.12A). Further, our earlier data showed that NPHP5 is not involved in this pathway (Figure 4.11.2D, 4.11.8 and 4.11.12A). In terms of BF assembly, we showed that NPHP5 recruits Kif3a, ninein, and Cep170 to organize BF (Figure 4.11.6A), prevents TCHP from being stabilized at, and recruited to, basal bodies (Figures 4.11.6A and 4.11.7A), but has no effect on the recruitment of CC2D2A, ODF2, and Sec15 (Figure 4.11.6A). We then proceeded to delineate the interrelationship between these proteins in BF assembly.

First, we individually depleted Kif3a, ninein, Cep170, TCHP, or ODF2 in quiescent RPE-1 cells and showed that such depletion does not preclude entry into quiescence (Ki67 negative, Figure 4.11.3) or the formation of basal bodies, as evidenced by the loss of one CP110 dot (Figure 4.11.3) and recruitment of IFT88 (Figure 4.11.4). Second, we examined the effects of ablating one protein on the localization of other SDA/BF proteins. Depletion of Kif3a led to a loss of two ninein or Cep170 dots, but had no effect on the localization of NPHP5, ODF2 or Sec15 (Figure 4.11.12B). TCHP, on the other hand, persisted on both the daughter centriole and basal body (Figure 4.11.12B). Depletion of ninein de-localized Cep170, but had negligible effects on the localization of NPHP5, Kif3a, TCHP, ODF2, or Sec15 (Figure 4.11.12B). Depletion of Cep170 had no effects on the localization of NPHP5, Kif3a, TCHP, ninein, ODF2, or Sec15 (Figure 4.11.12B). Depletion of ODF2 did not impinge on the localization of NPHP5 or Kif3a (Figure 4.11.12B); rather, it reduced the number of ninein and Cep170 dots, induced the mis-localization of Sec15, and caused TCHP to remain on the daughter centriole and basal body (Figure 4.11.12B). TCHP was normally absent from the basal body, as expected, and we found that depletion of TCHP does not impinge on the localization of NPHP5, Kif3a, ninein, Cep170, ODF2 or Sec15 (Figure 4.11.12B). On the basis of these results, we propose the following hierarchical pathway for BF assembly (Figure 4.11.12C). NPHP5 recruits Kif3a, which in turn prevents the recruitment of TCHP to basal bodies. ODF2 functions in parallel with NPHP5 and Kif3a to inhibit the recruitment of TCHP. Once TCHP is removed from basal bodies, ninein is brought in, followed by Cep170. Sec15 appears to function downstream of ODF2, but we were unable to determine its precise relationship with the other proteins in the BF assembly pathway due to sub-optimal knockdown efficiency.

To validate the BF assembly pathway, a series of experiments were carried out in which we ablated one protein to disrupt BF formation and asked if over-expression or depletion of a downstream or upstream player could restore its formation. Depletion of NPHP5 in quiescent RPE-1 cells resulted in the reduction of ninein dots/intensity, and this phenotype could be rescued by over-expression of NPHP5 or Kif3a (Figure 4.11.13A-B), co-depletion of TCHP (Figure 4.11.13C-D), or interestingly, over-expression of ODF2 (Figure 4.11.13A-B). Likewise, rescue of the ninein phenotype provoked by ODF2 depletion was achieved by over-expression of ODF2 (Figure 4.11.13A-B), co-depletion of TCHP (Figure 4.11.13C-D), or over-expression of NPHP5 or Kif3a (Figures 4.11.13A-B). Upon depletion of Kif3a in quiescent cells, only co-

depletion of TCHP (Figure 4.11.13C-D) or over-expression of Kif3a or ODF2 rescued the ninein phenotype (Figure 4.11.13A-B), whereas over-expression of NPHP5 showed no rescue (Figure 4.11.13A-B). Thus, our results confirm that the NPHP5-Kif3a and ODF2 axis converge at the level of TCHP to regulate BF assembly (Figure 4.11.12C), as deficiency in one axis could be compensated by increasing protein expression in the other axis or by reducing TCHP expression.

4.4.6. BF assembly correlates with ciliogenesis

The relationship between BF assembly and ciliogenesis remains poorly defined. NPHP5 depletion in quiescent RPE-1 cells simultaneously prevented ciliogenesis and BF assembly (Figures 4.11.2D, 4.11.2F, 4.11.3, 4.11.4, 4.11.6A-B and 4.11.10A-B). Likewise, depletion of Kif3a, ninein, Cep170, or ODF2 in quiescent RPE-1 cells suppressed cilia formation in addition to BF assembly (Figures 4.11.3 and 4.11.12B). On the other hand, ablation of TCHP, a negative regulator of ciliogenesis, in quiescent RPE-1 cells did not enhance ciliation or BF assembly to a significant degree (Figures 4.11.3 and 4.11.12B). In light of a positive correlation between BF assembly and ciliogenesis, we investigated whether restoration of the former might reinstate the latter. Cilia loss associated with NPHP5 or ODF2 depletion in quiescent RPE-1 cells could be rescued by over-expression of NPHP5, Kif3a, or ODF2 (Figure 4.11.14A-B), or co-depletion of TCHP (Figure 4.11.14C-D). Interestingly, impaired ciliogenesis induced by Kif3a depletion was rescued by over-expression of Kif3a or ODF2 (Figure 4.11.14A-B), or co-depletion of TCHP (Figure 4.11.14C-D), but not by over-expression of NPHP5 which functions upstream of Kif3a (Figures 4.11.12C, 4.11.14A-B). Our results suggest that the BF assembly pathway is identical to the ciliogenesis pathway and that BF formation is coupled to cilia formation.

4.5. Discussion

In this study, we demonstrated that SDAs and BF can be distinguished by their appearances. By using super-resolution microscopy, several SDA/BF components exhibit a ring-like structure, indicative of nine SDAs uniformly arranged on a circle, in cells that possess mother centrioles. On the other hand, the same SDA/BF components exhibit four dots which form three equidistant points on a circle in cells that form basal bodies. These observations suggest that there are nine SDAs and likely three to four BF. Future work will be needed to precisely address how SDAs are modified into BFs, or vice versa. Interestingly, during late G2/mitosis, SDAs apparently undergo extensive modification and are replaced by a halo (6,38), while certain SDA proteins reportedly diffuse away or disappear from the centrosome/spindle poles (17,27). Likewise, centrosomal staining of NPHP5 is greatly reduced in mitosis (34,35). It is tempting to think that this modification step might be necessary to prepare the cell for the next G0/G1 phase, where the decision to assemble SDAs versus BF hinges on whether or not the mother centrioles are converted to basal bodies.

A major finding from our study is that unlike other SDA/BF proteins known to date, NPHP5 is specifically required for BF assembly but not SDA assembly. We envision that although NPHP5 is targeted to SDAs of mother centrioles, this protein might be kept in an inactive state and barred from interacting with other SDA/BF proteins. During the conversion of mother centrioles to basal bodies, NPHP5 becomes activated, which allows it to interact with and recruit a subset of SDA/BF proteins for BF assembly. As NPHP5 is a relatively stable protein whose level does not fluctuate much in the cell cycle (35), it is plausible that its activation involves a post-translational mechanism. Further studies would be needed to decipher the mechanism by which NPHP5 transitions between inactive and active states.

We further showed in this study that a loss of SDA/BF component inhibits BF assembly and ciliogenesis without compromising basal body formation. We determined the assembly order of BF components and constructed, to our knowledge, the first-ever BF assembly pathway (Figure 4.11.12C). There are two noticeable differences between this pathway and the SDA assembly pathway (Figure 4.11.12A). First, the relationship of TCHP with its neighbouring proteins differs between SDA and BF assembly. ODF2 recruits TCHP to SDAs but prevents TCHP from being recruited to BF. Kif3a also prevents TCHP recruitment to BF, but their relationship in SDA assembly is currently unknown. TCHP recruits ninein to SDAs but inhibits its recruitment to BF.

Second, NPHP5 participates in the BF assembly by recruiting and interacting with Kif3a and ninein, and has an additional role in destabilizing TCHP. Given that the ubiquitin ligase CRL3^{KCTD17} targets TCHP for ubiquitination and proteolysis during BF assembly and ciliogenesis (39), it would be interesting to study if NPHP5 itself or in a complex with Kif3a/ninein is able to activate and/or enhance the activity of this enzyme, leading to TCHP degradation.

In addition, we showed that the assembly pathways for BF and cilia are identical and that rescue of BF loss restores ciliogenesis. How might BF assembly be linked to ciliogenesis? It is possible that BF defects disrupt the microtubule network which in turn impairs the transport of vesicles carrying ciliary building blocks to the basal body, thereby compromising ciliogenesis. The extent of BF defects required to impair ciliogenesis might vary from one system to another. Another possibility is that SDA/BF proteins we studied here are multifunctional and have a more direct role in ciliogenesis. Besides organizing BF, Kif3a functions as an anterograde motor for IFT during ciliogenesis (30,31). Likewise, NPHP5 regulates ciliary trafficking of the BBSome at the transition zone (37), while TCHP activates Aurora A kinase which might modulate HDAC6, leading to deacetylation and destabilization of axonemal microtubules (25,40). Further experiments will be needed to distinguish these possibilities.

4.6. Materials and methods

Cell culture and plasmids

Human RPE-1, ARPE-19, HK-2, HeLa, U2OS, PC-3, MCF-7, DU-5 and SAOS-2 cells were grown in DMEM (Wisent Inc, 319-005-CL) and supplemented with 10% FBS (Wisent Inc, 080150) at 37°C in a humidified 5% CO₂ atmosphere. The following proteins were expressed from plasmids in mammalian cells: pEGFP-C1, pEGFP-C1-NPHP5, pGL-FLKif3a (a gift from L. Wordeman; Addgene plasmid #13742), and pShuttle-CMV-GFP-hCenexin1 (isoform 11, a gift from K. Lee).

Antibodies

Antibodies used in this study included anti-NPHP5 (Santa Cruz Biotechnology, sc-134804 and Abcam, ab69927), anti-Kif3a (Proteintech, 13930-1-AP), anti-ninein (Santa Cruz Biotechnology, sc-376420), anti-Cep170 (Invitrogen, 41-3200), anti-ODF2/Cenexin1 (Santa Cruz Biotechnology, sc-393881), anti-TCHP (Santa Cruz Biotechnology, sc-515025 and Proteintech, 25931-1-AP), anti-CC2D2A (Sigma-Aldrich, HPA044124), anti-Cep83 (Proteintech, 26013-1-AP), anti-Cep164 (a gift from E. Nigg and Santa Cruz Biotechnology, sc-240226), anti- α -tubulin (Sigma-Aldrich, T5168), anti- γ -tubulin (Sigma-Aldrich, T3559 and Santa Cruz Biotechnology, sc-7396), anti-CP110 (Bethyl Laboratories, A301-344A), anti-CEP290 (Bethyl Laboratories, A301-659A), anti-centrin (Millipore, 04-1624), anti-POC5 (Bethyl Laboratories, A303-341A), anti-Sec15 (Sigma-Aldrich, SAB1104731), anti-GFP (Sigma-Aldrich, G1544), anti-IFT88 (Proteintech, 13967-1-AP), anti-glutamylated tubulin (GT335) (Adipogen life science, AG-20B-0020), anti-detyrosinated tubulin (DT) (Millipore, AB3201), and anti-Ki67 (Invitrogen, 180192Z and Cell signalling, 12202P).

Transmission electron microscopy

For ultra-structural characterization, cells were fixed with 2% glutaraldehyde (Electron Microscopy Sciences) and dehydrated through a series of graded ethanol dilutions. Samples were embedded in epoxy resin (Electron Microscopy Sciences). Ultrathin sections cut with a diamond knife (Diatome) (Electron Microscopy Sciences) on a Leica Microsystems UCT ultramicrotome were placed on formvar-coated nickel grids (Electron Microscopy Sciences) and stained with uranyl 2% (w/v) acetate and lead citrate (Electron Microscopy Sciences). Samples were observed with a FEI Tecnai 12 TEM (FEI) at an accelerating voltage of 120 kV and imaged with an AMT XR80C CCD camera (Advanced Microscopy Techniques Corp).

Immunoblotting and immunofluorescence

Immunoblotting and immunofluorescence were performed as described previously (41). Cells were lysed in a lysis buffer (50 mM HEPES/pH 7.4, 250 mM NaCl, 5 mM EDTA/pH 8, 0.1% NP-40, 1 mM DTT, 0.5 mM PMSF, 2 µg/ml leupeptin, 2 µg aprotinin, 10 mM NaF, 50 mM β-glycerophosphate and 10% glycerol) at 4°C for 30 minutes. Extracted proteins were recovered in the supernatant after centrifugation at 16,000g for 5 minutes. For immunoblotting, 100µg of extract was used and proteins were analyzed by SDS-PAGE and immunoblotted with primary antibodies and horseradish peroxidase (HRP)-conjugated secondary antibodies (Rockland Inc, 610-703-002 and 611-7302). For immunofluorescence staining, cells were fixed with cold methanol or 4% paraformaldehyde and permeabilized with 1% Triton X-100/PBS. Slides were blocked with 3% BSA in 0.1% Triton X-100/PBS and subsequently incubated with primary antibodies and secondary antibodies. Secondary antibodies used were Cy3- (Jackson ImmunoLabs, 711-165-151 and 715-165-152) or Alexa488- (Thermo Fisher Scientific, A11008, A11055, and A11001) conjugated donkey anti-mouse, anti-goat or anti-rabbit IgG). DAPI (Molecular Probes, D3571) stained for DNA and slides were mounted, observed, and photographed using a Leitz DMRB (Leica) microscope (100×, NA 1.3) equipped with a Retiga EXi cooled camera. Super-resolution 3D imaging was performed by using a Delta Vision OMX V4 system (Applied precision) equipped with a 100x, 1.514 oil immersion objective and 488 nm or 568 nm lasers. Image stacks of 2 µm in height with a z-distance of 0.125 µm were acquired with EMCCD camera (Photometrics), reconstructed in 3D using SoftWorx (Applied precision).

Quantitation of fluorescence intensity

A region of interest (ROI) was drawn around a fluorescent spot in the vicinity of the centrosome. The area of the ROI was used to determine the fluorescence intensity by using Volocity6 (PerkinElmer). Image conditions were identical in all cases and none were saturated as confirmed by the pixel intensity range.

Measurement of ring diameter

The diameter of a ring was measured by using Imaris 8.2 (Bitplane).

Microtubule re-growth assay

Cells were treated with 10 µM nocodazole (Sigma-Aldrich, M1404) for 1 hour at 4°C. After washing the cells several times with cold medium, they were placed in a pre-warmed medium at

37°C. Cells were fixed at various time points (0, 1, 5, 20 and 60 minutes) after 37°C and processed for immunofluorescence.

***In situ* PLA**

Duolink *in situ* PLA kit (Sigma, DUO92101-1KT) was used per manufacturer's instructions. In brief, cells grown on a glass coverslip were fixed, permeabilized, and incubated with blocking reagent for 1 hour at room temperature. Thereafter, the cells were incubated with primary antibody for 1 hour at room temperature, washed with Duolink Wash Buffer A twice, incubated with Plus and Minus PLA probes in a preheated humidity chamber for 1 hour at 37°C, washed with Duolink Wash Buffer A twice, incubated with the ligation solution for 30 minutes at 37°C, washed with Duolink Wash Buffer A twice, incubated with Duolink amplification solution for 100 minutes at 37°C, washed with Duolink Wash Buffer B twice, incubated anti- γ -tubulin-FITC for 45 minutes, and washed with Duolink Wash Buffer B once. Slides were mounted with the Duolink mounting medium containing DAPI.

RNA interference and expression of recombinant proteins

Synthetic siRNA oligonucleotides were purchased from Dharmacon and the sequences were: NS (non-specific): 5'-AATTCTCCGAACGTGTCACGT-3'; NPHP5 oligo2: 5'-ACCCAAGGATCTTATCTAT-3' (used for knocking down NPHP5); NPHP5 oligo5: 5'-CCCTAAGAATTGACACAAA-3' (targeted against 3'-UTR and used for knocking down NPHP5 in rescue experiments only); Cep290: 5'-AAATTAAGATGCTCACCGATT-3'; Kif3A: 5'-CAGATTGTCCTATGTTGCGCTGT-3' (targeted against 3'-UTR); ODF2 oligo2: 5'-GGTCAAGATGCAAAAAGGT-3' (used for knocking down ODF2); ODF2 oligo3'UTR: 5'-GGTCTTGTCTTAGCTACTAG-3' (targeted against 3'-UTR and used for knocking down ODF2 in rescue experiments only); TCHP: 5'-CAGGGCATTGTTCCATGGTTA-3'; Ninein: 5'-GCCGAGCTCTCTGAAGTAAA-3'; and Cep170: 5'-GAAGGAATCCTCCAAGTCA-3'. siRNA transfection were performed using siIMPORTER (Millipore, 64-101) according to per manufacturer's instructions. For RNA interference, cells were transfected with siRNA and harvested 72 hours after transfection. For experiments involving RNA interference and recombinant protein expression, cells were transfected with siRNA at 0 hour, transfected with an expression vector at 24 hour, and harvested at 72 hour time point.

Induction of primary cilia

Cells were induced to form primary cilia by serum withdrawal for at least 48 hours. Under this condition, the majority of RPE-1 and ARPE-19 cells, along with a significant percentage of HK-2 and HeLa cells, entered quiescence and formed cilia. In contrast, very few U2OS, PC-3, and MCF-7 cells entered quiescence and formed cilia. A certain percentage of MCF-7, DU-5, and SAOS-2 cells entered quiescence yet they did not form cilia. Cells positive and negative for Ki67 were deemed to be cycling and quiescent, respectively. Cells with one CP110 dot were deemed to possess basal bodies, whereas those with two/four CP110 dots possessed mother centrioles instead of basal bodies. Cilia were detected by staining cells with IFT88, glutamylated tubulin, and/or detyrosinated tubulin.

4.7. Acknowledgements

We thank all members of the Tsang laboratory for constructive advice, especially A. Das and J. Qian for their efforts and discussions on this project. WYT was a Canadian Institutes of Health Research New Investigator and a Fonds de recherche Santé Junior 2 Research Scholar. This work was supported by the Canadian Institutes of Health Research and the Natural Sciences and Engineering Research Council of Canada to WYT.

4.8. Author contributions

WYT designed all of the experiments with input from DH and MB. DH and MB performed the experiments and analyzed the corresponding results. WYT and DH wrote the paper, and all authors reviewed the paper.

4.9. Conflict of Interest

The authors declare no conflict of interest.

4.10. References

1. Bornens M (2012) The centrosome in cells and organisms. *Science* **335**, 422-426.
2. Kobayashi T and Dynlacht BD (2011) Regulating the transition from centriole to basal body. *J Cell Biol* **193**, 435-444.
3. Nigg EA and Stearns T (2011) The centrosome cycle: Centriole biogenesis, duplication and inherent asymmetries. *Nat Cell Biol* **13**, 1154-1160.
4. Seeley ES and Nachury MV (2010) The perennial organelle: assembly and disassembly of the primary cilium. *J Cell Sci* **123**, 511-518.
5. Goetz SC, Liem KF Jr and Anderson KV (2012) The spinocerebellar ataxia-associated gene Tau tubulin kinase 2 controls the initiation of ciliogenesis. *Cell* **151**, 847-858.
6. Vorobjev I A and Chentsov Yu S (1982) Centrioles in the cell cycle. I. Epithelial cells. *J Cell Biol* **93**, 938-949.
7. Ibrahim R, Messaoudi C, Chichon FJ, Celati C and Marco S (2009) Electron tomography study of isolated human centrioles. *Microsc Res Tech* **72**, 42-48.
8. Anderson R G (1972) The three-dimensional structure of the basal body from the rhesus monkey oviduct. *J Cell Biol* **54**, 246-265.
9. Kunimoto K, Yamazaki Y, Nishida T, Shinohara K, Ishikawa H, Hasegawa T, Okanou T, Hamada H, Noda T, Tamura A, Tsukita S and Tsukita S (2012) Coordinated ciliary beating requires Odf2-mediated polarization of basal bodies via basal feet. *Cell* **148**, 189-200.
10. Kodani A, Salomé Sirerol-Piquer M, Seol A, Garcia-Verdugo JM and Reiter JF (2013) Kif3a interacts with Dynactin subunit p150 Glued to organize centriole subdistal appendages. *EMBO J* **32**, 597-607.
11. Odor DL and Blandau RJ (1985) Observations on the solitary cilium of rabbit oviductal epithelium: its motility and ultrastructure. *Am J Anat* **174**, 437-453.
12. Hagiwara H, Ohwada N, Aoki T, Suzuki T and Takata K (2008) The primary cilia of secretory cells in the human oviduct mucosa. *Med Mol Morphol* **41**, 193-198.
13. Delgehyr N, Sillibourne J and Bornens M (2005) Microtubule nucleation and anchoring at the centrosome are independent processes linked by ninein function. *J Cell Sci* **118**, 1565-1575.

14. Gordon R E (1982) Three-dimensional organization of microtubules and microfilaments of the basal body apparatus of ciliated respiratory epithelium. *Cell Motil* **2**, 385-391.
15. Ishikawa H, Kubo A and Tsukita S (2005) Odf2-deficient mother centrioles lack distal/subdistal appendages and the ability to generate primary cilia. *Nat Cell Biol* **7**, 517-524.
16. Mogensen MM, Malik A, Piel M, Bouckson-Castaing V and Bornens M (2000) Microtubule minus-end anchorage at centrosomal and non-centrosomal sites: the role of ninein. *J Cell Sci* **113**, 3013-3023.
17. Guarguaglini G, Duncan PI, Stierhof YD, Holmström T, Duensing S and Nigg EA (2005) The forkhead-associated domain protein Cep170 interacts with Polo-like kinase 1 and serves as a marker for mature centrioles. *Mol Biol Cell* **16**, 1095-1107.
18. Huang N, Xia Y, Zhang D, Wang S, Bao Y, He R, Teng J and Chen J (2017) Hierarchical assembly of centriole subdistal appendages via centrosome binding proteins CCDC120 and CCDC68. *Nat Commun* **8**, 15057.
19. Gromley A, Jurczyk A, Sillibourne J, Halilovic E, Mogensen M, Groisman I, Blomberg M and Doxsey S (2003) A novel human protein of the maternal centriole is required for the final stages of cytokinesis and entry into S phase. *J Cell Biol* **161**, 535-545.
20. Chang P, Giddings TH Jr, Winey M and Stearns T (2003) Epsilon-tubulin is required for centriole duplication and microtubule organization. *Nat Cell Biol* **5**, 71-76.
21. Veleri S, Manjunath SH, Fariss RN, May-Simera H, Brooks M, Foskett TA, Gao C, Longo TA, Liu P, Nagashima K, Rachel RA, Li T, Dong L and Swaroop A (2014) Ciliopathy-associated gene Cc2d2a promotes assembly of subdistal appendages on the mother centriole during cilia biogenesis. *Nat Commun* **5**, 4207.
22. Mazo G, Soplop N, Wang WJ, Uryu K and Tsou MF (2016) Spatial control of primary ciliogenesis by subdistal appendages alters sensation-associated properties of cilia. *Dev Cell* **39**, 424-437.
23. Hehny H, Chen CT, Powers CM, Liu HL and Doxsey S (2012) The centrosome regulates the Rab11- dependent recycling endosome pathway at appendages of the mother centriole. *Curr Biol* **22**, 1944-1950.
24. Ibi M, Zou P, Inoko A, Shiromizu T, Matsuyama M, Hayashi Y, Enomoto M, Mori D, Hirotsune S, Kiyono T, Tsukita S, Goto H and Inagaki M (2011) Trichoplein controls

- microtubule anchoring at the centrosome by binding to Odf2 and ninein. *J Cell Sci* **124**, 857-864.
25. Inoko A, Matsuyama M, Goto H, Ohmuro-Matsuyama Y, Hayashi Y, Enomoto M, Ibi M, Urano T, Yonemura S, Kiyono T, Izawa I and Inagaki M (2012) Trichoplein and Aurora A block aberrant primary cilia assembly in proliferating cells. *J Cell Biol* **197**, 391-405.
 26. Tateishi K, Yamazaki Y, Nishida T, Watanabe S, Kunimoto K, Ishikawa H and Tsukita S (2013) Two appendages homologous between basal bodies and centrioles are formed using distinct Odf2 domains. *J Cell Biol* **203**, 417-425.
 27. Graser S, Stierhof YD, Lavoie SB, Gassner OS, Lamla S, Le Clech M and Nigg EA (2007) Cep164, a novel centriole appendage protein required for primary cilium formation. *J Cell Biol* **179**, 321-330.
 28. Chang J, Seo SG, Lee KH, Nagashima K, Bang JK, Kim BY, Erikson RL, Lee KW, Lee HJ, Park JE and Lee KS (2013) Essential role of Cenexin1, but not Odf2, in ciliogenesis. *Cell Cycle* **12**, 655-662.
 29. Hung HF, Hehnlly H and Doxsey S (2016) The Mother Centriole Appendage Protein Cenexin Modulates Lumen Formation through Spindle Orientation. *Curr Biol* **26**, 1248.
 30. Marszalek JR, Ruiz-Lozano P, Roberts E, Chien KR and Goldstein LS (1999) Situs inversus and embryonic ciliary morphogenesis defects in mouse mutants lacking the KIF3A subunit of kinesin-II. *Proc Natl Acad Sci U S A* **96**, 5043-5048.
 31. Takeda S, Yonekawa Y, Tanaka Y, Okada Y, Nonaka S and Hirokawa N (1999) Left-right asymmetry and kinesin superfamily protein KIF3A: new insights in determination of laterality and mesoderm induction by kif3A^{-/-} mice analysis. *J Cell Biol* **145**, 825-836.
 32. Sonnen KF, Schermelleh L, Leonhardt H and Nigg EA (2012) 3D-structured illumination microscopy provides novel insight into architecture of human centrosomes. *Biol Open* **1**, 965-976.
 33. Kobayashi T, Kim S, Lin YC, Inoue T and Dynlacht BD (2014) The CP110-interacting proteins Talpid3 and Cep290 play overlapping and distinct roles in cilia assembly. *J Cell Biol* **204**, 215-229.

34. Barbelanne M, Song J, Ahmadzai M and Tsang WY (2013) Pathogenic NPHP5 mutations impair protein interaction with Cep290, a prerequisite for ciliogenesis. *Hum Mol Genet* **22**, 2482-2494.
35. Das A, Qian J and Tsang WY (2017) USP9X counteracts differential ubiquitination of NPHP5 by MARCH7 and BBS11 to regulate ciliogenesis. *PLoS Genet* **13**, e1006791.
36. Sang L, Miller JJ, Corbit KC, Giles RH, Brauer MJ, Otto EA, Baye LM, Wen X, Scales SJ, Kwong M, Huntzicker EG, Sfakianos MK, Sandoval W, Bazan JF, Kulkarni P, Garcia-Gonzalo FR, Seol AD, O'Toole JF, Held S, Reutter HM, Lane WS, Rafiq MA, Noor A, Ansar M, Devi AR, Sheffield VC, Slusarski DC, Vincent JB, Doherty DA, Hildebrandt F, Reiter JF and Jackson PK (2011) Mapping the NPHP-JBTS-MKS protein network reveals ciliopathy disease genes and pathways. *Cell* **145**, 513-528.
37. Barbelanne M, Hossain D, Chan DP, Peränen J and Tsang WY (2015) Nephrocystin proteins NPHP5 and Cep290 regulate BBSome integrity, ciliary trafficking and cargo delivery. *Hum Mol Genet* **24**, 2185-2200.
38. Uzbekov R and Prigent C (2007) Clockwise or anticlockwise? Turning the centriole triplets in the right direction! *FEBS Lett* **581**, 1251-1254.
39. Kasahara K, Kawakami Y, Kiyono T, Yonemura S, Kawamura Y, Era S, Matsuzaki F, Goshima N and Inagaki M (2014) Ubiquitin-proteasome system controls ciliogenesis at the initial step of axoneme extension. *Nat Commun* **5**, 5081.
40. Pugacheva EN, Jablonski SA, Hartman TR, Henske EP and Golemis EA (2007) HEF1-dependent Aurora A activation induces disassembly of the primary cilium. *Cell* **129**, 1351-1363.
41. Hossain D, Javadi Esfehiani Y, Das A and Tsang WY (2017) Cep78 controls centrosome homeostasis by inhibiting EDD-DYRK2-DDB1^{VprBP}. *EMBO Rep* **18**, 632-644.

4.11. Figures

Cell line	Quiescent				Cycling			
	% of Ki67 -ve cells	% of cells with 1 CP110 dot	% of cells with 2/4 CP110 dots	% of ciliated cells	% of Ki67 -ve cells	% of cells with 1 CP110 dot	% of cells with 2/4 CP110 dots	% of ciliated cells
RPE-1	78 ± 4	77 ± 3	23 ± 3	73 ± 2	27 ± 3	22 ± 3	78 ± 3	19 ± 1
ARPE-19	80 ± 4	78 ± 6	22 ± 6	73 ± 2	27 ± 2	23 ± 1	77 ± 1	19 ± 1
HK-2	43 ± 2	41 ± 1	59 ± 1	37 ± 4	18 ± 2	13 ± 1	87 ± 1	11 ± 1
HeLa	36 ± 5	31 ± 2	69 ± 2	31 ± 3	9 ± 1	8 ± 1	92 ± 1	6 ± 2
U2OS	0 ± 0	4 ± 1	96 ± 1	0 ± 0	0 ± 0	4 ± 2	96 ± 2	0 ± 0
PC-3	6 ± 2	6 ± 1	94 ± 1	1 ± 2	0 ± 0	2 ± 2	98 ± 2	0 ± 0
MCF-7	7 ± 3	10 ± 1	90 ± 1	5 ± 1	3 ± 1	4 ± 1	96 ± 1	1 ± 1
DU-5	20 ± 1	4 ± 1	96 ± 1	0 ± 0	2 ± 1	3 ± 1	97 ± 1	0 ± 0
SAOS-2	18 ± 2	4 ± 1	96 ± 1	0 ± 0	2 ± 1	4 ± 1	96 ± 1	0 ± 0

Figure 4.11.1. Cell lines vary in their ability to enter quiescence, form basal bodies, and ciliate

RPE-1, ARPE-19, HK-2, HeLa, U2OS, PC-3, MCF-7, DU-5, and SAOS-2 cells grown in the presence (cycling) or absence (quiescent) of serum were stained with antibodies against CP110 and Ki67 or glutamylated tubulin (GT335). The percentage of Ki67 negative cells, the percentage of cells with 1 or 2/4 CP110 dots, and the percentage of ciliated cells are presented. At least 100 cells for each condition were scored, and the mean and standard error of three independent experiments are presented.

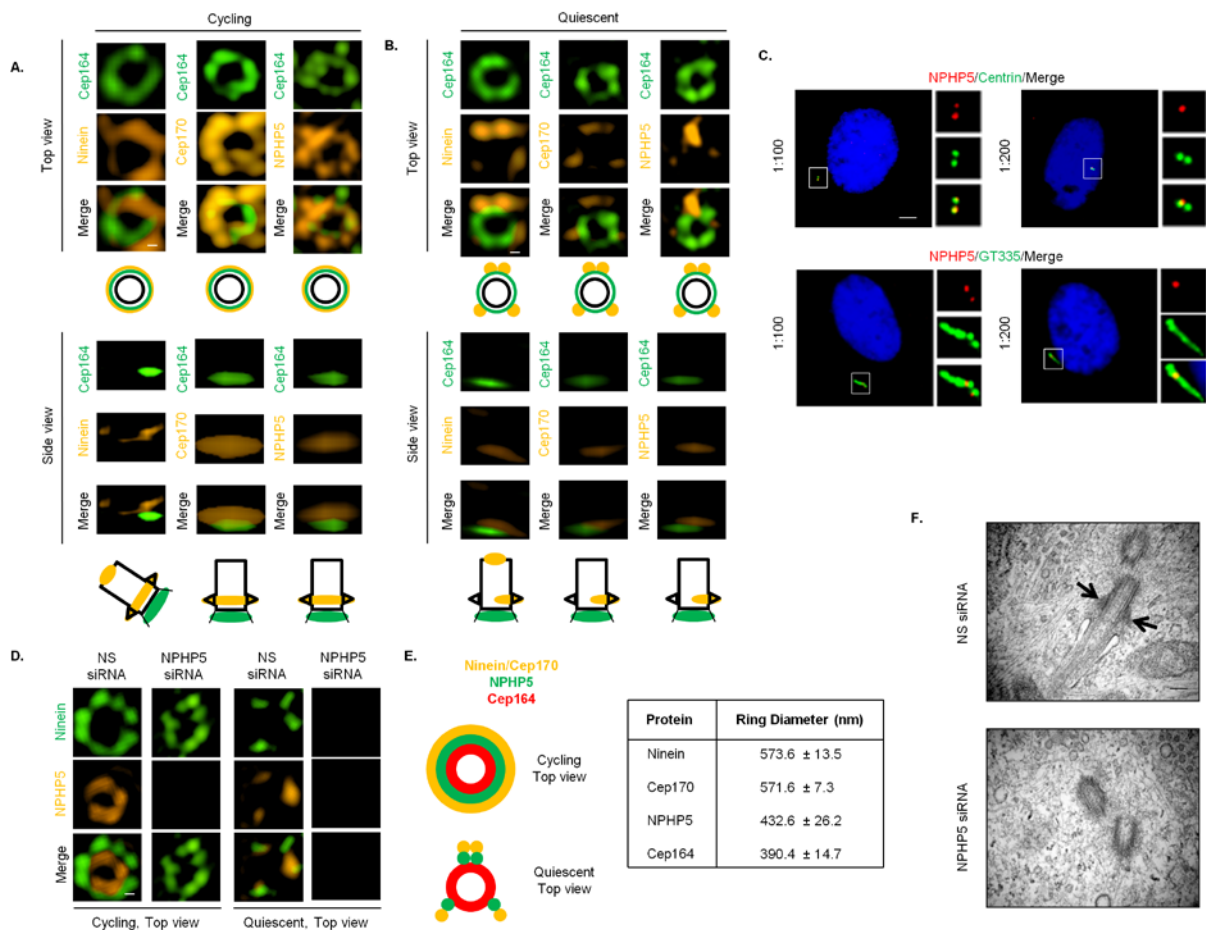


Figure 4.11.2. NPHP5 is a novel component of SDAs and BF, two distinguishable structures

A) Cycling or B) quiescent RPE-1 cells were stained with the indicated antibodies and images were acquired with 3D-SIM. Black circle and rectangle represent top-view and side-view of a mother centriole A) or basal body B). Scale bar, 0.1 μ m. C) Quiescent RPE-1 cells were stained with the indicated antibodies and with DAPI (blue). Two different dilutions of antibodies against NPHP5, 1:100 and 1:200, were used. Scale bar, 1 μ m. D) Cycling or quiescent RPE-1 cells transfected with NS (non-specific) or NPHP5 siRNAs were stained with the indicated antibodies and images were acquired with 3D-SIM. Scale bar, 0.1 μ m. E) (Left) 3D-SIM staining patterns of several proteins in cycling and quiescent RPE-1 cells are presented. (Right) Average ring diameter from the top view of cycling RPE-1 cells. n=5. F) Quiescent RPE-1 cells transfected with NS or NPHP5 siRNAs were analyzed by transmission electron microscopy. Scale bar, 0.1 μ m.

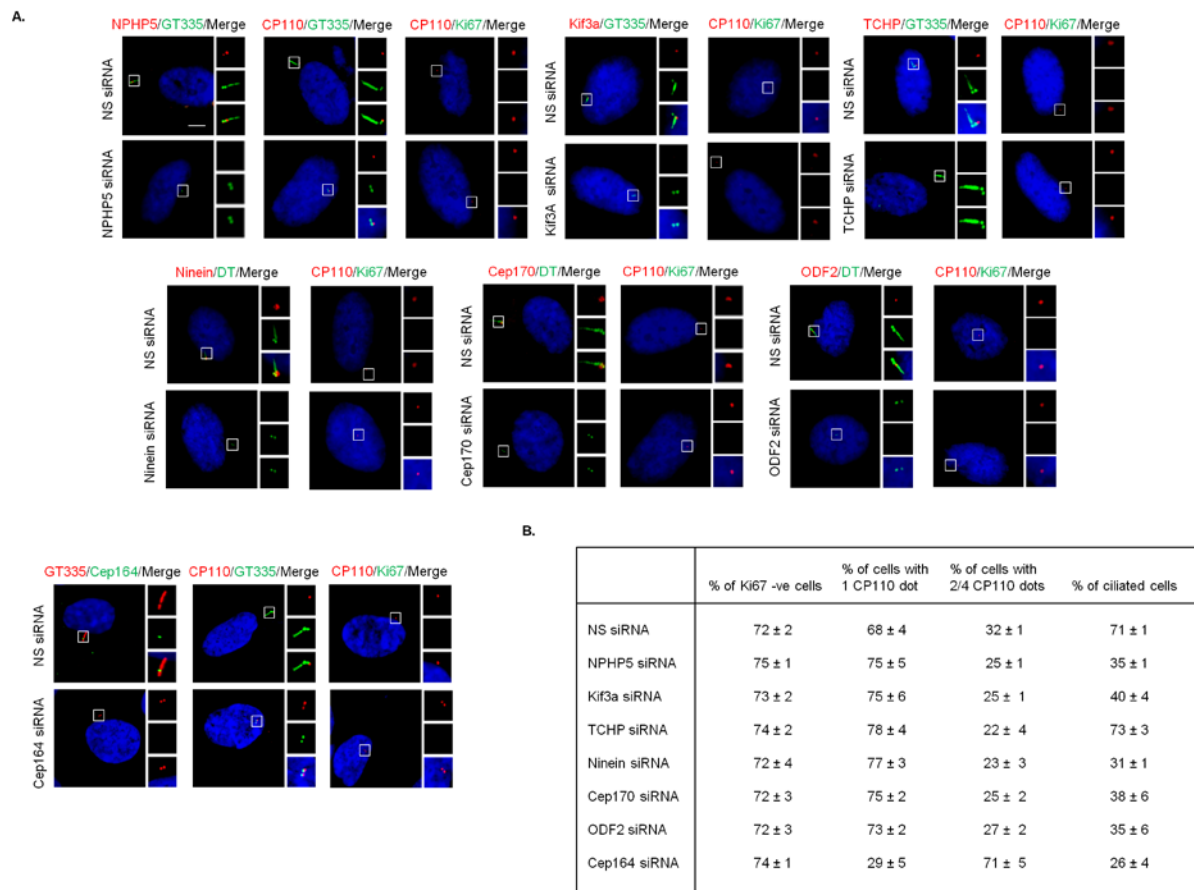


Figure 4.11.3. Ablation of BF components inhibits ciliogenesis without affecting entry into quiescence and basal body formation

A) Quiescent RPE-1 cells transfected with NS (non-specific) or the indicated siRNAs targeting SDA/BF components (NPHP5, Kif3a, TCHP, ninein, Cep170, ODF2) or a DA/TF component (Cep164) were stained with the indicated antibodies and with DAPI (blue). Scale bar, 1 μ m. B) Quiescent RPE-1 cells transfected with NS or the indicated siRNAs were stained with antibodies against CP110 and Ki67 or glutamylated tubulin (GT335), and with DAPI. The percentage of Ki67 negative cells, the percentage of cells with 1 CP110 dot or 2/4 CP110 dots, and the percentage of ciliated cells are presented. At least 100 cells for each condition were scored, and the mean and standard error of three independent experiments are presented.

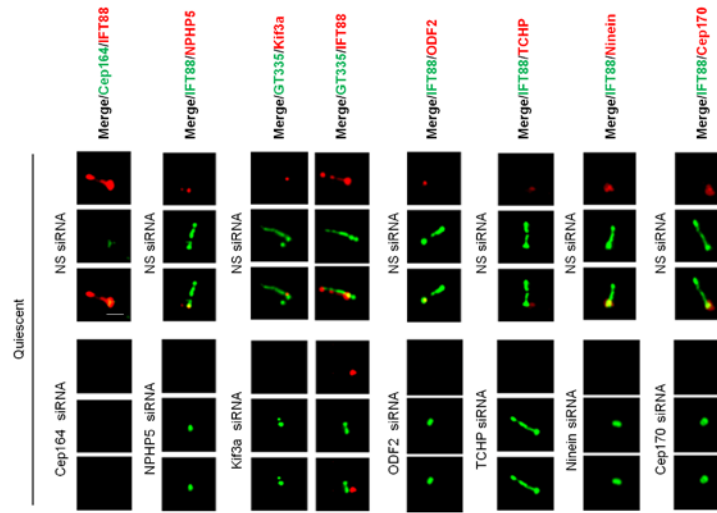


Figure 4.11.4. Ablation of BF components inhibits ciliogenesis without affecting recruitment of IFT88

Quiescent RPE-1 cells transfected with NS (non-specific) or the indicated siRNAs targeting SDA/BF components (NPHP5, Kif3a, TCHP, ninein, Cep170, ODF2) or a DA/TF component (Cep164) were stained with the indicated antibodies. Scale bar, 1 μ m.

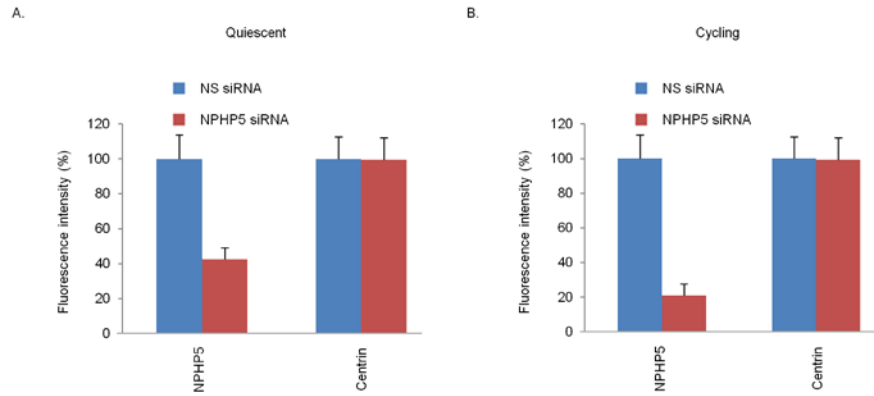


Figure 4.11.5. Knockdown efficiency of NPHP5 in cycling versus quiescent RPE-1 cells

A) Quiescent or B) cycling RPE-1 cells transfected with NS (non-specific) or NPHP5 siRNAs were stained with antibodies against NPHP5 and centrin. Fluorescence intensities of NPHP5 and centrin at the centrosome were quantitated and set to 100% in NS siRNA-transfected cells. For quantitation, at least 20 cells for each condition were analyzed, and the mean and standard error of three independent experiments are presented.

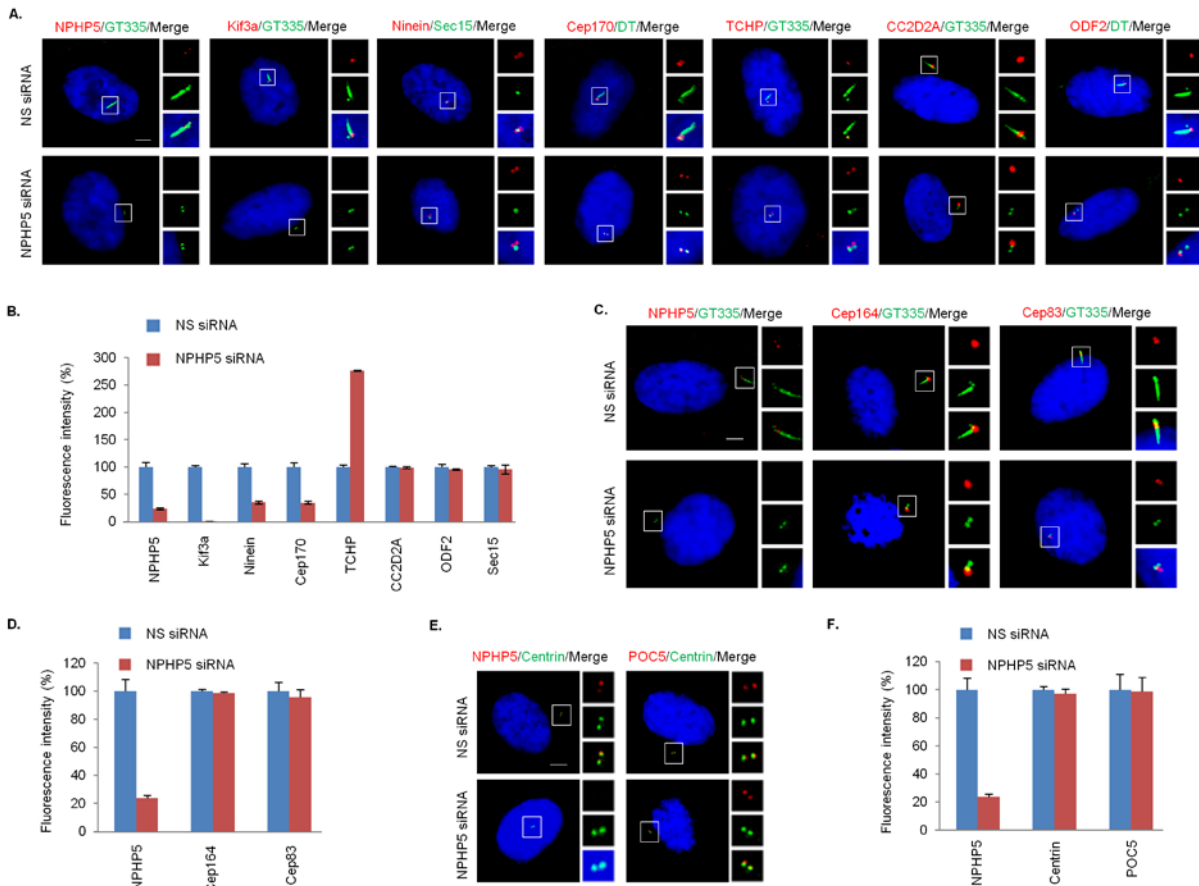


Figure 4.11.6. NPHP5 recruits Kif3a, ninein, and Cep170 to BF while preventing the recruitment of TCHP in quiescent RPE-1 cells

A, C, E) Quiescent RPE-1 cells transfected with NS (non-specific) or NPHP5 siRNAs were stained with the indicated antibodies and with DAPI (blue). Scale bar, 1 μ m. B, D, F) Fluorescence intensities of various proteins at the centrosome were quantitated and set to 100% in NS siRNA-transfected cells. For quantitation, at least 20 cells for each condition were analyzed, and the mean and standard error of three independent experiments are presented.

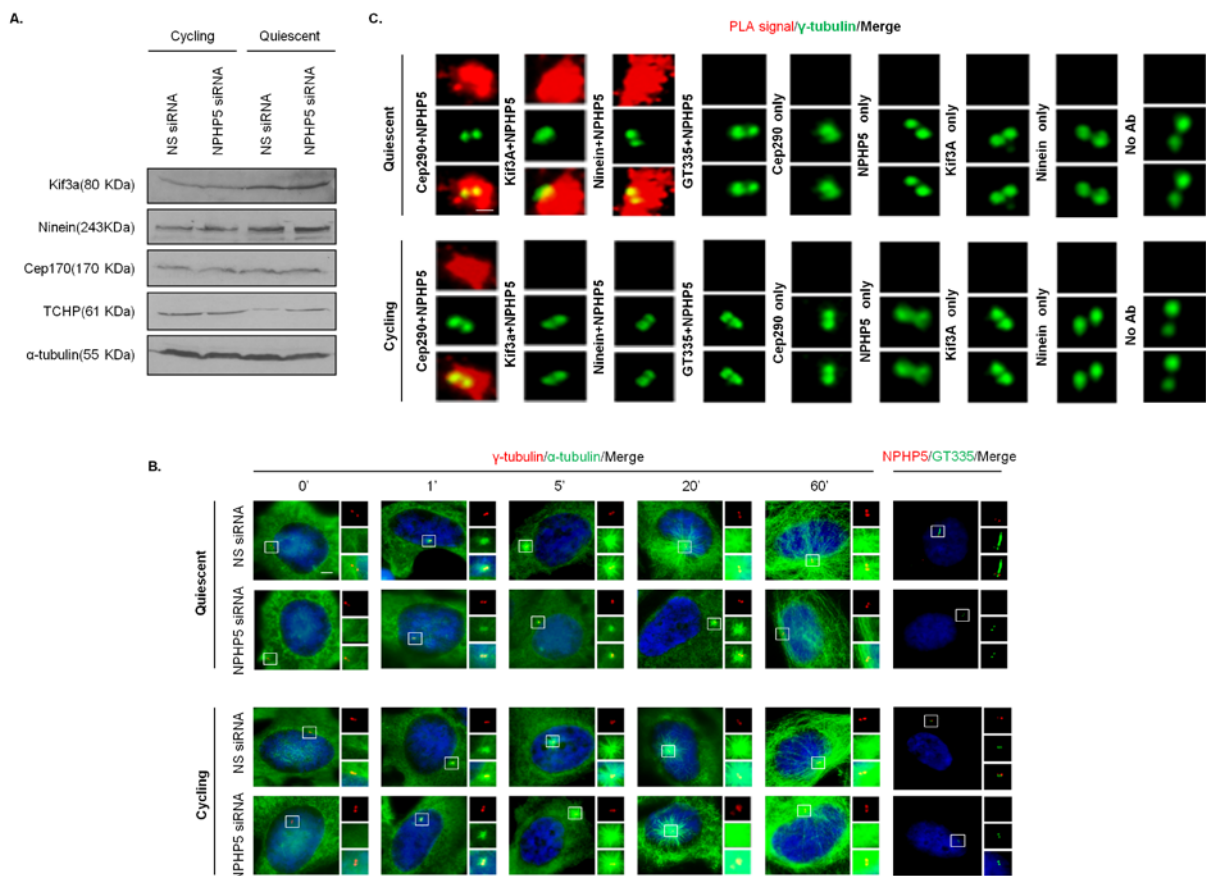


Figure 4.11.7. NPHP5 destabilizes TCHP, interacts with Kif3a and ninein at the centrosome, and is required for microtubule nucleation and anchoring in quiescent RPE-1 cells

A) Lysates from cycling or quiescent RPE-1 cells transfected with NS (non-specific) or NPHP5 siRNAs were analyzed by immunoblotting with the indicated antibodies. α -tubulin was used as a loading control. B) Quiescent or cycling RPE-1 cells transfected with NS or NPHP5 siRNAs and subjected to a microtubule re-growth assay were stained with the indicated antibodies and with DAPI (blue). Depletion of NPHP5 was monitored by staining cells with antibodies against NPHP5 (red) and glutamylated tubulin (GT335) (green). Scale bar, 1 μ m. C) *In situ* PLAs were performed on cycling or quiescent RPE-1 cells stained with the indicated combination of antibodies to reveal the location of close proximity/interaction (PLA signal, red) between two proteins. Cells were co-stained with γ -tubulin (green) to visualize the centrosome. No PLA signal was detected when NPHP5 and GT335 antibodies were used (negative control; no interaction between NPHP5 and glutamylated tubulin), one antibody was used, or two antibodies

were missing (no Ab). As positive control, a robust PLA signal was detected by using antibodies against NPHP5 and Cep290 under cycling and quiescent conditions. Scale bar, 1 μm .

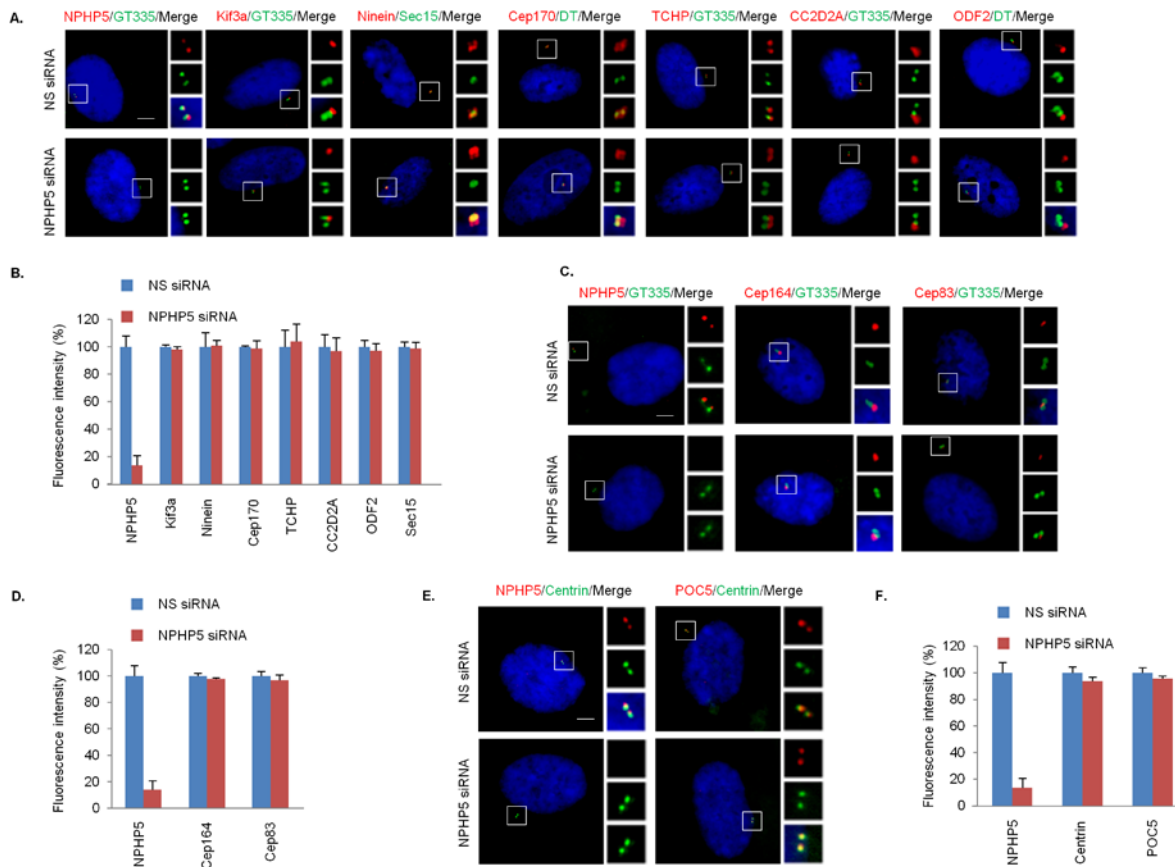


Figure 4.11.8. NPHP5 does not affect SDA assembly in cycling RPE-1 cells

A, C, E) Cycling RPE-1 cells transfected with NS (non-specific) or NPHP5 siRNAs were stained with the indicated antibodies and with DAPI (blue). Scale bar, 1 μ m. B, D, F) Fluorescence intensities of various proteins at the centrosome were quantitated and set to 100% in NS siRNA-transfected cells. For quantitation, at least 20 cells for each condition were analyzed, and the mean and standard error of three independent experiments are presented.

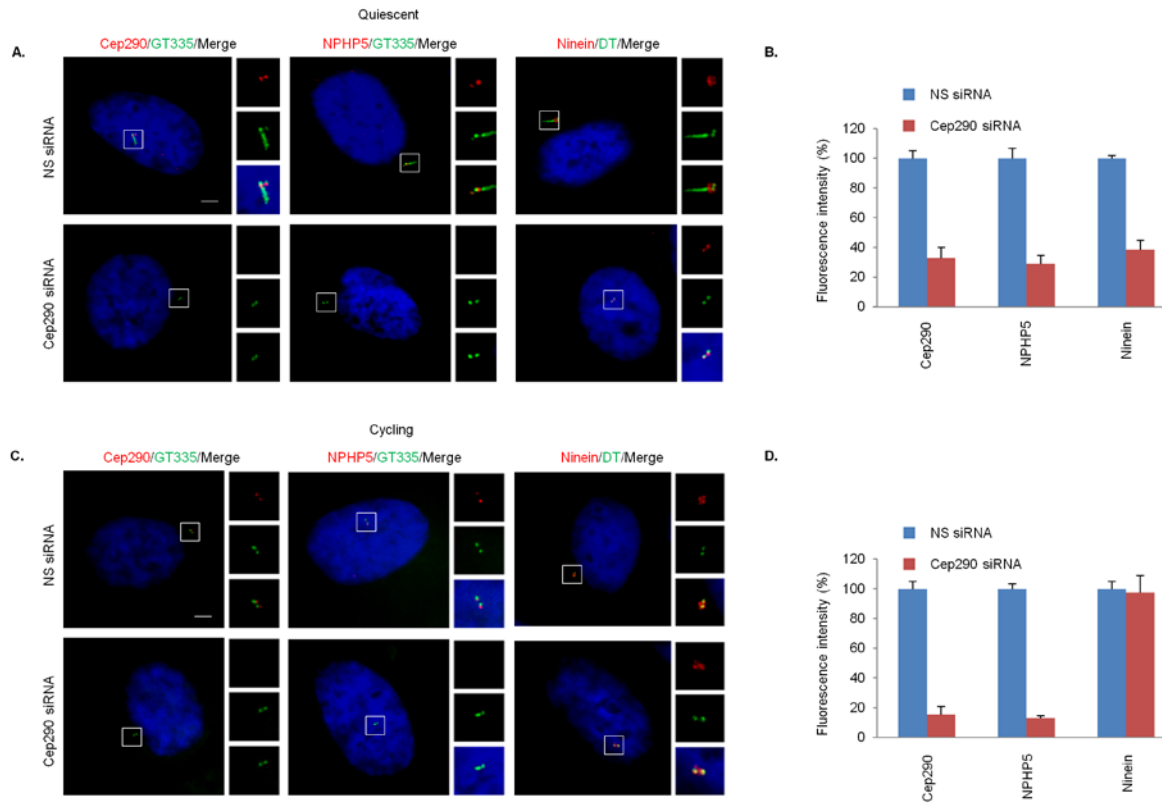


Figure 4.11.9. Cep290 specifically recruits ninein to BF but not SDAs

A) Quiescent or C) cycling RPE-1 cells transfected with NS (non-specific) or Cep290 siRNAs were stained with the indicated antibodies and with DAPI (blue). Scale bar, 1 μ m. B, D) Fluorescence intensities of various proteins at the centrosome were quantitated and set to 100% in NS siRNA-transfected cells. For quantitation, at least 20 cells for each condition were analyzed, and the mean and standard error of three independent experiments are presented.

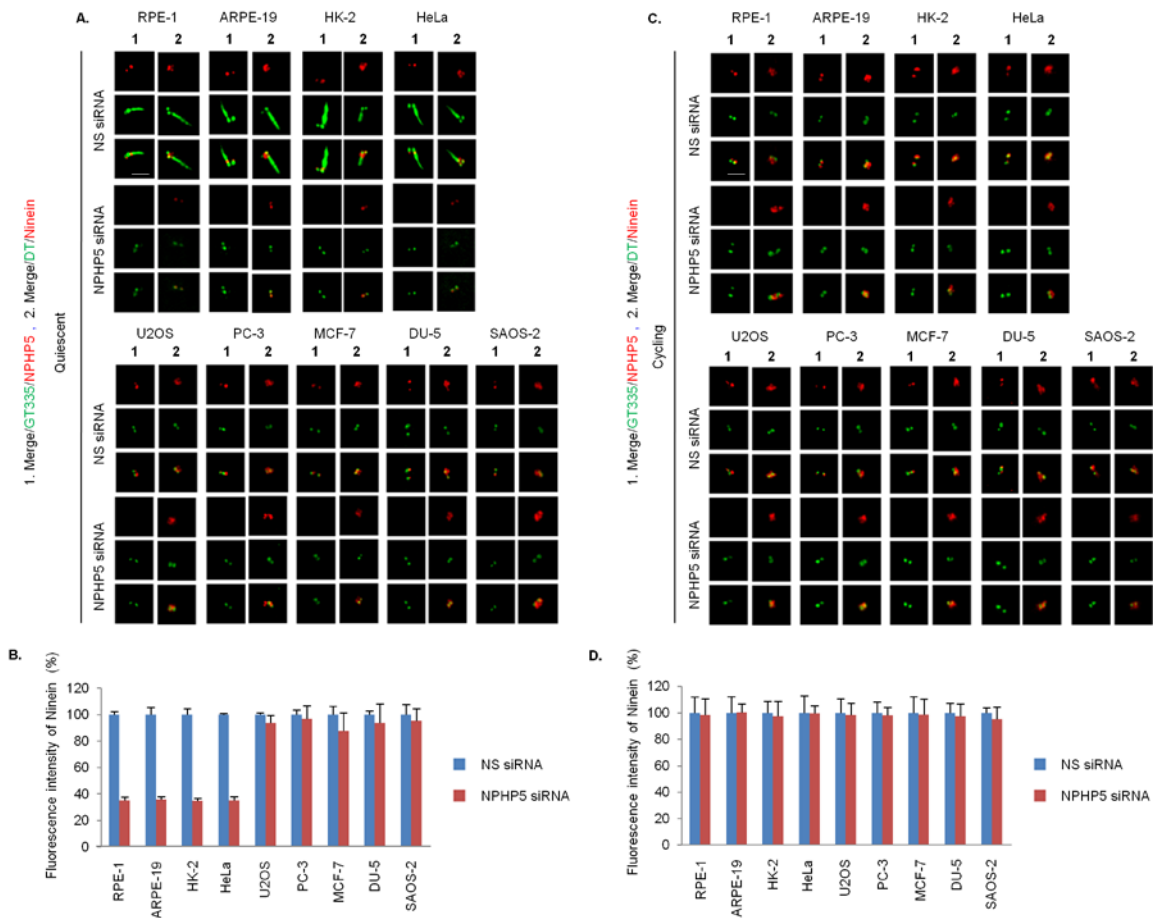


Figure 4.11.10. NPHP5-mediated BF assembly is cell type specific

A) Quiescent or C) cycling RPE-1, ARPE-19, HK-2, HeLa, U2OS, PC-3, MCF-7, DU-5, and SAOS-2 cells transfected with NS (non-specific) or NPHP5 siRNAs were stained with the indicated antibodies. Scale bar, 1 μ m. B, D) Fluorescence intensity of ninein at the centrosome was quantitated and set to 100% in NS siRNA-transfected cells. For quantitation, at least 20 cells for each condition were analyzed, and the mean and standard error of three independent experiments are presented.

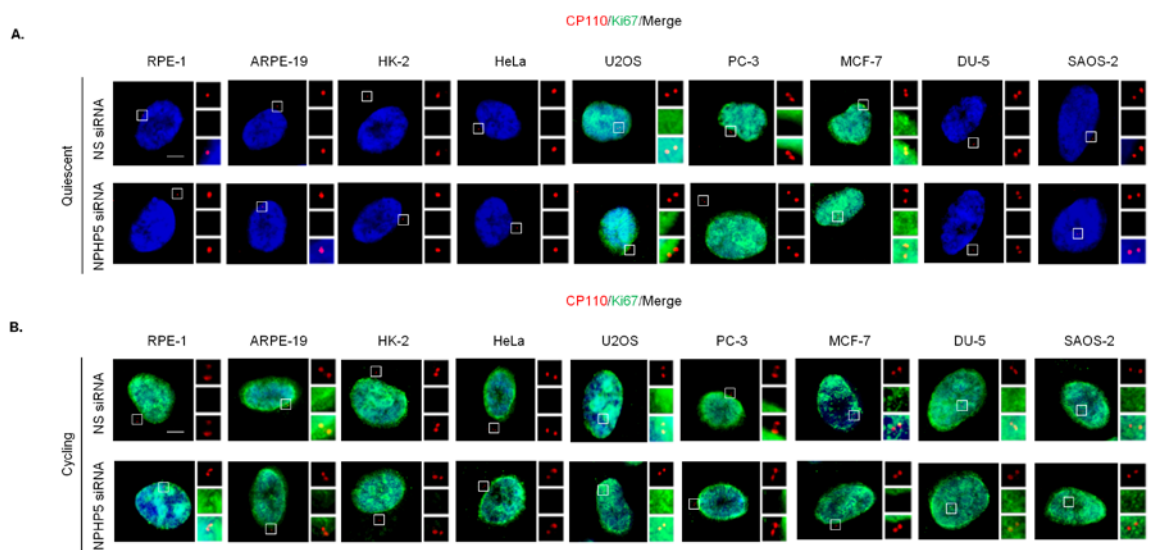


Figure 4.11.11. Ablation of NPHP5 does not affect entry into quiescence or basal body formation in quiescent RPE-1, ARPE-19, HK-2, and HeLa cells

A, B) RPE-1, ARPE-19, HK-2, HeLa, U2OS, PC-3, MCF-7, DU-5, and SAOS-2 cells transfected with NS (non-specific) or NPHP5 siRNAs and grown in the presence (cycling) or absence (quiescent) of serum were stained with antibodies against CP110 and Ki67, and with DAPI (blue).

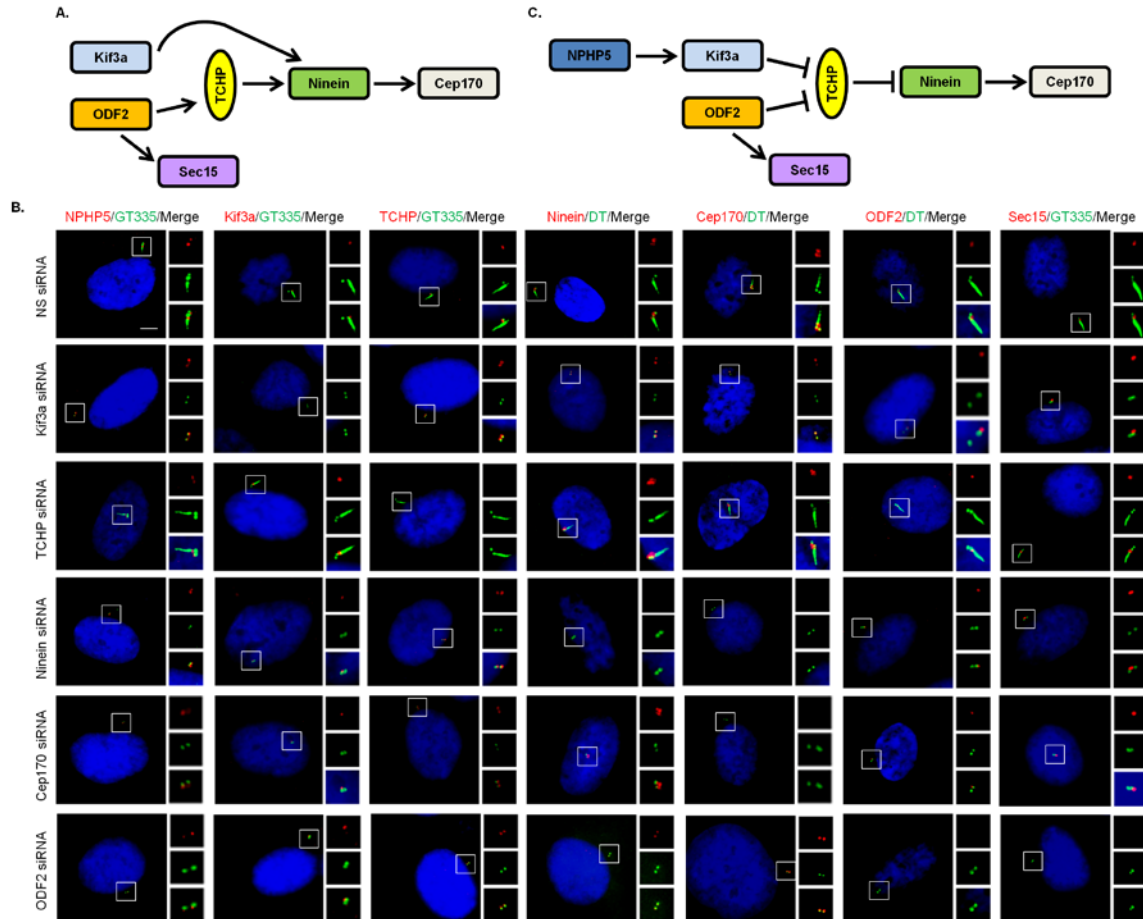


Figure 4.11.12. Hierarchical assembly of BF

A) Schematic model of SDA assembly based on the literature. B) Quiescent RPE-1 cells transfected with NS (non-specific) or the indicated siRNAs targeting SDA/BF components (Kif3a, TCHP, ninein, Cep170, ODF2) were stained with the indicated antibodies and with DAPI (blue). Scale bar, 1 μ m. C) Schematic model of BF assembly based on our results. Note the similarities and differences between the SDA and BF assembly pathways.

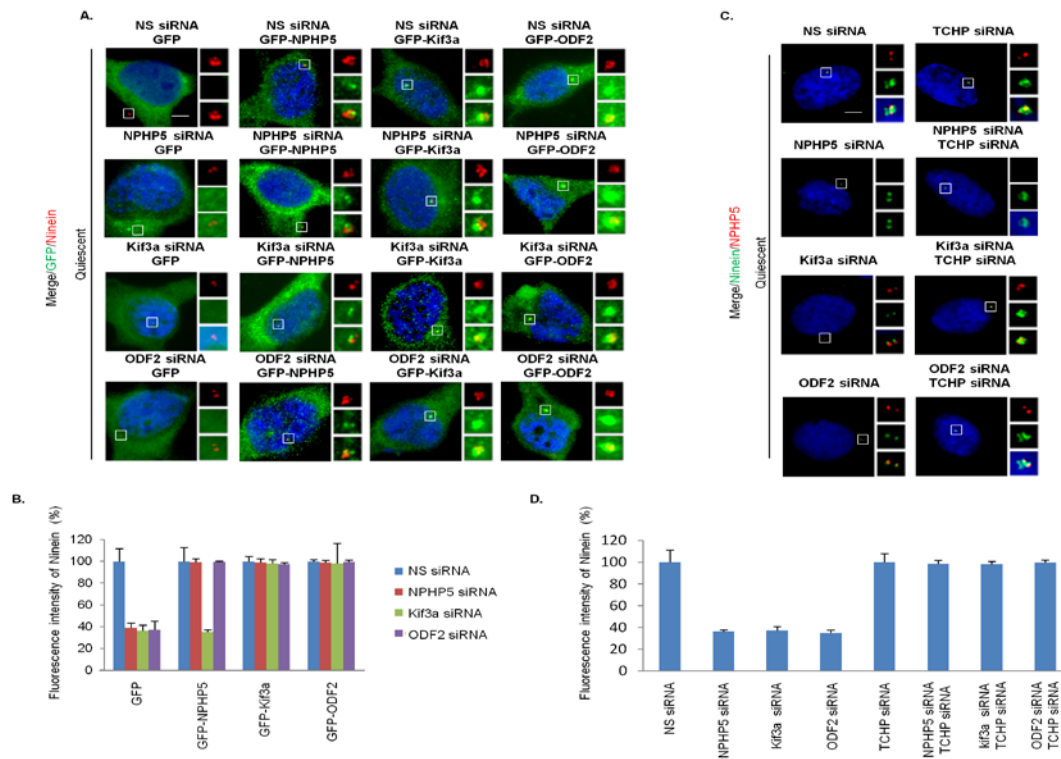


Figure 4.11.13. BF loss due to ablation of NPHP5, Kif3a or ODF2 can be rescued

A) Quiescent RPE-1 cells transfected with NS (non-specific) or the indicated siRNAs and plasmids expressing the indicated proteins were stained with the indicated antibodies and with DAPI (blue). Scale bar, 1 μ m. B) Fluorescence intensity of ninein at the centrosome was quantitated and set to 100% in NS siRNA-transfected cells. For quantitation, at least 20 cells for each condition were analyzed, and the mean and standard error of three independent experiments are presented. C) Quiescent RPE-1 cells transfected with the indicated siRNAs were stained with the indicated antibodies and with DAPI (blue). Scale bar, 1 μ m. D) Fluorescence intensity of ninein at the centrosome was quantitated and set to 100% in NS siRNA-transfected cells. For quantitation, at least 20 cells for each condition were analyzed, and the mean and standard error of three independent experiments are presented.

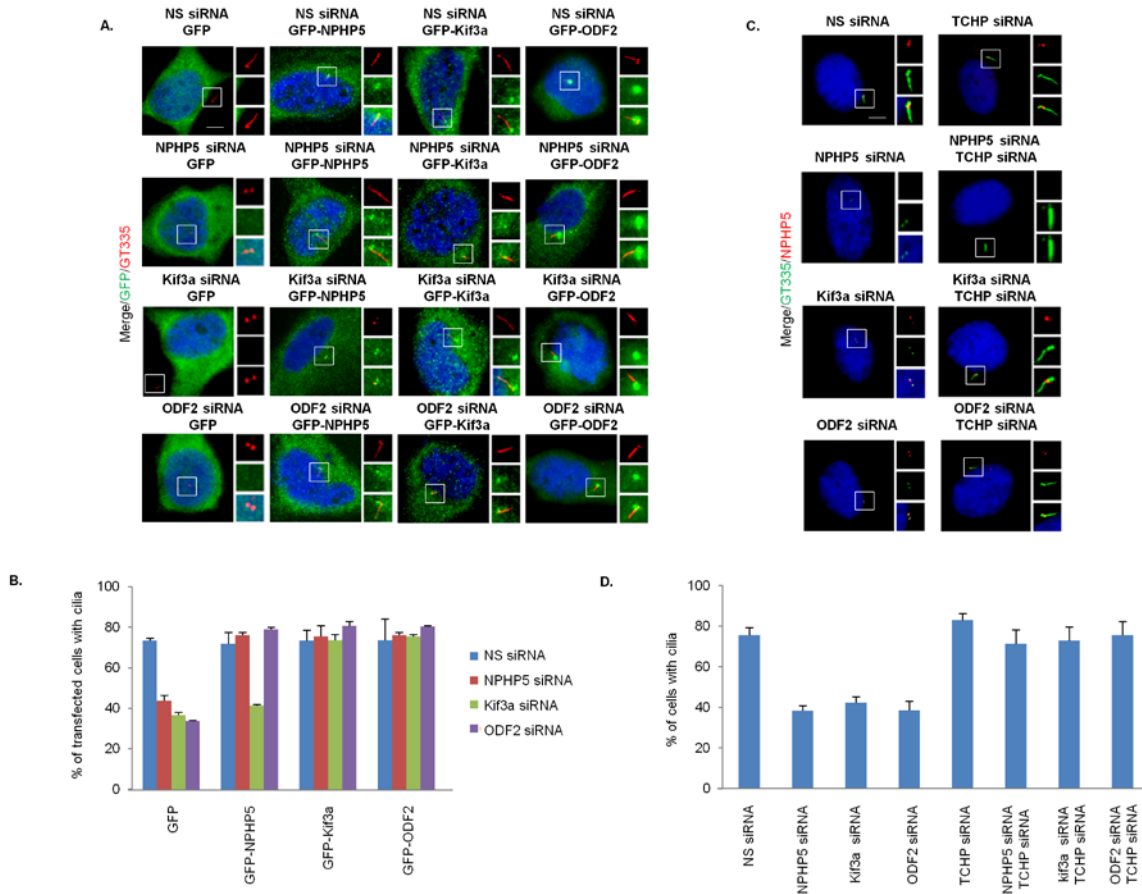


Figure 4.11.14. Cilia loss due to ablation of NPHP5, Kif3a or ODF2 can be rescued

A) Quiescent RPE-1 cells transfected with NS (non-specific) or the indicated siRNAs and plasmids expressing the indicated proteins were stained with the indicated antibodies and with DAPI (blue). Scale bar, 1 μ m. B) The percentage of GFP positive cells with cilia was scored. At least 100 cells for each condition were analyzed, and the mean and standard error of three independent experiments are presented. C) Quiescent RPE-1 cells transfected with the indicated siRNAs were stained with the indicated antibodies and with DAPI (blue). Scale bar, 1 μ m. D) The percentage of cells with cilia was scored. At least 100 cells for each condition were analyzed, and the mean and standard error of three independent experiments are presented.

Chapter 5

Conclusion and summary

At the onset of my project, the role of Cep78 in centrosome biology was unknown. My work here shows for the first time that Cep78 is a centrosomal protein that is localized at the distal end of the centriole in a cell cycle-dependent manner, suggesting that Cep78 plays an important role in the distal region of the centrosome. To identify the essential role of Cep78 at the centrosome, we did a proteomic screen for Cep78-interacting proteins. In this screen, we found many candidates. Among them, I confirmed the direct interaction between Cep78 and VprBP. VprBP acts as a substrate recognition subunit of both the RING-type CRL4^{VprBP} ubiquitin E3 ligase and the HECT-type EDD-DYRK2-DDB1^{VprBP} ubiquitin E3 ligase. Here, I showed that Cep78 inhibits the ubiquitination activity of EDD-DYRK2-DDB1^{VprBP}. In brief, the substrate is phosphorylated and recognized by DYRK2 and VprBP. It is believed that substrate recognition by VprBP is associated to bring the substrate in close proximity to EDD. Thereafter, ubiquitin molecules are transferred to the substrate from EDD. I showed that Cep78 specifically prevents the transfer of ubiquitin molecules from the EDD without compromising substrate phosphorylation and recognition by DYRK2 and VprBP, respectively. It is known that the subunits of EDD-DYRK2-DDB1^{VprBP} ubiquitin E3 ligase are localized in the nucleus and cytoplasm (161-165). In this study, I also confirmed the localization of a pool of EDD-DYRK2-DDB1^{VprBP} ubiquitin E3 ligase at the centrosome. There were two known substrates including TERT (nuclear) and katanin p60 (centrosomal) of EDD-DYRK2-DDB1^{VprBP} (164-166), and I identified a new substrate CP110 at the centrosome. Cep78 is only detected at the centrosome, which suggests that Cep78 regulates the centrosomal pool of EDD-DYRK2-DDB1^{VprBP} ubiquitin E3 ligase. Next, I reported that the ubiquitination of the centrosomal substrates katanin p60 and CP110 is inhibited by Cep78. Although Cep78 also inhibits the ubiquitination of TERT, Cep78 and TERT are presumably present in two different subcellular compartments (165). I speculate that this might be due to the use of cellular extracts where cells were broken and all the cellular contents were mixed in the ubiquitination experiment. This suggests that the inhibition of TERT ubiquitination by Cep78 might not be physically relevant. I also found that the loss of Cep78 leads to the elongated centriole, which is the same as for CP110 depletion. It is known that CP110 regulates the length of the centriole by forming a cap at the distal end of the centriole. Thus, I identified Cep78 as a new centrosomal protein that regulates centrosome homeostasis by

inhibiting the final step of the ubiquitination cascade catalyzed by EDD-DYRK2-DDB1^{VprBP} ubiquitin E3 ligase (165).

Several other questions remain unresolved in this study. For example, I reported that the Cep78 protein level is high during late G2 and decreases as the cell cycle proceeds to M until G1. How the protein level is maintained in a cell cycle-dependent manner has yet to be determined. One possible mechanism responsible for the Cep78 protein turnover is post-translational modification. For example, in our proteomic screen for Cep78-interacting proteins, we found many candidates, including several ubiquitin ligases besides EDD-DYRK2-DDB1^{VprBP} ubiquitin E3 ligase. I need to confirm the interaction between Cep78 and the candidate by immunoprecipitation/western blot. I also need to confirm the localization of this candidate at the centrosome. Thereafter, I will set up a ubiquitination assay to determine whether Cep78 is a substrate of this candidate. This will allow me to understand how the Cep78 protein level is maintained at the centrosome. Moreover, it is known that Cep78 possesses six LRR and one CC domain. In this thesis, I found that VprBP interacts with the LRR of Cep78. Disruption of LRR not only impaired the interaction between Cep78 and VprBP but also compromised the localization of Cep78 at the centrosome, whereas deletion of the CC domain did not affect either the interaction of Cep78 with VprBP or the localization of Cep78 at the centrosome. Therefore, the question arises regarding the function of the CC domain. The CC domain in the proteins is involved in many important biological functions such as acting as a molecular spacer (that either scaffolds a larger protein complex or separates the functional domains), regulation of gene expression, vesicle tethering, proper chromosome segregation, protein-protein interaction, etc (167). The centrosome has a subset of proteins that contain the CC domain. For example, SAS6 is responsible for forming the ‘cartwheel-like’ structure in procentriole, which is essential for stabilizing the centriole nine triplet microtubules. SAS6 comprises an N-terminal head group, a central CC domain and a less conserved C-terminal tail. Experimentally, it was shown that SAS-6 coiled-coil-mediated homodimer can assemble into a ring-like structure that looks like the central hub of a cartwheel. This also suggests that the CC domain of SAS6 interacts with another protein for cartwheel formation (14, 167, and 168). So, it might be possible that Cep78 uses its CC domain to interact with itself, forming a homodimer, or another protein, forming a heterodimer, and these dimers might have important functions at the centrosome.

In addition, it has been shown that the Cep78 protein level is considerably reduced in the CRC (132). Moreover, Cep78 is also required for centriole overduplication, and an abnormal centriole number can cause genomic instability and aneuploidy, which is a hallmark of cancer (31-33 and 129). Therefore, it is plausible that the deregulation of Cep78 is associated with many/other types of cancer. For instance, it was reported that the EDD-DYRK2-DDB1^{VprBP} substrate katanin p60 is expressed abruptly in prostate cancer bone metastasis (164). Given the abrupt expression of katanin p60, I predict that the level of Cep78 might be elevated, which would be in contrast to the reduced level of Cep78 observed in the CRC. Katanin has a microtubule-severing activity and is composed of two major subunits – an enzymatic subunit (p60) and a regulatory subunit (p80). The N-terminal domain of katanin p60 contains the AAA+ domain. NMR studies support the idea that this striking feature of katanin p60 resembles the microtubule interacting and trafficking domain. In mitosis, katanin p60 localizes to the minus end of the microtubule and regulates the length of spindle microtubules (169-171). Regulation of katanin p60 might be a crucial step that depends on many factors. As Cep78 regulates the katanin p60 protein turnover at the centrosome, it might be possible to reduce the expression of katanin p60 by modulating the Cep78 protein expression. For instance, transient reducing the endogenous Cep78 might stop the premature expression of katanin p60, which could play a role in preventing tumor migration.

As mentioned, katanin p60 is considered a microtubule-severing protein that has an important function in mitosis. Katanin p60 is required to sever the microtubule at the mitotic spindles, which is important for the proper segregation of sister chromatids. Experimentally, it was shown that the expression of p60 leads to the accumulation of cells with 4N and >4N DNA content, which leads to defective mitotic transition (164). As Cep78 regulates the protein turnover of the p60 in the centrosome, there might be a possibility that Cep78 participates in controlling the mitotic transition. For example, I can monitor the mitotic progression by expressing Cep78. This will provide a clue to understanding a new role of Cep78, which is required for proper mitotic progression.

It is known that VprBP interacts with the HIV-1 accessory protein Vpr and Vpr affects centrosome biology (145-154 and 172-174), but the molecular mechanisms are poorly understood. I started my work by using a simple test between the Vpr and Cep78, as both of these proteins have a common binding partner, VprBP. Interestingly, Vpr associated with Cep78

through VprBP at the centrosome and enhanced the ubiquitination activity of centrosomal EDD-DYRK2-DDB1^{VprBP}. Therefore, Vpr mediates the degradation of the previously characterized centrosomal native substrate CP110 (165, 174). The ubiquitination or protein level of Cep78 remains unchanged in the presence of Vpr, indicating that Cep78 is not a substrate of Vpr. Cep78 actually counteracts the ubiquitination and degradation of CP110 by Vpr. The down-regulation of CP110 by Vpr creates the elongated centriole phenotype that is expected. I also showed that the elongated centriole enhances the microtubule nucleation activity at the centrosome. It is known that microtubules are needed for HIV-1 trafficking inside the cell. Thus, our findings suggest that Vpr-mediated deregulation of centrosomal homeostasis could contribute to viral pathogenesis (174).

As there are several steps in the HIV-1 life cycle during the infection, we do not know at which step CP110 is targeted for degradation or whether the degradation of CP110 might have a direct or indirect role in viral pathogenesis. In the future, I will examine the possible role of Vpr-mediated degradation of CP110 by ablating the protein using either siRNA or CRISPR/Cas9 and testing how it affects different steps in HIV-1 pathogenesis. Therefore, I can monitor many parameters to identify the possible role of Vpr-mediated degradation of CP110. For example, I can monitor the rate of viral entry into the host cell or the transport of viral genetic material in and out of the nucleus from the cytoplasm in CP110-depleted cells. This could influence the rate of viral assembly and buds from the host cells, which can move to infect other cells.

In addition to the abovementioned phenotype, we and others found that Vpr causes centrosome amplification. Centrosome amplification is characterized by more than two centrosomes appearing in a cell. In mitosis, the two centrosomes establish the bipolar spindle poles, which are very important for proper chromosomal segregation. As the centrosome starts to duplicate in the S phase, it is possible that it does so more than once in a process called centrosome amplification. One possible mechanism that Vpr does the centrosome amplification is due to an increase of polo-like kinase-1 (PLK1). It has been shown that Vpr causes an elevated level of PLK1 (172). We know from the literature that PLK1 is the key player at the anaphase to loosen the connection between mother and daughter centrioles, allowing them to duplicate in the S phase. This happens with the complex action of PLK1 and separase. PLK1 actually phosphorylates the substrate SCC1 in the sister chromatid cohesion. Then, the phosphorylated SCC1 is cleaved by separase. This regulates the sister chromatid separation as well as

centrosome disengagement and duplication (10, 11). Thus, it might be possible that infection with HIV-1 increases the PLK1, which in turn allows the centrosome to duplicate more than once. From our results, it is clear that Vpr triggers centrosome amplification and centriole elongation in two different mechanisms. The mechanism of centrosome amplification induced by Vpr is not understood. It was suggested that Vpr does this either by G2/M arrest or by perturbing the regulation of the centrosome cycle (173). Interestingly, it was reported that centrosome amplification could also lead to increased microtubule nucleation (32), which is similar to what I report in this study. This might further enhance viral pathogenesis.

Furthermore, it would be interesting to study how many centrosomal proteins are targeted by the HIV-1 accessory protein Vpr. Besides CP110, katanin p60 is also the substrate of EDD-DYRK2-DDB1^{VprBP} ubiquitin E3 ligase at the centrosome. Vpr might target katanin p60 to deregulate centrosome homeostasis. I showed that the ubiquitination of Cep78 was unaffected in the presence of Vpr, and Cep78 counteracts the effect of Vpr at the centrosome. This suggests that Cep78 might not be the target of Vpr at the centrosome. According to the previous findings, EDD-DYRK2-DDB1^{VprBP} is thought to function in mitosis, where the Cep78 protein level is low (164-167). It is possible that Vpr could target EDD-DYRK2-DDB1^{VprBP} substrates in mitosis. Further proteomic screening for Vpr-interacting partners will identify new centrosomal proteins to examine whether these candidates might be involved in centrosome amplification, centriole elongation, or microtubule nucleation. This will provide new insights into why targeting of the centrosome by Vpr is beneficial for HIV-1 pathogenesis.

Next, I study another centrosomal protein called NPHP5. I have found that NPHP5 is a component of both SDAs and BF but regulates the organization of BF only. BF is equivalent to the SDAs of the mother centriole that only form during cilia formation. NPHP5 interacts and recruits Kif3a to the BF, which in turn contributes to organizing the downstream proteins such as ninein and Cep170. I also report that depletion of NPHP5 or BF protein inhibits ciliogenesis. Thus, the findings indicate that NPHP5 specifically regulates the hierarchical assembly of BF, which is linked to ciliogenesis.

Kif3a is a dual-functioning protein, as it possesses a motor domain. In addition to participating in BF organization and motor function, Kif3a also plays a role in centriole cohesion (engagement of mother and daughter centrioles) (115). As the depletion of NPHP5 mislocalizes the Kif3a, there is a possibility that NPHP5 depletion might give the same phenotype. In this

study, I have not determined whether NPHP5 is required for centriole cohesion. I found that the depletion of NPHP5/Kif3a inhibits the localization of ninein to the BF. Interestingly, one study showed that centriole cohesion was unaffected in the absence of ninein, whereas another study showed the opposite result (115, 175). These observations suggest that Kif3a, and possibly NPHP5 and ninein, have an additional role in regulating centriole cohesion. It might be tempting to speculate that NPHP5, Kif3a and ninein recruit a set of proteins to regulate centriole cohesion.

I showed that NPHP5 is localized in both SDAs and BF. Although the assembly pathway of BF and SDA are similar but not identical, NPHP5 specifically regulates the BF assembly pathway. Now, the question arises regarding the mechanism of the BF assembly by NPHP5. I speculate that NPHP5 is dispensable for SDA assembly because the protein may be functionally inactive. NPHP5 becomes functionally active during the BF assembly, and one possible mechanism responsible for the activation of NPHP5 is post-translational modification. To test this hypothesis, I can look at known post-translational modifications such as the phosphorylation of NPHP5 at both cycling conditions when SDA assembly is favourable and the serum-starved condition when the BF assembly is favourable. This could provide information on NPHP5-mediated BF organization. The other possibility is that the regulatory protein interacts with NPHP5 and keeps NPHP5 in an inactive state in cycling conditions when SDA assembly takes place. It seems plausible that the loss of the regulatory protein will release NPHP5 from inhibition in the serum-starved condition.

I also noticed that the BF are required for ciliogenesis. Previous findings revealed that the SDAs equivalent structure called the TFs has a role in ciliogenesis, but there is no clear information about how the BF participate in this process. Although ciliogenesis is affected in the absence of BF proteins, basal body formation is not affected (125). This suggests that other events of ciliogenesis are impaired after basal body formation. For example, Kif3a acts as an anterograde motor for IFT and transport of ciliary building blocks, it is possible that in the absence of NPHP5, the inability to recruit Kif3a to BF compromises Kif3a-mediated IFT and ciliogenesis. According to my observation, the number of BF is four instead of a ring-like pattern in SDAs. It has previously been shown that one basal foot forms in mice tracheal epithelial cells (125). They showed that in the absence of ODF2, not only is the basal foot formation impaired but also ciliary beating is affected. This suggests that motile cilia formation was unaffected. According to their findings, the basal foot has a role in the polarized organization of apical

microtubular lattice and basal bodies, which in turn coordinates the ciliary beating (125). It is known that the assembly process of motile and primary cilia is not the same (for example, vesicle recruitment is needed in primary cilia). Perhaps the remodelling of SDAs to BF is needed to reorganize the microtubule network, allowing efficient vesicle recruitment to occur during primary cilia assembly. It is possible that the transport of vesicles that carries ciliary building blocks to the basal body is impaired by disrupting the microtubule network in the absence of NPHP5 or BF protein, thereby impairing primary cilia formation, but sparing motile cilia formation.

As mutation in NPHP5 leads to retinal and renal disease, we and others showed that depletion of NPHP5 reduces the percentage of cells with cilia in RPE-1 cells (78, 134). One of the studies showed the localization and interaction of NPHP5 with other proteins in different cell lines. They found that NPHP5 interacts with Cep290 in NIH 3T3, IMCD3 and human RPE-1 cells, with NPHP1, NPHP4 and NPHP8 in NIH 3T3 cells, and with NPHP2 only in IMCD3 cells (78). These studies suggest that this is due to the distinct organization and function of these proteins in different cell lines. Thereafter, they performed the requirement of these proteins for cilia formation and found that the depletion of IFT88, NPHP5 and Cep290 but not NPHP1, NPHP4 and NPHP8 lead to defects in ciliogenesis. Then, they investigated whether they have any role other than ciliogenesis. They did a spheroid assay to allow the epithelial cells to form the polarized architecture in the IMCD3 cell line. Cells with IFT88 or Cep290 depletion develop affected or few spheroids and appear with few cilia, whereas the absence of NPHP5 causes spheroids to form, but defects are severe, and also there is less cilia. On the contrary, the depletion of NPHP1, NPHP 4, NPHP8 and NPHP2 have no problem with spheroid formation, but there are irregular lumens and the impaired localization of β catenin and obviously no cilia effects. These studies suggest that although NPHP5 interacts with other proteins, NPHP5 may have other roles distinct from ciliogenesis. They also performed some studies on the S12 cell line and found that the absence of NPHP5 and Cep290 had no apparent effects on cilia formation. Interestingly, they also found that Hh signal transduction was not affected by the absence of NPHP5 and Cep290 in the S12 cell line (78). The results of these studies suggest that the effect of BF formation linked to ciliogenesis by NPHP5 is cell type specific. It might be possible that NPHP5 is expressed in other cell types, but their association with other proteins or their regulation itself are different, which impedes it from performing BF assembly as well as cilia

formation. As NPHP5 mutation causes retinal failure in mice and dog models, we saw that BF formation and ciliogenesis is impaired in the absence of NPHP5 in RPE-1 cells (176).

References

1. Scheer U (2014) Historical roots of centrosome research: discovery of Boveri's microscope slides in Würzburg. *Philos Trans R Soc Lond B Biol Sci* **369**, 20130469.
2. Azimzadeh J and Bornens M (2007) Structure and duplication of the centrosome. *J Cell Sci* **120**, 2139-42.
3. Li S, Fernandez JJ, Marshall WF and Agard DA (2012) Three-dimensional structure of basal body triplet revealed by electron cryo-tomography. *EMBO J* **31**, 552-62.
4. Guichard P, Hachet V, Majubu N, Neves A, Demurtas D, Olieric N, Flückiger I, Yamada A, Kihara K, Nishida Y, Moriya S, Steinmetz MO, Hongoh Y and Gönczy P (2013) Native architecture of the centriole proximal region reveals features underlying its 9-fold radial symmetry. *Curr Biol* **23**, 1620-8.
5. Paintrand M, Moudjou M, Delacroix H and Bornens M (1992) Centrosome organization and centriole architecture: their sensitivity to divalent cations. *J Struct Biol* **108**, 107-28.
6. De Brabander M, Geuens G, Nuydens R, Willebrords R and De Mey J (1982) Microtubule stability and assembly in living cells: the influence of metabolic inhibitors, taxol and pH. *Cold Spring Harb Symp Quant Biol* **46**, 227-40.
7. Piel M, Meyer P, Khodjakov A, Rieder CL and Bornens M (2000) The respective contributions of the mother and daughter centrioles to centrosome activity and behavior in vertebrate cells. *J Cell Biol* **149**, 317-30.
8. Tsang WY and Dynlacht BD (2013) CP110 and its network of partners coordinately regulate cilia assembly. *Cilia* **2**, 9.
9. Tsou MF and Stearns T (2006) Mechanism limiting centrosome duplication to once per cell cycle. *Nature* **442**, 947-51.
10. Agircan FG, Schiebel E and Mardin BR (2014) Separate to operate: control of centrosome positioning and separation. *Philos Trans R Soc Lond B Biol Sci* **369**, 1650.
11. Tsou MF, Wang WJ, George KA, Uryu K, Stearns T and Jallepalli PV (2009) Polo kinase and separase regulate the mitotic licensing of centriole duplication in human cells. *Dev Cell* **17**, 344-54.
12. Kitagawa D, Vakonakis I, Olieric N, Hilbert M, Keller D, Olieric V, Bortfeld M, Erat MC, Flückiger I, Gönczy P and Steinmetz MO (2011) Structural basis of the 9-fold symmetry of centrioles. *Cell* **144**, 364-75.

13. Tang CJ, Lin SY, Hsu WB, Lin YN, Wu CT, Lin YC, Chang CW, Wu KS and Tang TK (2011) The human microcephaly protein STIL interacts with CPAP and is required for procentriole formation. *EMBO J* **30**, 4790-804.
14. Nakazawa Y, Hiraki M, Kamiya R and Hirono M (2007) SAS-6 is a cartwheel protein that establishes the 9-fold symmetry of the centriole. *Curr Biol* **17**, 2169–2174.
15. Habedanck R, Stierhof YD, Wilkinson CJ and Nigg EA (2005) The Polo kinase Plk4 functions in centriole duplication. *Nat Cell Biol* **7**, 1140–1146.
16. Kleylein-Sohn J, Westendorf J, Le Clech M, Habedanck R, Stierhof YD and Nigg EA (2007) Plk4-induced centriole biogenesis in human cells. *Dev Cell* **13**, 190–202.
17. Palazzo RE, Vogel JM, Schnackenberg BJ, Hull DR and Wu X (2000) Centrosome maturation. *Curr Top Dev Biol* **49**, 449-70.
18. Bornens M, Paintrand M, Berges J, Marty MC and Karsenti E (1987) Structural and chemical characterization of isolated centrosomes. *Cell Motil Cytoskeleton* **8**, 238-49.
19. Fry AM, Mayor T, Meraldi P, Stierhof YD, Tanaka K and Nigg EA (1998) C-Nap1, a novel centrosomal coiled-coil protein and candidate substrate of the cell cycle-regulated protein kinase Nek2. *J Cell Biol* **14**, 1563-74.
20. Bahe S, Stierhof YD, Wilkinson CJ, Leiss F and Nigg EA (2005) Rootletin forms centriole-associated filaments and functions in centrosome cohesion. *J Cell Biol* **171**, 27-33.
21. Gould RR and Borisy GR (1977) The pericentriolar material in Chinese hamster ovary cells nucleates microtubule formation. *J Cell Biol* **73**, 601–615.
22. Woodruff JB, Wueseke O and Hyman AA (2014) Pericentriolar material structure and dynamics. *Philos Trans R Soc B Biol Sci* **369**, 20130459–20130459.
23. Arquint C, Gabryjonczyk, AM and Nigg, EA (2014) Centrosomes as signalling centres. *Philos Trans R Soc B Biol Sci* **369**, 20130464–20130464.
24. Hurtado L, Caballero C, Gavilan MP, Cardenas J, Bornens M and Rios RM (2011) Disconnecting the Golgi ribbon from the centrosome prevents directional cell migration and ciliogenesis. *J Cell Biol* **193**, 917–933.
25. Mikule K, Delaval, B, Kaldis, P, Jurczyk, A, Hergert P and Doxsey, S (2007) Loss of centrosome integrity induces p38—p53—p21-dependent G1—S arrest. *Nat Cell Biol* **9**, 160–170.

26. Basto R, Lau, J, Vinogradova T, Gardiol A, Woods CG, Khodjakov A and Raff JW (2006) Flies without centrioles. *Cell* **125**, 1375–1386.
27. Joukov V, Walter JC and De Nicolo A (2016) Assays to study mitotic centrosome and spindle pole assembly and regulation. *Methods Mol Biol* **1413**, 207-35.
28. Manandhar G (2005) Centrosome reduction during gametogenesis and its significance. *Biol Reprod* **72**, 2-13.
29. Ohkura H (2015) Meiosis: an overview of key differences from mitosis. *Cold Spring Harb Perspect Biol* **7**, a015859.
30. Debec A, Sullivan W and Bettencourt-Dias M (2010) Centrioles: active players or passengers during mitosis? *Cell Mol Life Sci* **67**, 2173–2194.
31. Hansford S and Huntsman DG (2014) Boveri at 100: Theodor Boveri and genetic predisposition to cancer. *J Pathol* **234**, 142–145.
32. Godinho SA, Picone R, Burute M, Dagher R, Su Y, Leung CT, Polyak K, Brugge JS, Théry M and Pellman D (2014) Oncogene-like induction of cellular invasion from centrosome amplification. *Nature* **510**, 167–171.
33. Godinho SA and Pellman D (2014) Causes and consequences of centrosome abnormalities in cancer. *Philos Trans R Soc B Biol Sci* **369**, 20130467–20130467.
34. Ganem NJ, Godinho SA and Pellman D (2009) A mechanism linking extra centrosomes to chromosomal instability. *Nature* **460**, 278–282.
35. Gregan J, Polakova S, Zhang L, Tolić-Nørrelykke IM and Cimini D (2011) Merotelic kinetochore attachment: causes and effects. *Trends Cell Biol* **21**, 374–381.
36. Leber B, Maier B, Fuchs F, Chi J, Riffel P, Anderhub S, Wagner L, Ho AD, Salisbury JL, Boutros M and Krämer A (2010) Proteins required for centrosome clustering in cancer cells. *Sci Transl Med* **2**, 33-38.
37. Okamoto N, Kohmoto T, Naruto T, Masuda K and Imoto I (2018) Primary microcephaly caused by novel compound heterozygous mutations in ASPM. *Hum Genome Var* **5**, 18015.
38. O'Neill RS, Schoborg TA and Rusan NM (2018) Same but different: pleiotropy in centrosome-related microcephaly. *Mol Biol Cell* **29**, 241-246.
39. Barbelanne M and Tsang WY (2014) Molecular and cellular basis of autosomal recessive primary microcephaly. *Bio Med Res Int* **2014**, 1–13.

40. Beales P and Jackson PK (2012) Cilia – the prodigal organelle. *Cilia* **1**, 1.
41. Lodish H, Berk A, Zipursky SL, et al (2000) Cilia and Flagella: Structure and Movement. *Molecular Cell Biology*. **4th edition**, Section 19.4.
42. Reiter JF, Blacque OE and Leroux MR (2012) The base of the cilium: roles for transition fibres and the transition zone in ciliary formation, maintenance and compartmentalization. *EMBO Rep* **13**, 608-18.
43. Kobayashi T and Dynlacht BD (2011) Regulating the transition from centriole to basal body. *J Cell Biol* **193**, 435-44.
44. Ostrowski LE, Dutcher SK and Lo CW (2011) Cilia and models for studying structure and function. *Proc Am Thorac Soc* **8**, 423-9.
45. Flock A and Duvall AJ (1965) The ultrastructure of the kinocilium of the sensory cells in the inner ear and lateral line organs. *J Cell Biol* **25**, 1–8.
46. Mizuno N, Taschner M, Engel BD and Lorentzen E (2012) Structural studies of ciliary components. *J Mol Biol* **422**, 163-80.
47. Huang S, Hirota Y and Sawamoto K (2009) Various facets of vertebrate cilia: motility, signaling, and role in adult neurogenesis. *Proc Jpn Acad Ser B Phys Biol Sci* **85**, 324–336.
48. Garcia G, Raleigh DR and Reiter JF (2018) How the ciliary membrane is organized inside-out to communicate outside-in. *Curr Biol* **28**, R421-R43.
49. Mohri H, Inaba K, Ishijima S and Baba SA (2012) Tubulin-dynein system in flagellar and ciliary movement. *Proc Jpn Acad Ser B Phys Biol Sci* **88**, 397-415.
50. Venkatesh D (2017) Primary cilia. *J Oral Maxillofac Pathol* **21**, 8–10.
51. Gonçalves J and Pelletier L (2017) The ciliary transition zone: finding the pieces and assembling the gate. *Mol Cells* **40**, 243-253.
52. Geneva II, Tan HY and Calvert PD (2017) Untangling ciliary access and enrichment of two rhodopsin-like receptors using quantitative fluorescence microscopy reveals cell-specific sorting pathways. *Mol Biol Cell* **28**, 554-566.
53. Hossain D and Tsang WY (2018) The role of ubiquitination in the regulation of primary cilia assembly and disassembly. *Semin Cell Dev Biol* S1084-9521 [Epub ahead of print].

54. Tsang WY, Bossard C, Khanna H, Peränen J, Swaroop A, Malhotra V and Dynlacht BD (2008) CP110 suppresses primary cilia formation through its interaction with CEP290, a protein deficient in human ciliary disease. *Dev Cell* **15**, 187-97.
55. Lechtreck KF (2015) IFT-Cargo Interactions and Protein Transport in Cilia. *Trends Biochem Sci* **40**, 765-778.
56. Zhu B, Zhu X, Wang L, Liang Y, Feng Q and Pan J (2017) Functional exploration of the IFT-A complex in intraflagellar transport and ciliogenesis. *PLoS Genet* **13**, e1006627.
57. Katoh Y, Terada M, Nishijima Y, Takei R, Nozaki S, Hamada H and Nakayama K (2016) Overall architecture of the intraflagellar transport (IFT)-B complex containing Cluap1/IFT38 as an essential component of the IFT-B peripheral subunit. *J Biol Chem* **291**, 10962-75.
58. Porpora M, Sauchella S, Rinaldi L, Delle Donne R, Sepe M, Torres-Quesada O, Intartaglia D, Garbi C, Insabato L, Santoriello M, Bachmann VA, Synofzik M, Lindner HH, Conte I, Stefan E and Feliciello A (2018) Counterregulation of cAMP-directed kinase activities controls ciliogenesis. *Nat Commun* **9**, 1224.
59. Troilo A, Alexander I, Muehl S, Jaramillo D, Knobloch KP and Krek W (2014) HIF1 α deubiquitination by USP8 is essential for ciliogenesis in normoxia. *EMBO Rep* **15**, 77-85.
60. Sung CH and Li A (2011) Ciliary resorption modulates G1 length and cell cycle progression. *Cell Cycle* **10**, 2825-6.
61. Mitchison HM and Valente EM (2017) Motile and non-motile cilia in human pathology: from function to phenotypes. *J Pathol* **241**, 294-309.
62. Kim S and Tsiokas L (2011) Cilia and cell cycle re-entry: more than a coincidence. *Cell Cycle* **10**, 2683-90.
63. Seeley ES and Nachury MV (2010) The perennial organelle: assembly and disassembly of the primary cilium. *J Cell Sci* **123**, 511-8.
64. Sánchez I and Dynlacht BD (2016) Cilium assembly and disassembly. *Nat Cell Biol* **18**, 711–717.
65. Satir P, Heuser T and Sale WS (2014) A Structural basis for how motile cilia beat. *Bioscience* **64**, 1073–1083.
66. Nawroth JC, Guo H, Koch E, Heath-Heckman EAC, Hermanson JC, Ruby EG, Dabiri JO, Kanso E and McFall-Ngai M (2017) Motile cilia create fluid-mechanical

- microhabitats for the active recruitment of the host microbiome. *Proc Natl Acad Sci USA* **114**, 9510-9516.
67. Mitchell DR (2007) The evolution of eukaryotic cilia and flagella as motile and sensory organelles. *Adv Exp Med Biol* **607**, 130-40.
 68. Wheway G, Nazlamova L and Hancock JT (2018) Signaling through the Primary Cilium. *Front Cell Dev Biol* **6**:8.
 69. Christensen S, CA Clement CA, Brorsen SK, Ajbro KD, de Jesus M, Pedersen LB and Larsen LA (2012) Transforming growth factor beta (TGFβ) signaling is regulated at the pocket region of primary cilia. *Cilia* **1**, 023.
 70. Delling M, Indzhykulian AA, Liu X, Li Y, Xie T, Corey DP and Clapham DE (2016) Primary cilia are not calcium-responsive mechanosensors. *Nature* **531**, 656-60.
 71. Spasic M and Jacobs CR (2017) Primary cilia: cell and molecular mechanosensors directing whole tissue function. *Semin Cell Dev Biol* **71**, 42-52.
 72. May-Simera HL, Wan Q, Jha BS, Hartford J, Khristov V, Dejene R, Chang J, Patnaik S, Lu Q, Banerjee P, Silver J, Insinna-Kettenhofen C, Patel D, Lotfi M, Malicdan M, Hotaling N, Maminishkis A, Sridharan R, Brooks B, Miyagishima K, Gunay-Aygun M, Pal R, Westlake C, Miller S, Sharma R and Bharti K (2018) Primary cilium-mediated retinal pigment epithelium maturation is disrupted in ciliopathy patient cells. *Cell Rep* **22**, 189-205.
 73. Yoder BK (2007) Role of primary cilia in the pathogenesis of polycystic kidney disease. *J Am Soc Nephrol* **18**, 1381-8.
 74. Waters AM and Beales PL (2011) Ciliopathies: an expanding disease spectrum. *Pediatr Nephrol* **26**, 1039-56.
 75. Hildebrandt F, Benzing T and Katsanis N (2011) Ciliopathies. *N Engl J Med* **364**, 1533–1543.
 76. Ansley SJ, Badano JL, Blacque OE, Hill J, Hoskins BE, Leitch CC, Kim JC, Ross AJ, Eichers ER, Teslovich TM, Mah AK, Johnsen RC, Cavender JC, Lewis RA, Leroux MR, Beales PL and Katsanis N (2003) Basal body dysfunction is a likely cause of pleiotropic Bardet-Biedl syndrome. *Nature* **425**, 628-33.
 77. Forsythe E and Beales PL (2013) Bardet-Biedl syndrome. *Eur J Hum Genet* **21**, 8-13.

78. Sang L, Miller JJ, Corbit KC, Giles RH, Brauer MJ, Otto EA, Baye LM, Wen X, Scales SJ, Kwong M, Huntzicker EG, Sfakianos MK, Sandoval W, Bazan JF, Kulkarni P, Garcia-Gonzalo FR, Seol AD, O'Toole JF, Held S, Reutter HM, Lane WS, Rafiq MA, Noor A, Ansar M, Devi AR, Sheffield VC, Slusarski DC, Vincent JB, Doherty DA, Hildebrandt F, Reiter JF and Jackson PK (2011) Mapping the NPHP-JBTS-MKS protein network reveals ciliopathy disease genes and pathways. *Cell* **145**, 513-28.
79. Wolf MT (2015) Nephronophthisis and related syndromes. *Curr Opin Pediatr* **27**, 201-11.
80. Hildebrandt F, Attanasio M and Otto E (2009) Nephronophthisis: disease mechanisms of a ciliopathy. *J Am Soc Nephrol* **20**, 23-35.
81. Gerdes JM, Davis EE and Katsanis N (2009) The vertebrate primary cilium in development, homeostasis, and disease. *Cell* **137**, 32-45.
82. Gradilone SA, Pisarello MJL and LaRusso NF (2017) Primary cilia in tumor biology: the primary cilium as a therapeutic target in cholangiocarcinoma. *Curr Drug Targets* **18**, 958-963.
83. Han YG, Kim HJ, Dlugosz AA, Ellison DW, Gilbertson RJ and Alvarez-Buylla A (2009) Dual and opposing roles of primary cilia in medulloblastomadevelopment. *Nat Med* **15**, 1062-5.
84. Andersen JS, Wilkinson CJ, Mayor T, Mortensen P, Nigg EA and Mann M (2003) Proteomic characterization of the human centrosome by protein correlation profiling. *Nature* **426**, 570-574.
85. Jakobsen L, Vanselow K, Skogs M, Toyoda Y, Lundberg E, Poser I, Falkenby LG, Bennetzen M, Westendorf J, Nigg EA, Uhlen M, Hyman AA and Andersen JS (2011) Novel asymmetrically localizing components of human centrosomes identified by complementary proteomics methods. *EMBO J* **30**, 1520-35.
86. Sauer G, Körner R, Hanisch A, Ries A, Nigg EA and Silljé HH (2005) Proteome analysis of the human mitotic spindle. *Mol Cell Proteomics* **4**, 35-43.
87. Ren J, Liu Z, Gao X, Jin C, Ye M, Zou H, Wen L, Zhang Z, Xue Y and Yao X (2010) MiCroKit 3.0: an integrated database of midbody, centrosome and kinetochore. *Nucleic Acids Res* **38**, D155-60.

88. Friedberg F (2006) Centrin isoforms in mammals. Relation to calmodulin. *Mol Biol Rep* **33**, 243-52.
89. Levy YY, Lai EY, Remillard SP, Heintzelman MB and Fulton C (1996) Centrin is a conserved protein that forms diverse associations with centrioles and MTOCs in *Naegleria* and other organisms. *Cell Motil Cytoskeleton* **33**, 464.
90. Salisbury JL, Suino KM, Busby R and Springett M (2002) Centrin-2 is required for centriole duplication in mammalian cells. *Biochem Soc Trans* **12**, 1287-1292.
91. Resendes KK, Rasala BA and Forbes DJ (2008) Centrin 2 localizes to the vertebrates nuclear pore and plays a role in mRNA and protein export. *Mol Cell Biol* **28**, 755-69.
92. Dantas TJ, Daly OM, Conroy PC, Tomas M, Wang Y, Lalor P, Dockery P, Ferrando-May E and Morrison CG (2013) Calcium-binding capacity of centrin2 is required for linear POC5 assembly but not for nucleotide excision repair. *PloS One* **8**, e68487.
93. Azimzadeh J, Hergert P, Delouvé A, Euteneuer U, Formstecher E, Khodjakov A and Bornens M (2009) hPOC5 is a centrin-binding protein required for assembly of full-length centrioles. *J Cell Biol* **185**, 101-114.
94. Kobayashi T, Kim S, Lin YC, Inoue T and Dynlacht BD (2014) The CP110-interacting proteins Talpid3 and Cep290 play overlapping and distinct roles in cilia assembly. *J Cell Biol* **204**, 215-229.
95. Lee M, Seo MY, Chang J, Hwang DS and Rhee K (2017) PLK4 phosphorylation of CP110 is required for efficient centriole assembly. *Cell Cycle* **16**, 1225-1234.
96. Schmidt TI, Kleylein-Sohn J, Westendorf J, Le Clech M, Lavoie SB, Stierhof YD and Nigg EA (2009) Control of centriole length by CPAP and CP110. *Curr Biol* **19**, 1005-1011.
97. Al-Hakim AK, Bashkurov M, Gingras AC, Durocher D and Pelletier L (2012) Interaction proteomics identify NEURL4 and the HECT E3 ligase HERC2 as novel modulators of centrosome architecture. *Mol Cell Proteomics* **11**, M111.014233.
98. Loukil A, Tormanen K and Sütterlin C (2017) The daughter centriole controls ciliogenesis by regulating Neurl-4 localization at the centrosome. *J Cell Biol* **216**, 1287-1300.

99. D'Angiolella V, Donato V, Vijayakumar S, Saraf A, Florens L, Washburn MP, Dynlacht B and Pagano M (2010) SCF (Cyclin F) controls centrosome homeostasis and mitotic fidelity through CP110 degradation. *Nature* **466**, 138-42.
100. Chen Z, Indjeian VB, McManus M, Wang L and Dynlacht BD (2002) CP110, a cell cycle-dependent CDK substrate, regulates centrosome duplication in human cells. *Dev Cell* **3**, 339-50.
101. Kobayashi T, Tsang WY, Li J, Lane W and Dynlacht BD (2011) Centriolar kinesin Kif24 interacts with CP110 to remodel microtubules and regulate ciliogenesis. *Cell* **145**, 914-925.
102. Spektor A, Tsang WY, Khoo D and Dynlacht BD (2007) Cep97 and CP110 suppress a cilia assembly program. *Cell* **130**, 678-690.
103. Yadav SP, Sharma NK, Liu C, Dong L, Li T and Swaroop A (2016) Centrosomal protein CP110 controls maturation of the mother centriole during cilia biogenesis. *Development* **143**, 1491-501.
104. Bettencourt-Dias M and Carvalho-Santos Z (2008) Double life of centrioles: CP110 in the spotlight. *Trends Cell Biol* **18**, 8-11.
105. Tsang WY, Spektor A, Vijayakumar S, Bista BR, Li J, Sanchez I, Duensing S and Dynlacht BD (2009) Cep76, a centrosomal protein that specifically restrains centriole reduplication. *Dev Cell* **16**, 649-660.
106. Barbelanne M, Chiu A, Qian J and Tsang WY (2016) Opposing post-translational modifications regulate Cep76 function to suppress centriole amplification. *Oncogene* **35**, 5377-5387.
107. O'Toole E, Greenan G, Lange KI, Srayko M, Müller-Reichert T (2012) The role of γ -tubulin in centrosomal microtubule organization. *PLoS One* **7**, e29795.
108. Fuller SD, Gowen BE, Reinsch S, Sawyer A, Buendia B, Wepf R and Karsenti E (1995) The core of the mammalian centriole contains gamma-tubulin. *Curr Biol* **5**, 1384-93.
109. Teixidó-Travesa N, Villén J, Lacasa C, Bertran MT, Archinti M, Gygi SP, Caelles C, Roig J and Lüders J (2010) The gammaTuRC revisited: a comparative analysis of interphase and mitotic human gammaTuRC redefines the set of core components and identifies the novel subunit GCP8. *Mol Biol Cell* **21**, 3963-72.

110. Tanos BE, Yang HJ, Soni R, Wang WJ, Macaluso FP, Asara JM and Tsou MF (2013) Centriole distal appendages promote membrane docking, leading to cilia initiation. *Genes Dev* **27**, 163–8.
111. Wei Q, Ling K and Hu J (2015) The essential roles of transition fibers in the context of cilia. *Curr Opin Cell Biol* **35**, 98–105.
112. Wei Q, Xu Q, Zhang Y, Li Y, Zhang Q, Hu Z, Harris PC, Torres VE, Ling K and Hu J (2013) Transition fibre protein FBF1 is required for the ciliary entry of assembled intraflagellar transport complexes. *Nat Commun* **4**, 2750.
113. Oda T, Chiba S, Nagai T and Mizuno K (2014) Binding to Cep164, but not EB1, is essential for centriolar localization of TTBK2 and its function in ciliogenesis. *Genes Cells* **19**, 927-40.
114. Uzbekov R and Alieva I (2018) Who are you, subdistal appendages of centriole? *Open Biol* **8**, pii: 180062.
115. Kodani A, Salomé Sirerol-Piquer M, Seol A, Garcia-Verdugo JM and Reiter JF (2013) Kif3a interacts with Dynactin subunit p150 Glued to organize centriole subdistal appendages. *EMBO J* **32**, 597-607.
116. Serra R (2008) Role of intraflagellar transport and primary cilia in skeletal development. *Anat Rec (Hoboken)* **291**, 1049-6.
117. Quintyne NJ and Schroer TA (2002) Distinct cell cycle dependent roles for dynactin and dynein at centrosomes. *J Cell Biol* **159**, 245-54.
118. Chen TY, Syu JS, Han TY, Cheng HL, Lu FI and Wang CY (2015) Cell cycle-dependent localization of dynactin subunit p150 glued at centrosome. *J Cell Biochem* **116**, 2049-60.
119. Lee M and Rhee K (2015) Determination of mother centriole maturation in CPAP-depleted cells using the ninein antibody. *Endocrinol Metal (Seoul)* **30**, 53-7.
120. Veleri S, Manjunath SH, Fariss RN, May-Simera H, Brooks M, Foskett TA, Gao C, Longo TA, Liu P, Nagashima K, Rachel RA, Li T, Dong L and Swaroop A (2014) Ciliopathy-associated gene Cc2d2a promotes assembly of subdistal appendages on the mother centriole during cilia biogenesis. *Nat Commun* **5**, 4207.
121. Huang N, Xia Y, Zhang D, Wang S, Bao Y, He R, Teng J and Chen J (2017) Hierarchical assembly of centriole subdistal appendages via centrosome binding proteins CCDC120 and CCDC68. *Nat Commun* **8**, 15057.

122. Ibi M, Zou P, Inoko A, Shiromizu T, Matsuyama M, Hayashi Y, Enomoto M, Mori D, Hirotsune S, Kiyono T, Tsukita S, Goto H and Inagaki M (2011) Trichoplein controls microtubule anchoring at the centrosome by binding to Odf2 and ninein. *J Cell Sci* **124**, 857-864.
123. Hagiwara H, Ohwada N, Aoki T, Suzuki T and Takata K (2008) The primary cilia of secretory cells in the human oviduct mucosa. *Med Mol Morphol* **41**, 193-198.
124. Anderson RG. (1972) The three-dimensional structure of the basal body from the rhesus monkey oviduct. *J Cell Biol* **54**, 246-265.
125. Kunimoto K, Yamazaki Y, Nishida T, Shinohara K, Ishikawa H, Hasegawa T, Okanoue T, Hamada H, Noda T, Tamura A, Tsukita S and Tsukita S (2012) Coordinated ciliary beating requires Odf2-mediated polarization of basal bodies via basal feet. *J Cell Biol* **148**, 189-200.
126. Garcia G and Reiter JF (2016) A primer on the mouse basal body. *Cilia* **5**, 17.
127. Baffet AD, Martin CA, Scarfone I, Daly OM, David A, Tibelius A, Lattao R, Hussain MS and Woodruff JB (2013) Meeting report - building a centrosome. *J Cell Sci* **126**, 3259-3262.
128. Azimzadeh J, Wong ML, Downhour DM, Sánchez Alvarado A and Marshall WF (2012) Centrosome loss in the evolution of planarians. *Science* **335**, 461-463.
129. Brunk K, Zhu M, Bärenz F, Kratz AS, Haselmann-Weiss U, Antony C and Hoffmann I (2016) Cep78 is a new centriolar protein involved in Plk4-induced centriole overduplication. *J Cell Sci* **129**, 2713-8.
130. Namburi P, Ratnapriya R, Khateb S, Lazar CH, Kinarty Y, Obolensky A, Erdinest I, Marks-Ohana D, Pras E, Ben-Yosef T, Newman H, Gross M, Swaroop A, Banin E and Sharon D (2016) Bi-allelic truncating mutations in CEP78, encoding centrosomal protein 78, cause cone-rod degeneration with sensorineural hearing loss. *Am J Hum Genet* **99**, 1222-1223.
131. Nikopoulos K, Farinelli P, Giangreco B, Tsika C, Royer-Bertrand B, Mbefo MK, Bedoni N, Kjellström U, El Zaoui I, Di Gioia SA, Balzano S, Cisarova K, Messina A, Decembrini S, Plainis S, Blazaki SV, Khan MI, Micheal S, Boldt K, Ueffing M, Moulin AP, Cremers FPM, Roepman R, Arsenijevic Y, Tsilimbaris MK, Andréasson

- S and Rivolta C (2016) Mutations in CEP78 cause cone-rod dystrophy and hearing loss associated with primary-cilia defects. *Am J Hum Genet* **99**, 770-776.
132. Zhang M, Duan T, Wang L, Tang J, Luo R, Zhang R and Kang T (2003) Low expression of centrosomal protein 78 (CEP78) is associated with poor prognosis of colorectal cancer patients. *Chin J Cancer* **35**, 62.
133. Nesslinger NJ, Sahota RA, Stone B, Johnson K, Chima N, King C, Rasmussen D, Bishop D, Rennie PS, Gleave M, Blood P, Pai H, Ludgate C and Nelson BH (2007) Standard treatments induce antigen-specific immune responses in prostate cancer. *Clin Cancer Res* **13**, 1493-1502.
134. Barbelanne M, Song J, Ahmadzai M and Tsang WY (2013) Pathogenic NPHP5 mutations impair protein interaction with Cep290, a prerequisite for ciliogenesis. *Hum Mol Genet* **22**, 2482-2494.
135. Barbelanne M, Hossain D, Chan DP, Peränen J and Tsang WY (2015) Nephrocystin proteins NPHP5 and Cep290 regulate BBSome integrity, ciliary trafficking and cargo delivery. *Hum Mol Genet* **24**, 2185-2200.
136. Das A, Qian J and Tsang WY (2017) USP9X counteracts differential ubiquitination of NPHP5 by MARCH7 and BBS11 to regulate ciliogenesis. *PLoS Genet* **13**, e1006791.
137. Wilen CB, Tilton JC and Doms RW (2012) HIV: cell binding and entry. *Cold Spring Harb Perspect Med* **2**, pii: a006866.
138. Sattentau QJ and Moore JP (1993) The role of CD4 in HIV binding and entry. *Philos Trans R Soc Lond B Biol Sci* **342**, 59-66.
139. Klasse PJ (2012) The molecular basis of HIV entry. *Cell Microbiol* **14**, 1183–1192.
140. Frankel AD and Young JA (1998) HIV-1: fifteen proteins and an RNA. *Annu Rev Biochem* **61**, 1-25.
141. Zhao RY and Bukrinsky MI (2014) HIV-1 accessory proteins: VpR. *Methods Mol Biol* **1087**, 125-34.
142. Kogan M and Rappaport J (2011) HIV-1 accessory protein Vpr: relevance in the pathogenesis of HIV and potential for therapeutic intervention. *Retrovirology* **13**, 25.
143. Heinzinger NK, Bukrinsky MI, Haggerty SA, Ragland AM, Kewalramani V, Lee MA, Gendelman HE, Ratner L, Stevenson M and Emerman M (1994) The Vpr protein of

- human immunodeficiency virus type 1 influences nuclear localization of viral nucleic acids in nondividing host cells. *Proc Natl Acad Sci USA* **91**, 7311-5.
144. He J, Choe S, Walker R, Di Marzio P, Morgan DO and Landau NR (1995) Human immunodeficiency virus type 1 viral protein R (Vpr) arrests cells in the G2 phase of the cell cycle by inhibiting p34cdc2 activity. *J Virol* **69**, 6705-11.
 145. Wang X, Singh S, Jung HY, Yang G, Jun S, Sastry KJ, Park JI (2013) HIV-1 Vpr protein inhibits telomerase activity via the EDD-DDB1-VPRBP E3 ligase complex. *J Biol Chem* **288**, 15474-80.
 146. Hrecka K, Gierszewska M, Srivastava S, Kozaczekiewicz L, Swanson SK, Florens L, Washburn MP and Skowronski J (2007) Lentiviral Vpr usurps Cul4-DDB1[VprBP] E3 ubiquitin ligase to modulate cell cycle. *Proc Natl Acad Sci USA* **104**, 11778-83.
 147. Stinchcombe JC and Griffiths GM (2014) Communication, the centrosome and the immunological synapse. *Philos Trans R Soc Lond B Biol Sci* **369**, 20130463.
 148. Dieckmann NM, Frazer GL, Asano Y, Stinchcombe JC and Griffiths GM (2016) The cytotoxic T lymphocyte immune synapse at a glance. *J Cell Sci* **129**, 2881-6.
 149. Kloc M, Kubiak JZ, Li XC and Ghobrial RM (2014) The newly found functions of MTOC in immunological response. *J Leukoc Biol* **95**, 417-30.
 150. Prosser SL and Morrison CG (2015) Centrin2 regulates CP110 removal in primary cilium formation. *J Cell Biol* **208**, 693-701.
 151. Sloboda RD (2009) Posttranslational protein modifications in cilia and flagella. *Methods in Cell Biology* **94**, 347-363.
 152. Wloga D and Gaertig J (2010) Post-translational modifications of microtubules. *J Cell Sci* **123**, 3447-55.
 153. Pickart CM and Eddins MJ (2004) Ubiquitin: structures, functions, mechanisms. *Biochim Biophys Acta* **1695**, 55-72.
 154. Nakagawa T, Mondal K and Swanson PC (2013) VprBP (DCAF1): a promiscuous substrate recognition subunit that incorporates into both RING-family CRL4 and HECT-family EDD/UBR5 E3 ubiquitin ligases. *BMC Mol Biol* **14**, 22.
 155. Spratt DE, Walden H and Shaw GS (2014) RBR E3 ubiquitin ligases: new structures, new insights, new questions. *Biochem J* **458**, 421-437.

156. Kristariyanto YA, Abdul Rehman SA, Campbell DG, Morrice NA, Johnson C, Toth R and Kulathu Y (2015) K29-Selective ubiquitin binding domain reveals structural basis of specificity and heterotypic. Nature of K29 polyubiquitin. *Mol Cell* **58**, 83-94.
157. Passmore LA and Barford D (2004) Getting into position: the catalytic mechanisms of protein ubiquitylation. *Biochem J* **379**, 513-25.
158. Sadowski M and Sarcevic B (2010) Mechanisms of mono- and poly-ubiquitination: Ubiquitination specificity depends on compatibility between the E2 catalytic core and amino acid residues proximal to the lysine. *Cell Div* **5**, 19.
159. Ohtake F, Tsuchiya H, Saeki Y and Tanaka K (2018) K63 ubiquitylation triggers proteasomal degradation by seeding branched ubiquitin chains. *Proc Natl Acad Sci USA* **115**, E1401-E1408.
160. Kim HC and Huijbrechtse JM (2009) Polyubiquitination by HECT E3s and the determinants of chain type specificity. *Mol Cell Biol* **29**, 3307-3318.
161. Chu G and Chang E (1988) Xeroderma pigmentosum group E cells lack a nuclear factor that binds to damaged DNA. *Science* **242**, 564-7.
162. Becker W, Weber Y, Wetzel K, Eirmbter K, Tejedor FJ and Joost HG (1998) Sequence characteristics, subcellular localization, and substrate specificity of DYRK-related kinases, a novel family of dual specificity protein kinases. *J Biol Chem* **273**, 25893-902.
163. Henderson MJ, Russell AJ, Hird S, Muñoz M, Clancy JL, Lehrbach GM, Calanni ST, Jans DA, Sutherland RL and Watts CK (2002) EDD, the human hyperplastic discs protein, has a role in progesterone receptor coactivation and potential involvement in DNA damage response. *J Biol Chem* **277**, 26468-78.
164. Maddika S and Chen J (2009) Protein kinase DYRK2 is an E3-ligase specific molecular assembler. *Nat Cell Biol* **11**, 409-419.
165. Hossain D, Javadi Esfehiani Y, Das A and Tsang WY (2017) Cep78 controls centrosome homeostasis by inhibiting EDD-DYRK2-DDB1^{VprBP}. *EMBO Rep* **18**, 632-644.
166. Jung HY, Wang X, Jun S and Park JI (2013) Dyrk2-associated EDD-DDB1-VprBP E3 ligase inhibits telomerase by TERT degradation. *J Biol Chem* **288**, 7252-62.
167. Truebestein L and Leonard TA (2016) Coiled-coils: The long and short of it. *Bioessays* **38**, 903-16.

168. Qiao R, Cabral G, Lettman MM, Dammermann A and Dong G (2012) SAS-6 coiled-coil structure and interaction with SAS-5 suggest a regulatory mechanism in *C. elegans* centriole assembly. *EMBO J* **31**, 4334-47.
169. Ye X, Lee YC, Choueiri M, Chu K, Huang CF, Tsai WW, Kobayashi R, Logothetis CJ, Yu-Lee LY and Lin SH (2012) Aberrant expression of katanin p60 in prostate cancer bone metastasis. *Prostate* **72**, 291-300.
170. Rezaczkova L, Jiang K, Capitani G, Prota AE, Akhmanova A, Steinmetz MO and Kammerer RA (2017) Structural basis of katanin p60:p80 complex formation. *Sci Rep* **7**, 14893.
171. Matsuo M, Shimodaira T, Kasama T, Hata Y, Echigo A, Okabe M, Arai K, Makino Y, Niwa S, Saya H and Kishimoto T (2013) Katanin p60 contributes to microtubule instability around the midbody and facilitates cytokinesis in rat cells. *PLoS One* **8**, e80392.
172. Bolton DL, Barnitz RA, Sakai K and Lenardo MJ (2008) 14-3-3 theta binding to cell cycle regulatory factors is enhanced by HIV-1 Vpr. *Biol Direct* **3**, 17.
173. Chang F, Re F, Sebastian S, Sazer S and Luban J (2004) HIV-1 Vpr induces defects in mitosis, cytokinesis, nuclear structure, and centrosomes. *Mol Biol Cell* **15**, 1793-801.
174. Hossain D, Ferreira Barbosa JA, Cohen ÉA and Tsang WY (2018) HIV-1 Vpr hijacks EDD-DYRK2-DDB1^{DCAF1} to disrupt centrosome homeostasis. *J Biol Chem* **293**, 9448-9460.
175. Mazo G, Soplop N, Wang WJ, Uryu K and Tsou MF (2016) Spatial control of primary ciliogenesis by subdistal appendages alters sensation-associated properties of cilia. *Dev Cell* **39**, 424-437.
176. Ronquillo CC, Hanke-Gogokhia C, Revelo MP, Frederick JM, Jiang L and Baehr W (2016) Ciliopathy-associated IQCB1/NPHP5 protein is required for mouse photoreceptor outer segment formation. *FASEB J* **30**, 3400-3412.